

**NOVAL INNOVATIONS AND TECHNOLOGIES
IN COMPUTATIONAL SCIENCES AND THEIR
FUTURISTIC APPLICATIONS**

Editors

Dr. Vijayalakshmi Chintamaneni

Dr. Amit Kumar Dutta

Dr. Kaustubh Kumar Shukla

Dr. G Madhukar

Mrs. M Rekhasree



**SIDVI
Foundation**



**Bharti
Publications**

**Noval Innovations and Technologies
in Computational Sciences and
their Futuristic Applications**

Editors

Dr. Vijayalakshmi Chintamaneni

Dr. Amit Kumar Dutta

Dr. Kaustubh Kumar Shukla

Dr. G Madhukar

Mrs. M Rekhasree



Bharti Publications

New Delhi- 110002 (INDIA)

Copyright © 2024, Editors

Title: Noval Innovations and Technologies in Computational Sciences
and their Futuristic Applications

Editor-in-Chief: Dr. S. Akila

Editors: Dr. Vijayalakshmi Chintamaneni, Dr. Amit Kumar Dutta
Dr. Kaustubh Kumar Shukla, Dr. G Madhukar, Mrs. M Rekhasree

All rights reserved. No part of this publication may be reproduced or transmitted, in any form or by any means, without permission. Any person who does any unauthorized act in relation to this publication may be liable to criminal prosecution and civil claims for damages.

First Published, 2024

ISBN: 978-81-19757-24-4

Published by:

Bharti Publications

4819/24, 2nd Floor, Mathur Lane

Ansari Road, Darya Ganj, New Delhi-110002

Phone: 011-46172797, 011-23247537, 9899897381

E-mail : bhartipublications@gmail.com

Website : www.bhartipublications.com

Disclaimer: The author is solely responsible for the contents published in this book. The publisher does not take any responsibility for the same in any manner. Errors, if any, are purely unintentional and readers are requested to communicate such errors to the author or publisher to avoid discrepancies in future.

CONTENTS

- 1. Discovering the Most Efficient Route in Healthcare Using Python with Fuzzy Logic** 1-11
Dr. S. Akila, R. Sakthi Priya
- 2. Automated Product Expiry Alert System** 12-25
K. Manohari
- 3. Green and chemical synthesis of silver nanoparticles: A comparative study for structural, optical, morphological and antibacterial properties** 26-37
G. Azhagarasi, M. Jothibas, A. Muthuvel
- 4. Emergency Braking System AI Distance Sensors** 38-52
S. Navabharathy
- 5. Solving Game Theory Using Reverse Order Octagonal Fuzzy Numbers** 53-61
Ms. S. Farjana, M. Monisha, S. Karthiga
- 6. A Theoretical Perspective on Degradation of Fluorinated Hydrocarbons in the Atmosphere** 62-83
G. Manonmani, D. Ranjith Kumar, & M. Gnanaprakasam
- 7. Subject Notes-Taking System for Academic Performance** 84-89
S. Vidyavathi
- 8. Framework for Mechanized Powerfull Vehicle Mishap Detection and Better- Built Rescue System Based on Iot** 90-100
Snekha Praba J G

9. **A Study on College Atmosphere by Fuzzy Inference System Using Python** 101-110
P. Vishna Priya, R. Charulatha & A Sathyavathi
10. **Multiple Attribute Group Decision Making Problem Using Intuitionistic Triangular Fuzzy Numbers with Runge-Kutta Method** 111-128
S. Jenifer rose, K. Gopika & K. Shruthi
11. **Eco friendly synthesis and characterization zinc oxide nanoparticles nanoparticles and their antibacterial activity** 129-139
Muthuvel, N. Mahendran & V. Mohana
12. **Fraud Detection in Credit Card Online Transaction Using Hidden Markov Model** 140-147
Prabha N
13. **An Encryption and Decryption Technique Using a Complete Graph with Self-Invertible Matrix** 148-157
Ms. M. Rajeswari, N. Sharmila & S. Sarojiny
14. **A New Approaches of Nano RGB-Closed Set in Nano Topological Spaces** 158-167
Ms. R. Suganya, G. Harini & D. Priyanka Salomi
15. **Touchless Water Tap for Preventing Water Loss at Public Stand Posts** 168-178
A.S. Parveen Nisha, M. Kalaivani
16. **Analyzing the Shortest Path, Least Cost and Minimum Time by Using Graph Theory and PERT** 179-193
Ms. V. S. Selvi, Ms. R. Ranjani, Ms. V. Subashini & Ms. S. Charumathi

- 17. Analysis of Waiting Time in Hospital by Application of Queueing Theory** 194-202
Dr. N. Velmurugan, S. Pratheepa, K. Ragavi & T. Pragatheeswari
- 18. Predicting and Detecting of Kidney Problems Using Machine Learning Algorithm** 203-212
V. Vijayalakshmi
- 19. A New Era of Aviation: The Drone Revolution and Artificial Intelligence** 213-224
Dr. Kaustubh Kumar Shukla, Dr. Saket Kumar & Dr. C Venkataramanan

1

Discovering the Most Efficient Route in Healthcare Using Python with Fuzzy Logic

Dr. S. Akila* & R. Sakthi Priya**

* Associate Professor of Mathematics, Theivanai Ammal College for Women (Autonomous), Villupuram, Tamilnadu

** M.Sc. Mathematics, Theivanai Ammal College for Women (Autonomous), Villupuram, Tamilnadu

ABSTRACT

This paper uses Python to build the Fuzzy Shortest Path-Dijkstra's algorithm for healthcare routing. By incorporating fuzzy logic, it seeks to improve on conventional shortest path algorithms and make it possible to express uncertainty in healthcare data more realistically. The methodology computes pathways that take into account the ambiguity associated with medical information by utilizing Python tools for fuzzy logic, graph representation, and optimization. Making decisions is made better when fuzzy logic is applied to healthcare routing, especially when there are unknown medical facts. The project serves as an example of the viability and efficiency of using fuzzy logic to determine the best routes within healthcare networks.

Keywords: *B Fuzzy logic, Fuzzy Shortest Path, Weighted Directed Graph, Shortest Path Problem, Dijkstra's Algorithm, Modification Details.*

INTRODUCTION

Discovering the most efficient route in healthcare using Python with fuzzy logic involves leveraging advanced computational techniques to optimize healthcare logistics. By integrating Python, a versatile programming language, with fuzzy logic, a method for dealing with uncertainty and imprecision, healthcare systems can enhance their route planning processes. Fuzzy logic allows for the modeling of complex, real-world scenarios where precise data may be lacking or uncertain. Through Python's robust libraries and tools for data analysis and optimization, healthcare providers can streamline operations, such as patient transportation, supply chain management, and appointment scheduling, ultimately improving efficiency and patient outcomes. This approach enables healthcare organizations to navigate the complexities of patient care delivery with agility.

and precision, ultimately leading to better resource allocation and enhanced service delivery.

The evolution of graph theory, from foundational works by Balakrishnan (1997) and Wilson (1996) to more recent contributions by Chartrand (1997) and Arumugam and Ramachandran (2015), showcases its enduring relevance and applications. In the realm of fuzzy logic, Klir and Yuan's seminal work (1995) on "Fuzzy Sets and Fuzzy Logic" laid the groundwork, expanded upon by Novak, Perfiljeva, and Mockor (1999), while Atanassov's contributions (1986, 1989, 1999) advanced understanding in intuitionistic fuzzy sets. Mukherjee (2012) extended fuzzy logic applications to path finding in uncertain scenarios. Classical algorithms like Dijkstra's algorithm, explored by He (2022) and Alam and Faruq (2019), remain pivotal, while Wong et al. (2018) demonstrate its versatility in optimizing transportation routes. Python's emergence, highlighted by Torres Sanchez (2020) and Matthes (2021), has revolutionized algorithm implementation, fostering accessibility and empowering researchers and practitioners alike.

PRELIMINARIES

Fuzzy Logic

In Fuzzy Logic, the truth value of variables can be any real integer between 0 and 1, which makes it a form of many-valued logic. In situations where the truth value could vary from fully true to completely false, it is used to manage the idea of partial truth. On the other hand, variables in Boolean logic can have truth values that are limited to the integers 0 and 1.

Fuzzy Shortest Path

A Fuzzy shortest path, which is frequently represented using fuzzy logic, is a path in a network that is found by taking into consideration imprecise or erroneous data. Rather than relying solely on distances, it allows for data uncertainty, providing a more flexible method of determining the best course of action when details are not provided with accuracy.

WEIGHTED DIRECTED GRAPH

Similar to weighted graphs (also called undirected networks or weighted networks), weighted directed graphs (sometimes

called directed networks) are (simple) directed graphs with weights applied to their arrows.

SHORTEST PATH PROBLEM

In graph theory, the shortest path issue is determining the most cost-effective path between two vertices in a graph where each edge has a weight. Finding the route with the least amount of overall weight or expense is the aim. The problem has several real-world applications, including network routing, transportation, and optimization. It can be used to both directed and undirected graphs.

DIJKSTRA'S ALGORITHM

To determine the shortest path between nodes in a network, one popular graph search algorithm is Dijkstra's Method. The single-source shortest path problem can be solved with this algorithm, which bears Edsger W. Dijkstra's name. The shortest path tree or array of shortest distances from a source vertex to each other vertex in the graph is produced by the technique, which runs on graphs with non-negative edge weights.

MODIFICATION FOR FUZZY EDGE WEIGHTS IN DIJKSTRA'S ALGORITHM

When dealing with fuzzy edge weights in Dijkstra's Algorithm, we introduce a concept of uncertainty or imprecision in the weights of edges. Fuzzy logic is employed to model this uncertainty, allowing for a more flexible representation of edge weights. Below are the key modifications to the Dijkstra's Algorithm for handling fuzzy edge weights:

- ***Fuzzification:***

To transform sharp edge weights into fuzzy values, add a fuzzification step. The uncertainty present in real-world situations is simulated through fuzziness. Usually application-specific, this stage could entail taking unpredictability, variability, or imprecision into account.

- ***Fuzzy Arithmetic:***

Modify the distance calculations to involve fuzzy arithmetic. Instead of straightforward addition and comparison, fuzzy arithmetic operations are used. These operations consider the imprecision in the values, and fuzzy logic operators (e.g., fuzzy

addition, fuzzy multiplication) are applied to calculate fuzzy distances.

- **Fuzzy Comparison:**

Adjust the comparison criteria in the algorithm to accommodate fuzzy comparisons. Traditional comparisons are replaced with fuzzy comparisons that consider the degree of similarity between fuzzy values. This ensures that paths with fuzzy distances are properly evaluated.

- **Fuzzy Path Accumulation:**

During the exploration of neighbours, accumulate fuzzy distances along the paths. This involves incorporating fuzzy arithmetic to update tentative distances based on the fuzzy weights of edges.

- **Fuzzy Logic Functions:**

Implement fuzzy logic functions to handle the fuzziness of edge weights. These functions may include fuzzification functions, defuzzification functions (to convert fuzzy distances back to crisp values), and fuzzy comparison functions.

- **Adaptive Fuzzification:**

Based on the particulars of the application domain or the graph, take into consideration adaptive fuzzification. Through the use of adaptive fuzzification, the technique can dynamically adapt to differing levels of uncertainty in various graph regions.

Case study and result

In case study and its outcome, which is a real-world healthcare network graph. We also go over an algorithm and how to use Python to find the fuzzy shortest path between two healthcare facilities.

REAL LIFE HEALTHCARE NETWORK GRAPH

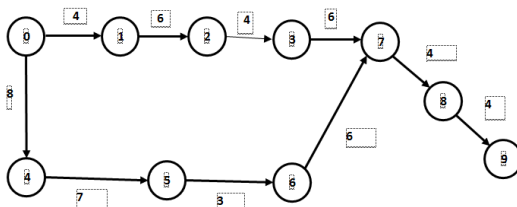


Figure: It is a Weighted Directed Graph (Network graph) consisting the two paths from GH Thiruvannainallur to GH Mundiypakkam to find the fuzzy shortest path.

Name of the places with place codes which we used in this Network.

Node No	Name of the place	Place Code
1	GH Thiruvannainallur	0
2	Emappur	1
3	Enathimangalam	2
4	Tirippichvadmed	3
5	Arasur	4
6	Pedagam	5
7	Kandamanadi	6
8	Villupuram	7
9	Ayyakkovilpattu	8
10	GH Mundiypakkam	9

ALGORITHM FOR PYTHON PROGRAMMING

Step 1: Initialize the **Fuzzy Logic** class with a static method **'fuzzify'** that simulates fuzzification based on some criteria. In this case, it generates a random number within a specific range.

Step 2: Set up initially the Graph class with the number of vertices **'num_vertices'**. This class initializes the graph with a 2D array (**'self.graph'**) representing the adjacency matrix.

Step 3: Define the **'print_solution'** method which prints the fuzzy distance of each vertex from the source vertex.

Step 4: Describe the **'find_min_distance_vertex'** method which finds the vertex with the minimum distance value from the source vertex among the vertices not yet visited.

Step 5: Explain the **'dijkstra'** method which implements Dijkstra's algorithm to find the shortest path from the source vertex to all other vertices in the graph. It includes fuzzification of distances using the **'fuzzify'** method.

Step 6: Initialize distance array `distances` with a maximum value for each vertex except the source vertex, which is set to 0. Initialize the visited array `visited` with all vertices marked as not visited. Also, initialize a dictionary '**previous_nodes**' to keep track of the previous node in the shortest path.

Step 7: Iterate through all vertices of the graph:

- Find the vertex with the minimum distance value from the source vertex using the '**find_min_distance_vertex**' method.
- Mark the selected vertex as visited.
- Update the distance value of adjacent vertices not yet visited if the current distance value plus the weight of the edge is less than the existing distance value. Apply fuzzification to the distances.

Step 8: Print the solution by calling the '**print_solution**' method with the updated distances.

Step 9: To print the outcome, use the call the '**print_result**' method, which traces back the shortest path from the target node to the source node using the '**previous_nodes**' dictionary.

PYTHON PROGRAMMING

```
import sys
import random
class FuzzyLogic:
    @staticmethod
    def fuzzify(value):
        # Simulate fuzzyfication based on some criteria
        return random.uniform(0.9, 1.1) # Adjust the range as needed
class Graph:
    def __init__(self, num_vertices):
        self.num_vertices = num_vertices
        self.graph = [[0 for _ in range(num_vertices)] for _ in range(num_vertices)]
    def print_solution(self, distances):
```



```

print("Vertex \tFuzzy Distance from Source")
for vertex, distance in enumerate(distances):
    print(vertex, "\t", distance)
    def find_min_distance_vertex(self, distances, visited):
        min_distance = sys.maxsize
        min_vertex = None
        for vertex in range(self.num_vertices):
            if distances[vertex] < min_distance and not visited[vertex]:
                min_distance = distances[vertex]
                min_vertex = vertex
        return min_vertex
    def dijkstra(self, source_vertex):
        distances = [sys.maxsize] * self.num_vertices
        distances[source_vertex] = 0
        visited = [False] * self.num_vertices
        previous_nodes = {vertex: None for vertex in
            range(self.num_vertices)}
        for _ in range(self.num_vertices):
            current_vertex = self.find_min_distance_vertex(distances,
                visited)
            visited[current_vertex] = True
            for neighbor_vertex in range(self.num_vertices):
                if (
                    self.graph[current_vertex][neighbor_vertex] > 0
                    and not visited[neighbor_vertex]
                    and distances[neighbor_vertex] >
                    distances[current_vertex] +
                    self.graph[current_vertex][neighbor_vertex]
                ):
                    # Introduce fuzzy logic here

```

```

        fuzz_factor =
FuzzyLogic.fuzzify(self.graph[current_vertex][neighbor_vertex])
        distances[neighbor_vertex] =
distances[current_vertex] + fuzz_factor *
self.graph[current_vertex][neighbor_vertex]
        previous_nodes[neighbor_vertex] = current_vertex
        self.print_solution(distances)
        return previous_nodes, distances

    def print_result(self, previous_nodes, start_node,
target_node):
        path = []
        current_node = target_node
        while current_node is not None:
            path.append(current_node)
            current_node = previous_nodes[current_node]
        path.reverse()
        print(f"We found the following best path from {start_node}
to {target_node}:")
        print("-> ".join(map(str, path)))

# Driver's code
if __name__ == "__main__":
    g = Graph(10)
    g.graph = [
        [0, 4, 0, 0, 8, 0, 0, 0, 0, 0],
        [0, 0, 6, 0, 0, 0, 0, 0, 0, 0],
        [0, 0, 0, 4, 0, 0, 0, 0, 0, 0],
        [0, 0, 0, 0, 0, 0, 0, 6, 0, 0],
        [0, 0, 0, 0, 0, 7, 0, 0, 0, 0],
        [0, 0, 0, 0, 0, 0, 3, 0, 0, 0],
    ]

```

```
[0, 0, 0, 0, 0, 0, 0, 6, 0, 0],
[0, 0, 0, 0, 0, 0, 0, 0, 4, 0],
[0, 0, 0, 0, 0, 0, 0, 0, 0, 4],
[0, 0, 0, 0, 0, 0, 0, 0, 0, 0],
]
source_vertex = 0
target_vertex = 9
previous_nodes, _ = g.dijkstra(source_vertex)
g.print_result(previous_nodes, source_vertex, target_vertex)
```

OUTPUT

```
Vertex  Fuzzy Distance from Source
0        0
1        4.188336416337637
2       10.493602579263133
3       14.099546997212203
4        7.797134603073242
5       15.363251678209956
6       18.113175778754925
7       20.151582163534613
8       24.360774492723625
9       28.23399142329736
```

We found the following best path from 0 to 9:

```
0 -> 1 -> 2 -> 3 -> 7 -> 8 -> 9
```

CONCLUSION

Fuzzy logic is added to Dijkstra's algorithm to allow for efficient decision-making in healthcare logistics, where distance uncertainties are present. By taking into account both sharp and fuzzy distances, this Python code effectively determines the shortest path between hospitals, enabling healthcare systems route patients more effectively. The technique improves flexibility to real-world healthcare circumstances by utilizing fuzzy logic, which eventually leads to better patient outcomes and operational efficiency.

BIBLIOGRAPHY

1. Vilem Novak , Irina Perfiljeva, & Jiri Mockor. (1999). *Mathematical Principles of Fuzzy Logic*. Dordrecht Kluwer Academic.
- A. Nagoor Gani, & M. Mohammed Jabarulla. (2010). On searching intuitionistic fuzzy shortest path in a network. *Applied Mathematical Sciences*, 4, 3447-3454.
2. Baoyi He. (2022). Application of Dijkstra algorithm in finding the shortest path. *Journal of Physics: Conference Series*.
3. C. M. Klein. (1991). Fuzzy shortest paths. *Fuzzy Sets and Systems*, 39,, 27-41.
4. David Torres Sanchez. (2020). A Python with a Collection of algorithm for the (Resource) Constrained Shortest Path Problem. *The Journal of Open sources Software*, 5(49).
5. Eric Matthes. (2021). *Python Crash Course*. William Pollock.
6. Gary Chartrand . (1997). *Introductory Graph Theory*. Courier Corporation.
7. George J. Klir, & Bo Yuan. (1995). *Fuzzy Sets and Fuzzy Logic Theory and Applications*. USA: prentice Hall PTR.
8. J.-R. Yu, & T.-H. Wei. (2007). Solving the fuzzy shortest path problem by using a linear multiple objective programming. *Journal of the Chinese Institute of Industrial Engineers*, 24, 360-365.
9. J.-S. Yao, & F.-T. Lin. (2003). Fuzzy shortest-path network problems with uncertain edge weights. *Journal of Information Science and Engineering*, 19, 329-351.
10. K. Atanassov. (1999). *Intuitionistic Fuzzy Sets: Theory and Applications*. Physica.
11. K. T. Atanassov. (1986). Intuitionistic fuzzy sets. *Fuzzy Sets and Systems*, 20, 87-96.
12. K. T. Atanassov. (1989). More on intuitionistic fuzzy sets. *Fuzzy Sets and Systems*, 33, 37-45.
13. L. Sujatha , & S. Elizabeth. (2011). Fuzzy shortest path problem based on similarity degree. *Applied Mathematical Sciences*, 5, 3263-3276.
14. Md. Almash Alam, & Md. Omar Faruq. (2019). Finding Shortest Path for Road Network Using Dijkstra's Algorithm. *Bangladesh Journal of Multidisciplinary Scientific Research*, 2.
15. Rini Wongo, Cin Cin, Suhartono, & Joseph. (2018). A Shortest Path Finding Application for Jakarta Public Transportation using Dijkstra Algorithm. *Journal of Computer Science*.

16. Robin J. Wilson. (1996). *Introduction to Graph Theory*. Englang: Addison Wesley Longman Limited.
17. S. Arumugam, & S. Ramachandran. (2015). *Invitation to Graph Theory*. Chennai: Scitech Publications (INDIA) PVT.LTD.
18. S. Mukherjee. (2012). Dijkstra's algorithm for solving the shortest path problem on networks under intuitionistic fuzzy environment. *Journal of Mathematical Modelling and Algorithms*, 11, 345-359.
19. S. Okada, & T. Soper. (2000). A shortest path problem on a network with fuzzy arc lengths. *Fuzzy Sets and Systems*, 109, 129-140.
20. Siddhartha Sankar Biswas, Bashir Alam, & M. N. Doja. (2013). An Algorithm for Extracting Instuitionistic Fuzzy Shortest Path in Graph. *Applied Computational Intelligence and Soft Computation*, 1-5.
21. V. K. Balakrishnan. (1997). *Graph Theory*. New York: McGraw-Hill.

ABSTRACT

Product expiry management System is very Convenient for manage the input, output and find the data to make the data specific, visualization and rationalization. It also provides the basic information maintenance function of employees, memberships and products that manage the function to add, delete and modify the basic information of Employees. Product controls is the process of managing products in order to meet customer demand. This study is to produce software which manages the sales activity done in a supermarket, maintaining the stock details, maintaining the records of the sales done for the products which have expired or about to expire.

1. INTRODUCTION

The Product Expiration System is a complete web-based application designed with HTML, CSS and PHP technology. The main aim of the project is to develop Product Expiration System Model software in which all the information regarding the stock of the organization to be mainted. It is an internet based application which has admin component to manage the inventory and maintenance of the inventory system.

This application is based on the management of stock of an organization. The application contains general organization profile, sales details, Purchase details and expiration dates presented in the organization. There is a provision of updating the inventory and generating different form of report.

Scope of the Research paper

The project is aimed at developing an alert system which notifies shop owners and managers of products/inventory which are about to expire. Faced with the challenges shop owners face with loses and health hazards brought about by expired products, the researcher aimed at developing a product/Inventory.

Expiration system that manages product expiration in a computerized manner. The Product expiration management system notifies/alerts the store manager on products expiring soon for prompt attention and decision. The system was built with PHP, MYSQL and Bootstrap Technologies

Products are considered as the business resources for the organization. This includes managing the product with appropriate way to review any time as per the requirement. Therefore, it is important to have a web-based Product Expiration System which has the ability to generate reports, report products expiry dates, maintain the balance of the stock, details about the purchase and sales in the organization, which helps to minimize loses to the business or negative health hazards to consumers. These web application can be used by large or small business organization for the management of their stock in the production houses. After analyzing the other Product Expiration systems, we decided to include some of common and key features that should be included in every Product Expiration system.

1.3 PROPOSED SYSTEM HIGHLIGHTS

Health hazards to consumers and huge loss to businesses have been the major challenges posed by expired products. Manually taking stock of products by small scale/medium scale business owners are still prone to human errors. When consumers are exposed to expired products, they may have various health challenges ranging from stomach upsets to food poisoning (which may result to death).

Apart from law suits the shop owner may face, he/she will be losing money if the products in the store expires without his/her notice. These challenges are the main reasons the researcher sought to develop a computerized system that notifies shop owners and managers of impending products that are about to expire. This system is significant in the sense that it will curb loses and prevent health hazards to consumers.

To develop a web Product Expiration system to assist business owners take stock and regulate product expiring dates, solves the tedious work and activities in calculating and taking stocks of large product for large business owners in which they end up missing expiry dates, mis-calculating and discarding some

important figures, with this Inventory system, business owners can now take stock, check product expiration dates, calculate their products left with just a click

PURPOSES

The system can aid Shop owners and managers make prompt and informed decisions of products that are about to expire. Clearance sales, Immediate Consumption of Products, Gifting of Product etc. could be good measures that can be taken to minimize loss to the business or prevent health hazards to consumers.

Product Expiration System is targeted to the small or medium organization which doesn't have proper records of their products, also for those organization that deals with products that expire, a proper system to keep track of product expiration is important

Applicabilities

When consumers search for and check expiration dates, the risk of purchasing and consuming a stale and denigrated quality product reduces. Since checking expiration dates has a significant impact on consumers' purchase and consumption decision making, the authors investigate what motivates consumers to search for expiration dates while shopping for and before consuming perishable grocery products. This research adapts and extends the information search model (Schmidt and Spreng 1996) by providing new insight on information search as not only a prepurchase but also a consumption stage activity. Findings suggest that expiration date search effort is influenced by perceived risk, time pressure while grocery shopping, and the motivation of checking expiration dates. These findings provide several implications for consumers and policymakers.

2 SYSTEM ANALYSIS

- System analysis is the process of gathering facts, interpreting facts and diagnosing problem by using the information for improvements on the system
- The act, process or profession of studying an activity (such as a procedure, a business, or a physiological function) typically by mathematical means in order to define its goals or

purposes and to discover operations and procedures for accomplishing them most efficiently.

2.1 Proposed system

- The proposed system is used to Expiry management makes it easy for businesses to keep track of which stocks are closest to their expiry dates. Hence, these stocks are sold first. With expiry management software, brands can prevent the loss of products.

2.2 Advantages of proposed system

- It develops the easy management of the inventory and also handle the inventory details like purchase details, manufacturer details and expiration dates of Products. It is used to maintain a record of batches of product brought to the store and keep a record of product brought to the store. This also helps to detect about to expire and expired products in the store.

2.3 Feasibility Study

- Preliminary investigation examine project feasibility, the likelihood the system will be useful to the organization. The main objective of the feasibility study is to test the Technical, Operational and Economical feasibility for adding new modules and debugging old running system. All system is feasible if they are unlimited resources and infinite time. There are aspects in the feasibility study portion of the preliminary investigation:

TECHNICAL FEASIBILITY

This study is carried out to check the technical feasibility, that is, the technical requirements of the system. Any system developed must not have a high demand on the available technical resources. This will lead to high demands on the available technical resources. This system can used to marking attendance in the fraction of second. The developed system must have a modest requirement, as only minimal or null changes are required for implementing this system.

3. SYSTEM SPECIFICATION

A system requirement is the analysis which is needed for the purposed system to run on a particular machine. It gives the

minimum requirements to execute the instruction in the machine. They are,

3.1 Software Requirement

The software requirement deal with the analysis of the software and operating system and the tools those are essential for the project.

1. Processor : AMD A4
2. Operating System : Windows family
3. Tool : Pycharm 3.7
4. Front End : Python,HTML
5. Back End : SQL (Xampp)

4. SYSTEM DESCRIPTION

4.1 TOOL DESCRIPTION

Python 3.8 IDE

The python integrated development environment is a creative launching pad that we can use to edit, debug and write code and then run the system. An integrated development environment (IDE) is a feature rich program that can be used for many aspects of software development.

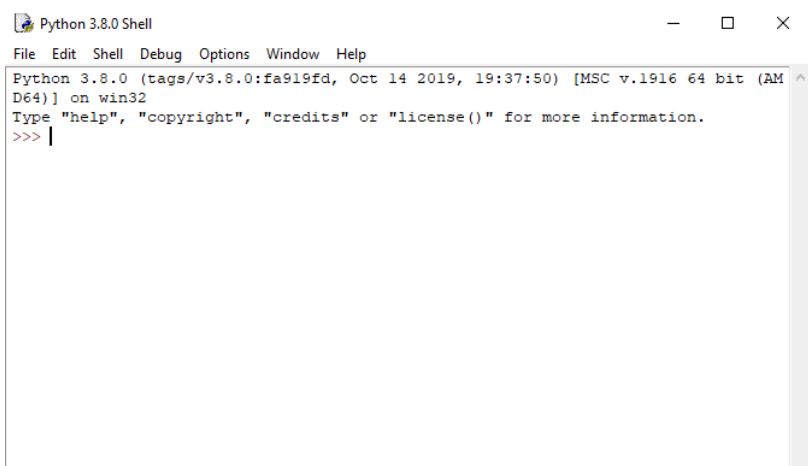
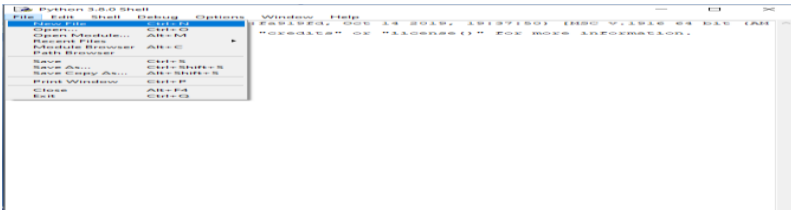


FIG 4.1.1. Python 3.8 Idle

- The image has several tools that we would use are:
- File tab consists of create new file, open the existing file, save the file with save and save as, print the file and close the file



IG 4.1.2. FILE TAB

- Edit tab consist of undo, redo, find and replace, go to, show call tip, show surroundings.

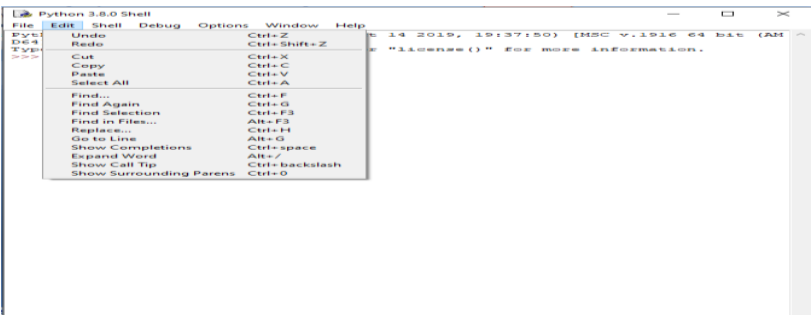


FIG 4.1.3 Edit Tab

- Shell tab is used to view the recent and previous history and restart the shell

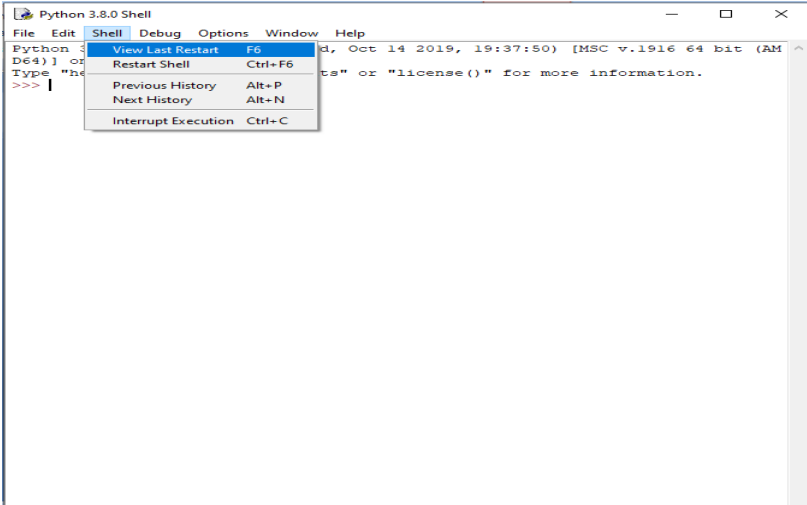


FIG 4.1.4 Shell Tab

- Debug tab used to debug the program and it consist of go to, stack viewer,Auto-open stack viewer.

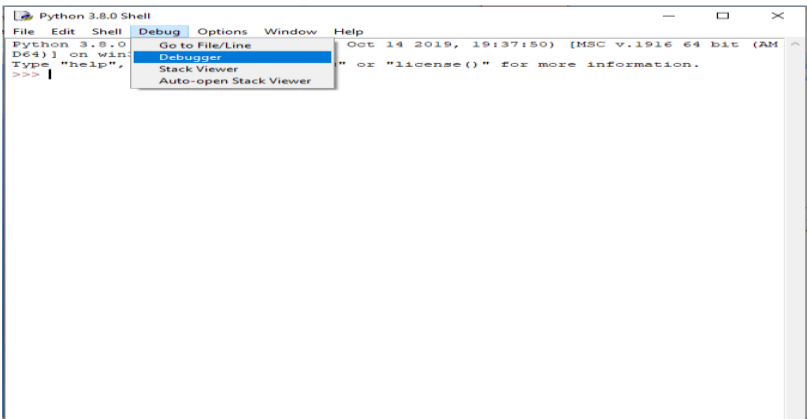


FIG 4.1.5. Debug tab

- Option tab consist of configure IDE, zoom height, Show line number and code context.

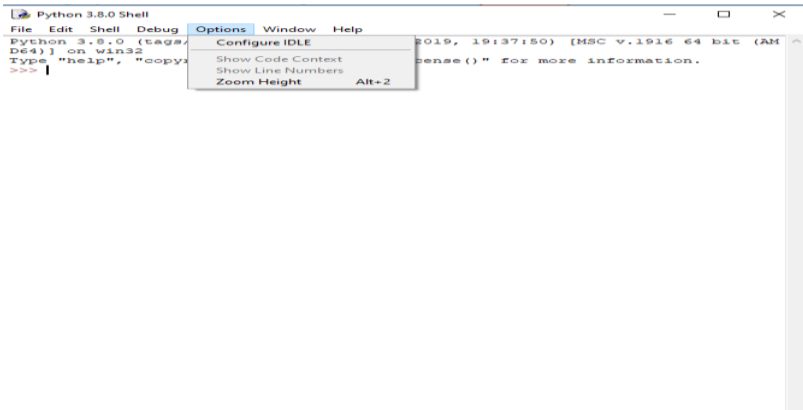


FIG 4.1.6. Option Tab

- Window tab consist of python 3.8 shell which activate shell window

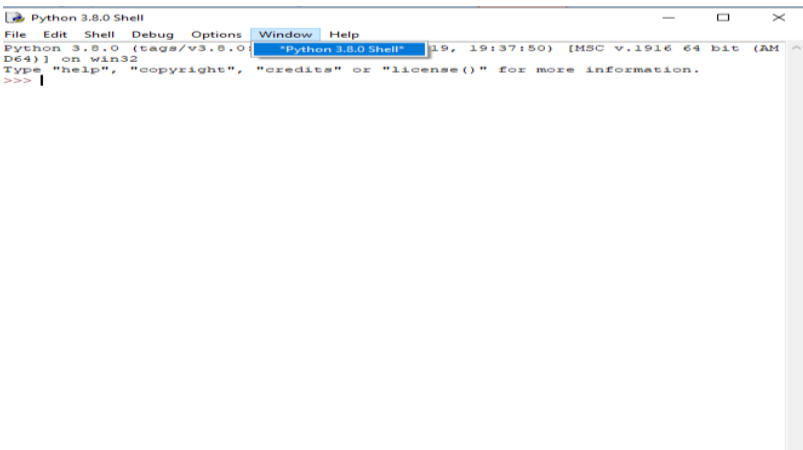


FIG 4.1.7. Window Tab

- Help tab allow the user to seek help from the IDE and it provide demo in it

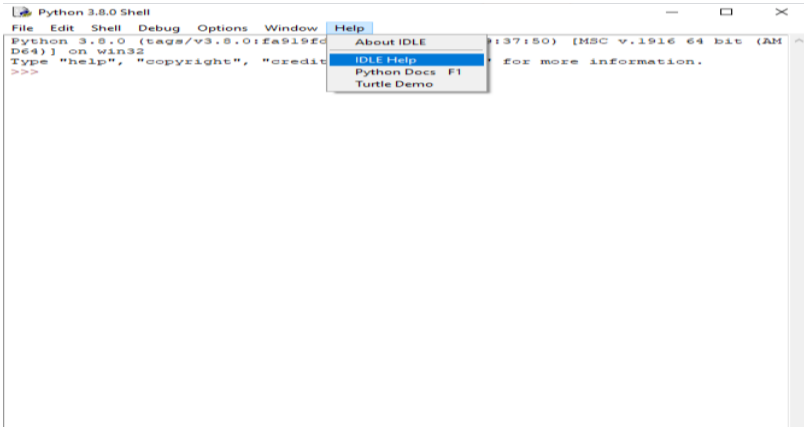


FIG 4.1.8. Help Tab

Features of Python:

- The image can be captured by the following coding in python. It can capture the image of the person in gray scale . Then save the image with name of the faculty.

```
ret, img = cap.read()

# Display countdown on each frame
# specify the font and draw the
# countdown using puttext
font = cv2.FONT_HERSHEY_SIMPLEX
cv2.putText(img, str(TIMER),
            (200, 250), font,
            7, (0, 255, 255),
            4, cv2.LINE_AA)

cv2.imshow('a', img)
cv2.waitKey(125)

# current time
cur = time.time()
```

FIG 4.1.9 Capture Image

Packages:

- *Tk-Tools*

Tk/Tcl has long been an integral part of Python. It provides a robust and platform independent windowing toolkit, that is available to Python programmers using the tkinter package, and its extension, the tkinter tix and the tkinter ttk modules. The tkinter package is a thin object-oriented layer on top of Tcl/Tk.

“pip install tk-tools”.

- *Opencv-Contrib-Python*

It's a package that contains pre-built OpenCV with dependencies and Python bindings, so there's no need to install OpenCV separately. ... We're proud to bring `opencv-python`, `opencv-python-headless`, `opencv-contrib-python` and `opencv-contrib-python-headless` home at OpenCV.org.

“pip install opencv-contrib-python”.

- *Datetime*

Datetime module supplies classes to work with date and time. These classes provide a number of functions to deal with dates, times and time intervals. Date and datetime are an object in Python, so when you manipulate them, you are actually manipulating objects and not string or timestamps

“pip install datetime”.

- *Pytest-Shutil*

The `shutil` module helps you automate copying files and directories. This saves the steps of opening, reading, writing and closing files when there is no actual processing. It is a utility module which can be used to accomplish tasks, such as: copying, moving, or removing directory trees

“pip install pytest-shutil”.

- *Python-CSV*

CSV (Comma Separated Values) is a simple file format used to store tabular data, such as a spreadsheet or database. A CSV file stores tabular data (numbers and text) in plain text. Each line of the file is a data record. ... For working CSV files in python, there is an inbuilt module called `csv`.

“pip install python-csv”.

- *Numpy*

NumPy can be used to perform a wide variety of mathematical operations on arrays. It adds powerful data structures to Python that guarantee efficient calculations with arrays and matrices and it supplies an enormous library of high-level mathematical functions that operate on these arrays and matrices

“pip install numpy”.

- *Pillow*

Pillow is a Python Imaging Library (PIL), which adds support for opening, manipulating, and saving images. The current version identifies and reads a large number of formats. Write support is intentionally restricted to the most commonly used interchange and presentation formats.

“pip install pillow”.

- ***Pandas***

Pandas is a widely-used data analysis and manipulation library for Python. It provides numerous functions and methods that expedite the data analysis and preprocessing steps.

“pip install pandas”.

- ***Face Recognition***

Face recognition is a method of identifying or verifying the identity of an individual using their face. There are various algorithms that can do face recognition but their accuracy might vary. Here it describe how to do face recognition using deep learning.

“pip install facerecognition”.

- ***DLIB***

It's a landmark's facial detector with pre-trained models, the dlib is used to estimate the location of 68 coordinates (x, y) that map the facial points on a person's face like image.

“pip install dlib”.

Haar cascade classifier

Haar Cascade classifiers are an effective way for object detection. This method was proposed by Paul Viola and Michael Jones in their paper [Rapid Object Detection using a Boosted Cascade of Simple Features](#). Haar Cascade is a machine learning-based approach where a lot of positive and negative images are used to train the classifier.

- **Positive images** – These images contain the images which we want our classifier to identify.
- **Negative Images** – Images of everything else, which do not contain the object we want to detect

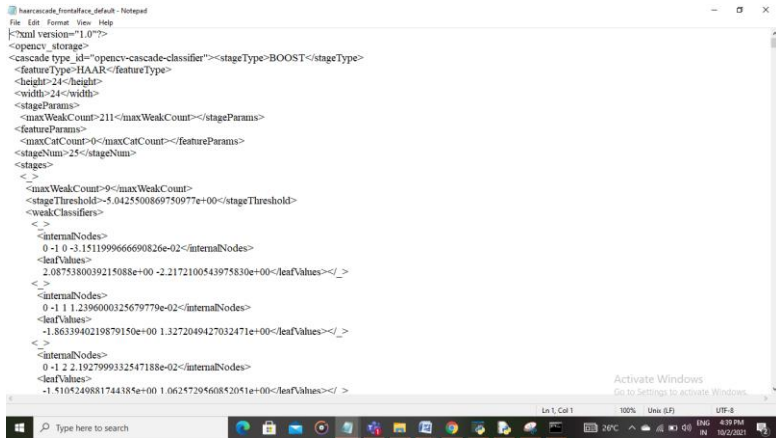


Fig 4.1.10. Haarcascade Classifier

METHODOLOGY

DATA SET CREATION:

The original database containing the images of the lectures is created by taking a live real time video of the lectures, and splitting the video into thirty frames, converting them to gray scale and storing only the faces of the student or faculty as images, then it training the respective images using the LBPH and then comparing the stored and trained images against the captured images to mark the attendance. The software used for splitting the video into frames is Open-CV.

PRODUCT INFORMATION

In this phase realized the documentation and control of large goods, so as to facilitate the management and decision of sales, and reduce a big burden for managers. These systems hardly notify the users of any product about to expire or has expired. which has led to loss of goods due to expiration. This project, product expiry alert management helps to improve the work efficiency of supermarket by providing daily, weekly or monthly expiry alerts of products. It also provides the basic information maintenance function of employees, memberships and products so that managers can through the function to add, delete, and modify the basic information of employees and the employees can through it to add, modify and delete the basic information of memberships and goods.

PRODUCT MATCHING

In this second phase once the video has begun capturing, simultaneously the Haar Cascade algorithm is applied to the video to get individual faces of the lectures and obtaining the distinct features of their face the parts of the face that are needed most for detection i.e, the ROI (Region of Interest) and processing and cropping out other regions of the face that do not play a role in the image processing and matching part. Once the faces are detected they are extracted and stored

PRODUCT DETECTION

In this third and most crucial phase of recognising the lecture, that is comparing captured image against the stored images in the database, this method is done by making use of the LBPH algorithm (Local Binary Pattern Histogram), each image stored in the database has it's from the captured video feed.

LBPH ALGORITHM

It is a Face Recognition algorithm it is used to recognize the face of a person. It is known for it's performance and how it is able to recognize the face of a person from both front face and side face. Frontal Haarcascade is used for face detection from the image, LBPH is used for face recognition and CNN is used for face mask detection system.

CONCLUSION

Today management is one of the most essential features of all form. Management provides sophistication to perform any kind of task in a particular form. This is pharmacy management system; it is used to manage most pharmacy related activities in the pharmacy. The primary aim of is to improve accuracy and enhance safety and efficiency in the pharmaceutical store. In this project it also includes that BAR CODE facility using the bar code reader. which will detect the expiry date and the other information about the related medicines. This may be also concluded by using pharmacy software, processing both new prescriptions and refills can be done quickly and simply with just a few keystrokes or mouse clicks with new, easy to learn and use Graphical User Interface (GUI) pharmacy management solution. A switch from product oriented to patient oriented which is one of the most important keys in pharmaceutical care. In other words that the pharmacist will have more time in

counseling his/her customers where the goal of patient counseling is one of the important solution to avoid medication error.

REFERENCES

1. Koluguri Neelima, K. Ashok Kumar—Advance Security System with Intruder Image Capture and Forward Through Email. July 2023. ISSN No 2348 4845
2. Nagula Shyam Kumar, Nivedita.M—IOT Based Advance Security System by Using Raspberry PI. . . July 2021. ISSN No 2348 4845
3. Rohini Jadhav, Harshal Patil, Prof. M. S. Wagh, “Automatic System Using RFID with High Alerting System” International Research Journal of Engineering and Technology (IRJET), volume-4, Issue4, April-2017
4. Sayali R. More, Ruchira J. Raut, Rasika K. Tandel, Snehal D. Yendhe, “Intelligent Alerting System,”
5. Karthik Krishnamurthi, Monica Bobby, Vidya. V, Edwin Baby, “Sensor based automatic control of product expiry” International Journal of Advanced Research in Computer Engineering and Technology (IJARCET) Volume 4 Issue 2, February 2015
6. J. Banuchandar, V. Kaliraj, P. Balasubramanian, S. Deepa, N. Thamilarasi, “Automated Unmanned Expiry Level Crossing System”, in International Journal of Modern Engineering Research (IJMER) Volume.2, Issue.1, Jan-Feb 2012 pp-458-

Green and Chemical Synthesis of Silver Nanoparticles: A Comparative Study for Structural, Optical, Morphological and Antibacterial Properties

G. Azhagarasi*, M. Jothibas** & A. Muthuvel**

*PG and Research Department of Physics,
Theivanai Ammal College for Women (Autonomous),
Villupuram, Tamil Nadu

** PG and Research Department of Physics,
T. B. M. L College, Porayar, Tamil Nadu

ABSTRACT

Two different methods (chemical and biological) are used to synthesize silver nanoparticles in this study. Both synthesized nanoparticles were characterized by FT-IR, XRD, PL, UV-visible, DLS, ZE and SEM with EDAX. The X-ray diffraction pattern confirmed the presence of crystalline, fcc structure of both synthesized NPs. The size of nanoparticles was 29 nm (chemical) and 18 nm (biological). The SEM analyses showed spherical shape with average size (36, 25) nm for the synthesized NPs by chemical and biological methods respectively. Furthermore, antibacterial activity proved biosynthesized Ag NPs to be more potent activity than chemically synthesized Ag NPs. There was also discussion about the possible antibacterial mechanisms of Ag NPs. In this study, concludes that the biosynthesize Ag NPs have smaller crystalline size, better morphology and significant antimicrobial activity as compared to that the chemically synthesized NPs.

Keywords: Silver, Chemical, biosynthesis, *T. procumbens*, XRD, Antibacterial.

INTRODUCTION

Nanotechnology is a new technology that can revolutionise various scientific fields. Nanomaterials have distinct chemical, physical and biological properties when compared to their macro scale complements [1]. The nanoparticles are being considered extensively for their structural, magnetic, optical, catalyst and biomedical fields. Today, noble metal nanoparticles, specifically Ag, Au, Pd, and Pt, are the most effectively studied [2]. Silver nanoparticles (Ag-NPs) have demonstrated their potential to be used in research and development centres due to

their unique chemical, physical and antimicrobial properties []. The nanoscale size of the particles, in particular, improved their antimicrobial activities via specific effects such as adsorption at bacterial surfaces [3]. Furthermore, used in environmental protection and biological application such as, drug delivery, gene delivery and nanomedicines etc. It has previously been reported that Ag NPs have good antibacterial, antioxidant, anti-inflammatory, antiviral and anticancer potential, with improved biodegradability and lower toxicity. For the synthesis of Ag NPs, many conventional chemical and physical methods have been used, including the Sol gel process, microwave, microemulsion, co-precipitation, solvothermal, laser and chemical vapour deposition [4-7]. These methods, on the other hand, are usually costly, time consuming and potentially harmful to the environment and living organisms. The chemical method for nanoparticles synthesis can result in the formation of multiple chemical molecules, increasing particle reactivity and toxicity and posing a risk to human health and the environment due to the unpredictability of their composition. Additional capping and stabilising agents are required in chemical and physical methods. The majority of synthesis methods make use of organic solvents and capping/reducing agents [8]. As a result, there is an obvious need for an alternative, simple, safe, cost effective and eco-friendly method of synthesising nanoparticles. As a result, there is an essential for "green synthesis", which provides several eco-friendly assistances by avoiding the habit of toxic chemicals in the synthesis process. There are three major sources of Ag NPs synthesis: fungi, bacteria and plant extracts. Because of the ease with which plants can be grown, using them for nanoparticles synthesis may be preferable to other biological methods. Plant mediated approaches can be also be easily scaled up for large scale nanoparticles synthesis. Plants play an important role in reducing the metal ions to nanoparticles and promoting their subsequent stability and acting as bioreactors and phytochemicals such as alkaloids and terpenoids, limonoids, sesquiterpenes, diterpenes, proteins and phenols [9].

Tridax procumbens (*T. procumbens*), a daisy-like plant, is one of the greatest commonly used plants in rural and tribal groups to treat a variety of ailments. This plant can be found in India's wastelands, roadsides, and hedges. *T. procumbens* has been used to treat fever, typhoid fever, diarrhoea, cough, asthma, and

epilepsy for centuries. Asad Syed et al., [10] evaluated that the antimicrobial and cytotoxic activity of the *T. procumbens* leaf extract. The different pharmaceutical properties of the plant extract were evaluated in other reports. Patil et al., [11] evaluated the antimicrobial activity of the synthesized magnetic iron nanoparticles using *T. procumbens* leaf extract. The current study focused on two different approaches for producing Ag NPs (Sol gel and biosynthesis). In the biosynthetic scheme, *T. procumbens* leaf extract was used. The properties (optical, morphological, structural and antibacterial) of the two Ag NPs variants were compared. Chemically synthesized Ag NPs and biosynthesized Ag NPs are referred to as chem Ag NPs and bio-Ag NPs.

2. MATERIALS AND METHODS

2.1 Chemicals

Silver nitrate (AgNO_3) and Sodium chloride (NaOH) were purchased from Sigma company Pvt. Ltd., India and deionized water was used for injection. All of the chemicals used in the Ag NPs synthesis experiments are pure and analytical reagents grade.

2.2. Preparation of leaf extract

T. procumbens leaves were obtained in the rural area of Porayar, Tamil Nadu, India. Healthy leaves of *T. procumbens* (25 g) were weighed, washed and boiled for 5 min in 100 mL of deionized water. The extract was filtered through Whatman No: 1 filter paper after cooling to room temperature and stored in the refrigerator for future investigation.

2.3. Synthesis of Ag NPs

2.3.1. Chemical synthesis Ag NPs

100 mL of 0.1 M AgNO_3 was mixed dropwise with 50 mL of a NaOH (0.5 M) solution to make Ag NPs. The reaction was continued for 80 °C for 3 h. After centrifugation at 10000 rpm for 10 min at 30 °C, the nanoparticles were collected and washed three times. To obtain the Ag NPs, the nanoparticles were dried at 100 °C and calcined for 2 h at 400 °C.

2.3.2. Green synthesis Ag NPs

Ag NPs were synthesized by mixing 20 mL of *T. procumbens* leaf extract. The above solution was heated at 80 °C for 3 h while

being constantly stirred with a magnetic stirrer. Centrifugation at 10000 rpm for 10 min at 30 °C was used to collect nanoparticles. The nanoparticles were washed three time, dried for 10 h at 80 °C, and then calcined fir 2 h at 400 °C.

2.4. Characterizations of the particles

The X-ray diffraction (SHIMADZU-XRD 6000) analysis was used to determine the crystal structure and phase of the synthesized nanoparticles. The scanning electron microscopy (SEM) was used to examine the morphology of the synthesized nanoparticles (Hitachi S-4500 Machine).The UV-Vis spectrophotometer was used to measure the absorption spectra (SHIMADZU-UV 1800). Fourier transform infrared (FT-IR) spectra in the range 4000-400 cm^{-1} were recorded (BRUKER: RFS 27).

2.5. Bacterial activities

The antibacterial activities of leaf extract, chem Ag NPs and bio-Ag NPs were tested using the disc diffusion methodon four types of bacteria: *B. subtilis*, *E. coli*, *S. aureus*, and *P. aeruginosa*. The 50 and 100 $\mu\text{g}/\text{mL}$ concentration of tested samples were poured onto each disk and placed on Muller Hinton agar plates. As a positive control, the antibiotic dis Ciprofloxacin was used. At 35°C, the plates were incubated for 24 h. The antibacterial activities of the samples on the tested bacterial strains was determined by forming an inhibitory zone around the wells.

3. RESULTS AND DISCUSSION

3.1 Structural analysis

The both synthesis of Ag NPs was primarily established by XRD analysis and results are given in Fig 1. The peaks obtained at $2\theta^\circ$ values of 38.07, 44.27, 64.47 and 77.42 can be attributed to the planes (111), (200), (220) and (311) respectively. All of the peaks match the Face Centre Cubic (FCC) structure of Ag NPs when compared to standard data (JCPDS No: 04-0784) [12]. Other than Ag, the XRD data revealed no impurity peaks, indicating that all products had good phase purity. Furthermore, the acquired diffraction reflections are well defined and have a high intensity, implying that the bio-Ag NPs are highly crystalline. The bio-Ag NPs, angle shifts, and diffraction planes were observed as a function of phytochemicals present in the leaf extract. The

positions of peaks in the bio-Ag NPs were slightly shifted towards the left side when compared to the chem Ag NPs, according to these findings.

Debye Scherer's formula was used to compute the average crystal size of both produced nanoparticles [12];

$$\text{The crystallite size (D)} = \frac{0.94\lambda}{\beta \cos\theta} \quad (1)$$

where, D is the crystalline size, θ is Bragg's diffraction angle, β is the angular peak width at half maximum in radian along (1 1 1) plane and λ is the wavelength of X-ray used (1.5406 Å). The micro-strain (ϵ), stacking fault (SF), dislocation density (δ) were calculated using the formula [11]:

$$\epsilon = \frac{\beta \cos\theta}{4} \quad (2)$$

$$\delta = \frac{1}{D^2} \quad (3)$$

$$SF = \left[\frac{2\pi^2}{45(3\tan\theta)^2} \right] \beta \quad (4)$$

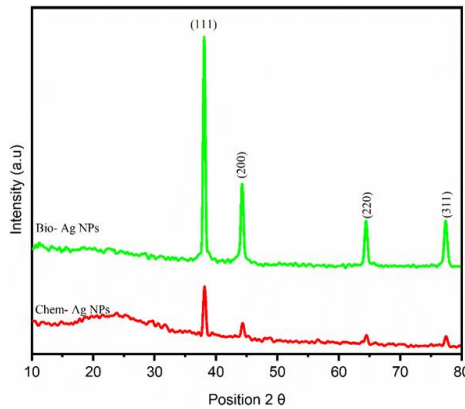


Figure 1 XRD pattern of the chem and bio-Ag NPs

Bio Ag NPs have a crystalline size of 18 nm, whereas chem Ag NPs have a crystalline size of 29 nm. The obtained crystallite size from the green synthesized Ag NPs (using *T. procumbens* leaf extract) is smaller from others leaf extracts (*Lagenaria siceraria*, *Solanum nigrum* and *Mimusopselengi*) used to synthesize Ag NPs.

The variation of structural parameters of the both synthesized Ag NPs are shown in Table 1. The dislocation density is inversely related to the crystalline size, but the micro strain is directly proportional. The small crystalline size of green synthesized nanoparticles will help greatly to improve antimicrobial activities.

3.2 Optical analysis

Figure 2a shows the room temperature absorption spectrum of Ag NPs synthesized by chemical and biological methods correspondingly. The absorbance peak for the chem Ag NPs was measured at 384 nm. The excitonic absorption peak of Ag NPs synthesized using the green method was found to be 424 nm. When comparing bio-Ag NPs to chem Ag NPs, a red shift was observed, and the shift of the absorption peak could be due to differences in particle size and configuration [13]. The maximum absorption in bio-Ag NPs may be due to phytochemicals present in leaf extract. The optical band gap energy of both produced nanoparticles was calculated using the following equation based on UV-Vis spectroscopy results [14];

$$(\alpha h\nu)^2 = B (h\nu - E_g)^{1/2} \quad (5)$$

where h is the Planck constant, α is the absorption coefficient, $h\nu$ is photon energy and B is a constant. Fig 2b shows the band gap energy of both synthesized Ag NPs. The green synthesized Ag NPs had a band gap of 2.92 eV (Fig 2b), which could be attributed to intrinsic Ag band gap absorption and electron transfer from the valence band to the conduction band.

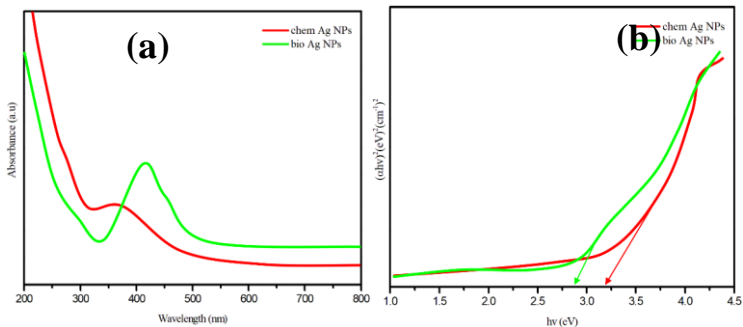


Figure 2 (a) UV-visible (b) band gap energy of the chem and bio-Ag NPs

The present band gap energy very low compared to that the chem Ag NPs ($E_g = 3.23$ eV) and others plant extract (*Mangifera indica* and *Acorus calamus*) use synthesized Ag NPs. The quantum confinement effect causes a shift in the valance band and conduction band, resulting in a lower band gap value observed in bio-Ag NPs. The band gap energy of the green synthesized Ag NPs was in good agreement value with the result published by Thirumagal et al.

3.4 Morphological analysis

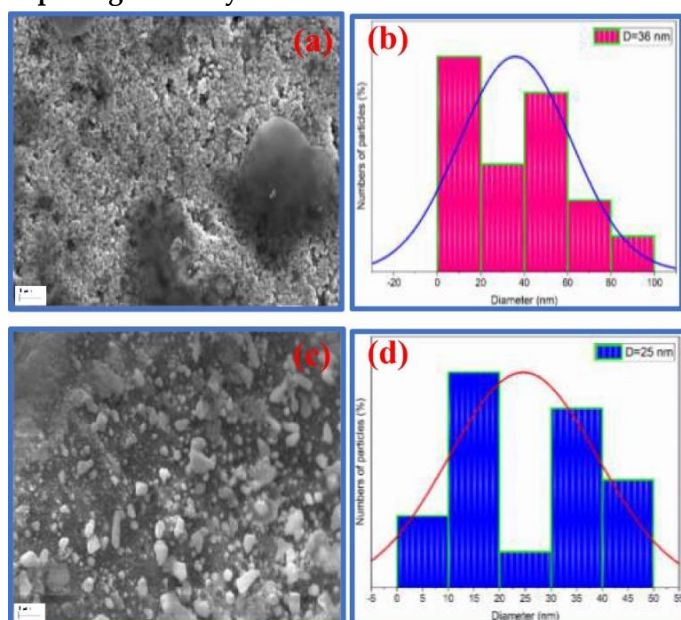


Figure 3 (a,c) SEM image (b,d) particles size of chem and bio Ag NPs

The structure, shape and size of the synthesized nanoparticles were determined using SEM examination. Fig 3 (a, c) shows the SEM images of chem Ag NPs and bio-Ag NPs respectively. The chem Ag NPs show the unique and spherical structure of the Ag NPs. Huge hexagonal arrays of nanoparticles have been formed from spherical bundles. The formation of Ag NPs during the first few minutes of the experiment causes many of the particles to agglomerate and develop in size, which causes many of the particles to agglomerate and grow in size. SEM images showed an average particle size of 36 nm. The strong aggregation of particles may be noticed in Fig 3 (c). Bio Ag NPs

are found to be 25 nm in size on average. From the results, the average particle size of bio-Ag NPs is smaller than that of chem Ag NPs. The presence of flavonoids in the leaf extract may also contribute to this. The flavonoids operate as a stabilising agent as well as a powerful reducing agent, reacting with Ag NPs and significantly lowering their size.

3.5 Functional groups analysis

The FT-IR analysis revealed details about the organic compound's specific molecular environment on the nanoparticles surface. Fig 4 shows the FT-IR spectra of the dried leaf extract of *T. procumbens*, chemically and biosynthesized Ag NPs. The leaf shows absorption peak at 2845.46, 2496.80, 1754.04, 1600.48, 1409.36 and 968.47 cm^{-1} . The peak at 2845.46 and 2496.80 cm^{-1} displays the presence of O-H stretching and methyl or methylene groups. The peak at 1754.04 and 1600.48 cm^{-1} illustrates the presence of carbonyl stretching and C-O functional groups [11]. The peak at 1409.36 cm^{-1} displays the presence of N-H stretching of aromatic benzene. The band about 968.46 cm^{-1} could be related to carboxylic acid stretching or binding [13]. The FT-IR analysis confirms the presence of carboxyl and amide groups in *T. procumbens* leaf extract. The carboxyl functional groups are the most abundant in flavonoids, flavonoids, proteins, alkaloids, phenolic compounds and vitamins [15]. The bio reduction of silver ions into Ag NPs is carried out by these phytochemicals.

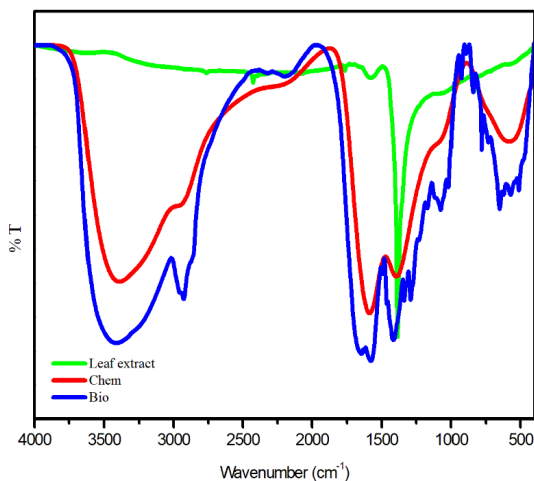


Figure 5 FT-IR spectra of leaf extract, chem and bio-Ag NPs

The FT-IR spectra of chem Ag NPs shows prominent peaks at 3434.68, 2968.04, 2248.71, 1608.40, 1409.56, 1240.86, 943.25 and 641.58 cm^{-1} . The presence of O-H stretching can be seen at the peak of 3434.68 cm^{-1} . The peaks at 2968.04 and 2248.71 cm^{-1} shows the stretching of C-H and C-C, respectively. The peaks in the 1600 to 1400 cm^{-1} range (1409.56 cm^{-1}) are due to the presence of aromatic rings of Ag NPs. The peak at 1240.86 cm^{-1} is due to the OH groups. The peak at 943.25 cm^{-1} due to the aromatic bending vibration of C-H groups. The important peak appeared at 641.58 cm^{-1} due to the Ag-O stretching vibrational mode. A significant broadening of the spectral area is found with bio-Ag NPs. The leaf extract is being affected by an additional peak that occurred around 1657.78 cm^{-1} . The principal reducing agents in leaf extract (flavonoids) could be accountable for the reduction of silver nitrate. The peak, though, does not appear in chemically synthesized Ag NPs and several of the peak positions in bio-Ag NPs are somewhat altered. During biosynthesis, leaf extract interacts with Ag NPs and solvent, causing the shift.

3.7. Antibacterial activities

The bacterial activities of *T. procumbens* leaf extract, chem Ag NPs and bio-Ag NPs for different concentrations was evaluated towards two different groups such as, gram negative (*E. coli*, *P. aeruginosa*) and gram positive (*B. subtilis*, *S. aureus*). The Ag NPs synthesized by biological method showed excellent antimicrobial activities against all tested bacterial strains (table 1). In general, the results showed that the zone of inhibition increased with increase in concentration. The *T. procumbens* leaf extract exhibited the highest inhibition zone at concentration of 100 $\mu\text{g}/\text{mL}$ for *E. coli* (5 mm), *P. aeruginosa* (4 mm), *B. subtilis* (3 mm) and *S. aureus* (2 mm).

Table 1 Antibacterial activity of leaf extract, chem and bio-Ag NPs against human pathogens

Bacteria's	50 μL				100 μL			
	leaf	chem	bio	standard	leaf	chem	bio	standard
<i>Bacillus subtilis</i>	2	4	8	11	3	11	18	25
<i>Staphylococcus aureus</i>	1	5	9	12	2	10	20	25

<i>Pseudomonas aeruginosa</i>	2	4	9	11	4	12	20	25
<i>Escherichia coli</i>	3	5	10	12	5	13	21	26

The chemAg NPs exhibited the highest zone inhibition at concentration at 100 $\mu\text{g}/\text{mL}$ for *E. coli* (13 mm), *P. aeruginosa* (12 mm), *B. subtilis* (11 mm) and *S. aureus* (10 mm). The bioAg NPs exhibited good antibacterial activities against all tested bacteria strains as compared with chemically synthesized Ag NPs at both concentrations. The inhibition zone was observed against *E. coli* (21 mm), *P. aeruginosa* (20 mm), *B. subtilis* (18 mm) and *S. aureus* (20 mm). A particulate drug delivery system's particle size and surface area are well recognised to have a major influence in their interactions with biological cells and the system's in vivo destiny. We hypothesised that the above-mentioned processes may provide bio-Ag NPs enhanced antibacterial activity as compared to chem Ag NPs. In comparison to gram-negative bacteria, the results showed that gram positive bacteria showed better action [16]. It happened because gram negative bacteria have a solid outer membrane and a hydrophobic nature. These results suggest that the use of *T. procumbens* leaf extract mediated green synthesis of Ag-NPs can be more efficient against gram negative bacteria like *E. coli*. Due to their small size and stability, the bio-Ag NPs showed enhanced antibacterial activity in the present study. The smaller nanoparticles have a larger surface area and higher reactivity, which enhances their antibacterial activity compared to chem Ag-NPs. Truong et al reported that the green synthesized Ag NPs with a size 10 nm demonstrated higher inhibitory activities against *S. aureus* and *E. coli* bacteria.

4. CONCLUSION

In summary, Ag NPs were synthesized by chemical and biological methods. The biological methods used to synthesis of Ag NPs is known to be much safer and more environmentally friendly than chemicals synthesis. The optical band gap value is 3.23 eV for chem Ag NPs and 2.92 eV for bios Ag NPs. The surface features are seeming obvious in SEM micrographs, indicating that CuO nanoparticles have been successfully prepared. Using XRD analysis, we calculated the average crystallite size of synthesised particles to be 29 nm for chem Ag NPs and 18 nm for bio-Ag NPs. Furthermore, biologically

synthesised Ag NPs using *T. procumbens* leaf extract showed to be an excellent antibacterial alternative to chemically synthesised materials. This study demonstrated that Ag NPs synthesised using the green method were more effective than Ag NPs synthesised using the chemical method, as well as the possibility of using Ag NPs in combination with antibiotics to prevent fatal diseases caused by pathogenic bacteria.

REFERENCES

1. N. Baig, I. Kammakakam, and W. Falath, Nanomaterials: a review of synthesis methods, properties, recent progress, and challenges, *Adv. Mater.*, (2021) 1821–1871, 2021.
2. S. B. Yaqoob, R. Adnan, R. M. Rameez Khan, and M. Rashid, Gold, Silver, and Palladium Nanoparticles: A Chemical Tool for Biomedical Applications, *Front. Chem.*, 8 (2020)
3. Almatroudi, Silver nanoparticles: synthesis, characterisation and biomedical applications, *Open Life Sci.*, 15 (2020) 819–839.
4. S. Maharjan, K.-S. Liao, A. J. Wang, Z. Zhu, B. P. McElhenny, J. Bao, and S. A. Curran, Sol-gel synthesis of stabilized silver nanoparticles in an organosiloxane matrix and its optical nonlinearity, *Chem. Phys.*, 532 (2020) 110610.
5. S. Özkar and R. G. Finke, Silver Nanoparticles Synthesized by Microwave Heating: A Kinetic and Mechanistic Re-Analysis and Re-Interpretation, *J. Phys. Chem. C*, 121 (2017) 27643–27654.
6. R. D. Rivera-Rangel, M. P. González-Muñoz, M. Avila-Rodriguez, T. A. Razo-Lazcano, and C. Solans, Green synthesis of silver nanoparticles in oil-in-water microemulsion and nano-emulsion using geranium leaf aqueous extract as a reducing agent, *Colloids Surf. A Physicochem. Eng.*, 536 (2018), 60–67.
7. Y. Dasaradhu and M. Arunachalam Srinivasan, Synthesis and characterization of silver nano particles using co-precipitation method, *Mater. Today: Proc.*, 33 (2020) 720–723.
8. A. Wani, S. Khatoon, A. Ganguly, J. Ahmed, A. K. Ganguli, and T. Ahmad, Silver nanoparticles: large scale solvothermal synthesis and optical properties, *Mater. Res. Bull.*, 45 (2010) 1033–1038.
9. D. O. Oseguera-Galindo, R. Machorro-Mejia, N. Bogdanchikova, and J. D. Mota-Morales, Silver nanoparticles synthesized by laser ablation confined in urea choline chloride deep-eutectic solvent, *Colloids Interface Sci. Commun.*, 12 (2016) 1–4.
10. Fernández-Arias, Zimbone, Boutinguiza, Val, Riveiro, Privitera, Grimaldi, and Pou, Synthesis and Deposition of Ag Nanoparticles by

- Combining Laser Ablation and Electrophoretic Deposition Techniques, *Coatings*, 9 (2019), 571.
11. Muthuvel, M. Jothibas, V. Mohana, and C. Manoharan, Green synthesis of cerium oxide nanoparticles using *Calotropis procera* flower extract and their photocatalytic degradation and antibacterial activity, *Inorg Chem Commun*, 119 (2020) 108086.
 12. N. Al-Zaqri, A. Muthuvel, M. Jothibas, A. Alsalmeh, F. A. Alharthi, and V. Mohana, Biosynthesis of zirconium oxide nanoparticles using *Wrightia tinctoria* leaf extract: Characterization, photocatalytic degradation and antibacterial activities, *Inorg Chem Commun*, 127 (2021) 108507.
 13. B. Anandh, A. Muthuvel, and M. Emayavaramban, Bio Synthesis and Characterization of Silver Nanoparticles Using *Lagenaria siceraria* Leaf Extract and their Antibacterial Activity *International Letters of Chemistry, Physics and Astronomy*, 38 (2014) 35–45.
 14. Hemlata, P. R. Meena, A. P. Singh, and K. K. Tejavath, Biosynthesis of Silver Nanoparticles Using *Cucumis prophetarum* Aqueous Leaf Extract and Their Antibacterial and Antiproliferative Activity Against Cancer Cell Lines, *ACS Omega*, 5 (2020) 5520–5528.
 15. M. Vanaja, G. Gnanajobitha, K. Paulkumar, S. Rajeshkumar, C. Malarkodi, and G. Annadurai, Phytosynthesis of silver nanoparticles by *Cissus quadrangularis*: influence of physicochemical factors, *J Nanostructure Chem*, 3 (2013) 1.
 16. Sengottaiyan, A. Aravinthan, C. Sudhakar, K. Selvam, P. Srinivasan, M. Govarthanan, K. Manoharan, and T. Selvankumar, Synthesis and characterization of *Solanum nigrum*-mediated silver nanoparticles and its protective effect on alloxan-induced diabetic rats, *J Nanostructure Chem*, 6 (2015) 41–48.

** Assistant Professor Department of Computer Science,
Theivanai Ammal College for Women, Villupuram*

ABSTRACT

In this project, we undertake a two-phase initiative to enhance examination security using advanced technologies. The first phase focuses on developing an AI-based examination system powered by deep learning techniques. a multichannel convolutional neural network (CNN) systems. This document presents the development of an innovative Emergency Braking System that combines AI and distance sensors to address the critical issue of collision avoidance in vehicles. The system leverages AI algorithms for real-time object detection and distance measurement to make rapid and precise decisions regarding emergency braking. By doing so, it contributes significantly to road safety and accident prevention.

Webcam camera that performs in real-time, and also provides a binary image at high resolution. For training and detection of objects CNN (convolutional neural network) is used for more accuracy. We can detect within seconds using YOLO. Using this we can detect images, create images. Yolo gives better output and taking less speed than others.

Problem statement

Here for the object detection problem is with detection of object in real time is not possible with more objects.so, we need to avoid it. We are worrying about the object classification, for labelling the image, not detecting all things. So, I'm introducing a new process.

Objective

The objective of this project is to design and implement an advanced Emergency Braking System for vehicles that integrates artificial intelligence (AI) and distance sensors. This system aims to enhance vehicle safety by automatically detecting potential collisions and applying emergency braking measures, thereby reducing the risk of accidents, and improving passenger safety.

INTRODUCTION

Examinations and assessments are essential components of education, providing a fair and standardized way to evaluate students' knowledge and skills. To maintain the integrity of examinations, it is imperative to develop innovative solutions

that can effectively detect and prevent fraudulent activities Road traffic accidents continue to be a major concern, and there is a pressing need for advanced safety features in vehicles. The integration of AI and distance sensors in an Emergency Braking System represents a significant technological advancement that has the potential to save lives by preventing collisions. This project introduces a solution that leverages the power of AI and distance sensors to enhance vehicle safer.

DIGITAL IMAGE PROCESSING

The identification of objects in an image and this process would probably start with image processing techniques such as noise removal, followed by (low-level) feature extraction to locate lines, regions and possibly areas with certain textures.

The clever bit is to interpret collections of these shapes as single objects, e.g. cars on a road, boxes on a conveyor belt or cancerous cells on a microscope slide. One reason this is an AI problem is that an object can appear very different when viewed from different angles or under different lighting. Another problem is deciding what features belong to what object and which are background or shadows etc. The human visual system performs these tasks mostly unconsciously but a computer requires skillful programming and lots of processing power to approach human performance. Manipulation of data in the form of an image through several possible techniques. An image is usually interpreted as a two-dimensional array of brightness values, and is most familiarly represented by such patterns as those of a photographic print, slide, television screen, or movie screen. An image can be processed optically or digitally with a computer.

BASICS OF IMAGE PROCESSING

Fundamentals of Digital Image

Image

An image is a two-dimensional picture, which has a similar appearance to some subject, usually a physical object or a person.

Image is a two-dimensional, such as a photograph, screen display, and as well as a three- dimensional, such as a statue. They may be captured by optical devices—such as cameras,

mirrors, lenses, telescopes, microscopes, etc. and natural objects and phenomena, such as the human eye or water.

The word image is also used in the broader sense of any two-dimensional figure such as a map, a graph, a pie chart, or an abstract painting. In this wider sense, images can also be rendered manually, such as by drawing, painting, carving, rendered automatically by printing or computer graphics technology, or developed by a combination of methods, especially in a pseudo-photograph.

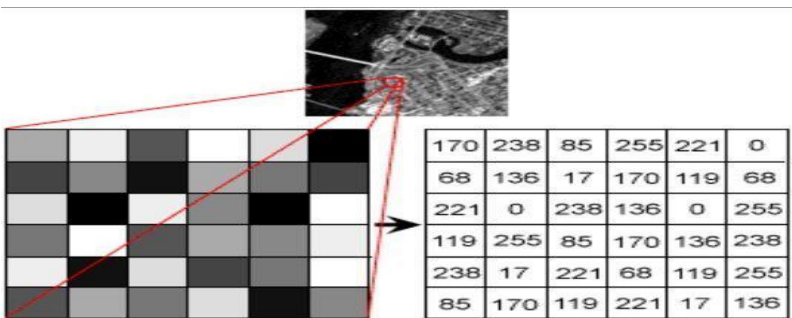
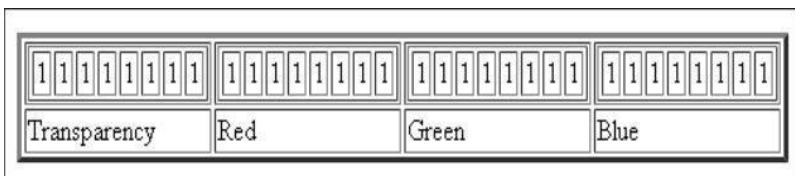


Fig1.1: Gray Scale Image Pixel Value Analysis

Each pixel has a color. The color is a 32-bit integer. The first eight bits determine the redness of the pixel, the next eight bits the greenness, the next eight bits the blueness, and the remaining eight bits the transparency of the pixel.



BIT Transferred for Red, Green and Blue plane (24bit=8bit red;8-bit green;8bit blue)

IMAGE FILE SIZES

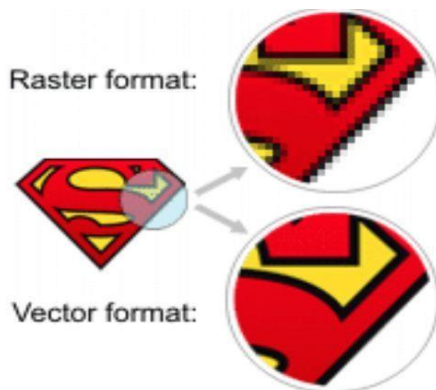
Image file size is expressed as the number of bytes that increases with the number of pixels composing an image, and the color depth of the pixels. The greater the number of rows and columns, the greater the image resolution, and the larger the file. Also, each pixel of an image increases in size when its color depth increases, an 8-bit pixel (1 byte) stores 256 colors, a 24-bit

pixel (3 bytes) stores 16 million colors, the latter known as true color. Image compression uses algorithms to decrease the size of a file. High resolution cameras produce large image files, ranging from hundreds of kilobytes to megabytes, per the camera's resolution and the image- storage format capacity. High resolution digital cameras record 12 megapixel (1MP = 1,000,000 pixels / 1 million) images, or more, in true color. For example, an image recorded by a 12 MP camera; since each pixel uses 3 bytes to record true color, the uncompressed image would occupy 36,000,000 bytes of memory, a great amount of digital storage for one image, given that cameras must record and store many images to be practical. Faced with large file sizes, both within the camera and a storage disc, image file formats were developed to store such large images.

IMAGE FILE FORMATS

Image file formats are standardized means of organizing and storing images. This entry is about digital image formats used to store photographic and other images.

Image files are composed of either pixel or vector (geometric) data that are rasterized to pixels when displayed (with few exceptions) in a vector graphic display. Including proprietary types, there are hundreds of image file types. The PNG, JPEG, and GIF formats are most often used to display images on the Internet.



HORIZONTAL AND VERTICAL PROCESS

In addition to straight image formats, Metafile formats are portable formats which can include both raster and vector

information. The metafile format is an intermediate format. Most Windows applications open metafiles and then save them in their own native form at.

Existing methods

Existing Method: in existing method we used neural network training with less object images with lables.so, the detection of more objects not possible.

- Works poor for multiple moving object detection.
- Single object detection
- Using neural network training we got less number of objects with less data.
- NN
- MOBILENET

Disadvantages

- Accuracy less with training
- Poor detection of objects
- Less objects will detect.
- Not getting proper accuracy result
- It can't work it as a real time video surveillance camera.

Proposed Method

- YOLO object feature comparison and recognition system.
- Deep learning (CNN)
- Pre-process

Advantages

- More objects detection done with yolo
- More accuracy with more gathering features.
- Using yolo object detection is very fast.
- Less time taken for the detection of objects.

Applications

- Face detection.
- Vegetables detection.
- At car accidents.

Algorithm:

- CNN: -

- Convolutional neural network. It is two stage of CNN. Using this we can detect object easily with grid lines for the classification.

Modules used

1. Opencv:-

- Used for object based applications.

2. Numpy:-

- It is used to algebraic, numerical, fourier and matrices etc...
- It is python library.

Software Requirements

- Python idle.
- Open CV modules.

ANALYSIS SYSTEM

Front to rear shunt collisions on straight road. Potentially front to rear shunt collisions on curves on geometry. The safety distance model considers the real-time headway as the safety evaluation parameter and provides the judgment basis for further warning and braking by calculating the safety critical value of the relative distance between the ego and front vehicles. The threshold algorithm includes five main algorithms.

Harware Requirements

- Windows OS PC.
- Minimum 4GB RAM.
- Management NIC
- Traffic Monitoring NIC
- Hard Disk Storage
- Minimum network during light usage
- Cores

AUTONOMOUS BRAKING

The Windows sensor includes an optional local scanning feature that enables static file analysis of applications before they are executed. This feature requires an additional 600MB of disk storage to store signature information and allow for signature updates.

IMAGE PROCESSING

Digital image processing, the manipulation of images by computer, is relatively recent development in terms of man’s ancient fascination with visual stimuli. In its short history, it has been applied to practically every type of images with varying degree of success. The inherent

subjective appeal of pictorial displays attracts perhaps a disproportionate amount of attention from the scientists and also from the layman. Digital image processing like other glamour fields, suffers from myths, mis-connect ions, mis-understandings and mis-information. It is vast umbrella under which fall diverse aspect of optics, electronics, mathematics, photography graphics and computer technology. It is truly multidisciplinary endeavor ploughed with imprecise jargon.

Several factors combine to indicate a lively future for digital image processing. A major factor is the declining cost of computer equipment. Several new technological trends promise to further promote digital image processing. These include parallel processing mode practical by low cost microprocessors, and the use of charge coupled devices (CCDs) for digitizing, storage during processing and display and large low cost of image storage arrays.

Fundamental Steps in Digital Image Processing:

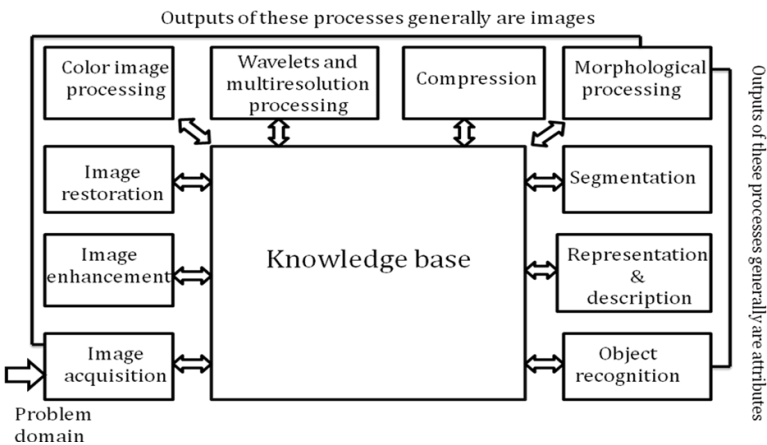


Fig 3.1: Basics steps of image Processing Image Acquisition

Image Acquisition is to acquire a digital image. To do so requires an image sensor and the capability to digitize the signal produced by the sensor. The sensor could be monochrome or color TV camera that produces an entire image of the problem domain every 1/30 sec. the image sensor could also be line scan camera that produces a single image line at a time. In this case, the objects motion past the line.

Scanner produces a two-dimensional image. If the output of the camera or other imaging sensor is not in digital form, an analog to digital converter digitizes it. The nature of the sensor and the image it produces are determined by the application.

Image Enhancement

Image enhancement is among the simplest and most appealing areas of digital image processing. Basically, the idea behind enhancement techniques is to bring out detail that is obscured, or simply to highlight certain features of interesting an image. A familiar example of enhancement is when we increase the contrast of an image because "it looks better." It is important to keep in mind that enhancement is a very subjective area of image processing.

Image restoration

Image restoration is an area that also deals with improving the appearance of an image. However, unlike enhancement, which is subjective, image restoration is objective, in the sense that restoration techniques tend to be based on mathematical or probabilistic models of image degradation.

Enhancement, on the other hand, is based on human subjective preferences regarding what constitutes a "good" enhancement result. For example, contrast stretching is considered an enhancement technique because it is based primarily on the pleasing aspects it might present to the viewer, whereas removal of image blur by applying a deblurring function is considered a restoration technique.

Color image processing

The use of color in image processing is motivated by two principal factors. First, color is a powerful descriptor that often simplifies object identification and extraction from a scene. Second, humans can discern thousands of color shades and

intensities, compared to about only two dozen shades of gray. This second factor is particularly important in manual image analysis. Segmentation.

Segmentation procedures partition an image into its constituent parts or objects. In general, autonomous segmentation is one of the most difficult tasks in digital image processing. A rugged segmentation procedure brings the process a long way toward successful solution of imaging problems that require objects to be identified individually.

On the other hand, weak or erratic segmentation algorithms almost always guarantee eventual failure. In general, the more accurate the segmentation, the more likely recognition is to succeed.

Digital image is defined as a two dimensional function $f(x, y)$, where x and y are spatial (plane) coordinates, and the amplitude off at any pair of coordinates (x, y) is called intensity or grey level of the image at that point. The field of digital image processing refers to processing digital images by means of a digital computer.

The digital image is composed of a finite number of elements, each of which has a particular location and value. The elements are referred to as picture elements, image elements, pels, and pixels. Pixel is the term most widely us.

CLASSIFICATION OF IMAGES

There are 3 types of images used in Digital Image Processing. They are

1. Binary Image
2. Gray Scale Image
3. Color Image.
4. BINARY IMAGE

A binary image is a digital image that has only two possible values for each pixel. Typically, the two colors used for a binary image are black and white though any two colors can be used. The color used for the object(s) in the image is the foreground color while the rest of the image is the background color.

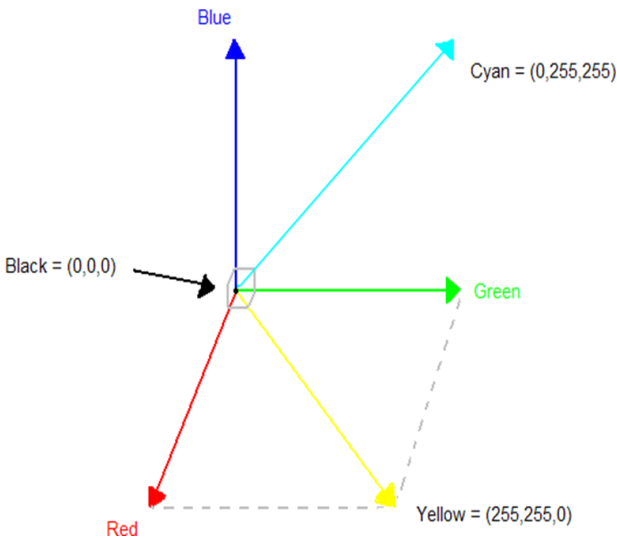
Gray Scale Image

A grayscale Image is digital image is an image in which the value of each pixel is a single sample, that is, it carries only intensity information. Images of this sort, also known as black-and-white, are composed exclusively of shades of gray(0-255), varying from black(0) at the weakest intensity to white(255) at the strongest.

Colour Image

A (digital) color image is a digital image that includes color information for each pixel. Each pixel has a particular value which determines its appearing color. This value is qualified by three numbers giving the decomposition of the color in the three primary colors Red, Green and Blue. Any color visible to human eye can be represented this way. The decomposition of a color in the three primary colors is quantified by a number between 0 and 255. For example, white will be coded as $R = 255, G = 255, B = 255$; black will be known as $(R, G, B) = (0,0,0)$; and say, bright pink will be : $(255,0,255)$

Vector representation of colors in a three dimensions space



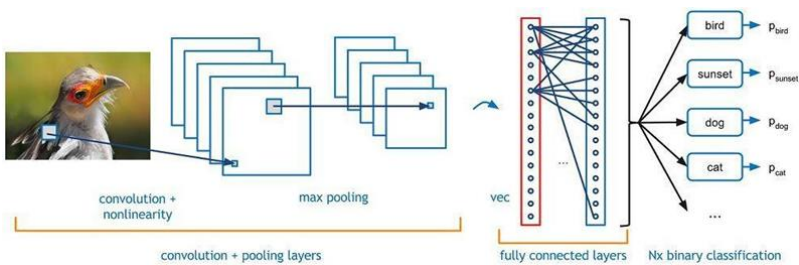
Hue Saturation Process of RGB SCALE Image

From the above figure, colors are coded on three bytes representing their decomposition on the three primary colors. It sounds obvious to a mathematician to immediately interpret colors as vectors in a three-dimension space where each axis stands for one of the primary colors. Therefore we will benefit from most of the geometric mathematical concepts to deal with our colors, such as norms, scalar product, projection, rotation or distance.

CONCLUSION

Convolution Neural Network Introduction

Convolutional neural networks. Sounds like a weird combination of biology and math with a little CS sprinkled in, but these networks have been some of the most influential innovations in the field of computer vision. 2012 was the first year that neural nets grew to prominence as Alex Krizhevsky used them to win that year's ImageNet competition (basically, the annual Olympics of computer vision), dropping the classification error record from 26% to 15%, an astounding improvement at the time. Ever since then, a host of companies have been using deep learning at the core of their services. Facebook uses neural nets for their automatic tagging algorithms, Google for their photo search, Amazon for their product recommendations, Pinterest for their home feed personalization, and Instagram for their search infrastructure.



The Problem Space

Image classification is the task of taking an input image and outputting a class (a cat, dog, etc.) or a probability of classes that best describes the image. For humans, this task of recognition is one of the first skills we learn from the moment we are born and is one that comes naturally and effortlessly as adults. Without

even thinking twice, we're able to quickly and seamlessly identify the environment we are in as well as the objects that surround us.

When we see an image or just when we look at the world around us, most of the time we are able to immediately characterize the scene and give each object a label, all without even consciously noticing. These skills of being able to quickly recognize patterns, generalize from prior knowledge, and adapt to different image environments are ones that we do not share with our fellow machines

Inputs and Outputs

When a computer sees an image (takes an image as input), it will see an array of pixel values. Depending on the resolution and size of the image, it will see a $32 \times 32 \times 3$ array of numbers (The 3 refers to RGB values). Just to drive home the point, let's say we have a color image in JPG form and its size is 480×480 . The representative array will be $480 \times 480 \times 3$. Each of these numbers is given a value from 0 to 255 which describes the pixel intensity at that point. These numbers, while meaningless to us when we perform image classification, are the only inputs available to the computer. The idea is that you give the computer this array of numbers and it will output numbers that describe the probability of the image being a certain class (.80 for cat, .15 for dog, .05 for bird, etc).

What We Want the Computer to Do

Now that we know the problem as well as the inputs and outputs, let's think about how to approach this. What we want the computer to do is to be able to differentiate between all the images it's given and figure out the unique features that make a dog a dog or that make a cat a cat. This is the process that goes on in our minds subconsciously as well. When we look at a picture of a dog, we can classify it as such if the picture has identifiable features such as paws or 4 legs.

In a similar way, the computer is able to perform image classification by looking for low level features such as edges and curves, and then building up to more abstract concepts through a series of convolutional layers. This is a general overview of what a CNN does. Let's get into the specifics.

Structure

Back to the specifics. A more detailed overview of what CNNs do would be that you take the image, pass it through a series of convolutional, nonlinear, pooling (down sampling), and fully connected layers, and get an output. As we said earlier, the output can be a single class or a probability of classes that best describes the image. Now, the hard part is understanding what each of these layers do. So let's get into the most important one.

First Layer - Math Part

The first layer in a CNN is always a Convolutional Layer. First thing to make sure you remember is what the input to this conv (I'll be using that abbreviation a lot) layer is. Like we mentioned before, the input is a $32 \times 32 \times 3$ array of pixel values. Now, the best way to explain a conv layer is to imagine a flashlight that is shining over the top left of the image. Let's say that the light this flashlight shines covers a 5×5 area. And now, let's imagine this flashlight sliding across all the areas of the input image.

In machine learning terms, this flashlight is called a filter (or sometimes referred to as a neuron or a kernel) and the region that it is shining over is called the receptive field. Now this filter is also an array of numbers (the numbers are called weights or parameters). A very important note is that the depth of this filter has to be the same as the depth of the input (this makes sure that the math works out), so the dimensions of this filter is $5 \times 5 \times 3$. Now, let's take the first position the filter is in for example. It would be the top left corner. As the filter is sliding, or convolving, around the input image, it is multiplying the values in the filter with the original pixel values of the image (aka computing element wise multiplications).

These multiplications are all summed up (mathematically speaking, this would be 75 multiplications in total). So now you have a single number. Remember, this number is just representative of when the filter is at the top left of the image. Now, we repeat this process for every location on the input volume. (Next step would be moving the filter to the right by 1 unit, then right again by 1, and so on). Every unique location on the input volume produces a number. After sliding the filter over all the locations, you will find out that what you're left with

is a $28 \times 28 \times 1$ array of numbers, which we call an activation map or feature map. The reason you get a 28×28 array is that there are 784 different locations that a 5×5 filter can fit on a 32×32 input image. These 784 numbers are mapped to a 28×28 array

First Layer - High Level Perspective

However, let's talk about what this convolution is actually doing from a high level. Each of these filters can be thought of as feature identifiers. When I say features, I'm talking about things like straight edges, simple colors, and curves. Think about the simplest characteristics that all images have in common with each other. Let's say our first filter is $7 \times 7 \times 3$ and is going to be a curve detector. (In this section, let's ignore the fact that the filter is 3 units deep and only consider the top depth slice of the filter and the image, for simplicity.)

As a curve detector, the filter will have a pixel structure in which there will be higher numerical values along the area that is a shape of a curve (Remember, these filters that we're talking about as just numbers!).

Introduction to Computer Vision

Using software to parse the world's visual content is as big of a revolution in computing as mobile was 10 years ago, and will provide a major edge for developers and businesses to build amazing products.

Computer Vision is the process of using machines to understand and analyze imagery (both photos and videos). While these types of algorithms have been around in various forms since the 1960's, recent advances in Machine Learning, as well as leaps forward in data storage, computing capabilities, and cheap high-quality input devices, have driven major improvements in how well our software can explore this kind of content.

REFERENCES

1. K. Lee and D. Kum, "Collision avoidance/mitigation system: Motion planning of autonomous vehicle via predictive occupancy map", *IEEE Access*, vol. 7, pp. 52846-52857, 2019.
2. NHTSA announces 2020 update on AEB installation by 20 automakers", Dec. 2020, [online] Available: <https://www.nhtsa.gov/press-releases/aeb-installation-update-2020>.

3. M. Park, S. Lee, C. Kwon and S. Kim, "Design of pedestrian target selection with funnel map for pedestrian AEB system", *IEEE Trans. Veh. Technol.*, vol. 66, no. 5, pp. 3597-3609, May 2017.
4. D. Lee, S. Kim, C. Kim and K. Huh, "Development of an autonomous braking system using the predicted stopping distance", *Int. J. Automot. Technol.*, vol. 15, no. 2, pp. 341-346, 2014.
5. S. Sim, "Camera device for vehicle", Oct. 2019.
6. Z. Zhang, R. Ma, L. Wang and J. Zhang, "Novel PMSM control for anti-lock braking considering transmission properties of the electric vehicle", *IEEE Trans. Veh. Technol.*, vol. 67, no. 11, pp. 10378-10386, Nov. 2018.
7. J. Lee et al., "Modeling of conducted EMI with current probe method for a motor-drive braking system", *Proc. IEEE Int. Symp. Electromagn. Compat.-EMC EUROPE*, Sep. 2017.
8. J. Lee et al., "Modeling of transfer impedance in automotive BCI test system with closed-loop method", *IEICE Trans. Commun.*, vol. E103-B, no. 4, pp. 405-414, 2020.
9. C. Jensen, "Toyota recalling 1 million vehicles for air bag and wiper problems", Jan. 2013, [online] Available: <https://wheels.blogs.nytimes.com/2013/01/30/toyota-recalling-1-million-vehicles-for-air-bag-and-wiper-problems/>.
10. Collision of two Washington metropolitan area transit authority metrorail trains near Fort Totten station", Jun. 2009, [online] Available: <https://www.washingtonpost.com/wp-srv/metro/documents/2009redlinecrashreport.pdf>
11. J. Lee, J. Song, D. Kim, J. Kim, Y. Kim and S. Jung, "Particle swarm optimization algorithm with intelligent particle number control for optimal design of electric machines", *IEEE Trans. Ind. Electron.*, vol. 65, no. 2, pp. 1791-1798, Feb. 2018.
12. B. Nguyen, B. Xue, P. Andreae and M. Zhang, "A new binary particle swarm optimization approach: Momentum and dynamic balance between exploration and exploitation", *IEEE Trans. Cybern.*, vol. 51, no. 2, pp. 589-603, Feb. 2019.

Ms. S. Farjana*, M. Monisha** & S. Karthiga**

* Assistant Professor, PG and Research, Department of Mathematics,
Theivanai Ammal College for women (Autonomous),
Villupuram, Tamilnadu

** M.sc Mathematics., PG and Research, Department of Mathematics,
Theivanai Ammal College for women (Autonomous),
Villupuram, Tamilnadu

ABSTRACT

In this paper, Reverse order octagonal fuzzy numbers are proposes a game theoretic model for solving allocation problem with two players and two resources. The model is solved using reverse order octagonal fuzzy number. Octagonal fuzzy number is capable of representing the uncertainty of the decision variable in a more accurate way. The result of the study show that proposed model can efficiently solve the resource allocation problem.

keywords: Fuzzy Numbers, Octagonal Fuzzy Numbers, Reverse Order Octagonal Fuzzy Number, Fuzzy Game Problem, Crisp Value, Fuzzy Ranking.

INTRODUCTION

Game theory is a branch of mathematics that is concerned with the analysis of strategic decision making. It has application in fields as divers as economics, politicalscience, and psychology, among others. One way to represent the preferences of decision-makers in game theory is through the use of fuzzy numbers, which allow for the expression of imprecision and uncertainty in decision-making.

Game theory is the study of mathematical models of strategic interactions among rational agents. It has applications in many fields of social science, used extensively in economics as well as in logic, systems science and computer science.

In recent years, there has been growing interest in the use of reverse order octagonal fuzzy numbers (ROOFNs) for the representation of preferences in game theory. ROOFNs are a type of fuzzy number that is particularly well-suited to the

representation of complex decision-making scenarios, such as those that arise in strategic games.

One of the key advantages of using ROOFNs in game theory is that they allow for a more nuanced and sophisticated analysis of decision-making. By capturing the imprecision and uncertainty inherent in decision-making, ROOFNs enable decision-makers to better understand the potential outcomes of different strategies and to make more informed decisions as a result.

The idea of game theory is to define an abstract framework to reason about how multiple agents should interact in an environment following a set of abstract rules. Because this theory is about the construction of this framework and not about solving potential real-world problems, it is by itself pure mathematics.

The usage of ROOFNs in game theory represents an exciting development in the field, and holds great promise for advancing our understanding strategic decision-making in a wide range of contexts.

2. PRELIMINARIES

2.1 Fuzzy set

Let $X = \{x\}$ denote a collection of objects denoted generically by x . Then a fuzzy set A in X is a set of ordered pairs ${}^\circ A = \{(x, \mu^{\circ}A(x)); x \in X\}$ where $\mu^{\circ}A(x)$ is termed as the grade of membership Space.

2.2 Normal set

A fuzzy set of universe set X is normal iff $x \in X \sup \mu^{\circ}A(x) = 1$

2.3 Convex set

A fuzzy set ${}^\circ A$ in universal set X is called convex if and only if

$$\mu^{\circ}A(x_1\lambda + (1 - \lambda)x_2) \geq \min [\mu^{\circ}A(x_1), \mu^{\circ}A(x_2)] \quad \forall x_1, x_2 \in X \text{ and } \lambda \in [0, 1].$$

2.4 Fuzzy Numbers

A Fuzzy number is a fuzzy set on the real line R , must satisfy the following conditions.

- (i) $\mu^{\circ}A(x)$ is piecewise continuous.
- (ii) There exists atleast $x \in R$ with $\mu^{\circ}A(x) = 1$
- (iii) ${}^\circ A$ must be convex and normal.

3. OCTAGONAL FUZZY NUMBERS

Fuzzy number \tilde{A}_0 is a octogonal fuzzy number denoted by $\tilde{A}_0(a_1, a_2, a_3, a_4, a_5, a_6, a_7, a_8)$ where $(a_1, a_2, a_3, a_4, a_5, a_6, a_7, a_8)$ are real numbers and its membership function $\mu_{\tilde{A}_0}(x)$ is given below

$$\mu_{\tilde{A}_0}(x) = \begin{cases} 0 & \text{for } x < a_1 \\ \frac{1(x - a_1)}{3(a_2 - a_1)} & \text{for } a_1 \leq x \leq a_2 \\ \frac{1}{3} + \frac{1(x - a_2)}{3(a_3 - a_2)} & \text{for } a_2 \leq x \leq a_3 \\ \frac{2}{3} + \frac{1(x - a_3)}{3(a_4 - a_3)} & \text{for } a_3 \leq x \leq a_4 \\ 1 & \text{for } a_4 \leq x \leq a_5 \\ 1 - \frac{1(x - a_5)}{3(a_6 - a_5)} & \text{for } a_5 \leq x \leq a_6 \\ \frac{2}{3} - \frac{1(x - a_6)}{3(a_7 - a_6)} & \text{for } a_6 \leq x \leq a_7 \\ \frac{1(a_8 - x)}{3(a_8 - a_7)} & \text{for } a_7 \leq x \leq a_8 \\ 0 & \text{otherwise} \end{cases}$$

4. REVERSE ORDER OCTAGONAL FUZZY NUMBERS

A fuzzy number \tilde{A}_0 is a reverse order octagonal Fuzzy Number denoted by \tilde{A}_0

$(-a_1, -a_2, -a_3, -a_4, a_5, a_6, a_7, a_8)$ where $(-a_1, -a_2, -a_3, -a_4, a_5, a_6, a_7, a_8)$ are real number and its memberships function $\mu_{\tilde{A}_0}(x)$.

5. RANKING OF OCTAGONAL FUZZY NUMBERS

A number of approaches have been proposed for the ranking of fuzzy numbers. $\tilde{A}_0(a_1, a_2, a_3, a_4, a_5, a_6, a_7, a_8)$, a ranking method is derived based on the following formula.

$$R(\tilde{A}_0) = \left(\frac{2a_1 + 3a_2 + 4a_3 + 5a_4 + 5a_5 + 4a_6 + 3a_7 + 2a_8}{18} \right) \left(\frac{5}{18} \right)$$

6. MATHEMATICAL FORMULATION OF FUZZY GAME PROBLEM

Illustrate two-person zero-sum game in which all the entries in the payoff matrix are Icosidodecahedron fuzzy numbers. Let the player P has 'i' strategies and player Q has 'j' strategies. Here it is simulated that each player has to choose from amongst the pure

strategies. Player P is always assumed to be winner and player Q is always assumed to be loser. The payoff ixj is

$$P = \begin{vmatrix} p_{11} & p_{12} & \dots & p_{1i} \\ p_{21} & p_{22} & \dots & p_{2i} \\ \vdots & & & \\ \vdots & & & \\ p_{j1} & p_{j2} & \dots & p_{ji} \end{vmatrix}$$

7. ALGORITHM FOR SOLVING A GAME PROBLEM USING FUZZY

Step1: First, we have to examine whether a saddle point will exist or not. If it exist in the given problem, then we need to find it in a direct way. However, if it does not exist, then we need to follow the second step.

Step2: compare column strategies.

- I. In the given pay-off matrix, if the element of column $A \leq$ elements of Column B, that is, Column A strategy will fully dominate over column B strategy, then according to the rule we need to delete column B strategy from the given pay-off matrix.
- II. In the given pay-off matrix, we tally each column strategy with all other column strategies and omit high strategies as far as possible.

Step3: compare row strategies.

- I. In the given pay-off matrix, if the elements of Row $A \geq$ elements of Row B, Row A strategy will dominate over Row B strategy. So, omit Row B strategy from the given payoff matrix.
- II. In the all possible row strategies and omit low strategies given pay-off matrix, we tally each row strategy with as far as possible.
- III. The game may decrease to a single cell giving an order about the value of the game and optimal master plan of the players. If not, then moves to step4.

Step4: The dominance rule should not be based on the dominance of pure strategies only. A given approach can be dominated if it gives us a poor result to an usual of two or more other pure master plan.

7.1 Saddle point

If in a game, the max-min value equals the mini-max value, then game is said to have a saddle point and the corresponding strategies which give the saddle point are called optimal strategies.

The amount of payoff at an equilibrium point is called the crisp game value of the game matrix. Solution of all $i \times j$ Matrix Game [14] consider the general game matrix $P = [p_{ij}]$.

To solve this game we proceed as follows:

- Test for a saddle point
- If there is no saddle point, solve by finding equalizing strategies.

The optimal mixed strategies for player

A = $(p_1; p_2; p_3)$ and for player B = $(q_1; q_2; q_3)$, where

$$p_1 = \left(\frac{p_{22} - p_{12}}{(p_{11} + p_{22}) - (p_{12} + p_{21})} \right), p_2 = 1 - p_1$$

$$q_1 = \left(\frac{p_{22} - p_{12}}{(p_{11} + p_{22}) - (p_{12} + p_{21})} \right), q_2 = 1 - q_1$$

$$V = \left(\frac{(p_{11} \times p_{22}) - (p_{12} \times p_{21})}{(p_{11} + p_{22}) - (p_{12} + p_{21})} \right)$$

Example 1: Consider the following Reverse Order octagonal fuzzy game problem.

Player B

Player A	$(-9, -7, -6, -5, 5, 12, 9, 8)$	$(-10, -8, -7, -4, 14, 17, 18, 10)$	$(-11, -9, -8, -17, 18, 9, 15, 14)$
	$(-5, -4, -2, -4, 5, 13, 2, 1)$	$(-4, -5, -3, -2, 1, 8, 9, 2)$	$(-1, -3, -10, -15, 8, 19, 17, 8)$
	$(-6, -8, -15, -12, 9, 15, 16, 17)$	$(-1, -10, -14, -12, 10, 11, 13, 12)$	$(-15, -13, -10, -5, 8, 7, 6, 7)$

Solution : By the definition of Reverse Order octagonal fuzzy number $^{\circ}A(x)$ is calculated as

Step 1: Convert the reverse order octagonal fuzzy problem into a crisp value problem

$a_{11} = (-9, -7, -6, -5, 5, 12, 9, 8)$	$R(a_{11}) = \frac{(2(-9)+3(-7)+4(-6)+5(-5)+5(5)+4(12)+3(9)+2(8))}{18} \left(\frac{5}{18}\right) = 0.3240$
$a_{12} = (-10, -8, -7, -4, 14, 17, 18, 10)$	$R(a_{12}) = \frac{(2(-10)+3(-8)+4(-7)+5(-4)+5(18)+4(17)+3(18)+2(10))}{18} \left(\frac{5}{18}\right) = 0.8796$
$a_{13} = (-11, -9, -8, -17, 18, 9, 15, 14)$	$R(a_{13}) = \frac{(2(-11)+3(-9)+4(-8)+5(-17)+5(18)+4(9)+3(5)+2(4))}{18} \left(\frac{5}{18}\right) = 0.5092$
$a_{21} = (-3, -4, -2, -4, 5, 13, 2, 1)$	$R(a_{21}) = \frac{(2(-3)+3(-4)+4(-2)+5(-4)+5(5)+4(13)+3(2)+2(1))}{18} \left(\frac{5}{18}\right) = 0.3240$
$a_{22} = (-4, -5, -3, -2, 1, 8, 9, 1)$	$R(a_{22}) = \frac{(2(-4)+3(-5)+4(-3)+5(-2)+5(1)+4(8)+3(9)+2(1))}{18} \left(\frac{5}{18}\right) = 0.3240$
$a_{23} = (-1, -3, -10, -15, 8, 19, 17, 8)$	$R(a_{23}) = \frac{(2(-1)+3(-3)+4(-10)+5(-15)+5(8)+4(19)+3(17)+2(8))}{18} \left(\frac{5}{18}\right) = 0.8796$
$a_{31} = (-6, -8, -15, -12, 9, 15, 16, 17)$	$R(a_{31}) = \frac{(2(-6)+3(-8)+4(-15)+5(-12)+5(9)+4(15)+3(16)+2(7))}{18} \left(\frac{5}{18}\right) = 0.4629$
$a_{32} = (-1, -10, -14, -12, 10, 11, 13, 11, 2)$	$R(a_{32}) = \frac{(2(-1)+3(-10)+4(-14)+5(-12)+5(10)+4(11)+3(13)+2(12))}{18} \left(\frac{5}{18}\right) = 0.1388$
$a_{33} = (-15, -13, -10, -5, 8, 7, 6, 7)$	$R(a_{33}) = \frac{(2(-15)+3(-13)+4(-10)+5(-5)+5(8)+4(7)+3(6)+2(7))}{18} \left(\frac{5}{18}\right) = 0.2469$

Step2: The pay-off matrix

Player B

Player A $\begin{pmatrix} 0.3240 & 2.4691 & 0.5092 \\ 0.5401 & 0.3240 & 0.8796 \\ 0.4629 & 0.1388 & 0.2469 \end{pmatrix}$

Step 3: There is no saddle point since Max(mini)is not equal to Min (Max).

Step4: Using dominance the pay-off matrix

Player B

Player A $\begin{pmatrix} 0.3240 & 2.4691 & 0.5092 \\ 0.5401 & 0.3240 & 0.8796 \\ 0.4629 & 0.1388 & 0.2469 \end{pmatrix}$

Step5: The required pay-off matrix becomes

Player B

Player A $\begin{pmatrix} 0.3240 & 2.4641 \\ 0.5401 & 0.3240 \end{pmatrix}$

Here $p_{11} = 0.3240$, $p_{12} = 2.4641$, $p_{21} = 0.5401$ and $p_{22} = 0.3240$

$q_1 = 0.9082$, $q_2 = 0.0918$ and $q_1 = 0.9082$, $q_2 = 0.0918$

$V = 0.52$

Example 2: Consider the following Reverse Order octogonal fuzzy game problem.

Player B

$$\text{Player A} \left(\begin{matrix} (-7, -5, -4, -2, 12, 10, 8, 7) & (-2, -4, -18, -9, 30, 18, 2, 5) & (-8, -18, -10, -2, 18, 19, 15, 14) \\ (-15, -2, -4, -8, 15, 16, 7, 9) & (-13, -5, -3, -9, 11, 13, 15, 12) & (-11, -9, -8, -12, 17, 15, 16, 12) \\ (-16, -2, -8, -5, 8, 2, 12, 18) & (-13, -10, -11, -2, 18, 19, 15, 5) & (-10, -5, -4, -3, 14, 5, 12, 11) \end{matrix} \right)$$

Solution: By the definition of Reverse Order octogonal fuzzy number $^{\circ}A(x)$ is calculated as

Step 1: Convert the reverse order octogonal fuzzy problem into a crisp value problem

$a_{11} = (-7, -5, -4, -2, 12, 10, 8, 7)$	$R(a_{11}) = \frac{(2(-7)+3(-5)+4(-4)+5(-2)+5(12)+4(10)+3(8)+2(7)) \left(\frac{5}{18}\right)}{18} = 1.2800$
$a_{12} = (-2, -4, -18, -9, 30, 18, 2, 5)$	$R(a_{12}) = \frac{(2(-2)+3(-4)+4(-18)+5(-9)+5(30)+4(18)+3(2)+2(5)) \left(\frac{5}{18}\right)}{18} = 1.6203$
$a_{13} = (-8, -18, -10, -2, 18, 19, 15, 14)$	$R(a_{13}) = \frac{(2(-8)+3(-18)+4(-10)+5(-2)+5(18)+4(19)+3(15)+2(14)) \left(\frac{5}{18}\right)}{18} = 1.8364$
$a_{21} = (-15, -2, -4, -8, 15, 16, 7, 9)$	$R(a_{21}) = \frac{(2(-15)+3(-2)+4(-4)+5(-8)+5(15)+4(16)+3(7)+2(9)) \left(\frac{5}{18}\right)}{18} = 1.3271$
$a_{22} = (-13, -5, -3, -9, 11, 13, 15, 12)$	$R(a_{22}) = \frac{(2(-13)+3(-5)+4(-3)+5(-9)+5(11)+4(13)+3(15)+2(12)) \left(\frac{5}{18}\right)}{18} = 1.4043$
$a_{23} = (-11, -9, -8, -12, 17, 15, 16, 12)$	$R(a_{23}) = \frac{(2(-11)+3(-9)+4(-8)+5(-12)+5(17)+4(15)+3(16)+2(12)) \left(\frac{5}{18}\right)}{18} = 1.1728$
$a_{31} = (-16, -2, -8, -5, 8, 2, 12, 18)$	$R(a_{31}) = \frac{(2(-16)+3(-2)+4(-8)+5(-5)+5(8)+4(2)+3(12)+2(18)) \left(\frac{5}{18}\right)}{18} = 1.0030$
$a_{32} = (-13, -10, -11, -2, 18, 19, 15, 5)$	$R(a_{32}) = \frac{(2(-13)+3(-10)+4(-11)+5(-2)+5(18)+4(19)+3(15)+2(5)) \left(\frac{5}{18}\right)}{18} = 1.7129$
$a_{33} = (-10, -5, -4, -3, 14, 5, 12, 11)$	$R(a_{33}) = \frac{(2(-10)+3(-5)+4(-4)+5(-3)+5(14)+4(5)+3(12)+2(11)) \left(\frac{5}{18}\right)}{18} = 1.2654$

Step2: The pay-off matrix

Player B

$$\text{Player A} \begin{pmatrix} 1.2800 & 1.6203 & 1.8364 \\ 1.3271 & 1.4043 & 1.1728 \\ 1.0030 & 1.7129 & 1.2654 \end{pmatrix}$$

Step 3: There is no saddle point since Max(mini)is not equal to Min (Max).

Step4: Using dominance the pay-off matrix

Player B

$$\text{Player A} \begin{pmatrix} 1.2800 & 1.6203 & 1.8364 \\ 1.3271 & 1.4043 & 1.1728 \\ 1.0030 & 1.7129 & 1.2654 \end{pmatrix}$$

Step5: The required pay-off matrix becomes

Player B

Player A $\begin{pmatrix} 1.2800 & 1.8364 \\ 1.3271 & 1.1728 \end{pmatrix}$

Here $p_{11} = 1.2800$, $p_{12} = 1.8364$, $p_{21} = 1.3271$ and $p_{22} = 1.1728$

$p_1 = 0.9337$, $p_2 = 0.06$ and $q_1 = 0.9337$, $q_2 = 0.06$

$V = 1.31$

CONCLUSION

The reverse order octagonal fuzzy numbers has emerged as a novel approach for solving game theory problems. This method offers the potential to represent and handle uncertain or imprecise information in a game theory setting, leading to improved decision-making. However, the effectiveness of this approach may vary depending on the specific problem and data quality. Further research is required to explore the full potential and limitations of reverse order octagonal fuzzy numbers in game theory.

REFERENCES

1. R. Gajalakshmi, G. Charles Rabinson "Solving Game Theory Using Reverse Order Pentagonal Fuzzy Number", Journal of algebraic statistics, Volume 13, No. 3, 2022, p. 1785-1790 .
2. Pathinathan. T and Ponnivalavan.K., 2015, "Reverse order Triangular, Trapezoidal and Pentagonal Fuzzy Numbers", Annals of Pure and Applied Mathematics, Vol. 9, No. 1, 2015, 107-117.
3. Rajarajeswari. P, Sahaya Sudha. A "Ranking of Hexagonal Fuzzy Numbers for Solving Multi Objective Fuzzy Linear Programming Problem", International Journal of Computer Applications, Volume 84 - No 8, December 2013.
4. J. Jon Arockiaraj and N. Sivasankari, "Solution of Fuzzy Game Problem Using Hexagonal Fuzzy Numbers", International Journal of Mathematics And its Applications", Volume 4, Issue 4(2016) 381-387.
5. Rajarajeswari.P and SahayaSudha A and Karthika.R, "A new Operations on hexagonal fuzzynumber" International Journal of Fuzzy Logic Systems (IJFLS) Vol.3, No3, July 2013.
6. S.H Nasserri, "A new method for solving fuzzy linear programming by solving linear programming". Applied Mathematical Sciences, 2 (2008), 37-46.

7. HakanSonerAplak and OrhanTurkbey, 2013, "Fuzzy logic based game theory applications in multi-criteria decision making process", Journal of Intelligent & Fuzzy Systems 25: 359-371.

A Theoretical Perspective on Degradation of Fluorinated Hydrocarbons in the Atmosphere

G. Manonmani*, D. Ranjith Kumar** & M. Gnanaprakasam***

* Sravathi Artificial Intelligence Technology Pvt. Ltd, Bangalore

** School of Chemical Engineering, Yeungnam University, Gyeongsan, Korea

*** PG & Research Department of Physics, Theivanai Ammal College for Women (Autonomous), Villupuram

ABSTRACT

Chemical reactions involve the conversion of one low-energy compound into another, potentially including intermediates and transition states. Understanding atmospheric chemical reactions is crucial for comprehending the degradation of pollutants and their environmental impact. Given the complex nature of these reactions, a combination of experimental and theoretical methods is essential for thorough characterization. The main goal of theoretical modelling is to identify stationary points on the potential energy surface of a reaction complex. Chlorofluorocarbon (CFC) compounds have caused substantial harm to the ozone layer. Over the years, CFCs, widely used as refrigerants and aerosol can propellants, released millions of tons into the atmosphere. Due to their volatility and resistance to chemical reactions, CFCs persist in the atmosphere, reaching the upper troposphere and infiltrating the stratosphere. In response, manufacturing companies have successfully identified alternatives, such as hydrochlorofluorocarbons (HCFCs) and hydrofluorocarbons (HFCs). HCFCs are hydrocarbons where some hydrogen atoms are substituted with chlorine or fluorine, while HFCs lack chlorine. The C-H bonds in HCFCs and HFCs act as "handles," enabling additional chemical reactions in the troposphere, leading to their faster degradation and removal before reaching the stratosphere. Despite the extensive use of halogenated hydrocarbons in various applications, international legislation has phased out the production and use of halofluorocarbons, bromofluorocarbons (halons), and CFCs. This measure was implemented due to the recognized threat posed by these substances to the Earth's ozone layer.

1. INTRODUCTION:

In the troposphere, the primary location for chemical reactions, volatile organic compounds (VOCs)¹ and radicals play crucial

roles. The key classes of VOCs encompass alkanes, alkenes, aromatic hydrocarbons, and oxygenated VOCs. Various chemical processes, including photolysis, reactions with hydroxyl radicals in daylight, reactions with nitrate radicals during evening and night hours, and interactions with ozone (O_3) as well as chlorine (Cl) atoms in coastal and marine regions, transform these VOCs.^{2, 3, 4} Fluorinated compounds exhibit environmental persistence and have been shown to bioaccumulate, contributing significantly to climate change. Nevertheless, various measures have contributed to a reduction in the climate impact of halocarbons. Hydrofluoroethers (HFEs), among other halocarbons, serve as substitutes for ozone-depleting chemicals in refrigeration and air conditioning systems.⁵ The implementation of improved leakage rates, as mandated by the United States Environmental Protection Agency, represents one of the straightforward approaches to lowering atmospheric concentrations of these chemicals.⁶

A chlorofluorocarbon (CFC) consists of volatile derivatives of methane and ethane in combination with halogenated elements like chlorine and fluorine. Hence, the common formulae of CFCs can be expressed as CCl_nF_{4-n} and $C_2Cl_nF_{6-n}$ with non-zero value of 'n' (Table 1). The fact that the use of CFCs would lead to the destruction of atmospheric ozone was predicted as early as in 1974.⁷ The chemical stability of CFCs allows them to gradually diffuse and be transported from the lower atmosphere (i.e., troposphere) to the stratosphere. Their photolysis releases chlorine atoms which then participate in a series of reactions, the ClO_x catalytic cycle, which leads to the catalytic destruction of ozone. Overall, these chain reactions are identified to play key roles in the destruction of stratospheric ozone.^{7, 8, 9, 10} In such reactions, one chlorine atom can destroy several thousand ozone molecules in the stratosphere.^{11, 12} Besides their role in ozone destruction, the release of CFCs has other important implications for the global environment

Order	Full name	Acronym
<i>A. CFCs and CCl₄</i>		
1	Trichlorofluoromethane	CFC-11
2	Dichlorodifluoromethane	CFC-12
3	1,1,2-Trichloro-1,2,2-trifluoroethane	CFC-113
4	1,2-Dichloro-1,1,2,2,-tetrafluoroethane	CFC-114
5	Chloropentafluoroethane	CFC-115
6	Carbon tetrachloride	CCl ₄
<i>B. HCFCs</i>		
7	Monochlorodifluoromethane	HCFC-22
8	Dichlorotrifluoroethane	HCFC-123
9	Monochlorotetrafluoroethane	HCFC-124
10	Dichlorofluoroethane	HCFC-141b
11	Monochlorodifluoroethane	HCFC-142b
12	Dichloropentafluoropropane	HCFC-225ca
13	Dichloropentafluoropropane	HCFC-225cb
<i>C. HFCs</i>		
14	Trifluoromethane	HFC-23
15	Difluoromethane	HFC-32
16	Pentafluoroethane	HFC-125
17	1,1,1,2-tetrafluoroethane	HFC-134a
18	1,1,1-trifluoroethan	HFC-143a
19	1,1-difluoroethane	HFC-152a
20	1,1,1,2,3,3,3-heptafluoropropane	HFC-227ea
21	1,1,1,3,3,3-hexafluoropropane	HFC-236fa
22	1,1,1,3,3-pentafluoropropane	HFC-245fa
23	1,1,2,2,3-pentafluoropropane	HFC-245ca
24	1,1,1,2,3-pentafluoropropane	HFC-245eb
25	1,1,1,3,3-pentafluorobutane	HFC-365mfc
26	1,1,1,2,2,3,4,5,5,5-decafluoro-pentan	HFC-4310mee

Table 1: Common CFCs and related compounds

due to their effects on the absorption of infrared radiation (IR) from the surface of the earth.¹³⁻¹⁶ such, their contribution to the man-made greenhouse effect is estimated to be about 20%, while those by common greenhouse gases (CO₂, CH₄, N₂O, and tropospheric ozone) are estimated to be 50, 15, 5, and 7%, respectively.¹⁷

The concentration of chlorofluorocarbons (CFCs) in the atmosphere increased rapidly in four decades since their introduction in 1930s. The rise in atmospheric chlorine levels caused by CFC emissions has however been designated as the main cause of the Antarctic ozone 'hole' in the late 1970s as well as depletion of ozone over parts of the Northern Hemisphere.^{18,}

19 In brief, the original Montreal Protocol in 1987 controlled only CFCs as ODSs in developed countries. It furthermore required to begin phasing out of CFCs in 1993 and to achieve a 50% reduction by 1998 relative to 1986 consumption levels. Although CFCs were the only target of control in the original Protocol, halons, CCl_4 , and CH_3CCl_3 were added in the London Amendment in 1990. Then, HCFCs and CH_3Br were added as ODSs in the Copenhagen Amendment (1992) and Montreal Amendment (1997), respectively. The latest revision of the Beijing Amendment in 1999 included tightened controls on the production and trade of HCFCs and Halon-1011 (Bromochloromethane).

First developed in the early 1930s, CFCs were used widely in both household and industrial applications because of their unique properties (e.g., low toxicity, low or zero flammability, low gasphase thermal conductivity, good chemical stability, low corrosiveness during use, reasonable cost, etc.).^{20, 21} The use of these CFCs is diverse, including refrigerants, solvents, propellants, and foam blowing agents. Historically, CFC-11 was used in aerosol propellant mixtures, although its functions have been gradually replaced with others since 1990.²² Although CFC-12 was developed as a refrigerant in the 1930s, it was also used frequently as an aerosol propellant.^{23, 24} In addition, other CFCs like CFC-113, -114, and -115 are commonly used in solvents, propellants, and refrigerants, respectively.^{25, 26}

The presence of halogenated hydrocarbons in the troposphere was first reported by the chemical inertness of CFCs enables them to reside for the duration of tens to hundreds of years in the atmosphere.²⁶ The only realistic sink mechanism for tropospheric CFCs is their transport into the stratosphere. Once in the stratosphere, CFCs can be photochemically destroyed by ultraviolet (UV) photolysis and by excited oxygen atoms ($\text{O}(1\text{D})$).^{27 - 32} As the key property of CFC substitutes, HFCs and HCFCs can be removed effectively in the troposphere through reaction with OH. Although OH-initiated reactions occur predominantly in the troposphere, the reactions leading to the complete destruction of these alternatives are not rapid enough relative to the time required for transport from troposphere to stratosphere. Because the vertical transport of air mass (from the troposphere to the stratosphere) occurs primarily in the tropical

regions³³ processes occurring in the tropical tropopause layer (TTL) are crucial in determining timescales of such transport for chemical species released into troposphere.³⁴ Because of this gap, a certain fraction of the alternative compounds can reach the stratosphere the extent of which depends on their lifetimes.³⁵

The OH-initiated photooxidation of CFC alternatives can lead to the production of partially oxidized halogen compounds (e.g. $\text{CF}_3\text{C}(\text{O})\text{F}$ from HFC-134a, CH_2FCF_3) via H-atom abstraction and subsequent O_2 addition channels. Other major halogen-containing transformation products also include hydroperoxide (ROOH) and alkyl peroxy nitrates (ROONO₂). Chlorine-initiated oxidation for HCFCs and HFCs has also been reported to proceed in a similar manner to OH-initiated oxidation. These oxidation transformation products of HFCs and HCFCs can then be degraded by the reaction with OH, photolysis, thermal decomposition, or uptake into clouds, depending on their chemical properties. The fate of oxidation products such as $\text{C}(\text{O})\text{X}_2$ and $\text{HC}(\text{O})\text{X}$ depends on whether they are generated in the troposphere or in the stratosphere. Removal in the stratosphere is largely dominated by photolysis, whereas in the troposphere, heterogeneous processes such as rainout and uptake by cloud droplets or surface waters followed by hydrolysis may be important relative to photolysis or reaction with the OH radical.³⁶

In addition, a compound like CF_3CHO , known as the oxidation transformation products of HFC-143a (CH_3CF_3), can be subject to further degradation into CF_3 , CF_3CO , and $\text{CF}_3\text{C}(\text{O})\text{OO}$ radicals, ultimately forming more stable products (e.g., CF_3COOH , $\text{CF}_3\text{C}(\text{O})\text{OONO}_2$, etc.) by photolysis and/or OH oxidation in the atmosphere.³⁶ In general, these transformation products have tropospheric lifetimes of less than a month, except for $\text{HC}(\text{O})\text{F}$.³⁶ CFCs remain in the atmosphere for a long time because of their chemical inertness and high volatility.³⁸ Hence, the atmospheric lifetimes of organic compounds containing chlorine and bromine are often accounted for by their relations to the ODP in the stratosphere. The atmospheric lifetime of a given compound can thus be computed by assessing the relationship between its rate of source (or sink) and atmospheric burden, i.e., dividing the burden (Tg) of a target compound by its mean global sink rate (Tgyr⁻¹) in a steady state (i.e., with unchanging

burden).³⁹⁻⁴² The wide ranges of lifetimes of HCFCs and HFCs to be in the range of 1.4 (HFC152a) to 260 years (HFC-23).¹¹

Nevertheless, another class of unsaturated compounds termed Hydrofluoroolefins (HFOs) justified their use as CFC replacements. Due to their high reactivity in the atmosphere with the available oxidants, they were also found to be short-lived, have low GWPs and do not cause ozone depletion (~zero Ozone depletion potential, ODP). Due to this eco-friendly nature, HFOs reasonably pose insignificant vandalism to the Earth's atmosphere. But, it is also paramount that before these compounds enter the tropospheric environment, complete information on their photo-oxidation mechanism needs to be well understood, as this will help in deciding the best CFC alternative among the variety of available HFOs. In general, for any VOC, the degree of damage caused by the molecule can be deliberated based on the lifetime of a compound. For procuring such information, their degradation with OH and NO₃ radicals, Cl atoms and ozone needs to be well examined. These cleansing agents in the Earth's atmosphere are responsible for the fate of an emitted molecule. Among all the available oxidants, OH radicals play a pivotal role in governing the lifespan of a HFO or any VOC for that matter, with a 12 hour weighted-average concentration of 1×10^6 radical cm⁻³. In addition to this, Cl atoms too play a vital hand particularly in Marine Boundary layer (MBL) conditions, with a typical concentration of 1.3×10^5 atoms cm⁻³.⁴³ However; several research groups have utilized both experimental techniques as well as sophisticated computational tools to explore the kinetics of HFOs with OH radicals.

2. A BRIEF HISTORY OF ATMOSPHERIC CHEMICAL REACTIONS INVOLVING CFCS:

(Parth Gupta et al.,)⁴⁴ theoretically studied the reaction of CF₂=CHCF₃ and CF₂=CHCF₂CF₃ with OH radicals. It was understood that the addition of the OH radical onto the double bond was the major path for their atmospheric degradation. Moreover, the mechanistic approach to understand the photooxidation reaction of these HFOs with OH radicals formed various harmful fluorinated acids and aldehydes, which are known to increase cloud acidity in the Earth's atmosphere. On the contrary, as the computed lifetimes are not high enough as other HFCs, HCFCs and HFEs, the amount of these fluorinated

compounds generated by the degradation of these HFOs will be minimal. Calculated GWPs and the POCPs were also found to be negligible thereby reflecting minimal damage to the Earth's atmosphere. Hence, these molecules due to their less-threatening effects on the atmosphere promise to be successful alternatives to high GWP CFCs and HCFCs.

(Makroni Lilly et al.)⁴⁵ studied Theoretical studies on the kinetics of reactions of $\text{CHF}_2\text{CF}_2\text{OCH}_2\text{CF}_3$ with Cl atoms were performed. The H-abstraction reaction of $\text{CHF}_2\text{CF}_2\text{OCH}_2\text{CF}_3$ with Cl atoms shows a significant variational effect. The fitted three 466 parameter expression over a temperature range of 250–1000 K for overall rate coefficient is $k_{\text{Cl}}(\text{CHF}_2\text{CF}_2\text{OCH}_2\text{CF}_3 + \text{Cl}) = 5.24 \times 10^{-22} T^{3.2} \exp(-580/T)$ (in $\text{cm}^3 \text{ molecule}^{-1} \text{ s}^{-1}$ 467). Our calculations 468 also reveal that H-abstraction from the $-\text{CH}_2-$ group for $\text{CHF}_2\text{CF}_2\text{OCH}_2\text{CF}_3 + \text{Cl}$ reaction is the 469 primary reaction pathways over the whole temperature range of our study. The GWP value for 470 $\text{CHF}_2\text{CF}_2\text{OCH}_2\text{CF}_3$ at the 100-year horizon is found to be 601. $\text{CHF}_2\text{CF}_2\text{OC}(\text{O})\text{CF}_3$, 471 $\text{CHF}_2\text{CF}_2\text{OCHO}$, $\text{CHF}_2\text{CF}_2\text{O}_2\text{CF}_2\text{CHF}_2$, $\text{CHF}_2\text{CF}_2\text{OH}$, COF_2 , HF etc. are expected to be the 472 possible products after atmospheric decomposition of $\text{CHF}_2\text{CF}_2\text{OC}\cdot\text{HCF}_3$ radical.

(Manonmani et al.)⁴⁶ studied a detailed theoretical insight on the mechanism, thermochemistry and kinetics of reaction of HFO-1234zc with OH radical in the gas phase and on silicate clusters have been studied by using electronic structure calculations. The OH addition reactions at C3 carbon atoms of HFO-1234zc are more favourable in gas phase which leads to the formation of HFO-1234zc-OH adduct intermediate. The dual level dynamic approach is used to calculate the rate constant, and the rate constant calculated for the favourable intermediate, at 298 K is equal to $1.64 \times 10^{-13} \text{ cm}^3 \text{ molecule}^{-1} \text{ s}^{-1}$ which is comparable with the previous experimental result. It is found that HFO-1234zc is easily adsorbed on H_4SiO_4 , $\text{H}_6\text{Si}_2\text{O}_7$, $\text{H}_8\text{Si}_3\text{O}_{10}$ and $\text{H}_{12}\text{Si}_6\text{O}_{18}$ clusters and the thermochemistry results show that the initial reactions are highly feasible on silicate clusters. More specifically, the rate constant calculated for H-atom abstraction reaction on silicate cluster is higher by four orders of magnitude than that of the gas phase reaction. The rate constant calculated for the initial reactions on silicate clusters show that both H-atom and OH-addition reactions are equally probable. This

indicates that the mineral dust particles play a significant role on the atmospheric reaction of HFO-1234zc, and their interaction implicates the balance of HFOs in the troposphere. The subsequent reactions for intermediates formed from the initial H-atom abstraction reaction and OH-addition reactions with O₂, HO₂, NO radicals and H₂O molecule were studied. The products, 3-tetrafluoro-2-hydroperoxy-propan-1-ol, 3-tetrafluoro-1-hydroperoxy-propan-2-ol and 3-tetrafluoro-prop-2-en-1-yl-hydroperoxide formed from subsequent reactions are harmful and toxic in nature, particularly to aquatic organisms. However, the HFO-1234zc is a short-lived gas with lifetime of 2 days with very low ozone formation potential. Hence, HFO-1234zc can be used as an alternative to every level of chlorofluorocarbons, in controlled manner.

(Sandhiya et al.)⁴⁷ reported a detailed study on the mitigation potential for HFCs towards global warming through their phase down as per Kigali Amendment. HFC-125, HFC-134a, HFC-143a, HFC-152a and HFC-227ea are the major HFCs employed in cooling sector in India. Over the years, 2000 to 2021, the HFC emissions have decreased gradually on a global level. However, the percentage contribution of HFCs emissions from India to the global has increased over the years. The GWP weighted emissions of HFCs are estimated for scenarios with and without Kigali Amendment. With Kigali Amendment fully in action, the estimated HFC reduction target in 2050 is ~0.03 Gt CO₂ eq. The lifetime of the HFCs in different layers of atmosphere indicate that HFC-143a has a longer lifetime in the troposphere, stratosphere and mesosphere. The HFC-152a and HFC-134a have shorter lifetimes in the troposphere, owing to the fact that these HFCs are strongly oxidized by abundantly available OH radical in the troposphere. Thus, in addition to GWP, the atmospheric oxidation potential of HFCs needs to be considered for determining the complete fate of HFCs. This strongly brings the point of addressing the atmospheric oxidation potential of HFCs as one of the important policy relevant metrics to include the HFCs that need to be banned in Kigali Amendment. Though, the national and international agencies thrive hard to combat climate change resulting from HFCs, the recent measurements on the increase of emissions of five CFCs that were banned as per Montreal protocol has again raised concern.

The latest study (Western et al.,)⁴⁸ discovered an increase in emissions for CFC-113a, CFC-114a, and CFC-115 between 2010 and 2020, despite their phased-out status. Serving as feedstock's for HFCs, their emissions surged from 1.6 ± 0.2 to 4.2 ± 0.4 Gg yr⁻¹ over the same period. This escalation highlights that the renewability of HFCs depends not only on their respective GWPs but also on their entire lifecycle, spanning from production to emission. Consequently, the study underscores the necessity for the Kigali Amendment's ban on HFCs to consider atmospheric oxidation potential, product toxicity, and chemical stability as crucial policy metrics, in addition to GWP.

However, certain limitations in the study need addressing, such as accounting for all by-product emissions from HFC and HFE production in emission estimates, developing abatement scenarios, and including product toxicity in mitigating climate and clean air policies related to CFC alternatives. These aspects require a comprehensive study, representing the outlook of future work. To enhance Kigali Amendment implementation, future research should focus on the entire lifecycle of HFCs, assess the renewability of all fourth-generation synthetic halocarbons in addressing climate change, and consider all by-product emissions from HFC production in emission estimates and abatement scenarios, explore atmospheric degradation processes, and incorporate product toxicity in mitigating climate and clean air policies concerning CFC alternatives. Revisiting policy mechanisms and implementing amendments that account for these factors is imperative.

3. ALTERNATIVES FOR CHLOROFLUOROCARBONS (CFCS):

To mitigate the adverse effects of chlorofluorocarbons (CFCs) on the atmosphere, substitutes have been devised. These alternatives strive to deliver comparable functionalities while reducing environmental impact. Key replacements encompass:

3.1 Hydrochlorofluorocarbons (HCFCs):

Comprising hydrogen, chlorine, fluorine, and carbon atoms, HCFCs contribute to ozone depletion, albeit with a lower ozone-depleting potential than CFCs. Nevertheless, HCFCs are undergoing a phase-out process under the Montreal Protocol due to their environmental impact.

3.2 Hydrofluorocarbons (HFCs):

Devoid of chlorine, HFCs do not contribute to ozone layer depletion. Introduced as substitutes for CFCs and HCFCs, HFCs are utilized in diverse applications like refrigeration, air conditioning, and insulation. Nevertheless, due to their elevated global warming potential, HFCs play a role in climate change. Initiatives are in progress to phase out high-GWP HFCs and shift towards alternatives with lower global warming potential.

3.3 Hydrocarbons (HCs):

Regarded as eco-friendly substitutes for CFCs and HFCs, hydrocarbon refrigerants like propane (R-290) and isobutane (R-600a) boast zero ozone depletion potential and low global warming potential. These hydrocarbons find application in domestic refrigerators, freezers, and air conditioning systems.

3.4 Natural Refrigerants:

Increasingly popular as substitutes for synthetic refrigerants, natural refrigerants such as ammonia (NH₃), carbon dioxide (CO₂), and water (H₂O) have minimal environmental impact and play a role in lowering greenhouse gas emissions. Widely employed in industrial refrigeration systems, these natural refrigerants are actively being investigated for various other applications.

3.5 Hydrofluoroolefins (HFOs):

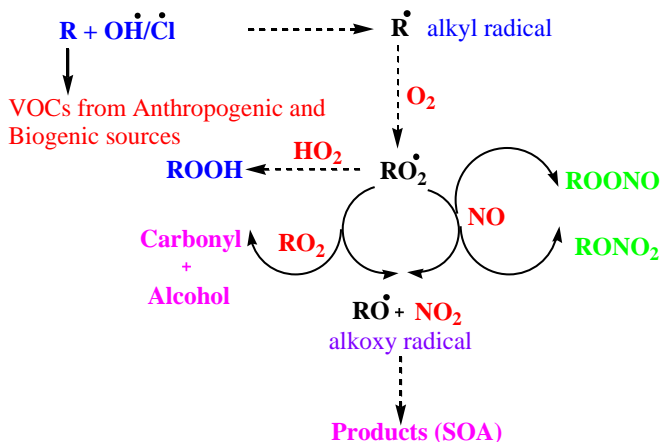
HFOs represent a new generation of refrigerants intended to supplant high-GWP HFCs. Possessing a low global warming potential, they are increasingly utilized in diverse applications, including air conditioning and refrigeration.

3.6 Alternative Technologies:

Advancements in technology have given rise to alternative cooling and heating systems, such as magnetic cooling and thermoelectric cooling, aiming to decrease dependence on synthetic refrigerants. Beyond refrigerants, the shift away from CFCs and other ozone-depleting substances entails a blend of regulatory measures, technological innovation, and market-driven initiatives, all geared towards endorsing environmentally sustainable alternatives.

4. REACTION SCHEME FOR ATMOSPHERIC REACTION OF VOLATILE ORGANIC COMPOUNDS:

Numerous organic compounds are released into the troposphere, and a series of reactions play a crucial role in the oxidation of these compounds. The subsequent transformations of alkyl radicals, generated from the initial reactions of volatile organic compounds (VOCs), hold equal significance. These reactions are accountable for the creation of diverse secondary organic aerosol products, posing a significant threat to life on Earth and disrupting the delicate balance of the atmosphere.⁴⁹ The overall framework for the primary and secondary reactions of VOCs is illustrated in Scheme 4.1. Initially, the alkyl radical of a volatile organic compound (VOC) is generated through either the abstraction of a hydrogen atom by $\text{OH}^\bullet/\text{Cl}^\bullet$ or the addition of $\text{OH}^\bullet/\text{Cl}^\bullet$ to the VOC. Subsequently, the resulting alkyl radical intermediate engages in a reaction with molecular oxygen in the atmosphere, resulting in the formation of a peroxy radical intermediate.⁵⁰ This peroxy radical possesses adequate energy to undergo reactions with reactive atmospheric species like HO_2 and NO_x ($x=1, 2$) radicals. Alternatively, it may undergo unimolecular decomposition and isomerization reactions.^{50, 51}



Scheme 4.1: General reaction scheme of VOCs with atmospheric oxidants.

It's noteworthy that the HO_2 radical serves as a significant chemical sink in the lower atmosphere, playing a crucial role in transforming both primary and secondary pollutants.⁵² When

the peroxy radical reacts with NO_2 , it results in the creation of a peroxyxynitrate adduct, a hazardous pollutant formed through the oxidation reactions of volatile organic compounds (VOCs).⁵³ Effectively studying the atmospheric implications of VOCs involves characterizing and identifying the products arising from primary and secondary reactions by exploring various theoretical methods and reaction pathways.

5. THEORETICAL PERSPECTIVE ON THE REACTION MECHANISM OF POTENTIAL ENERGY SURFACE

The potential energy surface (PES) serves as a mathematical and schematic representation depicting the relationship between molecular structure and energy. For a molecule with N atoms, the PES encompasses $(3N-6)$ coordinate dimensions. When the first derivative of energy is zero at a specific point on the PES that point is referred to as a stationary point.^{54, 55} This stationary point could be a local minimum, global minimum, or a saddle point with maximum energy.⁵⁴ In the context of a chemical reaction, the reactant, product, and intermediate all correspond to minimum energy points, while the transition state (TS) aligns with the maximum energy point. To discern the nature of a stationary point, it is essential to evaluate the second derivative of the PES, known as the Hessian. Diagonalizing the Hessian matrix yields eigenvectors associated with the normal modes of vibrations, and the eigenvalues are proportional to the square of the vibrational frequency. At a local minimum, all the modes possess positive frequencies, while the maximum energy point (transition state) exhibits one negative eigenvalue. Essentially, a transition state is a first-order saddle point, implying that in one specific direction within nuclear configuration space, the energy is at its maximum, whereas in all other orthogonal directions, the energy is at its minimum. While obtaining the PES theoretically is possible by gridding the PES at each point in

Principle, practical limitations arise due to the substantial increase in computational costs, especially for larger systems.

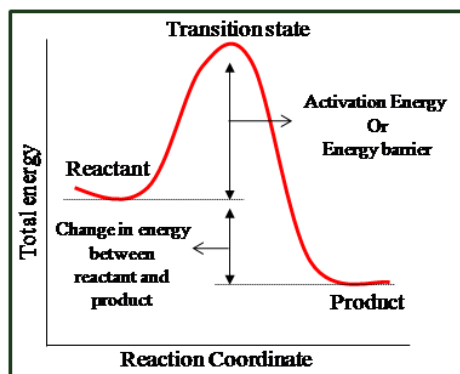


Figure 5.1: Schematic representation of a PES.

Hence, the reaction PES is constructed based on reaction coordinate, the molecular structural parameter corresponding to bond formation or bond breaking. The schematic representation of PES for a reaction system is shown in Figure 5.1. The energy difference between the TS and the reactant (omitting zero point vibrational energy) is called as an activation energy (E_a) or energy barrier of the reaction. Thus, E_a is considered as an energy barrier that must be crossed by the reactant before getting converted into product.

6. PREDICTION OF TRANSITION STATE (TS) AND INTRINSIC REACTION COORDINATE (IRC) CALCULATION

In the investigation of chemical reactions, the identification of the transition state (TS) on the potential energy surface (PES) holds great significance. Predicting the TS remains a complex and challenging task in the study of reaction mechanisms. Within a chemical reaction, the transition state structure represents a specific configuration along the reaction coordinate with the highest energy in the minimum energy path. The Synchronous Transit Quasi Newton (STQN) method,⁵⁶ introduced by H. B. Schlegel and Co-workers,⁵⁷ is widely employed for TS location. This method utilizes a quadratic synchronous transit (QST) approach to approach the quadratic region of the TS. In STQN, the TS is identified by making successful guesses⁵⁷ and then utilizing either a quasi-Newton or eigenvector following algorithm to complete the optimization of the TS.

Within the STQN framework, two methods, QST2 and QST3, are utilized for TS location. QST2 requires the specification of two molecules, the reactant and product, as input. It generates a guessed TS structure midway between the reactant and product and optimizes this structure for a first-order saddle point. On the other hand, QST3 requires the specification of three molecules (reactant, product, and guessed TS structure) as input. QST3 identifies the highest energy point between the reactant and product using the guessed input and optimizes the TS structure. The outcome of these methods provides the structure of the TS. Once the TS geometry is obtained, intrinsic reaction coordinate (IRC) calculations can be performed to confirm whether the TS genuinely connect the specified reactant and product. The IRC path calculation, proposed by Fukui in 1970, represents the path of a chemical reaction, defined as the steepest descent path in mass-weighted Cartesian coordinates on the PES, starting from the TS. The IRC path is followed when the reaction system descends from the TS to the reactant or product on the PES with infinitesimal velocity.⁵⁸

7. THERMODYNAMIC PROPERTIES:

Thermochemistry focuses on the variations in thermal properties that occur during chemical reactions. Its fundamental objective is to ascertain the amount of heat transferred between a system and its surroundings throughout the course of a chemical reaction. The key thermochemical parameters associated with chemical reactions include enthalpy, entropy, and Gibbs free energy. The enthalpy, ΔH for a chemical reaction is defined as,

$$\Delta H_f = \Delta H_f(\text{product}) - \Delta H_f(\text{reactant}) \quad (7.1)$$

The enthalpy of a reaction may be positive or negative, depending on whether heat is gained or lost, where ΔH_f denotes the heat of formation. If $\Delta H_f(\text{product}) > \Delta H_f(\text{reactant})$, ΔH_f is positive, indicating an endothermic reaction, where the reacting system absorbs heat from the surroundings. Conversely, if $\Delta H_f(\text{product}) < \Delta H_f(\text{reactant})$, ΔH_f is negative, signifying an exothermic reaction, where the reaction releases energy to the surroundings. The energy associated with molecular vibrations at 0 K is referred to as zero-point vibrational energy (ZPVE or ZPE). When calculating thermochemical parameters, it is essential to include ZPE correction. The relationship between the change in enthalpy (ΔH) and entropy (ΔS) is encapsulated in

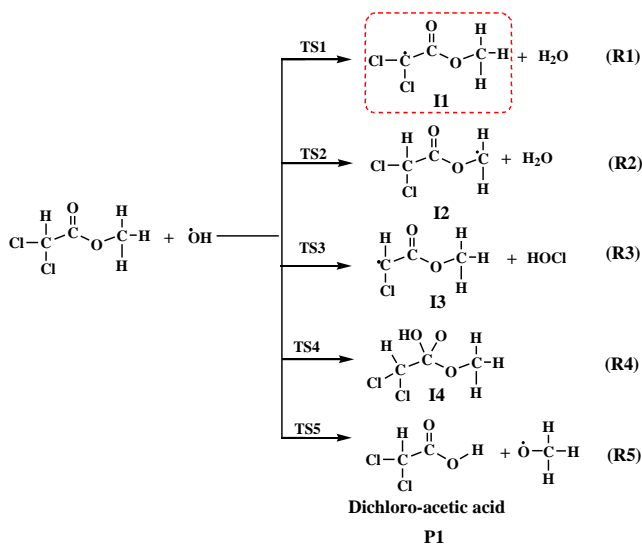
Gibbs free energy (ΔG). This energy, available for useful work in a system at constant temperature and pressure, is termed the Gibbs free energy of the system. The change in Gibbs free energy in a chemical reaction is,

$$\Delta G = \Delta H - T\Delta S \quad (7.2)$$

here, ΔH is the change in enthalpy, T is the temperature and ΔS is the change in entropy. The change in Gibbs free energy is linked to the spontaneity criterion of a chemical change and plays a pivotal role in determining the equilibrium position of the reaction.⁵⁹ Entropy, a thermochemical quantity, can be conceptualized as a measure of randomness or disorder, representing the number of states (i.e., energy levels) available to a system to occupy. If the change in Gibbs free energy is negative ($\Delta G < 0$), the reaction is deemed spontaneous (exoergic). Conversely, if ΔG is positive, the reaction is classified as non-spontaneous (endoergic). A prerequisite for a chemical reaction to occur is that ΔS should be positive.

8. MODELLING ATMOSPHERIC REACTION OF METHYLDICHLOROACETATE WITH HYDROXYL RADICAL:

The reaction between MDCA and the OH radical is thoroughly examined through electronic structure calculations.



Scheme 1: A schematic representation of the potential initial reaction between methylchloroacetate and the OH radical.

The study investigated the potential energy profiles, energy barriers, and thermochemical parameters for each step involved in various reaction pathways. Scheme 1 illustrates five initial reaction pathways: hydrogen and chlorine atom abstraction, OH addition reaction, and C-O bond breaking, where OH addition reactions were examined. Subsequent to the initial reaction, the reaction of oxygenated free radicals with alkyl, alkoxy, and alkyl peroxy radical intermediates was explored to discern potential exit pathways and end products.

9. ATMOSPHERIC IMPLICATIONS:

The degradation of hydrofluoroolefins (HFOs) through reactions with OH radicals and the subsequent transformation of secondary products contribute to the production of ozone, peroxy nitrates, and secondary organic aerosol in the atmosphere. The generation of ozone is a growing environmental concern due to its detrimental effects on both the environment and life on Earth, being a major contributor to smog formation. Previous research has indicated that the reaction of ROO• and HO₂ radicals with NO leads to the atmospheric formation of ozone and NO₂.⁴⁶ Therefore, the ozone production is heavily dependent on the reaction of ROO radicals, formed from the initial oxidation reactions of HFOs.⁴⁶ The dissociation of NO₂ also plays a role in ozone formation. Consequently, the quantity of NO₂ molecules generated during the degradation of atmospheric pollutants determines the potential for ozone formation in the atmosphere. The formation of ozone molecules is contingent upon the number of carbon and hydrogen atoms present in the molecule. Taking CF₂CHCHF₂ as an example, the maximum number of ozone molecules that can be formed is 5 (nC + nH = 5). During the OH radical-initiated oxidation reaction of HFO-1234zc, the observed ozone formation is 0.113 ppm.⁴⁶ Past studies have reported that the ozone creation potential of halocarbons falls within the range of 0-27 ppm,⁶⁰ suggesting that halocarbons may not significantly contribute to ozone formation in the atmosphere. Consequently, it is concluded that the ozone creation through the degradation of HFO-1234zc oxidation reaction is not deemed significant.

10. CONCLUSION:

The Earth's atmosphere comprises distinct layers that do not readily mix. The sun emits radiation, encompassing visible light (detectable by the human eye) and ultraviolet light (more energetic than visible light and invisible to the human eye). In the stratosphere, ultraviolet light reacts with O_2 molecules, forming atomic oxygen. Subsequently, atomic oxygen reacts with an O_2 molecule, resulting in the creation of ozone (O_3). This reaction leads to the formation of a substantial concentration of ozone molecules, constituting the ozone layer in the stratosphere. The absorption of ultraviolet light in the stratosphere serves as a protective shield for Earth's surface against the harmful effects of the sun.

Chlorofluorocarbons (CFCs), volatile organic compounds containing carbon, chlorine, and fluorine, have the potential to reach the stratosphere. There, they can react with ultraviolet light to generate chlorine atoms and other chlorine-containing species. These substances catalyze the conversion of ozone to O_2 , thereby diminishing the ozone concentration in the stratosphere. One strategy developed to minimize further damage to Earth's ozone layer involves replacing chlorofluorocarbons with hydrochlorofluorocarbons (HCFCs) or hydrofluorocarbons (HFCs). Fluorinated compounds, encompassing chlorofluorocarbons (CFCs), hydrochlorofluorocarbons (HCFCs), hydrofluorocarbons (HFCs), and related substances, have significantly contributed to both ozone depletion and climate change. The imperative to mitigate their impact on climate change underscores the essential phase-out of HFCs and other high-global-warming-potential (GWP) compounds. International agreements, exemplified by the Montreal Protocol, have played a pivotal role in regulating the production and usage of fluorinated compounds, aiming to safeguard the ozone layer. Amendments to the Montreal Protocol specifically target the cessation of ozone-depleting substances and the adoption of safer alternatives. However, challenges persist in addressing the climate impact of substitutes, necessitating ongoing regulation and innovative solutions.

Initiatives to reduce the environmental impact of fluorinated compounds concentrate on transitioning to safer alternatives with lower ozone-depletion potential and diminished global

warming potential. This transition involves embracing natural refrigerants like ammonia and carbon dioxide, alongside the development of low-GWP synthetic compounds such as hydrofluoroolefins (HFOs). The promotion of energy efficiency and sustainable practices plays a pivotal role in mitigating the climate impact of fluorinated compounds. Sustained efforts to phase out high-GWP compounds, advocate alternative solutions, and curb emissions are indispensable for preserving the Earth's atmosphere and combating climate change.

ACKNOWLEDGEMENTS:

We thank Dr. A. Muthuvel and Ms. G. Azhagarasi, PG & Research Department of Physics, Theivanai Ammal College for Women (Autonomous), Villupuram, for helpful discussions for this Book Chapter.

REFERENCES

1. Vereecken, L and Francisco, J. S. *Chem. Soc. Rev.*, 2012, 41, 6259.
2. Atkinson, R and Arey, J, *Chem. Rev.*, 2003, 103, 4605.
3. Sandhiya, L, Kolandaivel, P and Senthilkumar, K *Struct. Chem.*, 2012, 23, 1475.
4. Gnanaprakasam, .M, Sandhiya, .L and Senthilkumar, .K *Comput. Theor. Chem.* 1131, (2018), 40-50.
5. Papadimitriou, V. C., Lazarou, Y. J., Talukdar, R. K., and Burkholder, J. B., *J. Phys. Chem. A*, **2011**, 115 (2), 167-181.
6. Tokuhashi, K., Takahashi, A., Kaise, M., Kondo, S., Sekiya, A., Fujimoto, E., *Chem. Phys. Let.*, 325, 2000, 189-195.
7. Molina, M., Rowland, F.S., 1974. Stratospheric sink for chlorofluoromethanes: chlorine atom catalyzed destruction of ozone. *Nature*, 249, 810e812.
8. Rowland, F. S., Molina, M. J., 1975, Chlorofluoromethanes in the environment. *Rev. Geophys.* 13 (1), 1e35.
9. Ramaswamy, V., Boucher, O., Haigh, J., Hauglustaine, D., Haywood, J., Myhre, G., Nakajima, T., Shi, G.Y., Solomon, S., 2001. Radiative forcing of climate change. The Scientific Basis, Contribution of Working Group I to the Third Assessment Report of the Intergovernmental Panel on Climate Change. Cambridge University Press, Cambridge, U.K., p. 881. Chapter 6
10. Stemmler, K., Folini, D., Ubl, S., Vollmer, M.K., Reimann, S., O'Doherty, S., Grealley, B. R., Simmonds, P.G., Manning, A.J., 2007. European emissions of HFC36mfc, a chlorine-free substitute for the

- foam blowing agents HCFC-141b and CFC-11. *Environ. Sci. Technol.* 41, 1145e1151
11. WMO (World Meteorological Organization), 2007. Scientific assessment of ozone depletion: 2006. Global Ozone Research and Monitoring Project Report No. 50, 572 pp., Geneva, Switzerland.
 12. WMO (World Meteorological Organization), 1999. Scientific Assessment of Ozone Depletion: 1998. Global Ozone Research and Monitoring Project e Report No. 44, World Meteorological Organization, Geneva, Switzerland, 732 pp.
 13. Ramanathan, V., 1975. Greenhouse effect due to chlorofluorocarbons e climatic implications. *Science*, 190, 50e52.
 14. Hansen, J., Lacis, A., Prather, M., 1989. Greenhouse effect of chlorofluorocarbons and other trace gases. *J. Geophys. Res.* 94, 16417e16421.
 15. Solomon, S., Daniel, J.S., 1996. Impact of the Montreal Protocol and its amendments on the rate of change of global radiative forcing. *Clim. Change*, 32, 7e17.
 16. Ramanathan, V., Feng, Y., 2009. Air pollution, greenhouse gases and climate change: global and regional perspectives. *Atmos. Environ.* 43, 37e50.
 17. Dekant, W., 1996. Toxicology of chlorofluorocarbon replacements. *Environ. Health Perspect.* 104, 75e83.
 18. Solomon, S., Garcia, R.R., Rowland, F.S., Wuebbles, D.J., 1986. On the depletion of Antarctic ozone. *Nature*, 321, 755e758.
 19. Prather, M., Spivakovsky, C.M., 1990. Tropospheric OH and the lifetimes of hydrochlorofluorocarbons. *J. Geophys. Res.* 95 (D11), 18,723e18,729.
 20. Ehhalt, D., Prather, M., Dentener, F., Derwent, R., Dlugokencky, E., Holland, E., Isaksen, I., Katima, J., Kirchhoff, V., Matson, P., Midgley, P., Wang, M., 2001. Atmospheric chemistry and greenhouse gases. The Scientific Basis Contribution of Working Group I to the Third Assessment Report of the Intergovernmental Panel on Climate Change. Cambridge University Press, Cambridge, U.K., p. 881 (Chapter 4).
 21. UNEP (United Nations Environment Programme), 2009. Handbook for the Montreal Protocol on Substances that Deplete the Ozone Layer, eighth ed. UNEP Ozone Secretariat, Nairobi, Kenya.
 22. McCulloch, A., Ashford, P., Midgley, P.M., 2001. Historic emissions of fluorotrichloromethane (CFC-11) based on a market survey. *Atmos. Environ.* 35, 4387e4397.

23. Midgley Jr., T., 1937. From the periodic table to production. *Indust. Eng. Chem.* 29 (2), 241e244.
24. McCulloch, A., Midgley, P.M., Ashford, P., 2003. Releases of refrigerant gases (CFC-12, HCFC-22 and HFC-134a) to the atmosphere. *Atmos. Environ.* 37, 889e902.
25. McCulloch, A., 1999. CFC and Halon replacements in the environment. *J. Fluorine Chem.* 100, 163e173.
26. Metz, B., Kuijpers, L., Solomon, S., Anderson, S.O., Davidson, O., Pons, J., de Jager, D., Kestin, T., Manning, M., Meyer, L., 2005. Safeguarding the Ozone Layer and the Global Climate System: Issues Related to Hydrofluorocarbons and Perfluorocarbons. Cambridge University Press, Cambridge, USA.
27. Lovelock, J.E., Maggs, R.J., Wade, R.J., 1973. Halogenated hydrocarbons in and over the Atlantic. *Nature*, 241 (5386), 194e196
28. Hubrich, C., Zetzsch, C., Stuhl, F., 1977. Ber. Bunsenges. *Phys. Chem.* 81, 437e442.
29. Hubrich, C., Stuhl, F., 1980. The ultraviolet absorption of some halogenated methanes and ethanes of atmospheric interest. *J. Photochem.* 12, 93e107.
30. Simon, P.C., Gillotay, D., Vanlaethem-Meurée, N., Wisenberg, J., 1988a. *Ann. Geophys.* 6, 239e248. Simon, P.C., Gillotay, D., Vanlaethem-Meurée, N., Wisenberg, J., 1988b. Ultraviolet absorption cross-sections of chloro and chlorofluoro-methanes at stratospheric temperatures. *J. Atmos. Chem.* 7, 107e135.
31. Mérienne, M.F., Coquart, B., Jenouvrier, A., 1990. Temperature effect on the ultraviolet absorption of CFC13, CF2Cl2 and N2O. *Planet. Space Sci.* 38, 617e625.
32. Sander, S.P., Finlayson-Pitts, B.J., Friedl, R.R., Golden, D.M., Huie, R.E., Keller-Rudek, H., Kolb, C.E., Kurylo, M.J., Molina, M.J., Moortgat, G.K., Orkin, V.L., Ravishankara, A.R., Wine, P.W., 2006. Chemical kinetics and photochemical data for use in atmospheric studies. Evaluation No. 15, NASA JPL Publication 06-2.
33. Holton, J.R., Haynes, P.H., McIntyre, M.E., Douglass, A.R., Rood, R.B., Pfister, L., 1995. Stratosphere-troposphere exchange. *Rev. Geophys.* 33 (4), 403e439.
34. Mohanakumar, K., 2008. Stratosphere-Troposphere Exchange, In *Stratosphere Troposphere Interactions*. Springer.
35. Prinn, R.G., Zander, R., Cunnold, D.M., Elkins, J.W., Engel, A., Fraser, P.J., Gunson, M.R., Ko, M.K.W., Mahieu, E., Midgley, P.M., Russell III, J.M., Volk, C.M., Weiss, R.F., 1999. Long-lived ozone-related compounds, Chapter 1 in *Scientific Assessment of Ozone Depletion*:

- 1998, Global Ozone Research and Monitoring Project Report No. 44, World Meteorological Organization, Geneva.
36. Wine, P.H., Chameides, W.L. 1990. Possible atmospheric lifetimes and chemical reaction mechanisms for selected HCFCs, HFCs, CH₃CCl₃ and their degradation products against dissolution and/or degradation in seawater and cloud water. In Scientific Assessment of Stratospheric Ozone: 1989, Volume II, Appendix: AFEAS Report, World Meteorological Organization Global Ozone Research and Monitoring Project eReport No. 20, Geneva, 271e295.
 37. Brasseur, G. P., Orlando, J. J., Tyndall G.S., 1999. In: Atmospheric Chemistry and Global Change.
 38. Molina, M., Rowland, F.S., 1974. Stratospheric sink for chlorofluoromethanes: chlorine atom catalyzed destruction of ozone. *Nature*, 249, 810e812.
 39. Ko, M.K.W., Sze, N.D., 1982. A 2-D model calculation of atmospheric lifetimes for N₂O, CFC-11 and CFC-12. *Nature*, 297, 317e319. doi:10.1038/297317a0.
 40. Cunnold, D.M., Weiss, R.F., Prinn, R.G., Hartley, D., Simmonds, P.G., Fraser, P.J., Miller, B., Alyea, F.N., Porter, L., 1997. GAGE/AGAGE measurements indicating reductions in global emissions of CCl₃F and CCl₂F₂ in 1992e1994. *J. Geophys. Res.* 102 (D1), 1259e1269.
 41. Ehhalt, D., Prather, M., Dentener, F., Derwent, R., Dlugokencky, E., Holland, E., Isaksen, I., Katima, J., Kirchhoff, V., Matson, P., Midgley, P., Wang, M., 2001. Atmospheric chemistry and greenhouse gases. In: Houghton, J.T., Ding, Y., Griggs, D.J., Noguer, M., van der Linden, P.J., Dai, X., Maskell, K., Johnson, C.A. (Eds.), *Climate Change 2001: The Scientific Basis Contribution of Working Group I to the Third Assessment Report of the Intergovernmental Panel on Climate Change*. Cambridge University Press, Cambridge, U.K., p. 881 (Chapter 4).
 42. R. Prinn, R. Weiss, B. Millar, J. Jaung, F. Alyea, D. Cunnold, P. Fraser, D. Hartley, P. Simmonds, *Science*, 1995, 269, 187–192.
 43. C. W. Spicer, E. G. Chapman, B. J. Finlayson-Pitts, R. A. Plastridge, J. M. Hubbe, J. D. Fast, C. M. Berkowitz, *Nature*, 1998, 394, 353–356.
 44. Partha Gupta, Rajakumar Balla, A Dual Level Direct Dynamics Study for the Reaction of CF₂=CHCF₃ (HFC-1225zc) and CF₂=CHCF₂CF₃ (HFC-1327cz) towards OH Radicals. *Chemistry Select*, 4, 2019, 4827-4838.
 45. Makroni Lily, Bidisha Baidya, Wenliang Wang, Fengyi Liu, Asit K. Chandra, Atmospheric chemistry of CHF₂CF₂OCH₂CF₃: Reactions with Cl atoms, fate of CHF₂CF₂OC•HCF₃ radical, formation of OH

- radical and Criegee Intermediate. *Atmospheric Environment*, 242, 2020, 117805.
46. G. Manonmani et al. A computational perspective on the chemical reaction of HFO-1234zc with OH radical in gas phase and in the presence of mineral dust. *J. Phy. Chem. A*, 2022, 126, 51, 9564-9576.
 47. L. Sandhiya et al. Mitigation potential of banned hydrofluorocarbons (HFCs) towards global warming - An assessment of Kigali Amendment in the Indian scenario. *Journal of Cleaner Production*, 428(4):139315.
 48. Western, L.M., Vollmer, M.K., Krummel, P.B., Adcock, K.E., Fraser, P.J., Harth, C.M., Langenfelds, R.L., Montzka, S.A., Mühle, J., O'Doherty, S., Oram, D.E., Reimann, S., Rigby, M., Vimont, I., Weiss, R.F., Young, D., Laube, J.C., 2023. Global increase of ozone-depleting chlorofluorocarbons from 2010 to 2020. *Nat. Geosci.* <https://doi.org/10.1038/s41561-023-01147-w>, 2023.
 49. Zhao, Y. L.; Saleh, R.; Saliba, G.; Presto, A. A.; Gordon, T. D.; Drozd, G. T. *Proc. Natl. Acad. Sci.* **2017**, 27, 6984.
 50. Atkinson, R.; Arey, J. *Chem. Rev.* **2003**, 103, 4605.
 51. Sun, X.; Zhang, C.; Zhao, Y.; Bai, Y.; Zhang, J.; Wang, Q. *Environ. Sci. Technol.* **2012**, 46, 8148.
 52. Xiaomin, S.; Chenxi, Z.; Yuyang, Z.; B., J.; Qingzhu, Z.; Wang, W. *Environ. Sci. Technol.* **2012**, 46, 8148.
 53. Gnanaprakasam, M.; Sandhiya, L.; Senthilkumar, K. *Theor. Chem. Acc.* **2017**, 136:131, 1.
 54. Levine, I. N. *Quantum Chemistry, Fifth Edition, Prentice Hall of India Pvt. Ltd.* **2008**.
 55. Peng, C.; Schlegel, H. B. *Israel J. Chem.* **1993**, 33, 449.
 56. Fukui, K. *Acc. Chem. Res.* **1981**, 14, 363.
 57. Schlegel, H. B., (2003), Exploring potential energy surfaces for chemical reactions: an overview of some practical methods. *J. comp. chem.*, 24, (12), 1514-1527
 58. Picot, D.; Ohanessian, G.; Frison, G. *Inorg. Chem.* **2008**, 47, 8167.
 59. Sommerfeld, A., *Thermodynamics and Statistical mechanics, Published by Levant Books*, **2005**.
 60. Derwent, R.; Jenkin, M.; Saunders, S., Photochemical ozone creation potentials for a large number of reactive hydrocarbons under European conditions. *Atmospheric Environment* **1996**, 30, (2), 181-199.

**PG & Research Department of Computer Science Theivanai Ammal
College for Women (Autonomous), Villupuram*

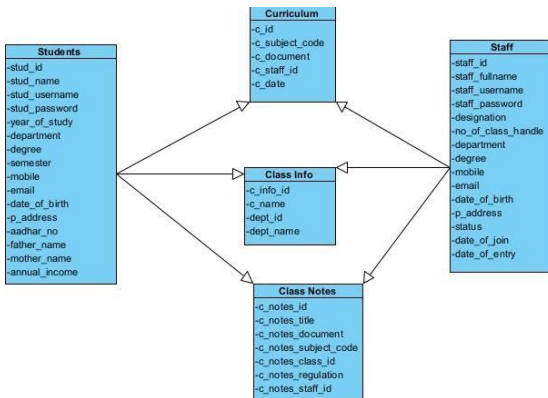
ABSTRACT

It becomes quite difficult to handle the crucial notes when needed because most notes are shared over WhatsApp or other messaging apps. This framework will provide a straightforward method for sharing documents for educational purposes. On the framework, multiple users can work at once. The teachers will find it easy to distribute the notes to every single kid. Teachers and students in universities will use the framework, and schools may also use it. Many students struggle to prepare during test season since they either don't have the lecture notes from their professors or they weren't enrolled in college. This system will offer a way to access the notes with ease. Finding the correct person to hire with their passed notes is difficult. The note circulation system eliminates this issue. It provides a platform where users can propose people based on the needs specified in their notes. This project is developed for current and arrear students to prepare for the examination and improve their knowledge also they learn to read the material in various formats - PDF, Document, PowerPoint format, or video. The particular subject handling staff uploads the syllabus and class notes in different formats in a particular subject department and regulation-wise. Students only view or read the documents or videos to improve their knowledge and prepare for the examination. This system does not allow downloading documents. This application was developed as an Android mobile application because of its hand-holding application; it's easy to use for students and staff.

INTRODUCTION

This is a really helpful project. Instead of physically checking his register to look for records, the user can now use the software to search it by making specific selections. The user does not need to enter the majority of the information. All documents about our topic appear automatically. The main objective of this note-sharing website is to allow students to exchange their notes online, which is very advantageous for teachers and universities. This is beneficial for universities or other organizations that are now providing online courses due to the pandemic. However, with the integration of portable Android mobile applications

with online document-sharing services. The class notes-sharing platform in hand hand-held Android mobile application will appear there in the Dashboard, My Notes, and My Account. You can view all of the notes and documents for a particular course, along with information like name Description, Type, uploaded by, Uploaded On and you can even download the notes to see its content. In the New Notes view all the notes that you have uploaded. Through My Account, the user can make changes to his profile. He can view all of the notes that the teacher or user has uploaded while in the admin section, and he can choose which notes to accept or disapprove. The notes that other users have uploaded can also be removed by him.



LITERATURE REVIEW

Nowadays, note-taking remains a fundamental aspect of academic success, whether through traditional pen-and-paper methods or digital platforms. While traditional note-taking fosters active engagement and deeper processing, digital systems offer advantages in organization, accessibility, and multimedia integration. The choice between these methods should consider individual preferences, learning styles, and technological literacy. Moreover, the integration of cognitive strategies can enhance the effectiveness of note-taking practices, ultimately contributing to improved academic performance.

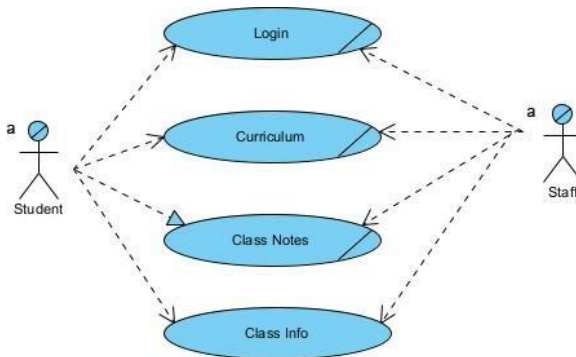
EXISTING SYSTEM

Notion is an all-in-one workspace that combines note-taking, project management, and collaboration features. It provides users with the flexibility to create customizable notes using text,

tables, multimedia content, and embedded files. Notion's hierarchical structure allows for easy organization of notes into pages, databases, and linked content. It also supports real-time collaboration and integrates with third-party applications, enhancing productivity and knowledge management.

PROPOSED SYSTEM

EduNote+ is a proposed subject notes-taking system designed to enhance academic performance by providing students with a comprehensive and user-friendly platform for capturing, organizing, and reviewing course materials. Leveraging digital technology, EduNote+ aims to address the limitations of traditional note-taking methods while integrating cognitive strategies to promote effective learning outcomes.



FUTURE ENHANCEMENTS

This project, "Subject notes-taking system for academic performance," may be expanded in the future by putting in place a tagging system that automatically groups notes according to relevance, subjects, or keywords. Based on these tags, users may then quickly search and filter notes to obtain reliable information. Additionally, the subject staff will send students their notes, which they can download. It appears that staff and students will find great benefit from this undertaking in the future.

MODULE

The Primary goal for my project is to send class notes and syllabus to all related students via mobile application.

Modules: There are two main modules

1. Staff
2. Student

In my project, I divided it into two main users first one is Staff and Students. The staff uploads the syllabus for the current curriculum, and study class notes for related class students, the student module, and students can only read the document in various formats like notes/documents/video/pdf/ppt.

1. Staff Module

The main user is the admin; it creates an account for all kinds of staff. The admin module has the following sub-modules:

Login Module-Staff can access the mobile application first and enter into this login module to enter their username and password, if given the correct information log the application otherwise it denotes the error username and password is wrong.

2. Student Registration Module

The Student registration module is creating new student information on the database; The following fields are created for each student. "stud_name, stud_username, stud_password, degree, email, mobile, year_of_study, department, p_address, last_edu_qualification, percentage, father_name, mother_name, annual_income, date_of_birth, parent_mobile_no, date_of_entry "If the Student already exists the system intimate the student's information already exists otherwise all student data is saved into the database.

Upload Curriculum Modul-Faculty uploads the curriculum documents to the database, in curriculum documents format like as pdf only, by using hand held mobile device.

Upload Class Notes Module- Faculty uploads the documents to database class notes in various formats like notes/documents/video/pdf/ppt using a hand-held mobile device.

TECHNIQUES AND ALGORITHM USING IN MODULE

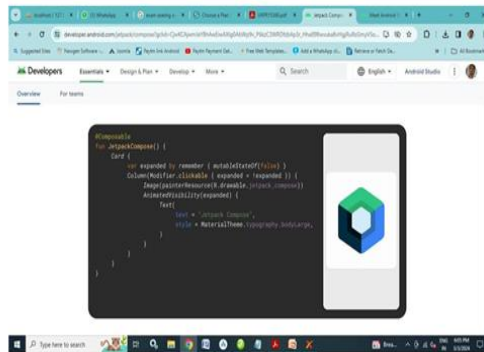
Android Studio

Among the many features of Android Studio are the following:

Build system: A flexible Gradle-based build system that allows you to customize the build process, create APKs, and reuse code.
Code editor: An advanced code editor for building common app features.
Tools: Tools for development, debugging, testing, and performance. Build better apps faster with Jetpack Compose.

Android recommends Jetpack Compose as a contemporary toolset for creating native user interfaces.

It streamlines and expedites Android UI development. Develop your project more quickly with less code, stronger tools, and user-friendly Kotlin AP.



CONCLUSION

This project "Subject Notes-Taking System for Academic Performance" has several advantages. Keeping track of the notes and managing the project's levels are both simple tasks. It is simple to keep up with the topic. Furthermore, tracking by hand is not necessary. The project's future potential is incredibly vast. In the future, the project may be deployed on an intranet. Due to the project's remarkable development adaptability, upgrades can be made shortly as and when necessary. Any association can utilize the suggested note-management software to execute the entire project in a much better, more accurate, and error-free manner. The project's long-term scope is as follows. This system is exclusive to a specific association individual. The system will create unique IDs for teachers and students. The message alert will be used with the mailing framework. Thus I conclude that I have completed this project with the below future enhancements to be done.

REFERENCES

1. <https://www.studocu.com/in/document/national-institute-of-technology-meghalaya/mechanical-engineering/pdfcoffee-this-pdf-includes-project-report-on-notes-management>
2. Introduction to Communication Systems Communication Model, Transmission Line, and Data Communication Elmustafa Sayed Ali Ahmed Red Sea University, Sudan
3. Monitoring Student Learning in the Classroom Kathleen Cotton
4. https://www.researchgate.net/publication/362301918_Student_Management_System_Group_Project_ReFaculty_Attendance_Monitoring_Using_RFID_With_Overload_Computation_And_Email_Notification_for_City_College_of_Calamba_Edmund_O._Mati_Jr.
5. Uncovering the Role of Biophysical Factors and Socioeconomic Forces Shaping Soil Sensitivity to Degradation: Insights from Italy Filippo gambella
6. Jones, S. (2020). "Digital Note-Taking: Enhancing Learning Outcomes in Higher Education." *Journal of Educational Technology & Society*, 23(2), 14-25.
7. Li, X., & Zhang, Y. (2019). "A Review of Digital Note-Taking Methods for Students in Higher Education." *International Journal of Emerging Technologies in Learning*, 14(7), 64-76.
8. Smith, J. K., & Boland, M. (2018). "The Cornell Note-Taking System: A Review of Research and Best Practices." *Journal of College Reading and Learning*, 48(2), 133-145.
9. Wang, L., & Li, S. (2017). "An Overview of Natural Language Processing Techniques for Text Analysis in Educational Contexts." *Educational Technology & Society*, 20(2), 122-136.
10. Zhang, H., & Liu, D. (2021). "Integration of Note-Taking Techniques in Digital Learning Environments: A Review." *Computers & Education*, 167, 104203.
11. Zhao, L., & Lu, Y. (2019). "The Role of Multimedia Note-Taking in Improving Learning Performance: A Meta-Analysis." *Journal of Educational Computing Research*, 57(5), 1257-1279.
12. *Educational Technology Research and Development*, 68(3), 1415-1443.
13. National Center for Biotechnology Information. (n.d.). "Sentiment Analysis in Text Mining." Retrieved from <https://www.ncbi.nlm.nih.gov/pmc/articles/PMC5987332/>.
14. Yildirim, S., & Güven, İ. (2020). "A Comprehensive Review of Named Entity Recognition (NER) Studies." *International Journal of Advanced Computer Science and Applications*, 11(11), 408-414.
15. Laranjo, L., Dunn, A. G., Tong, H. L., Kocaballi, A. B., Chen, J., Bashir, R., & Lau, A. Y. (2018). "Conducting Systematic Reviews of Text and Opinion." *Journal of the American Medical Informatics Association*, 25(12), 1429-1437.

**Assistant Professor, Department of Computer Applications Theivanai Ammal College for Women, Villupuram, Tamil Nadu*

ABSTRACT

Presently a day, innovation quickly development, yet in addition individuals don't endure his/her life later street mishap on the grounds that there are no crisis offices accessible in our country. So, this paper holds an advanced innovation which works much better with the crisis offices. This venture illuminate about a mishap that is happened to vehicle to save group and the relatives of the voyaging people. This uses vibration sensor which can recognize the unexpected vibration when a mishap is happened and furthermore involved Infrared Sensor (IR) in distance computation for alarming. More benefits of this framework the data ship off the salvage group by utilizing IOT innovation and find the situation by GPS beneficiary modems as scope and longitude. Here and there individuals can't arrive at clinics brief later a mishap due to the gridlock, shortfall of rescue vehicle, absence of a system to opportune proliferate data to the suitable power. To guarantee the wellbeing of lives, this paper proposes a mechanized IoT based powerful mishap discovery framework. Following an occurrence, the information data is shipped off the web server, moment SMS is sent to the victim's associates and furthermore to the significant specialists, for example, close by police headquarters, nearby health offices and rescue vehicle administration. To assess the exhibition of the framework, a recreated street situation has been planned. Attributable to the escalated improvement in innovation, different canny and independent frameworks have been imagined.

Keywords: Intelligent Transportation Systems (ITS), Internet of Things (IoT), IR (Infrared Sensor), VTS (Vehicle Tracking System), Printed Circuit Boards (PCBs), GPS, GSM, Wi-Fi module, rescue system.

INTRODUCTION

The colleagues are frequently told long later the occurrence. The general circumstance is deteriorated by the way that the following and reachability of the mishap spot in a metropolitan region is a significantly troublesome. Hence in this paper, a programmed mishap identification and salvage framework is centered on utilizing IoT by which the kinfolk of the victim, closest police headquarters, the nearest clinical center and grid lock signal server will be notified immediately with the location

where the mishap occurred. For the better interaction, the nearest clinical center will be notified with the victims blood group along with the location where mishap occurred. Closest rescue vehicle administration will likewise be alarmed through the web with the area of the mishap. The total framework will altogether work on the brief co-appointment of the important activities later a mishap. In the field of IoT, the articles impart and trade data to offer progressed keen types of assistance to the clients. In South Asian urban communities, the quantity of vehicles is on a consistent ascent, subsequently, street mishaps are expanding alarmingly. The mishaps predominantly happen for surge driving and overwhelming. The total number of accident-related deaths in our country, 2017-18 stood at 1,53,987 approximately indicate an increase of 2% over the figures for 2017-18. India, despite the fact that it will be perceived as one of the highly populated and agricultural nations, both financially and socially, the passing rate is 7.75 per 10,000 of populace. India has the third largest road network, the total number of vehicles in the year 2017-2018 stood at 296.8 million. The quantity of certified drivers is 205 million, out of which 26% are unskilled. This large number of bottlenecks adds more difficulties to the fast exchange of the casualty to the close by emergency clinic. Since various savvy frameworks are available to save the life of victim, there ought to be a mechanical arrangement in cases connected with a mishap. These frameworks would be helpful in diminishing the loss of human life and occurrence of gridlocks.

LITERATURE REVIEW

“An Approach on Automated Rescue System with Intelligent Traffic Lights for Emergency Service” proposed by Sanjana.K.R, in the year of 2015. They use the framework which will detect roadside accidents with the help of sensor. Using GSM, the victim’s family members get the notification about the accident. It fully computerized. Detect the accident place, using Google guide, controls traffic light, arriving at emergency medical center at a time. It executed in huge populated nations.

Keen Car: An IoT Based Accident Detection System proposed by Arif Shaik in the year of 2018. They did not use any programmed warning for accident detection to rescue systems. It fully based on Internet of Things (IoT). An indication from an accelerometer

and a GPS sensor is sent to the cloud, a notification will be sent. The indication will show the effectiveness of accident and location. Using GPS, the rescue system reached. IoT Based Accident Detection and Rescue System proposed by S.L.V. Prasad, in the year of 2020. They use self-accident detection technique. It does not depend on external inputs to detect accidents. It uses accident-detection sensor, GPS receiver, ESP 32 that work collectively to detect accidents instantly and will send location coordinates to an ambulance. It includes another setup in ambulance to observe the victim's health condition. The ambulance contains BP sensor, pulse sensor, and glucose dripping sensor along with Arduino-nano and display.

METHODOLOGIES

1. Smart vehicle - A shrewd vehicle is planned with GPS and vibration sensor to distinguish a mishap. On making a shrewd salvage framework to right away work with post-mishap co-appointment. An exploratory model is intended to all the more likely show the convenience of the general structure.
2. Microcontroller - A Microcontroller is a low-cost microcomputer, which is designed to perform the specific tasks of embedded systems like displaying microwave's information, receiving remote signals, etc. Whenever a user vehicle meets with an accident, the vibration sensor detects and gives its output. The output is then detected by the microcontroller.
3. Vibration sensor - A vibration sensor is a device that measures the amount and frequency of vibration in our vehicle. This vibration sensor then detects and gives its output to the microcontroller whenever the vehicle meets with an accident.
4. IR sensor - IR sensor is an electronic device that emits the light in order to sense some object of the surroundings. An IR sensor can measure the heat of an object as well as detects the motion. It detects the motion of a 3rd party vehicle around our vehicle within a certain meters and directs to the microcontroller to give us a buzzer sound.
5. GPS/GSM Module - A GPS module contains tiny processors and antennas that directly receive data sent by satellites through dedicated RF frequencies and a GSM module is a

hardware device that uses GSM mobile telephone technology to provide a data link to a remote network. These modules are used for the sharing of victims' location to the respective rescue offices.

EXISTING SYSTEM

The existing system only use the information about the vehicle's vibrating measurements to detect the accident and that is doesn't work in network fewer areas. And after occurrence of the accident, controlling of traffic takes high time. This drawback can be overcome by proposed system.

Disadvantages:

- It has low reliability
- Poor control system

PROPOSED SYSTEM

The main principle of the project is the immediate detection and rescue management. No most recent innovation can deflect mishaps totally and don't have a clue where and when a mishap might happen. If vehicle is normal, no messages have been sent to salvage group. And the vibration level of the vehicle is monitored in all the time, if it reaches the threshold level then the action has been taken automatically. Whenever mishap occurred, the vibration sensor detects the mishap happened with vehicle. The controller gets the input from sensor and sends the mishap alert

information message to the salvage group. GPS/GSM module finds the area of mishap and sends location to the salvage group and kinfolk of victim. The message sent to the nearby clinical center also contains the victim's blood group. It will facilitate connectivity to the nearest police station and hospital and provide medical help through IOT technology. This paper also proposed the special feature added to the vehicle that is the buzzer will be ringing if any other objects or the vehicle comes closest to the client vehicle within the 10 feet distance. This action is being controlled by the IR sensor, microcontroller and buzzer respectively.

Advantages:

- Fast recovery and quick process.

- Monitor all hazards and threats in both network coverage and no network areas.
- Wireless monitoring and user friendly.

SYSTEM DESIGN

The main framework of this system contains the hardware components such as power supply (4V), microcontroller/ arduino, vibration sensor, GPS/GSM module and LED display. The second setup contains the framework of hardware components combined with the main system are the IR sensor and buzzer. These components are frame worked as a system by initiated from the microcontroller which is the center of the framework. Then the vibration sensor is connected to the microcontroller which is connected to the GPS/GSM module, LED display respectively. The microcontroller/arduino controls the entire activity of the system as it contains the IC where data are embedded in it. This completes the framework of setup one. The setup two is designed by connecting the IR sensor to the microcontroller/arduino and the distance range is fixed to 10feet from the sensor. Microcontroller then connected to the buzzer to ring if any object or vehicle is detected. These two frameworks are combined in one complete system by testing generally coordinated modules that have passed incorporated testing as its feedback. Model is intended to more readily show thehandiness of the general structure.

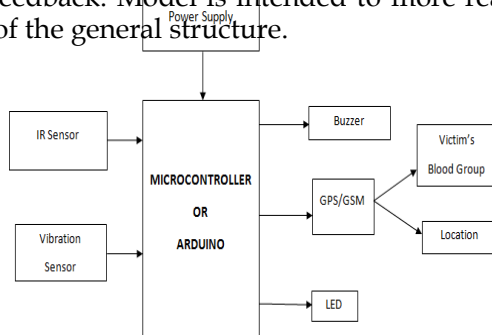


Fig. 1 System Framework

SYSTEM WORKING

In this section, our practical approach is going to be discussed that has been taken to solve the problem. In the setup one, when a power supply (4V) is given to the system, a sensor named

vibration sensor has been used which detects the vibration of the vehicle by monitoring vibration range. When a vibration sensor detects the vibration range more than 1000Hz, it is considered being a mishap occurred. Then the vibration sensor sends the indication to the microcontroller. After the mishap is detected, the data about the vehicle is sent to the salvage group and victim's kinfolk by the GPS/GSM module. The data contains the mishap alert text message and the area of mishap to the nearby police station, victim's kinfolk. Nearby clinical center receives the blood group of the victim along with the alert message and location. To check whether the alert message sent successfully, it is displayed through the LED display.



Fig. 2 Flow chart for mishap detection

The setup two that contains the IR sensor that senses the motion of any object that is considered to be a vehicle within the distance of 10 feet around the client's vehicle and sends the intimation to the microcontroller that alerts the client by ringing the buzzer.

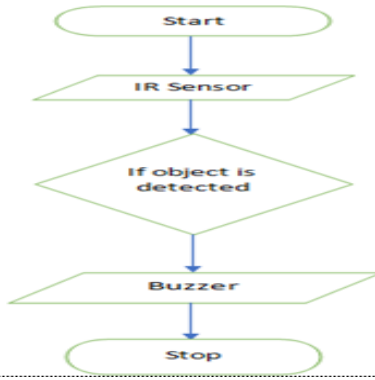


Fig.3 Flow chart for IR sensor unit

7 RESULTS



Fig.4 Full Setup



Fig. 5 Initial Vibration Level



Fig.6 Alert SMS sent to USER 1



Fig.7 Alert SMS sent to USER 2

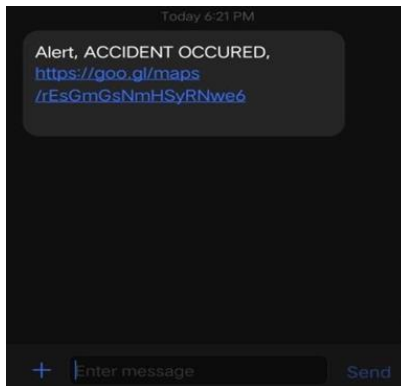


Fig.8 SMS Receivedby USER 1

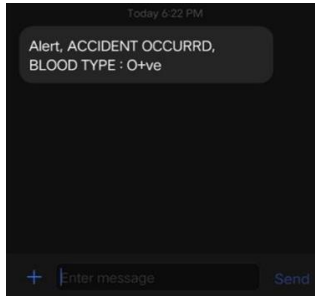


Fig. 9 SMS Received by USER 2

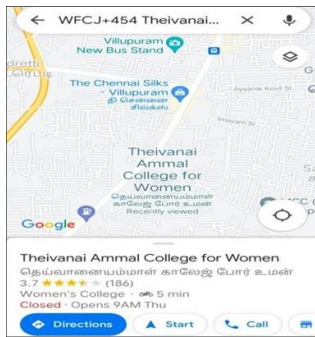


Fig.10 Location of the Mishap



Fig.11IR Sensor detects the object

CONCLUSION

This paper has successfully implemented the plan of two setups which is combined into one module to detect the mishap and send detailed data about the victim and mishap area progressively. When the mishap occurred, the received vibration of the vehicle will be sensed by the Vibration sensor. Then the details data is transferred to the salvages groups. This setup improves the communication level between the groups by making it faster. This setup helps to prevent the loss of life and also reduce the gridlocks caused by the mishap. The setup two is succeeded by getting the buzzer sound when any objects like vehicles or any other that approaches the client's vehicle within the 10feet distance. Thus the setup two is succeeded by using IR sensor. This paper concludes the improved mishap detections and quick communication to the salvage group by saving the victim's life and prevents the mishaps to be occurred.

FUTURE ENHANCEMENT

Up to this point, the system can collect data successfully from sensors and communicates with GSM/GPS using microcontroller. In upcoming future, this system can be improved by developing an android app that contains data like photos, names, age, blood groups and health status records of who are travelling in a vehicle. This enhancement further includes the notice of mishap aware at minimum of three nearest hospitals if critically occurs and shows the shortest lane to get to the mishap spot. The one more process is, if the mishap is not that much of cause, the victim would be able to send the message that sent to the salvage systems.

REFERENCES

1. Khan.A.R., Suri.P, Tejaswani.S.P., Paigude.T.A. "Automatic Accident Detection". International Journal for Engineering Science and computer-, Volume 8, Issue March 2018.
2. Bhoite, P.A., Gopal, K., Saga, W., Sisodia, T., Satish, P. "Accident Detection System Using Arduino", International Science and technology journal- Volume 7, Issue 4, 2018.
3. S. G. Fernandez, R. Palanisamy, K. Vijayakumar "GPS & GSM Based Accident Detection and Auto Intimation", Indonesian Journal of Electrical Engineering and Computer Science. Vol.11, No.1, July 2018, pp 336-361.

4. Al Wadhahi, N.T.S., Hussain, S.M., Yosof, K.M., Hussain, S.A. and Singh, A.V., 2018, August. Accidents Detection and Prevention System to reduce Traffic Hazards using IR Sensors. In 2018 7th International Conference on Reliability, Infocom Technologies and Optimization (Trends and Future Directions) (ICRITO) (pp. 737-741). IEEE.
5. K. Sangeetha, P. Archana, M. Ramya, P. Ramya. IOSR Journal of Engineering (IOSRJEN), Vol. 04, Issue 02 (February. 2014) | V5 | PP 53-57.
6. Shaik, A., Bowen, N., Bole, J., Kunzi, G., Bruce, D., Abdelgawad, A. and Yelamarthi. K., 2018, December. Smart car: An IoT based accident detection system. In 2018 IEEE Global Conference on Internet of Things (GCIoT) (pp. 1-5).
7. Jung Lee, "An accident detection system on highway through CCTV with calogero-moser system", Conference on Communications (APCC) 2012 18th Asia-Pacific.
8. Yong-Kul Ki, Jin-Woo Kim and Doo-Kwon Baik, "A Traffic Accident Detection Model using Metadata Registry", Conference on Software Engineering Research Management and Applications, 2006.
9. Md. Syedul, Jubayer Amin, M Jalil and B.I.Reaz, "Accident Detection and Reporting System using GPS GPRS and GSM Technology", IEEE/OSAIIAPR International Conference on Informatics Electronics & Vision in 2012.
10. Kattukkaran, N., George, A. and Haridas, T.M., 2017, January. Intelligent accident detection and alert system for emergency medical assistance. In 2017 International Conference on Computer Communication and Informatics (ICCCI) (pp. 1-6). IEEE.
11. N. Virtanen, A. Schirokoff, and J. Luoma, "Impacts of an automatic emergency call system on accident consequences," in 18th ICTCT Workshop: Transport Telematics and Safety, Helsinki, Finland, 2005.
12. R. K. Megalingam, R. N. Nair, and S. M. Prakhya, "Wireless Vehicular Accident Detection and Reporting System, " in 2nd International Conference on Mechanical and Electrical Technology (ICMET), Singapore, 2010, pp. 636-640.

P. Vishna Priya*, **R. Charulatha**** & **A Sathyavathi****

**Assistant professor, PG and Research Department of Mathematics, Theivanai Ammal College for women (Autonomous), Villupuram, Tamilnadu*

*** PG and Research department of Mathematics, Theivanai Ammal College for Women (Autonomous), Villupuram, Tamilnadu*

ABSTRACT

In this paper we use fuzzy inference system (Mamdani model) to analyse the college atmosphere through circulating questionnaires among students.

Keywords: *Membership functions, Fuzzification, Defuzzification, Fuzzy Inference System, Mamdani model.*

INTRODUCTION:

Preliminaries:

Lotfi Zadeh developed a kind of fuzzy logic controller known as the Mamdani model in the 1970s. In systems where there is ambiguous or imprecise information, it is utilized for decision-making. The model can be applied in a variety of domains, including expert systems, artificial intelligence, and control systems. It mimics human reasoning by using fuzzy rules and language variables

MEMBERSHIP FUNCTIONS:

The Sigmoidal function:

Sigma ($x, [a, c]$), as given in the following equation by $f(x, a, c)$ is a mapping on a vector x , and depends on two parameters a and c

$$f(x; \sigma, c) = \frac{1}{1 + e^{-a(x-c)}}, \text{ } a \text{ is slope and } c \text{ is crossover point.}$$

THE GAUSSIAN FUNCTION:

The symmetric Gaussian function depends on two parameters σ and c as given by

$$f(x; \sigma, c) = e^{-\frac{(x-c)^2}{2\sigma^2}}, c \text{ is center and } \sigma \text{ is width.}$$

THE TRAPEZOIDAL FUNCTION:

The trapezoidal curve is a function of a vector, x , and depends on four scalar parameters a, b, c , and d , as given by,

$$f(x; a, b, c, d) = \max\left\{\min\left[\frac{x-a}{b-a}, 1, \frac{d-x}{d-c}\right], 0\right\}$$

FUZZIFICATION:

Input variables are assigned degrees of membership in various classes.

The purpose of fuzzification is to map the inputs from a set of sensors (or features of those sensors) to values from 0 to 1 using a set of input membership functions.

E.g. A temperature input might be graded according to its degree of coldness, coolness, warmth or heat

DEFUZZIFICATION:

Fuzzy outputs are combined into discrete values needed to drive the control mechanism. (e.g. A cooling fan).

FUZZY INFERENCE SYSTEM:

The process of creating a fuzzy logic mapping from a given input to an output is known as fuzzy inference. After that, the mapping offers a foundation on which judgments can be formed or trends identified. Fuzzy inference incorporates all of the components of,

- Membership Functions
- Logical Operations
- If-Then Rules.

MAMDANI MODEL:

Mamdani-style inference anticipates fuzzy sets as the output membership functions. Each output variable has a fuzzy set following the aggregation process that needs to be defuzzed.

To solve a Mamdani model, we follow these steps:

1. Input Fuzzification:

Convert crisp input values into fuzzy sets using the defined membership functions.

2. Rule Evaluation:

Using the fuzzy input values as a basis, apply the fuzzy rules to find each rule's degree of membership.

3. Aggregation of Rule Outputs:

Combine the output memberships of all applicable rules.

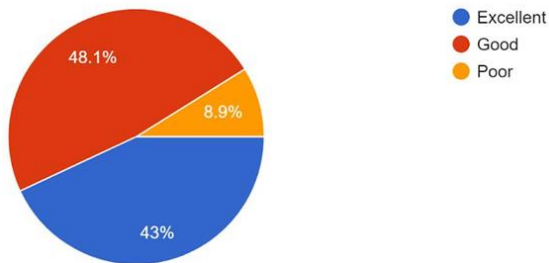
4. Defuzzification:

Convert the aggregated fuzzy output into a crisp value.

The above process is executed in python by collecting data through : <https://forms.gle/T8epqu1fzXYsQkpT6>

Data collected in pie chart format

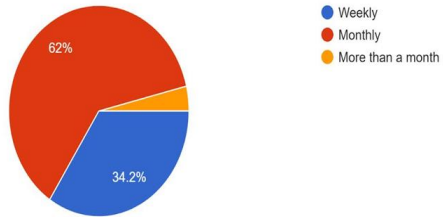
1. How will you characterize the academic atmosphere in the college ?
79 responses



Noval Innovations and Technologies in Computational 104

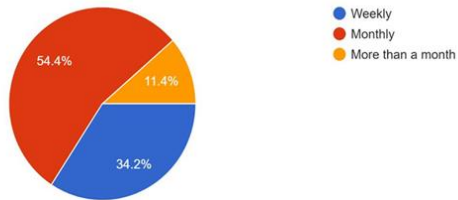
2. How often do your college conduct social activities ?

79 responses



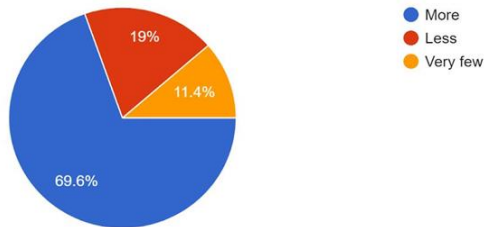
3. How often do your college conduct extracurricular activities?

79 responses



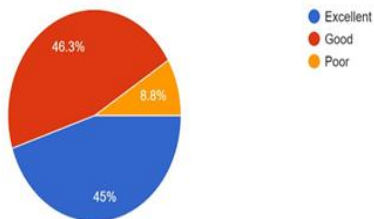
4. How diverse is the students in your college?

79 responses



5. How are the recreational activities (Eg:reading, dancing, singing) & other facilities in campus?

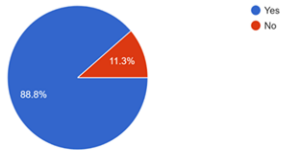
80 responses



Noval Innovations and Technologies in Computational 105

6. Does your college conducts any notable annual / traditional events that contributes to the college atmosphere?

80 responses



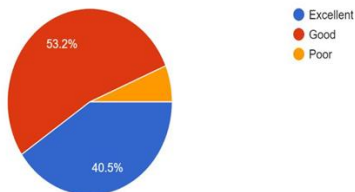
7. Do you feel safe in your campus?

80 responses



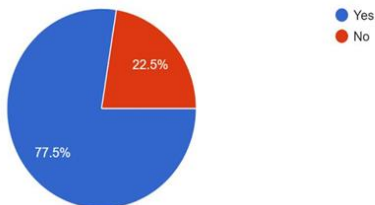
8. How is the support system for students such as counselling and academic advising?

79 responses

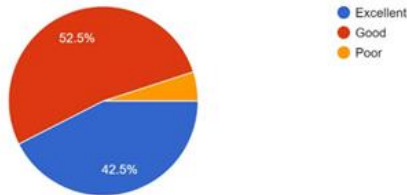


9. Are there any opportunities for students to engage with the surrounding areas ?

80 responses



10. How will you describe the overall atmosphere in campus ?
80 responses



Mamdani model in Python coding :

```
import numpy as nps
import matplotlib.pyplot as plt
def triangular(x, a, b, c):
result= np. Zeros like(x)
mask1 = (x >= a) & (x < b) & (b != a)
mask2 = (x >= b) & (x <= c) & (c != b)
result[mask1] = (x[mask1] - a) / (b - a)
result[mask2] = (c - x[mask2]) / (c - b)
return np.clip(result, 0, 1)
academic_atmosphere = np.arange(0, 101, 1)
academic_atmosphere = np.arange(0, 101, 1)
extracurricular_activities = np.arange(0, 101, 1)
diversity_of_students = np.arange(0, 101, 1)
recreational_activities = np.arange(0, 101, 1)
annual_events = np.arange(0, 101, 1)
securedness = np.arange(0, 101, 1)
support_system = np.arange(0, 101, 1)
surrounding_area_engagement = np.arange(0, 101, 1)
overall_atmosphere = np.arange(0, 101, 1)
excellent_academic_atmosphere=triangular(academic_atmosphere, 0, 43,100)
```

good_academic_atmosphere = triangular(academic_atmosphere, 0, 48, 100)

poor_academic_atmosphere = triangular(academic_atmosphere, 0, 9, 100)

weekly_social_activities = triangular(social_activities, 0, 34, 100)

monthly_social_activities = triangular(social_activities, 0, 62, 100)

more_than_a_month_social_activities=triangular(social_activities, 0, 4, 100)

weekly_extracurricular_activities=triangular(extracurricular_activities, 0, 34,100)

monthly_extracurricular_activities=triangular(extracurricular_activities, 0, 54, 55)

more_than_a_month_extracurricular_activities=triangular(extracurricular_activities, 0, 12, 100)

more_diversity_of_students = triangular(diversity_of_students, 0, 70, 100)

less_diversity_of_students = triangular(diversity_of_students, 0, 19, 100)

very_few_diversity_of_students=triangular(diversity_of_students, 0, 11, 100)

excellent_recreational_activities=triangular(recreational_activities, 0, 45 , 100)

good_recreational_activities = triangular(recreational_activities, 0, 46 , 100)

poor_recreational_activities = triangular(recreational_activities, 0, 9 , 100)

yes_annual_events = triangular(annual_events, 0, 89, 100)

no_annual_events = triangular(annual_events, 0 , 11 , 100)

yes_securedness = triangular(securedness, 0, 100, 100)

no_securedness = triangular(securedness, 0, 0, 100)

excellent_support_system = triangular(support_system, 0, 41, 100)

```

good_support_system = triangular(support_system, 0, 53,100)
poor_support_system = triangular(support_system, 0, 2, 100)
yes_surrounding_area_engagement=triangular(surrounding_are
a_engagement, 0, 78 , 77)
no_surrounding_area_engagement=triangular(surrounding_are
a_engagement, 0, 22, 100)
excellent_overall_atmosphere = triangular(overall_atmosphere,
0, 43, 100)
good_overall_atmosphere = triangular(overall_atmosphere, 0,
52, 100)
poor_overall_atmosphere = triangular(overall_atmosphere, 0, 5,
100)
plt.plot(academic_atmosphere, excellent_academic_atmosphere,
label='excellent academic atmosphere')
plt.plot(academic_atmosphere, good_academic_atmosphere,
label='good academic atmosphere')
plt.plot(academic_atmosphere,poor_academic_atmosphere,label
='poor academic atmosphere') plt.legend()
plt.title('Academic Atmosphere Membership Functions')
plt.xlabel('Academic Atmosphere')
plt.ylabel('Membership Degree')
plt.show()
plt.plot(social_activities, weekly_social_activities, label='weekly
social activities')
plt.plot(social_activities,monthly_social_activities,label='monthl
y social activities')
plt.plot(social_activities,more_than_a_month_social_activities,
label='more than a month social activities')

plt.legend()
plt.title('Social Activities Membership Functions')
plt.xlabel('Social Activities')
plt.ylabel('Membership Degree')

```

```

plt.show()

overall_atmosphere_membership = np.fmax(np.fmax(np.fmax(
np.fmin(excellent_academic_atmosphere,weekly_social_activitie
s),
np.fmin(good_academic_atmosphere,monthly_extracurricular_a
ctivities)
np.fmin(poor_academic_atmosphere,more_than_a_month_social
_activities)), ...)

# Combine membership functions of other rules as needed

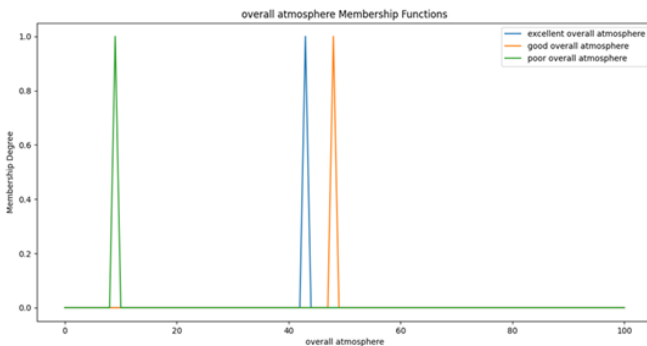
# Defuzzify the aggregated membership function to obtain crisp
characterization

defuzzified_atmosphere=np.sum(overall_atmosphere*overall_at
mosphere_membership)/np.sum(overall_atmosphere_membersh
ip)

# Determine crisp characterization based on defuzzified value
if defuzzified_atmosphere < 33.3:
characterization = "Poor"
elif defuzzified_atmosphere < 66.6:
characterization = "Good"
else:
characterization = "Excellent"

print(f"Overall Atmosphere Characterization: {characterization}")

```



INFERENCE

Hence the excellent overall atmosphere has a range of 40-50%,

The good overall atmosphere has a range of 50-60%,

The poor overall atmosphere has a range of 0-10%.

*(Every triangular membership functions has its peak at 1 since the declaration is such that it has atmost value at 1)

CONCLUSION

The aim of the work is to model and analyse data coming from responses to questionnaires of college atmosphere. The method used is Fuzzy Inference System (FIS) specifically Mamdani model is used in python. Also we may quickly determine an institution's overall performance if we have knowledge of a few of its components. The model can manage uncertainties and offer a more thorough evaluation by building fuzzy sets and rules based on these variables.

REFERENCES

1. Fuzzy set theory fuzzy logic and their applications" , S.Chand & company pvt ltd
2. "Journal of artificial socities and social simulation 21(3) 2"
<https://www.jass.org/21/3/2.html>
3. [https://www.sciencedirect.com/topics/mathematics/fuzzy-set-theory#:~:text=Fuzzy%20set%20theory%20was%20initiated,transitive%20fuzzy%20relation%20\(see%20II.](https://www.sciencedirect.com/topics/mathematics/fuzzy-set-theory#:~:text=Fuzzy%20set%20theory%20was%20initiated,transitive%20fuzzy%20relation%20(see%20II.)
4. https://www.philadelphia.edu.jo/academics/qhamarshseh/uploads/Lecture%2018_Difference%20Types%20of%20Membership%20Functions%201.pdf
5. https://www.researchgate.net/profile/Mohamed-Mourad-Lafifi/post/What_is_the_greatest_lower_bound_for_fuzzy_gaussian_membership_function_Is_it_as_trivial_as_the_value_0/attachment/59ds6507379197b80779a9474/AS%3A502963024400384%401496927137203/download/4-membership-functions.pdf
6. <https://www.engpaper.com/free-research-papers-and-projects-on-fuzzy-logic.html>

Multiple Attribute Group Decision Making Problem Using Intuitionistic Triangular Fuzzy Numbers with Runge-Kutta Method

S. Jenifer rose*, K. Gopika** & K. Shruthi**

* Assistant Professor, Department of Mathematics Theivanai Ammal College for Women (Autonomous), Villupuram, Tamil Nadu

** Department of Mathematics, Theivanai Ammal College for women (Autonomous), Villupuram, Tamil Nadu

ABSTRACT

Solving one of the most important researches in the recent trends becomes (MAGDM) Multiple Attribute Group Decision Making problems. The information or data is in the form of Intuitionistic Triangular Fuzzy Number (ITrFN). The methods are applied in decision making problems using second, third and fourth order in Runge-Kutta methods. The Intuitionistic Triangular Fuzzy Weighted Geometric (ITrFWG) operator and the Intuitionistic Triangular Fuzzy Hybrid Geometric (ITrFHG) operator are used to combine the decision matrix. The correlation coefficient is used for ranking the best alternatives. To show the effectiveness of the method by Numerical illustration.

Keywords: MAGDM, Intuitionistic Trapezoidal Fuzzy Number, ITrFWG, ITrFHG using Runge-Kutta Methods.

1. INTRODUCTION

Multiple Attribute Group Decision Making problems are wide spread in real life condition. In the process of MAGDM problems with intuitionistic fuzzy information and the attribute values taken in the form of intuitionistic triangular fuzzy number. A MAGDM problem is to find a desirable solution from a finite number of feasible alternatives assessed on multiple attribute quantitative and qualitative. Atanassov [1,2] are introduced the concept of intuitionistic fuzzy set (IFS) and characterized by a membership and a non-membership function, which is generalization of the concept of fuzzy set. Atanassov & Gargov [3] are research the concept of interval valued intuitionistic fuzzy sets. Atanassov [4,5] are proposed some operators over interval valued intuitionistic fuzzy sets and new operations defined over

the intuitionistic fuzzy sets. Burillo [6] are provide the definition of intuitionistic fuzzy number. John Robinson & Amirtharaj [7,8] are proposed a short primer on the correlation co-efficient of vague sets and a search for the correlation co-efficient of triangular and trapezoidal intuitionistic fuzzy sets for multiple attribute group decision making

Aggregation operators with MAGDM problems are used in the field of mathematics, physics, economics, natural sciences, computer engineering and so on. Jenifer Rose & Akila [11] are introduced multiple attribute group decision making methods using intuitionistic triangular fuzzy set. Wei Wu et al. [14,15] are proved by some arithmetic aggregation with intuitionistic trapezoidal fuzzy numbers and their application to group decision making and an approach to multiple attribute group decision making with interval intuitionistic trapezoidal fuzzy information. J. R. Dormand, P. J. Prince,[17] A family of embedded Runge-Kutta formula Kanthasami thilagavathi [16] are using second, third, fourth method by runge-kutta methods in numerical methodology. In this paper basic concepts of IFS, ITrFN and Intuitionistic trapezoidal fuzzy sets are presented. Some aggregation operators are discussed and the procedure for decision making using the correlation co-efficient for ITrFNs is also presented. A numerical example is proposed to explain the developed decision making model.

2. BASIC DEFINITIONS

2.1 TRIANGULAR FUZZY NUMBER

A Fuzzy Number $\tilde{A}(a_1, a_2, a_3)$ is a Triangular fuzzy number if its membership function $\mu_{\tilde{A}}(x)$ is given by

$$\mu_{\tilde{A}}(x) = \begin{cases} \frac{x - a_1}{a_2 - a_1}, & a_1 \leq x \leq a_2, \\ \frac{x - a_3}{a_2 - a_3}, & a_2 \leq x \leq a_3 \text{ where } a_1, a_2, a_3 \text{ are real numbers} \\ 0, & \text{otherwise.} \end{cases}$$

2.2 INTUITIONISTIC TRIANGULAR FUZZY NUMBER (ITrFN)

A ITrFN is an IFS in R with the following membership function $\mu_A(x)$ and non-membership function $\gamma_A(x)$:

$$\mu_A(x) = \begin{cases} \frac{x - a_1}{a_2 - a_1}, & \text{for } a_1 \leq x \leq a_2, \\ \frac{a_3 - x}{a_3 - a_2}, & \text{for } a_2 \leq x \leq a_3, \\ 0, & \text{otherwise.} \end{cases} \gamma_A(x) = \begin{cases} \frac{x - a_1}{a_2 - a_1'}, & a_1' \leq x \leq a_2, \\ \frac{a_3 - x}{a_3' - a_2'}, & a_2 \leq x \leq a_3', \\ 1, & \text{otherwise.} \end{cases}$$

Here $a_1' \leq a_1 \leq a_2 \leq a_3 \leq a_3'$, This ITrFN is denoted by $(a_1, a_2, a_3; a_1', a_2, a_3')$. This ITrFN is also stated as:

$$A = \left\langle ([a_1, a_2, a_3]; \mu_A), ([a_1', a_2, a_3']; \nu_A) \right\rangle.$$

Let $a_1 = ([a_1, b_1, c_1]; u_{a_1}^-, v_{a_1}^-)$, $a_2 = ([a_2, b_2, c_2]; u_{a_2}^-, v_{a_2}^-)$ be two intuitionistic triangular fuzzy numbers. Then,

1. $a_1 + a_2 = ([a_1 + a_2, b_1 + b_2, c_1 + c_2]; u_{a_1}^- + u_{a_2}^- - u_{a_1}^- u_{a_2}^-, v_{a_1}^- \cdot v_{a_2}^-)$
2. $a_1 \cdot a_2 = ([a_1 \cdot a_2, b_1 \cdot b_2, c_1 \cdot c_2]; u_{a_1}^- \cdot u_{a_2}^- - u_{a_1}^- + u_{a_2}^-, v_{a_1}^- \cdot v_{a_2}^-)$
3. $\lambda a_1 = ([\lambda a_1, \lambda b_1, \lambda c_1]; 1 - (1 - u_{a_1}^-) \lambda, v_{a_1}^- \lambda), \lambda \geq 0$
4. $a_1^\lambda = ([a_1^\lambda, b_1^\lambda, c_1^\lambda]; (u_{a_1}^-)^\lambda, 1 - (1 - v_{a_1}^-)^\lambda), \lambda \geq 0$

3. AGGREGATION OPERATORS ON INTUITIONISTIC FUZZY SETS

3.1 BASIC DEFINITIONS

Definition 1: Let $\alpha_i (i = 1, 2, \dots, n)$ be a collection of intuitionistic triangular fuzzy number, and let operators on intuitionistic triangular fuzzy set weighted geometric $ITrFWG : \Omega^n \rightarrow \Omega$, if

$$\begin{aligned} ITrFWG_W(\alpha_1, \alpha_2, \dots, \alpha_n) &= \prod_{i=1}^n \alpha_i^{w_i} \\ &= \left(\left[\prod_{i=1}^n (a_i)^{w_i}, \prod_{i=1}^n (b_i)^{w_i}, \prod_{i=1}^n (c_i)^{w_i} \right]; \prod_{i=1}^n (u_{\alpha_i})^{w_i}, 1 - \prod_{i=1}^n (1 - v_{\alpha_i})^{w_i} \right) \end{aligned}$$

Definition 2: Let $\alpha_i (i = 1, 2, \dots, n)$ be a collection of intuitionistic triangular fuzzy number. A intuitionistic triangular fuzzy hybrid

geometric (ITrFHG) operator of dimension n is a mapping $ITrFHG : \Omega^n \rightarrow \Omega$, which has an associated vector $w = (w_1, w_2, \dots, w_n)^T$ with $\sum_{i=1}^n w_i = 1, w_i \in [0, 1]$ such that

$$ITrFWG_{\omega, w}(\alpha_1, \alpha_2, \dots, \alpha_n) = \beta_{\sigma(1)}^{w_1} \otimes \beta_{\sigma(2)}^{w_2} \otimes \dots \otimes \beta_{\sigma(n)}^{w_n}$$

$$= \left(\prod_{i=1}^n (a_{\sigma(i)})^{w_i}, \prod_{i=1}^n (b_{\sigma(i)})^{w_i}, \prod_{i=1}^n (c_{\sigma(i)})^{w_i} \right); \prod_{i=1}^n (u_{\beta_{\sigma(i)}})^{w_i}, 1$$

$$- \prod_{i=1}^n (1 - v_{\beta_{\sigma(i)}})^{w_i}$$

Where, $\beta_{\alpha(i)}$ is the i th largest of the weighted intuitionistic triangular fuzzy number $\beta_i(\beta_i, \alpha_i (i = 1, 2, \dots, n))$ $\omega = (\omega_1, \omega_2, \dots, \omega_n)$ is weight vector of $\alpha_i (i = 1, 2, \dots, n)$ with $\sum_{i=1}^n w_i = 1, \omega_i \in [0, 1]$.

3.2 INTUITIONISTIC FUZZY WEIGHTED GEOMETRIC OPERATOR

Let $\alpha_j = (\mu_{\alpha_j}, \nu_{\alpha_j}) (j = 1, 2, \dots, n)$ be a collection of IFNs, and let $IFWG : \theta^n \rightarrow \theta$ explained as:

If $IFWG_w(\alpha_1, \alpha_2, \dots, \alpha_n) = w_1 \alpha_1 \oplus w_2 \alpha_2 \oplus \dots, w_n \alpha_n$ Then the function IFWG is called an intuitionistic fuzzy weighted averaging (IFWG) operator, where $w = (w_1, w_2, \dots, w_n)^T$ is the weight vector of $\alpha_j, (j = 1, 2, \dots, n)$, with $w_j \in [0, 1]$.

3.3 INTUITIONISTIC FUZZY HYBRID GEOMETRIC OPERATOR

Let $\tilde{\alpha}_j (j = 1, 2, \dots, n)$ be a collection of intuitionistic fuzzy numbers.

An Intuitionistic Fuzzy Hybrid Geometric (IFHG) operator of dimension n is a mapping $IFHG : \Omega^n \rightarrow \Omega$ that has an associated

vector $\omega = (\omega_1, \omega_2, \dots, \omega_n)^T$ such that $\omega_j \in [0, 1]$ and $\sum_{j=1}^n \omega_j = 1$.

$IFHG_{\omega, w}(\tilde{\alpha}_1, \tilde{\alpha}_1, \dots, \tilde{\alpha}_n) = \ddot{\tilde{\alpha}}_{\sigma(1)}^{\omega_j} \otimes \ddot{\tilde{\alpha}}_{\sigma(2)}^{\omega_j} \dots \otimes \ddot{\tilde{\alpha}}_{\sigma(n)}^{\omega_j}$ where $\ddot{\tilde{\alpha}}_{\sigma(j)}^{\omega_j}$ is

the j th largest of the weighted intuitionistic fuzzy numbers

$\ddot{\tilde{\alpha}}_j^{\omega_j} (\ddot{\tilde{\alpha}}_j^{\omega_j} = \ddot{\tilde{\alpha}}_j^{n\omega_j}, j = 1, 2, \dots, n)$. $w = (w_1, w_2, \dots, w_n)^T$ is the

weight vector of $\tilde{\alpha}_j$ with $w_j \in [0, 1]$ and $\sum_{j=1}^n w_j = 1$, and n is the

balancing coefficient, in such case, if the vector

$$w = (w_1, w_2, \dots, w_n)^T \text{ approaches } (1/n, 1/n, \dots, 1/n)^T, \text{ then the}$$

$$\text{Vector } (\tilde{\alpha}_1^{n\omega_1}, \tilde{\alpha}_1^{n\omega_2}, \dots, \tilde{\alpha}_1^{n\omega_n})^T \text{ approaches } (\tilde{\alpha}_1, \tilde{\alpha}_1, \dots, \tilde{\alpha}_n)^T.$$

$$\text{IFHG}_{w,\omega}(\tilde{\alpha}_1, \tilde{\alpha}_1, \dots, \tilde{\alpha}_n) = \prod_{j=1}^n \tilde{\alpha}_{\sigma(j)}^{\omega_j} = \left(\prod_{j=1}^n \tilde{\mu}_{\tilde{\alpha}_{\sigma(j)}}^{\omega_j}, 1 - \prod_{j=1}^n (1 - \tilde{\nu}_{\tilde{\alpha}_{\sigma(j)}}^{\omega_j}) \right)^{\omega_j}.$$

4. AN APPROACH TO GROUP DECISION MAKING WITH INTUITIONISTIC TRIANGULAR FUZZY INFORMATION

Let $A = \{A_1, A_2, \dots, A_n\}$ be a discrete set of alternatives, and $G = \{G_1, G_2, \dots, G_n\}$ be the set of attributes, $w = \{w_1, w_2, \dots, w_n\}$ is the weighting vector of the attribute $G_j (j = 1, 2, \dots, n)$ where $w_j \in [0, 1] \sum_{j=1}^n w_j = 1$ Let

$D = \{D_1, D_2, \dots, D_t\}$ be the set^{j=1} of decision makers, $\omega = \{\omega_1, \omega_2, \dots, \omega_p\}$ be the weighting vector of decision makers, with $\omega_j \in [0, 1] \sum_{j=1}^p \omega_j = 1$ Suppose that,

$R_k = \left(\tilde{r}_{ij}^{(k)} \right)_{m \times n} = \left([a_{ij}^{(k)}, b_{ij}^{(k)}, c_{ij}^{(k)}]; \mu_{ij}^{(k)}, \nu_{ij}^{(k)} \right) 0 \leq a_{ij}^{(k)} \leq b_{ij}^{(k)} \leq c_{ij}^{(k)} \leq 1$
 $0 \leq \mu_{ij}^{(k)} + \nu_{ij}^{(k)} \leq 1$ is the normalized intuitionistic triangular fuzzy decision matrix, where $i = 1, 2, \dots, n; j = 1, 2, \dots, n; k = 1, 2, \dots, t$. Then the intuitionistic triangular fuzzy positive ideal solution and intuitionistic triangular fuzzy negative ideal solution are defined as follows: $r^+ = \left([a^+, b^+, c^+]; \mu^+, \nu^+ \right) = \left([1, 1, 1]; 1, 0 \right)$, $r^- = \left([a^-, b^-, c^-]; \mu^-, \nu^- \right) = \left([0, 0, 0]; 0, 1 \right)$. In the following, the ITrFWG and ITrFHG operator are applied to MAGDM problem based on intuitionistic triangular fuzzy information

4.1 METHODS OF RUNGE-KUTTA:

4.1.1 SECOND ORDER METHOD :

The Runge-Kutta second order method is a numerical technique used to solve an ordinary differential equation of the form

$$\frac{dy}{dx} = f(x, y), \quad y(x_0) = y_0.$$

The second order becomes,

$$y_{i+1} = y_1 + \frac{1}{2} (K+L)$$

With $K = h f(x_i, y_i)$

$L = h f(x_i+h, y_i+K)$ For $i = 0, 1, 2, \dots, n$.

4.1.2 THIRD ORDER METHOD :

The Runge-Kutta third order method is a numerical technique used to solve an ordinary differential equation of the form

$$\frac{dy}{dx} = f(x, y), \quad y(x_0) = y_0.$$

Third order method becomes,

$$y_{i+1} = y_i + \frac{h}{6} (K + 4L + M)$$

Where $K = f(x_i, y_i)$

$$L = f(x_i + \frac{1}{2}h, y_i + \frac{1}{2}hK)$$

$$M = f(x_i + h, y_i - hK + 2hL)$$

4.1.3 FOURTH ORDER METHOD :

The Runge-Kutta fourth order method is a numerical technique used to solve an ordinary differential equation of the form

$$\frac{dy}{dx} = f(x, y), \quad y(x_0) = y_0.$$

fourth order method becomes,

$$y_{i+1} = y_i + \frac{1}{6} (k + 2L + 2M + P)$$

Where $K = h f(x_i, y_i)$

$$L = h f(x_i + \frac{1}{2}h, y_i + \frac{1}{2}K)$$

$$M = h f(x_i + \frac{1}{2}h, y_i + \frac{1}{2}L)$$

$$P = h f(x_i + h, y_i + M).$$

4.2 EXAMPLES:

4.2.1 SECOND ORDER METHOD

Do the steps of Runge-Kutta methods of second order for the equation

$$\frac{dy}{dx} = x+y ; y(1)=2; h=0.2$$

Given: $\frac{dy}{dx} = x+y ; y(1)=2; h=0.2$

Since $\frac{dy}{dx} = f(x,y) ; y(x_0)=y_0; h=0.2$

Therefore, $h=0.2, x_0 = 1, y_0 = 2, f(x,y) = x+y$

Then by using second order method,

$$Y_{i+1} = y_1 + (\frac{1}{2}) (K + L)$$

where,

$$K = hf(x_i, y_i)$$

$$L = hf(x_i + h, y_i + K)$$

Iteration 1:

Put $i=0$

$$K = hf(x_i, y_i)$$

$$= (0.2) (1+2)$$

$$K = 0.6$$

$$L = hf(x_i + h, y_i + K)$$

$$= (0.2) [(1+0.2)+(2+0.6)]$$

$$L = 0.76$$

$$Y_{i+1} = y_i + (1/2) (K + L)$$

$$Y_1 = 2 + (1/2) (0.6 + 0.76)$$

$$\mathbf{Y_1 = 2.68}$$

Similarly,

$$Y_2 = 3.5536, Y_3 = 4.7, Y_4 = 6.6$$

Now, $Y = y_1 + y_2 + y_3 + y_4$

$$= 2.68 + 3.5536 + 4.7 + 6.6$$

$$\mathbf{Y = 17.5336}$$

$$\omega_1 = y_1 / Y$$

$$= 2.68 / 17.5336$$

$$\omega_1 = 0.1528$$

similarly,

$$\omega_2 = 0.2026$$

$$\omega_3 = 0.268$$

$$\omega_4 = 0.3764$$

Therefore,

$$\omega = (0.1528, 0.2026, 0.268, 0.3764) \dots \dots \dots (1)$$

4.2.2 THIRD ORDER METHOD

Do the steps of Runge-Kutta methods of third order for the equation

$$\frac{dy}{dx} = 2xy ; y(0)=1; h=0.1$$

Given:

$$\frac{dy}{dx} = 2xy ; y(0)=1; h=0.1$$

Since $\frac{dy}{dx} = f(x,y) ; y(x_0)=y_0; h=0.1$

Therefore, $h=0.1, x_0 = 0, y_0 = 1, f(x,y) = 2xy$

Using 3rd ordered method

$$Y_{i+1} = y_i + (h/6) (K + 4L + M)$$

where,

$$K = f(x_i, y_i)$$

$$L = f[x_i + (1/2)h, y_i + (1/2)hK]$$

$$M = f(x_i + h, y_i -hk + 2hL)$$

Iteration 1:

Put $i=0$

$$K = f(x_i, y_i)$$

$$= 2(0)(1)$$

$$K = 0$$

$$L = f[x_i + (1/2)h, y_i + (1/2)hK]$$

$$= [(0+(1/2)(0.1) + 1+(1/2)(0.1)]$$

$$L = 1.1$$

$$M = f(x_i + h, y_i -hk + 2hL)$$

$$=(0+0.1 + 1-(0.1)(0) + 2(0.1)(1.1))$$

$$M = 0.156$$

$$Y_{i+1} = y_i + (h/6) (K + 4L + M)$$

$$Y_1 = 1(0.1/6) (0+4(1.1)+0.078)$$

$$Y_1 = 1.0759$$

Similarly,

$$Y_2 = 1.1039$$

$$Y_3 = 1.1605$$

$$Y_4 = 1.2447$$

Now, $Y = y_1 + y_2 + y_3 + y_4$

$$= 1.0759 + 1.1039 + 1.1605 + 1.2447$$

$$Y = 4.585$$

$$\omega_1 = y_1 / Y$$

$$= 1.0759 / 4.585$$

$$\omega_1 = 0.2346$$

similarly,

$$\omega_2 = 0.2407$$

$$\omega_3 = 0.2531$$

$$\omega_4 = 0.2714$$

Therefore,

$$\omega = (0.2346, 0.2407, 0.2531, 0.2714) \dots \dots \dots (2)$$

4.2.3 FOURTH ORDER METHOD

Do the steps of Runge-Kutta methods of fourth order for the equation

$$\frac{dy}{dx} = x+y ; y(1)=0; h=0.1$$

Given:

$$\frac{dy}{dx} = x+y ; y(1)=0; h=0.1$$

Since $\frac{dy}{dx} = f(x,y) ; y(x_0)=y_0; h=0.1$

Therefore, $h=0.1, x_0 = 1, y_0 = 0, f(x,y)= x+y$

Using Fourth Order Method: $Y_{i+1} = y_i + (\frac{1}{6}) (K + 2L + 2M + P)$

where,

$$K = hf(x_i, y_i)$$

$$L = hf[x_i + (\frac{1}{2}) h, y_i + (\frac{1}{2})K]$$

$$M = hf[x_i + (\frac{1}{2}) h, y_i + (\frac{1}{2})L]$$

$$P = hf(x_i + h, y_i + M)$$

Iteration 1:

Put $i=0$

$$\begin{aligned} K &= hf(x_i, y_i) \\ &= (0.1) (1 + 0) \end{aligned}$$

$$K = 1.1$$

$$L = hf[x_i + (\frac{1}{2}) h, y_i + (\frac{1}{2})K]$$

$$L = 0.16$$

$$\begin{aligned} M &= hf[x_i + (\frac{1}{2}) h, y_i + (\frac{1}{2})L] \\ &= 0.1 (1+(\frac{1}{2})0.1+ 0+(\frac{1}{2})0.16) \end{aligned}$$

$$M = 0.018$$

$$\begin{aligned} P &= hf(x_i + h, y_i + M) \\ &= 0.1f(1 + 0.1, 0 + 0.018) \end{aligned}$$

$$P = 0.1118$$

$$Y_{i+1} = y_i + (\frac{1}{6}) (K + 2L + 2M + P)$$

$$Y_1 = 0+(1/6) (1.1 + 2(0.16) + 2(0.018) + 0.1118)$$

$$Y_1 = 0.2623$$

Similarly,

$$Y_2 = 0.41$$

$$Y_3 = 0.5847$$

$$Y_4 = 1.448$$

$$\begin{aligned} \text{Now, } Y &= y_1+y_2+y_3+y_4 \\ &= 0.2623 + 0.41 + 0.5847 + 1.448 \end{aligned}$$

$$Y = 2.705$$

$$\begin{aligned} \omega_1 &= y_1 / Y \\ &= 0.2623 / 2.705 \end{aligned}$$

$$\omega_1 = 0.097$$

similarly,

$$\omega_2 = 0.1515$$

$$\omega_3 = 0.2161$$

$$\omega_4 = 0.5353$$

Therefore,

$$\omega = (0.097, 0.1515, 0.2161, 0.5353) \dots \dots \dots (3)$$

5. ALGORITHM :

In the following, to apply the Intuitionistic Fuzzy Weighted Geometric (ITrFWG) operator and in the Multiple Attribute Group Decision Making (MAGDM) problem based on intuitionistic fuzzy information. The method involves the following steps:

Step 1: To obtain the intuitionistic fuzzy matrix.

Step 2: Utilize the intuitionistic triangular fuzzy weighted geometric

$$ITrFWG_w(\alpha_1, \alpha_2, \dots, \alpha_n) = \prod_{i=1}^n \alpha_i^{w_i} = \left(\left[\prod_{i=1}^n (a_i)^{w_i}, \prod_{i=1}^n (b_i)^{w_i}, \prod_{i=1}^n (c_i)^{w_i} \right]; \prod_{i=1}^n (u_{\alpha_i})^{w_i}, 1 - \prod_{i=1}^n (1 - v_{\alpha_i})^{w_i} \right)$$

where ω_j be the weighting vector of the attributes.

Step 3: Utilize the intuitionistic fuzzy ordered weighted geometric (IFOWG) operator,

$$ITrFHG_{\omega, w}(\tilde{\alpha}_1, \tilde{\alpha}_2, \dots, \tilde{\alpha}_n) = \tilde{\beta}_{\sigma(1)}^{w_1} \otimes \tilde{\beta}_{\sigma(2)}^{w_2} \otimes \dots \otimes \tilde{\beta}_{\sigma(n)}^{w_n} = \left(\left[\prod_{i=1}^n (a_{\sigma(i)})^{w_i}, \prod_{i=1}^n (b_{\sigma(i)})^{w_i}, \prod_{i=1}^n (c_{\sigma(i)})^{w_i} \right]; \prod_{i=1}^n (\mu_{\beta_{\sigma(i)}})^{w_i}, 1 - \prod_{i=1}^n (1 - v_{\beta_{\sigma(i)}})^{w_i} \right)$$

where W_j be the associated weighting vectors of the decision makers.

Step 4: Using correlation coefficient between the collective overall preference values and the positive ideal value where,

$$C(A, B) = \sum_{i=1}^n [\mu_A(x_i) \mu_B(x_i) + \nu_A(x_i) \nu_B(x_i)]$$

Step 5: The correlation coefficient of the intuitionistic fuzzy set A and B is given,

$$K_{ITrFS}(A, B) = \frac{c_{ITrFS}(A,B)}{\sqrt{E_{ITrFS}(A)+E_{ITrFS}(B)}}$$

Step 6: Ranking the alternatives and select the best one.

Step 7: Stop the process.

6. NUMERICAL ILLUSTRATION

In the following, going to develop an illustrative example of the new approach in a decision making problem.

Let us consider an investor wants to invest some money in an enterprise in order to get high profits. Initially an investor considers five possible alternatives:

- A_1 is a food company
- A_2 is a chemical company
- A_3 is a computer company
- A_4 is a car company
- A_5 is a TV company

In order to evaluate these investments, the investor uses a group of experts. This group of experts considers that the key factor is the economic environments of the economy. After careful analysis, they consider four possible attributes:

- S_1 : Risk Analysis
- S_2 : Growth Analysis
- S_3 : Social-Political Impact Analysis
- S_4 : The Environmental Impact Analysis

The five possible alternatives (A_1, A_2, A_3, A_4, A_5) are to be evaluated using the intuitionistic fuzzy numbers by weighting vector, $\omega = (0.3345, 0.2456, 0.3467, 0.0732)^T$ under the above four attributes. And the weighting vector, $W = (0.3394, 0.3289, 0.2314, 0.1003)^T$ under the above five alternatives of the decision makers and construct respectively, the decision matrices (5×4) are

$$\begin{aligned}
 R1 &= \begin{bmatrix} ([0.5, 0.6, 0.7]; 0.4, 0.1) & ([0.1, 0.2, 0.4]; 0.4, 0.3) & ([0.4, 0.5, 0.6]; 0.1, 0.5) & ([0.5, 0.6, 0.7]; 0.3, 0.4) \\ ([0.2, 0.4, 0.6]; 0.3, 0.2) & ([0.5, 0.6, 0.8]; 0.2, 0.5) & ([0.1, 0.4, 0.6]; 0.3, 0.2) & ([0.2, 0.4, 0.6]; 0.2, 0.6) \\ ([0.3, 0.5, 0.7]; 0.4, 0.6) & ([0.5, 0.8, 0.9]; 0.3, 0.1) & ([0.3, 0.6, 0.9]; 0.1, 0.5) & ([0.4, 0.5, 0.7]; 0.4, 0.2) \\ ([0.2, 0.6, 0.8]; 0.3, 0.6) & ([0.1, 0.3, 0.6]; 0.4, 0.2) & ([0.2, 0.3, 0.4]; 0.4, 0.5) & ([0.1, 0.5, 0.9]; 0.3, 0.6) \\ ([0.4, 0.6, 0.7]; 0.1, 0.2) & ([0.4, 0.7, 0.9]; 0.8, 0.1) & ([0.3, 0.4, 0.5]; 0.3, 0.2) & ([0.6, 0.7, 0.9]; 0.4, 0.1) \end{bmatrix} \\
 R2 &= \begin{bmatrix} ([0.4, 0.7, 0.9]; 0.5, 0.3) & ([0.7, 0.8, 0.9]; 0.2, 0.4) & ([0.1, 0.3, 0.5]; 0.4, 0.1) & ([0.2, 0.3, 0.5]; 0.1, 0.5) \\ ([0.3, 0.5, 0.6]; 0.4, 0.2) & ([0.2, 0.4, 0.6]; 0.5, 0.4) & ([0.1, 0.2, 0.3]; 0.3, 0.2) & ([0.2, 0.7, 0.9]; 0.3, 0.6) \\ ([0.5, 0.7, 0.8]; 0.5, 0.2) & ([0.2, 0.6, 0.9]; 0.4, 0.2) & ([0.3, 0.6, 0.9]; 0.4, 0.5) & ([0.2, 0.4, 0.5]; 0.4, 0.3) \\ ([0.3, 0.4, 0.5]; 0.1, 0.6) & ([0.2, 0.5, 0.8]; 0.3, 0.4) & ([0.5, 0.7, 0.9]; 0.5, 0.3) & ([0.7, 0.8, 0.9]; 0.3, 0.4) \\ ([0.2, 0.5, 0.6]; 0.1, 0.6) & ([0.3, 0.4, 0.8]; 0.1, 0.2) & ([0.2, 0.4, 0.6]; 0.5, 0.3) & ([0.4, 0.6, 0.8]; 0.2, 0.4) \end{bmatrix} \\
 R3 &= \begin{bmatrix} ([0.5, 0.6, 0.7]; 0.4, 0.1) & ([0.1, 0.2, 0.4]; 0.4, 0.3) & ([0.4, 0.5, 0.6]; 0.1, 0.5) & ([0.5, 0.6, 0.7]; 0.6, 0.3) \\ ([0.5, 0.6, 0.7]; 0.2, 0.5) & ([0.1, 0.2, 0.4]; 0.4, 0.3) & ([0.5, 0.6, 0.7]; 0.6, 0.3) & ([0.3, 0.4, 0.8]; 0.3, 0.6) \\ ([0.2, 0.4, 0.6]; 0.2, 0.6) & ([0.1, 0.4, 0.6]; 0.7, 0.2) & ([0.1, 0.2, 0.4]; 0.4, 0.3) & ([0.2, 0.4, 0.6]; 0.1, 0.2) \\ ([0.1, 0.2, 0.8]; 0.3, 0.4) & ([0.3, 0.4, 0.6]; 0.3, 0.6) & ([0.2, 0.7, 0.9]; 0.3, 0.2) & ([0.1, 0.2, 0.8]; 0.1, 0.6) \\ ([0.4, 0.5, 0.6]; 0.1, 0.5) & ([0.1, 0.2, 0.8]; 0.3, 0.4) & ([0.3, 0.4, 0.7]; 0.1, 0.6) & ([0.4, 0.6, 0.8]; 0.7, 0.1) \end{bmatrix} \\
 R4 &= \begin{bmatrix} ([0.2, 0.3, 0.4]; 0.7, 0.2) & ([0.3, 0.4, 0.5]; 0.5, 0.4) & ([0.1, 0.2, 0.3]; 0.1, 0.2) & ([0.3, 0.4, 0.7]; 0.4, 0.1) \\ ([0.4, 0.6, 0.8]; 0.1, 0.2) & ([0.2, 0.4, 0.6]; 0.4, 0.2) & ([0.1, 0.3, 0.5]; 0.1, 0.4) & ([0.1, 0.5, 0.8]; 0.7, 0.2) \\ ([0.1, 0.2, 0.5]; 0.5, 0.2) & ([0.6, 0.7, 0.8]; 0.3, 0.6) & ([0.1, 0.4, 0.8]; 0.1, 0.5) & ([0.2, 0.4, 0.6]; 0.4, 0.5) \\ ([0.5, 0.6, 0.7]; 0.6, 0.3) & ([0.1, 0.2, 0.3]; 0.2, 0.3) & ([0.3, 0.4, 0.5]; 0.2, 0.5) & ([0.3, 0.4, 0.6]; 0.3, 0.5) \\ ([0.3, 0.4, 0.7]; 0.3, 0.4) & ([0.4, 0.5, 0.7]; 0.3, 0.2) & ([0.4, 0.5, 0.7]; 0.3, 0.5) & ([0.4, 0.6, 0.9]; 0.5, 0.2) \end{bmatrix}
 \end{aligned}$$

Step 1: Utilize the given intuitionistic triangular fuzzy matrix and using ITrFWG operator to derive the individual overall preference intuitionistic triangular fuzzy values by Runge-Kutta methods.

$$ITrFWG_w(\tilde{\alpha}_1, \tilde{\alpha}_2, \dots, \tilde{\alpha}_n) = \prod_{i=1}^n \tilde{\alpha}_i^{w_i} = \left(\left[\prod_{i=1}^n (a_i)^{w_i}, \prod_{i=1}^n (b_i)^{w_i}, \prod_{i=1}^n (c_i)^{w_i} \right]; \prod_{i=1}^n (u_{\alpha_i}^-)^{w_i}, 1 - \prod_{i=1}^n (1 - v_{\alpha_i}^-)^{w_i} \right)$$

$$\begin{aligned}
 \tilde{r}_{11} &= ([(0.5)^{0.1528} \times (0.1)^{0.2026} \times (0.4)^{0.268} \times (0.5)^{0.3764}, (0.6)^{0.1528} \times (0.2)^{0.2026} \\ &\quad \times (0.5)^{0.268} \times (0.6)^{0.3764}, (0.7)^{0.1528} \times (0.4)^{0.2026} \times (0.6)^{0.268} \\ &\quad \times (0.7)^{0.3764}; (0.4)^{0.1528} \times (0.4)^{0.2026} \times (0.1)^{0.268} \times (0.3)^{0.3764}, 1 \\ &\quad - [(1 - 0.1)^{0.1528} \times (1 - 0.3)^{0.2026} \times (1 - 0.5)^{0.268} \times (1 - 0.4)^{0.3764}])
 \end{aligned}$$

$$\tilde{r}_{11} = ([0.3051,0.4568,0.5987]; 0.2476,0.3721)$$

Similarly,

$$\tilde{r}_{12} = ([0.1996,0.4286,0.6354]; 0.237,0.4403)$$

$$\tilde{r}_{13} = ([0.4024,0.5776,0.6300]; 0.2602,0.3503)$$

$$\tilde{r}_{14} = ([0.1339,0.4043,0.6552]; 0.3435,0.5112)$$

$$\tilde{r}_{15} = ([0.4314,0.5885,0.7399]; 0.3449,0.1435)$$

$$\tilde{r}_{21} = ([0.238,0.4166,0.6162]; 0.1663,0.3605)$$

$$\tilde{r}_{22} = ([0.1768,0.4243,0.5804]; 0.3447,0.4185)$$

$$\tilde{r}_{23} = ([0.2565,0.5274,0.7085]; 0.4139,0.3292)$$

$$\tilde{r}_{24} = ([0.6952,0.6312,0.8033]; 0.2909,0.4121)$$

$$\tilde{r}_{25} = ([0.2819,0.4822,0.7088]; 0.1833,0.3769)$$

$$\tilde{r}_{31} = ([0.3399,0.4574,0.3501]; 0.3214,0.3352)$$

$$\tilde{r}_{32} = ([0.2977,0.4123,0.6572]; 0.3600,0.4613)$$

$$\tilde{r}_{33} = ([0.1443,0.3322,0.5382]; 0.2392,0.3056)$$

$$\tilde{r}_{34} = ([0.1505,0.3297,0.7249]; 0.1984,0.4874)$$

$$\tilde{r}_{35} = ([0.5184,0.4210,0.7387]; 0.3022,0.3902)$$

$$\tilde{r}_{41} = ([0.2083,0.3179,0.4783]; 0.3144,0.2110)$$

$$\tilde{r}_{42} = ([0.2022,0.4285,0.6654]; 0.2755,0.2458)$$

$$\tilde{r}_{43} = ([0.1867,0.6426,0.6681]; 0.2693,0.4864)$$

$$\tilde{r}_{44} = ([0.2597,0.3699,0.5084]; 0.2756,0.4364)$$

$$\tilde{r}_{45} = ([0.3828,0.5176,0.7695]; 0.3636,0.3249)$$

Step 2: Utilize the ITrFHG operator to derive the collective overall preference intuitionistic triangular fuzzy values using runge-kutta 3rd and 4th ordered method.

$$\tilde{r}_{11} = ([0.3051,0.4568,0.5987]; 0.2476,0.3721)$$

$$\tilde{r}_{21} = ([0.2380,0.4166,0.6162]; 0.1663,0.3605)$$

$$\tilde{r}_{31} = ([0.3399,0.4574,0.3501]; 0.3214,0.3352)$$

$$\tilde{r}_{41} = ([0.2083,0.3179,0.4783]; 0.3144,0.2110)$$

,

$$\begin{aligned}
 a_1^{(1)} &= a_1^{n \times W_1} = (0.3051)^{4 \times 0.2346} = 0.3282, a_2^{(1)} = a_2^{n \times W_2} = 0.2510, \\
 a_3^{(1)} &= a_3^{n \times W_3} = 0.3353, a_4^{(1)} = a_4^{n \times W_4} = 0.1821, b_1^{(1)} = b_1^{n \times W_1} = 0.4793, \\
 b_2^{(1)} &= b_2^{n \times W_2} = 0.4303, b_3^{(1)} = b_3^{n \times W_3} = 0.4529, b_4^{(1)} = b_4^{n \times W_4} = 0.2881, \\
 c_1^{(1)} &= c_1^{n \times W_1} = 0.6179, c_2^{(1)} = c_2^{n \times W_2} = 0.6273, c_3^{(1)} = c_3^{n \times W_3} = 0.3456, \\
 c_4^{(1)} &= c_4^{n \times W_4} = 0.4490, \mu_1^{(1)} = \mu_1^{n \times W_1} = 0.2698, \mu_2^{(1)} = \mu_2^{n \times W_2} = 0.1778, \\
 \mu_3^{(1)} &= \mu_3^{n \times W_3} = 0.3169, \mu_4^{(1)} = \mu_4^{n \times W_4} = 0.2847, \gamma_1^{(1)} = \gamma_1^{n \times W_1} = 0.3954, \\
 \gamma_2^{(1)} &= \gamma_2^{n \times W_2} = 0.3744, \gamma_3^{(1)} = \gamma_3^{n \times W_3} = 0.3306, \gamma_4^{(1)} = \gamma_4^{n \times W_4} = 0.1847
 \end{aligned}$$

$$ITrFHG_{\alpha, \beta}(\tilde{\alpha}_1, \tilde{\alpha}_2, \dots, \tilde{\alpha}_n) = \left(\left[\prod_{i=1}^n (a_{\sigma(i)})^{\beta_i}, \prod_{i=1}^n (b_{\sigma(i)})^{\beta_i}, \prod_{i=1}^n (c_{\sigma(i)})^{\beta_i} \right]; \left[\prod_{i=1}^n (\mu_{\beta_{\sigma(i)}})^{\beta_i}, 1 - \prod_{i=1}^n (1 - \nu_{\beta_{\sigma(i)}})^{\beta_i} \right] \right)$$

$$\begin{aligned}
 \tilde{r}_1 &= ([(0.3282)^{0.097} \times (0.251)^{0.1515} \times (0.3353)^{0.2161} \times (0.1821)^{0.5353}, (0.4793)^{0.097} \\
 &\quad \times (0.4303)^{0.1515} \times (0.4529)^{0.2161} \times (0.2881)^{0.5353}, (0.6179)^{0.097} \\
 &\quad \times (0.6273)^{0.1515} \times (0.3456)^{0.2161} \times (0.449)^{0.5353}]; (0.2698)^{0.097} \\
 &\quad \times (0.1778)^{0.1515} \times (0.3169)^{0.2161} \times (0.2847)^{0.5353}, 1 \\
 &\quad - [\times (1 - 0.3954)^{0.097} \times (1 - 0.3744)^{0.1515} \times (1 - 0.3306)^{0.2161} \\
 &\quad \times (1 - 0.1847)^{0.5353}])
 \end{aligned}$$

$$\tilde{r}_1 = ([0.2309, 0.3547, 0.4604]; 0.2699, 0.2709)$$

Similarly,

$$\tilde{r}_2 = ([0.2031, 0.4112, 0.6380]; 0.2842, 0.3360)$$

$$\tilde{r}_3 = ([0.1863, 0.5265, 0.6298]; 0.2653, 0.4016)$$

$$\tilde{r}_4 = ([0.2383, 0.3789, 0.5862]; 0.2514, 0.5596)$$

$$\tilde{r}_5 = ([0.3817, 0.4835, 0.7436]; 0.3029, 0.3208)$$

Step 3: To calculate the correlation coefficient between collective overall values

$(\tilde{r}_i) = ([a_i, b_i, c_i]; \mu_i, \nu_i)$ and the intuitionistic triangular fuzzy positive ideal solution

$$\tilde{r}^+ = ([1, 1, 1]; 1, 0), \text{ is}$$

Now we calculate the correlation

coefficient,

$$\pi_1 = 1 - \mu - \gamma$$

$$K_{ITrFS}(A,B) = \frac{c_{ITrFS}(A,B)}{\sqrt{E_{ITrFS}(A)+E_{ITrFS}(B)}}$$

$$\tilde{r}_1 = ([0.2309,0.3547,0.4604]; 0.2699,0.2709)$$

$$\tilde{r}_2 = ([0.2031,0.4112,0.6380]; 0.2842,0.3360)$$

$$\tilde{r}_3 = ([0.1863,0.5265,0.6298]; 0.2653,0.4016)$$

$$\tilde{r}_4 = ([0.2383,0.3789,0.5862]; 0.2514,0.5596)$$

$$\tilde{r}_5 = ([0.3817,0.4835,0.7436]; 0.3029,0.3208)$$

$$E_{ITrFS}(A)_1 = \frac{1}{n} \sum_{i=1}^n \left[\frac{a_1+4b_1+c_1}{6} \right]^2 [\mu_A^2(x_i) + \gamma_A^2(x_i) + \pi_A^2(x_i)]$$

$$= \frac{1}{1} \left[\frac{0.2309+4(0.3547)+0.4604}{6} \right]^2 [(0.2699)^2 + (0.2709)^2 + (0.4592)^2]$$

$$E_{ITrFS}(A)_1 = 0.4416$$

Similarly,

$$A_2 = 0.0580$$

$$A_3 = 0.0812$$

$$A_4 = 0.0627$$

$$A_5 = 0.0874$$

$$E_{ITrFS}(B)_1 = \frac{1}{n} \sum_{i=1}^n \left[\frac{a_1+4b_1+c_1}{6} \right]^2 [\mu_B^2(x_i) + \gamma_B^2(x_i) + \pi_B^2(x_i)]$$

$$= \frac{1}{1} \left[\frac{1+4(1)+1}{6} \right]^2 [(1)^2 + (0)^2 + (0)^2]$$

$$E_{ITrFS}(B)_1 = 1 \quad (\text{to all B, are same value})$$

$$C_{ITrFS}(A_1, B_1) = \frac{1}{2}$$

$$[\mu_A^2(x_i)\mu_B^2(x_i) + \gamma_A^2(x_i)\gamma_B^2(x_i) + \pi_A^2(x_i)\pi_B^2(x_i)]$$

$$C_{ITrFS}(A_1, B_1) = [(0.3517)(1)][(0.2699)(1)]$$

$$C_{ITrFS}(A_1, B_1) = 0.0949$$

Similarly,

$$(A_2, B_2) = 0.1177$$

$$C_{ITrFS} (A_3, B_3) = 0.1292$$

$$C_{ITrFS} (A_4, B_4) = 0.0980$$

$$C_{ITrFS} (A_5, B_5) = 0.1545$$

$$K_{ITrFS}(A_1, B_1) = \frac{c_{ITrFS}(A,B)}{\sqrt{E_{ITrFS}(A)+E_{ITrFS}(B)}} \\ = \frac{0.0949}{\sqrt{(0.4416)(1)}}$$

$$K_{ITrFS}(A_1, B_1) = 0.14280$$

Similarly,

$$K_{ITrFS}(A_2, B_2) = 0.4888$$

$$K_{ITrFS}(A_3, B_3) = 0.4534$$

$$K_{ITrFS}(A_4, B_4) = 0.2503$$

$$K_{ITrFS}(A_5, B_5) = 0.5227$$

Step 4: Rank all the alternatives, A_i ($i = 1, 2, 3, 4, 5$).

$$A_1 < A_4 < A_3 < A_2 < A_5$$

Hence, the best alternative is, A_1 .

7. CONCLUSION

In this paper, we proposed with respect to MAGDM problems, where the attribute weights and the expert weights the form of runge-kutta methods and the attribute values takes form a intuitionistic triangular fuzzy numbers (ITrFNs). Some arithmetic operations of ITrFNs and runge-kutta methods where presented and different operators, namely ITrFWG operator and ITrFHG operator were also utilized. Aggregates the all weighted arguments into a collective data. The correlation coefficient method for ITrFNs was introduced to choose the best alternative value. Finally, our proposed method is developed an validate the effectiveness by given illustrative examples.

REFERENCES

1. K. Atanassov, (1986). *Intuitionistic fuzzy sets*. Fuzzy Sets and Systems, 20(1), 87–96. doi:10.1016/S0165-0114(86)80034-3.
2. K Atanassov, (1989). *More on intuitionistic fuzzy sets*. Fuzzy Sets and Systems, 33(1), 37–45. doi:10.1016/0165-0114(89)90215-7.
3. Atanassov, K., & Gargov, G. (1989). *Interval valued intuitionistic fuzzy sets*. Fuzzy Sets and Systems, 31, 343-349.
4. Atanassov, K. (1994). *Operators over interval-valued intuitionistic fuzzy sets*. Fuzzy Sets and Systems, 64, 159-174.
5. Atanassov, K. (1994). *New operations defined over the intuitionistic fuzzy sets*. Fuzzy Sets and Systems, 61(2), 137-142.
6. Akila. S & John Robinson. P, (2019). *Multiple attribute group decision making methods using numerical methods of intuitionistic Triangular fuzzy sets*. Journal of Physics: Conference Series. 1377 (2019) 012022 doi:10.1088/1742-6596/1377/1/012022
7. P. Burillo, H. Bustince, V. Mohedano, Some definitions of intuitionistic fuzzy number, Fuzzy based expert systems, fuzzy Bulgarian enthusiasts, September (1994), 28-30, Sofia, Bulgaria.
8. Changyong liang, shuping zhao, junling zhang (2014), *Aggregation Operators on Triangular Intuitionistic Fuzzy Numbers and its Application to Multi-Criteria Decision Making Problems*, Foundations of computing and decision sciences, Vol. 39, DOI: 10.2478/fcds-2014-0011, ISSN 0867-6356.
9. D. F. Li, (2005). *Multi attribute decision making models and methods using intuitionistic fuzzy sets*. Journal of Computer and System Sciences, 70(1), 73–85. doi:10.1016/j.jcss.2004.06.002.
10. D. F. Li, (2010c). *A ratio ranking method of triangular intuitionistic fuzzy numbers and its application to MADM problems*. Computers & Mathematics with Applications (Oxford, England), 58(6), 1557–1570. doi:10.1016/j.camwa.2010.06.039 .
11. Jenifer rose. S, & Akila. S (2020) . *Multiple Attribute Group Decision making methods using intuitionistic triangular Fuzzy set*. 0950-0707, doi:16.10089/STD.
12. J. P. Robinson, & E. C. H. Amirtharaj, (2011b). *Extended TOPSIS with correlation coefficient of Triangular Intuitionistic fuzzy sets for Multiple Attribute Group Decision Making*. International Journal of Decision Support System Technology, 3(3), 15–40. doi:10.4018/jdsst.2011070102.
13. J.P. Robinson, Amirtharaj, E.C.H, (2012b). *A Search for the Correlation coefficient of Triangular and Trapezoidal intuitionistic*

- Fuzzy sets for Multiple Attribute Group Decision Making. In Mathematical Modeling and Scientific Computation (pp. 333- 342).*
14. John P. Robinson, V. Poovarasan,(2015). *A Robust MAGDM Method for Triangular Intuitionistic Fuzzy Sets*. International Journal of Pure and Applied Mathematics, Volume 101 No. 5 2015, 753-762 ISSN: 1311-8080.
 15. J. P. Robinson, & Amirtharaj, E. C. H. (2015). *MAGDM problems with correlation coefficient of Triangular fuzzy IFS*. International Journal of Fuzzy System Applications, 4(1), 1-32. doi:10.4018/IJFSA.2015010101
 16. J.R. Dormand, P. J. Prince, (1980) Department of Mathematics and Statistics, Teesside Polytechnic, Middlesbrough, Cleveland UK. *A Family of embedded Runge-Kutta formulae* [https://10.1016/0771-050X\(80\)90013-3](https://10.1016/0771-050X(80)90013-3)
 17. P. John Robinson, (2016) *Multiple Attribute Group Decision Analysis for Intuitionistic Triangular and Trapezoidal Fuzzy Numbers*. International Journal of Fuzzy System Applications, 5(3), 45-76. DOI: 10.4018/IJFSA.2016070104.
 18. Jeeva, S., Robinson, J.P.: *Application of Sumudu Transform in Intuitionistic Fuzzy MAGDM Problems*, International Journal of Pure and Applied Mathematics, 119(11), 109-117 (2017) .
 19. J.P. Robinson, & Jeeva, S. (2018): *Application of Double Sumudu Transform in MAGDM problems with Intuitionistic Triangular Fuzzy Sets*. International Journal of Research in Advent Technology, 6(7), pp. 1620-1628.
 20. Robinson, J.P, & Jeeva, S. *Application of Double Sumudu Transform in MAGDM problems with Intuitionistic Triangular Fuzzy Sets*, International Journal of Research in Advent Technology, 6(7), 1620-1628 (2018) .
 21. M.Dong, S. Li, & H. Zhang, (2015). *Approaches to group decision making with incomplete information based on power geometric operators and triangular fuzzy AHP*, Expert Systems with Applications, 42(21), 7846-7857 .
 22. G. Wei, *Some arithmetic aggregation operators with intuitionistic trapezoidal fuzzy numbers and their application to group decision making*, Journal of Computers (2010), 5 (3), 345-351.

A. Muthuvel*, N. Mahendran & V. Mohana*****

*PG & Research Department of Physics, Theivanai Ammal College for Women
(Autonomous), Villupuram, Tamil Nadu

**PG & Research Department of Physics, Idhaya College for Women,
Kumbakonam, Tamil Nadu

***Research Department of Physics, Government arts and science college,
Kallakurichi, Tamil Nadu

ABSTRACT

The aim of the current study was to synthesize nanoparticles of Zinc oxide (ZnO) using extract of *Plectranthus Amboinicus* leaves and their antibacterial properties. The biosynthesized nanoparticles were analysed using XRD, FT-IR, SEM with EDAX and UV-visible analysis. The synthesized nanoparticles had a mean size of 12 nm measured by XRD which was highly pure, and their spherical shape was confirmed by SEM. The UV-Visible confirmed that ZnO nanoparticles have a direct band gap energy at 3.364 eV. The highest zone of inhibition was observed against *Escherichia coli*.

Keywords: Zinc Oxide, Nanoparticles, XRD, Antibacterial.

1. INTRODUCTION

The synthesis of nanoparticles has been considered as the preference field in the nanotechnology sector due to the properties of materials based on size. The green synthesis of metal nanoparticles is an interesting issue of nanoscience [1]. Numerous efforts have been made to development of semiconductor nanoparticles in the last two decades due to their novel optical, chemical, photoelectrochemical and electronic properties which are different from that of bulk. Zinc oxide (ZnO) is a well know n-type wide-bandgap ($E_g = 3.37$ eV) semiconductor [2]. Because of the strong UV absorption properties of ZnO, they are increasingly used in personal care products, such as cosmetics and sunscreen [3]. In addition, ZnO NPs have superior antibacterial, antimicrobial, and excellent UV blocking properties. Therefore, in the textile industry, the finished fabrics by adding ZnO NPs exhibited the attractive functions of ultraviolet and visible light resistance, antibacterial,

and deodorant [4]. The biological method of the synthesis of ZnO nanoparticles is gaining importance due to its simplicity, eco-friendliness and extensive antimicrobial activity [5]. The use of eco-friendly biosynthesized nanoparticles as an alternative to the chemically synthesized ones would help control chemical toxicity in the environment. To overcome the limitations of these conventional methods, green synthesis has been emerged as an eco-friendly alternative for low-cost development of nanoparticles, which are highly efficient and biocompatible and can be used in a variety of applications [6]. Green synthesis of nanoparticles is an approach of synthesizing nanoparticles using microorganisms and plants having biomedical applications [7]. This approach is an environment-friendly, cost-effective, biocompatible, safe, green approach [8]. Green synthesis includes synthesis through plants, bacteria, fungi, algae etc. They allow large scale production of ZnO NPs free of additional impurities [9]. Nanoparticles synthesized from biomimetic approach show more catalytic activity and limit the use of expensive and toxic chemicals. Biosynthesis of nanoparticles is an approach of synthesizing nanoparticles using microorganisms and plants having biomedical applications.

Plectranthus Amboinicus (Lour.) Spreng (Syn. *Coleus amboinicus*, *Coleus aromaticus*, *Plectranthus aromaticus*) belongs to the family Lamiaceae (Labiatae). It is popularly known as Indian oregano. The leaves have many medicinal uses especially for the treatment of cough, sore throats and nasal congestion. *Plectranthus amboinicus* (*P. amboinicus*) contains butylanisole, β -caryophyllene, quercetin, ursolic acids, triterpenic acids, α -pinene, β -pinene, thymol etc and possess antioxidant, and antimicrobial properties [10]. Green synthesis includes synthesis through plants, bacteria, fungi, algae etc. Herein, we report for the first-time synthesis of ZnO NPs using *Plectranthus amboinicus* leaf extract as reducing agent. The present chapter utilized *Plectranthus amboinicus* leaf extract for reducing zinc nitrate to ZnO nanoparticles which were synthesized and characterized using several techniques: UV-Visible spectroscopy (UV-vis), Scanning electron microscopy (SEM), X-ray diffraction (XRD), Fourier transform infrared spectroscopy (FTIR), and X-ray spectroscopy (EDX) analysis. Also, antibacterial activity against human pathogens bacteria.

2. MATERIAL AND METHODS

2.1 Materials

The chemicals such as Zinc acetate dihydrate ($\text{Zn}(\text{CH}_3\text{COO})_2 \cdot 2\text{H}_2\text{O}$) and all the chemicals and reagents were procured from Merck chemical reagent co. Distilled water ingredients utilized in this work purchased from the leaves of plant *Plectranthus amboinicus* collected from in and around garden, Nagapattinam, Tamil Nadu, India.

2.2 Preparation of Leaf Extract

Fresh leaves of plants that is, *Plectranthus amboinicus* free from were collected from Villupuram. Whipped with tissue paper. The collected leaves were washed twice with tap water, followed by washing through double-distilled (dd) water for multiple times to remove dust particles from the surface of the leaves. The washed leaves were shade-dried for 5 days. 5g of the fine cut leaves were taken in a 250 mL glass beaker with 100mL of distilled water. These were boiled for 1hour, the colour of aqueous solution turned from watery to light yellow. The extract was cooled to room temperature and filtered using filter paper. The extract was stored in the refrigerator for further use.

2.3 Biosynthesis of ZnO Nanoparticles Using *Plectranthus Amboinicus* Leaf Extract

Briefly, it was prepared by stirring 2 M zinc acetate in 50 mL of deionized water for 30 min at 85°C. On order to prepare a NaOH solution, 4 gm NaOH powder was added to 50 mL of distilled water and stirred simultaneously at 85°C for 30 min. The two solutions were then vigorously stirred together. The 15 mL leaf extract was mixed with the solution drop by drop during this stirring process. After stirring continuously for to 2 h using a magnetic stirrer, white precipitate was obtained. To remove the impurities, the precipitate was filtered and repeatedly washed with distilled water followed by ethanol. After, the precipitate was dried at 400°C for 4 h and the obtained ZnO powder was subjected for further characterization.

3 RESULT AND DISCUSSION

3.1 X - ray diffraction analysis

The X - ray diffraction was taken to further conform the ZnO phase of the nanoparticles. The XRD patterns of biosynthesized

ZnO nanoparticles is shown in Figure 1. The diffraction peaks at 28.39, 29.41, 31.41, 34.46, 36.17, 40.59, 47.46, 56.48, 62.73, 66.26, 67.83, 68.94, 72.54 and 76.92. The XRD peak were identified as (100), (002), (101), (110), (102), (103), (112), (201) and (202). There were no other impurity peaks in the plots, indicating that the synthesized ZnO nanoparticles are of high phase purity. The cramped and strong diffraction peaks indicate the well crystalline nature of the ZnO. The size of ZnO nanoparticles was obtained by the Scherrer's formula used to calculate the particle size through powder X-diffractometer is given as;

$$D = 0.9\lambda / \beta \cos\theta \tag{1}$$

where D is the particle size. λ is the wavelength of source used (Cu, K α) β is the full width at half maximum of ZnO (101) line θ is the diffracting angle. The particle size of biosynthesized ZnO nanoparticles was found to be 12 nm and characterized the prepared sample by XRD. These plane values are closely matched with wurtzite structure of ZnO reflection lines of hexagonal wurtzite ZnO (JCPDS36-1451) [10].

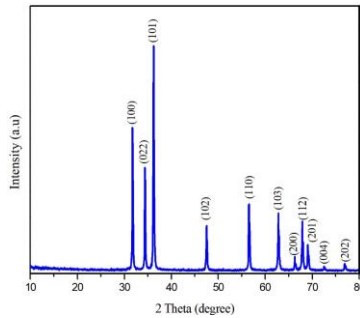


Figure 1 XRD pattern of biosynthesized ZnO nanoparticles

3.2 UV - visible analysis

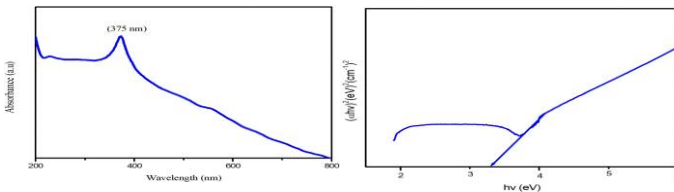


Figure 2 a) UV-visible spectra and b) band gap energy of biosynthesized ZnO nanoparticles

The UV - visible spectrum of biosynthesized ZnO nanoparticles is shown in Figure 1a. The presence of ZnO nanoparticles is indicated by the surface plasmon resonance peak at 372 nm exposed in Figure 1a. The absorption peak of the synthesized ZnO nanoparticles is nearly the same as that of those recorded in the literature [11]. The band gap energy of biosynthesized ZnO nanoparticles was determined using UV - visible spectroscopy data, using the equation (2) as a reference [12],

$$(\alpha h\nu)^2 = B (h\nu - E_g)^{1/2} \quad (2)$$

Where A is the photon energy ($h\nu$), E_g is bandgap energy, and α and n are absorption coefficient. Figure 2 b shows the optical band gap energy of biosynthesized ZnO nanoparticles. In biosynthesized ZnO nanoparticles, the measured band gap was 3.66 eV. In this case, it is likely that an intrinsic ZnO band gap absorption and electron transfer between the valance band and conduction band are responsible for this phenomenon [12]. The biosynthesized ZnO nanoparticles with minimum band gap energy could be used in antibacterial activity.

3.4 Scanning Electron Microscopy Analysis

The morphology of synthesized ZnO nanoparticles by *Plectranthus Amboinicus* leaf extract was recovered from the SEM micrograph image as displayed in Figure 3a. The SEM micrograph images of ZnO nanoparticles were exhibited mostly in hexagonal shape. With apparently separated nature. The separation between nanoparticles plays an essential role in achieving high efficiency of application purposes of nanoparticles [13]. The SEM micrograph apparently expressed the synthesized ZnO nanoparticles were separated with narrow space in among the nanoparticles. The large surface area, small sized ZnO nanoparticles has higher activity in antibacterial activity also many fields [14]. The spots present in the surface of ZnO nanoparticles revealed some capping agents included in the synthesis process from *Plectranthus Amboinicus* leaf extract. The average particles size of biosynthesized ZnO nanoparticle is found to be 38 nm. Figure b showed the particle size distribution graph of ZnO nanoparticles by *Plectranthus Amboinicus* leaf extract. The size was in good accordance with DLS and XRD analyzer study. The received hexagonally shaped nanoparticles of SEM micrograph was quite coordinated with Geetha et al. and Susan Azizi et al. The elemental composition of the ZnO

nanoparticles is revealed by EDX spectra and shown in Figure 4. The EDX analysis confirmed the presence of zinc oxide nanoparticles. The spectra showed strong signal peaks for zinc (Zn) atoms and weak signal energy peak for oxygen (O) atom. The presence of weak plant metabolites was also observed with appearance of weak peaks for elements like carbon and nitrogen. Figure 3 (c-d) shows a surface plot analysis of synthesized nanoparticle images. It has been demonstrated that biosynthesised ZnO nanoparticles have the highest porosity, thus allowing more dye molecules to absorb, which would improve the performance of the antibacterial.

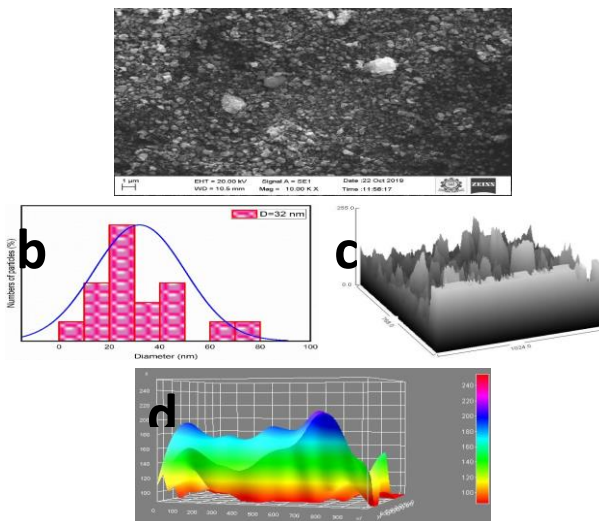


Figure 3 a) SEM image b) particles size distribution c-d) surface plot analysis of biosynthesized ZnO nanoparticles

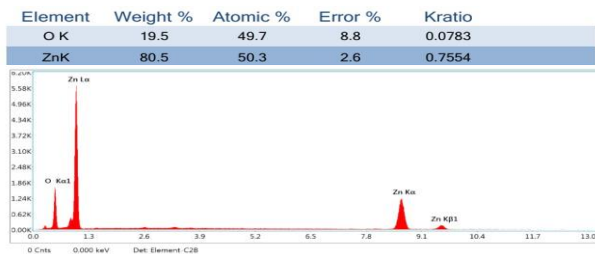


Figure 4 EDS spectrum of the biosynthesized ZnO nanoparticles

3.4 Fourier Transform Infrared Analysis

The FT-IR spectra of a biosynthesized ZnO nanoparticles and plant extract are shown in Figure 6.6. The existence of major functional groups such as -OH stretching vibration (3360.53 cm^{-1}), C - H stretching vibration (2998.35 cm^{-1}), amine N - H group of protein (1439.03 cm^{-1}) and cellulose (871.22 cm^{-1}) and alkenes was observed in the leaf extract. FT-IR analysis confirmed the presence of carboxyl groups in leaf extract. The bio-reduction of Zinc ions into Zinc oxide nanoparticles is carried out from these groups. The observed IR band 3431.41 cm^{-1} corresponding to the O - H bending vibration of water molecules in the spectra provided by the study of biosynthesized ZnO nanoparticles [15]. The presence of an alcohol group has been indicated by the strong and broad peak observed at 2336.30 cm^{-1} , which correspond to a (C - H) bond.

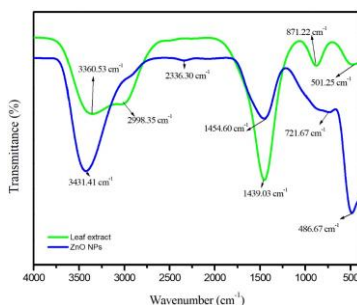


Figure 5 FT-IR spectra of *Plectranthus Amboinicus* leaf extract and biosynthesized ZnO nanoparticles

The peak at 1454.60 cm^{-1} held emerged due to the N - H stretching band and symmetric stretching vibration of carboxyl side groups present in amino acid residues of the protein molecules. The peaks observed about from 400 cm^{-1} to 1900 cm^{-1} obtained due to Zn - O bond. The strong peak at 486.67 cm^{-1} represented Zn - O stretching vibration. The peak at 721.67 cm^{-1} described the free surface of Zn - O bonding. The IR spectrum was used to assess the relationship between chemical constituents as well as the absorption bands of the synthesised sample. Against this backdrop, it was undoubtedly possible to observe the biomolecules present in plant extract, as they play an important role in the green synthesis of nanoparticles for reduction and stabilisation of nanoparticles. We discovered that the phytochemicals present in the detected peaks contributed to the stability and formation of ZnO nanoparticles during biogenic

reduction. We also discovered the functional groups of reducing agents through which the nanoparticles formed. The finding is consistent with that biosynthesized ZnO nanoparticles using *Echinochloa frumentaces*.

3.5 Antibacterial Activity

The antibacterial activity of *Plectranthus Amboinicus* leaf extract synthesised ZnO nanoparticles was determined for both Gram - positive and Gram - negative bacteria using disc diffusion and zone of inhibition methods. Figure 6 and Table 1 show the results that were received. The in different concentrations of tested samples in 5 $\mu\text{g}/\text{mL}$ and 10 $\mu\text{g}/\text{mL}$ were also examined in this study. The leaf extract of *Plectranthus Amboinicus* showed the maximum inhibition zone at concentration of 10 $\mu\text{g}/\text{mL}$ for *Escherichia coli* (12 mm), *Pseudomonas Aeruginosa* (10 mm), *Staphylococcus aureus* (10 mm) and *Bacillus subtilis* (9 mm). When compared to leaf extract at a concentration of 10 g/mL , the biosynthesized ZnO nanoparticles demonstrated respectable bacterial activity against all microorganisms. The inhibition zone was observed against *Escherichia coli* (24 mm), *Pseudomonas Aeruginosa* (21 mm), *Staphylococcus aureus* (20 mm) and *Bacillus subtilis* (19 mm). A particulate drug delivery system's particle size and surface area are well known to play a significant role in their interactions with biological cells and the system's in vivo fate. Because of their size and large surface area, ZnO nanoparticles produce electronic effects, which can increase the nanoparticles' binding strength with bacteria. We hypothesised that the aforementioned mechanisms could explain ZnO nanoparticles' superior antibacterial activity when compared to *Plectranthus amboinicus* leaf extract. ZnO nanoparticles have a greater zone of inhibition against gram-negative bacteria than gram-positive bacteria at all concentrations. Because of the diversity in cell wall structure, the aforementioned recognised different sensitivity of zone of inhibition rate against gramme positive and gramme negative [16]. The outer membrane of gram-negative bacteria is solid and hydrophobic. According to these findings, green-synthesis of ZnO nanoparticles using *Plectranthus amboinicus* leaf extract may be effective against gram-negative bacteria like *Escherichia coli*. This could be due to the presence of more phenols, flavonoids, saponins, and secondary metabolites in *Plectranthus amboinicus*, such as rutin, nimbinene, meliacin, and quercertion.

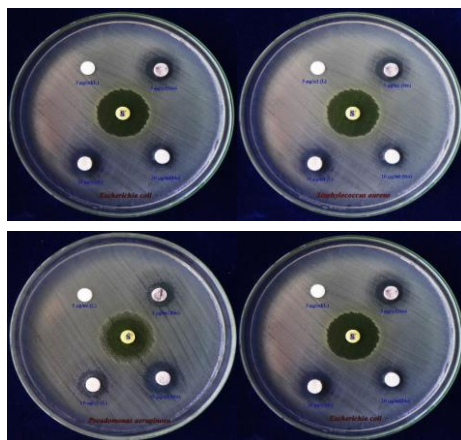


Figure 6 Antibacterial activity of *Plectranthus Amboinicus* leaf extract and biosynthesized ZnO nanoparticles against human pathogenic bacteria at different concentrations

Table 2 Antibacterial activity of *Plectranthus amboinicus* leaf extract and biosynthesized ZnO nanoparticles against human pathogenic bacteria

Bacteria's	Zone of inhibition (mm)				Standard
	5 µg/mL		10 µg/mL		
	Leaf	Bio ZnO	Leaf	Bio ZnO	
<i>Bacillus subtilis</i>	1	9	5	19	24
<i>Staphylococcus aureus</i>	2	10	8	20	25
<i>Pseudomonas aeruginosa</i>	4	10	9	21	26
<i>Escherichia coli</i>	6	12	12	24	26

4 CONCLUSION

ZnO nanoparticles were synthesized by using *Plectranthus amboinicus* leaf extract. The obtained ZnO nanoparticles were in the hexagonal wurtzite structure. The FTIR spectrum was confirmed the ZnO nanoparticles done by biogenic reduction process. From UV - visible study, the ZnO nanoparticles by leaf extract was confirmed by SPR band appeared at 375 nm. The photoluminescence study of ZnO nanoparticles by *Plectranthus amboinicus* extract indicated good optical applications due to red shoulder emission and observed fewer surface defects. The SEM micrograph showed a large surface area of hexagonal structured ZnO nanoparticles with separation within the nanoparticles. The manufactured ZnO nanoparticles manifested good antibacterial activity against gram negative bacteria.

REFERENCES

1. Virkutyte, J., & Varma, R. S. (2011). Green synthesis of metal nanoparticles: biodegradable polymers and enzymes in stabilization and surface functionalization. *Chemical Science*, 2(5), 837-846.
2. Li, B., & Wang, Y. (2010). Facile synthesis and photocatalytic activity of ZnO-CuO nanocomposite. *Superlattices and Microstructures*, 47(5), 615-623.
3. Liao, C., & Kannan, K. (2014). Widespread occurrence of benzophenone-type UV light filters in personal care products from China and the United States: an assessment of human exposure. *Environmental science & technology*, 48(7), 4103-4109.
4. Malhotra, S. P. K., & Mandal, T. (2019). Zinc oxide nanostructure and its application as agricultural and industrial material. *Contamin. Agric. Environ. Health Risks Remed*, 1, 216.
5. Fouda, A., Saied, E., Eid, A. M., Kouadri, F., Alemam, A. M., Hamza, M. F., ... & Hassan, S. E. D. (2023). Green synthesis of zinc oxide nanoparticles using an aqueous extract of punica granatum for antimicrobial and catalytic activity. *Journal of Functional Biomaterials*, 14(4), 205.
6. Zhou, J., Yang, Y., & Zhang, C. Y. (2015). Toward biocompatible semiconductor quantum dots: from biosynthesis and bioconjugation to biomedical application. *Chemical reviews*, 115(21), 11669-11717.
7. Ahmad, F., Ashraf, N., Ashraf, T., Zhou, R. B., & Yin, D. C. (2019). Biological synthesis of metallic nanoparticles (MNPs) by plants and microbes: their cellular uptake, biocompatibility, and biomedical applications. *Applied microbiology and biotechnology*, 103, 2913-2935.
8. Ong, C. B., Ng, L. Y., & Mohammad, A. W. (2018). A review of ZnO nanoparticles as solar photocatalysts: Synthesis, mechanisms and applications. *Renewable and Sustainable Energy Reviews*, 81, 536-551.
9. Husain, S., Rahman, F., Ali, N., & Alvi, P. A. (2013). Nickel sub-lattice effects on the optical properties of ZnO nanocrystals. *J. Optoelectron. Eng*, 1(1), 28-32.
10. Talam, S., Karumuri, S. R., & Gunnam, N. (2012). Synthesis, characterization, and spectroscopic properties of ZnO nanoparticles. *International Scholarly Research Notices*, 2012.
11. Muthuvel, A., Jothibas, M., & Manoharan, C. (2020). Synthesis of copper oxide nanoparticles by chemical and biogenic methods: photocatalytic degradation and in vitro antioxidant activity. *Nanotechnology for Environmental Engineering*, 5(2), 14.
12. Muthuvel, A., Jothibas, M., & Manoharan, C. (2020). Effect of chemically synthesis compared to biosynthesized ZnO-NPs using

- Solanum nigrum leaf extract and their photocatalytic, antibacterial and in-vitro antioxidant activity. *Journal of Environmental Chemical Engineering*, 8(2), 103705.
13. Berry, C. C., & Curtis, A. S. (2003). Functionalisation of magnetic nanoparticles for applications in biomedicine. *Journal of physics D: Applied physics*, 36(13), R198.
 14. Sharma, S., Kumar, K., Thakur, N., Chauhan, S., & Chauhan, M. S. (2020). The effect of shape and size of ZnO nanoparticles on their antimicrobial and photocatalytic activities: a green approach. *Bulletin of Materials Science*, 43, 1-10.
 15. Nithya, K., & Kalyanasundharam, S. (2019). Effect of chemically synthesis compared to biosynthesized ZnO nanoparticles using aqueous extract of *C. halicacabum* and their antibacterial activity. *OpenNano*, 4, 100024.
 16. Dahiya, P., & Purkayastha, S. (2012). Phytochemical screening and antimicrobial activity of some medicinal plants against multi-drug resistant bacteria from clinical isolates. *Indian journal of pharmaceutical sciences*, 74(5), 443.

**Assistant Professor, Department of Computer Applications
Theivanai Ammal College for Women, Villupuram, Tamil Nadu*

ABSTRACT

Nowadays, the usage of credit cards has dramatically increased. As master card becomes the foremost popular mode of payment for both online also as regular purchases, cases of fraud associated with it are also rising. In this paper, we model the sequence of operations in master card transaction processing employing a Hidden Markov Model (HMM) and show how it are often used for the detection of frauds. At the same time, we plan to confirm that genuine transactions aren't rejected. We present detailed experimental results to means the effectiveness of our approach and compare it with other techniques available within the literature.

INTRODUCTION

Credit-card-based purchases are often Categorized into two types :1) physical card and 2) virtual card. In a physical- card based purchase, the cardholder presents his card physically to a merchant for creating a payment. to hold out fraudulent transactions in this kind of purchase, an attacker possesses to steal the creditcard. If the cardholder doesn't realize the loss of card, it can cause a substantial loss to the master card company. Within the second quite purchase, just some important information a few card (card number, expiration date, secure code) is required to form the payment. Such purchases are normally done on the online or over the phone. To commit fraud in these kinds of purchases, a fraudster simply must know the cardboard details. Most of the time, the important cardholder isn't aware that someone else has seen or stolen his card information. The only because of detect this sort of fraud is to research the spending patterns on every card and to figure out any inconsistency with reference to the "usual" spending patterns. Fraud detection supported the analysis of existing purchase data of cardholder could also be a promising because of reduce the speed of successful credit card frauds. Since

humans tend to exhibit specific behavior profiles, every cardholder are often represented by a group of patterns containing information about the standard purchase category, the time since the last purchase, the number of money spent, etc. Deviation from such patterns could also be a possible threat to the system.

LITERATURE REVIEW

Credit card fraud detection using a neural network has been proposed by Ghosh and Reilly. They've done It. created a detection method based on a large dataset a sample of credit card account transactions that have been categorized These transactions are examples of fraud instances that have occurred as a result of the transactions to cards that have been misplaced, cards that have been stolen, and application fraud counterfeiting, mail-order fraud, and non- received mail are all examples of fraud. (NRI) fraud is a concern have recently utilized PGNNs (parallel granular neural networks) for Increasing the speed with which data is mined and insight is gained In order to detect credit card fraud, a discovery method is used. For this, a whole system has been implemented purpose.

METHODS AND MATERIALEXISTING SYSTEM

In case of the prevailing system the fraud is detected after the fraud is completed that, the fraud is detected after the complaint of the card holder. And so the cardboard holder faced plenty of trouble before the investigation finish.

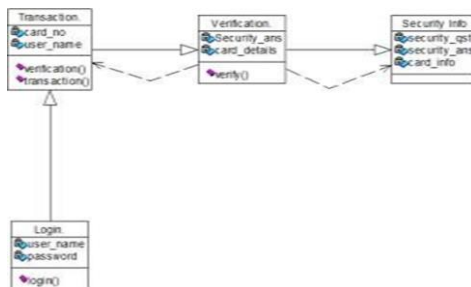


FIGURE 1. Class Diagram

PROPOSEDSYSTEM

In proposed system, we present a Hidden Markov Model (HMM). Which doesn't require fraud signatures and yet is during a position to detect frauds by considering a cardholder's

spending habit? Card transaction processing sequence by the model of an HMM. The details of things purchased in Individual transactions are usually not known to any Fraud Detection System (FDS) running at the bank that issues credit cards. It tries to hunt out any anomaly within the transaction supported the spending profile of the cardholder, shipping address, and billing address, etc. If the FDS confirms the transaction to be of fraud, and the issuing bank declines the transaction.

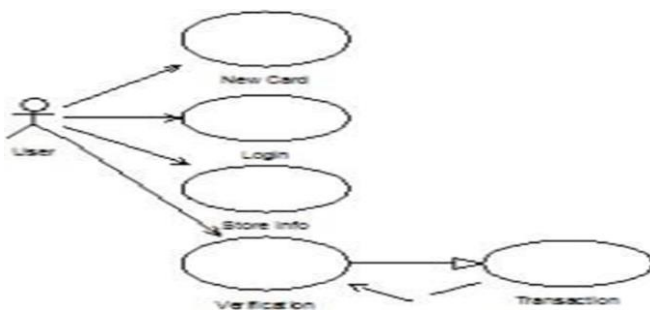


FIGURE 2. Use Case Diagram

MODULE

- A brand newcard
- Signin
- Information onsecurity
- Business transaction
- Confirmation

DESCRIPTION OF THE MODULE

A brand-new card

The consumer provides information in this module. Information on registering a new card. The data is all about their contact information.

Sign in

They make their own login and password. Visitors are presented in the Login Form module. with a username and password formfields. User provides a valid username and password they will be access to a combination extra materials available on the website. What extra resources will they have? Separate settings can be made for access to.

Information on security

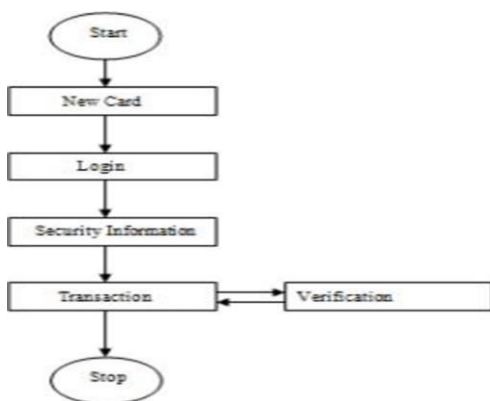
It will be found in the Security Information Module. the specifics of the information and the location of the store database. If the card is lost, the security information is lost as well.

Business transaction

The method and apparatus for preauthorizing transactions involve providing a transaction. A seller and a communication device holder of a credit card. A credit card is initiated by the credit card owner. By informing a creditor of the transaction number on a credit card and storing it there, a distinct piece of information that identifies a certain transaction to be completed made by a credit card user who has been given permission to use the card to be used at a later date. The data is regarded as reliable system information "Only if the data is correct is it stored in the database. PIC stands for personal identification code. with regards to communication. The "network data" will be used in the future. Authorize the transaction in question.

Verification

Information on verification is provided with in relation to a transaction involving an initiator and a recipient The first is a verification-seeking party, and the second is a verification-seeking party. Information provided by a third party for verification



Techniques and Algorithm Using HMM Model

Which additional resources they are going to have access to are often configured separately. HMM Model was used to map the

credit card transaction. We begin by performing a processing operation in terms of an HMM. When choosing on our observation symbols first model. We convert the x price into M price by quantifying the purchasing values x . $V_1; V_2; V_M$, etc., producing the observation at the issuing bank, symbols are used. The pricing range in reality each symbol can be customized based on the Individual cardholders' spending habits. These costs are by using a dynamic algorithm, ranges can be determined. On the basis of the values of each cluster, a clustering method was developed. Transactions of the cardholder, as shown in Section 5.2 $V_k, k = 1; 2; M$ is used to denote both the initial and final values. The sign for observation, as well as the related the price range we only analyze three price ranges in this study. low (l), medium (m), and high (h) The issuing bank handling the FDS is unaware of this information regarding the merchant's nature of business. As a result, the cardholder's purchase type The FDS can't see it because it's hidden. All potential types are included in this set. The set of all potential purchases and, equivalently, the set of all possible purchases Merchants' lines of business make up a hidden set. the HMM's states It worth noting at this point that implies the merchant's line of business is well-known Because this information is confidential, the acquiring bank

should be contacted. Provided at the time of a merchant's registration Furthermore, some shops may deal in a variety of products. (Wal-Mart, K Mart, and Target, for example, sell tens of thousands of different commodities things). These are the types of businesses that fall into this category

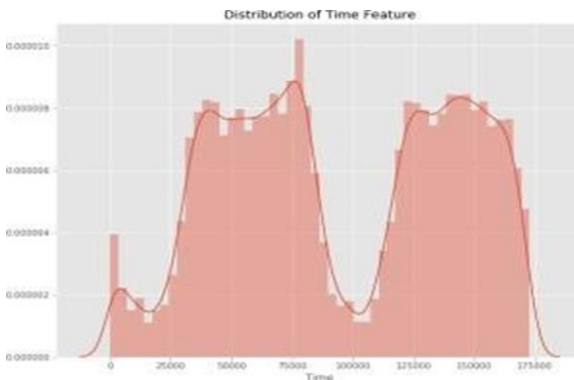


FIGURE 4. Fraudulent vs non- fraudulent

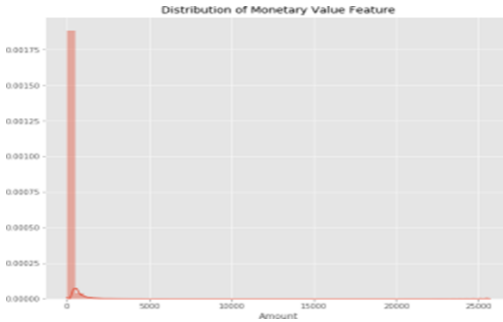


FIGURE 5. Distribution of time future

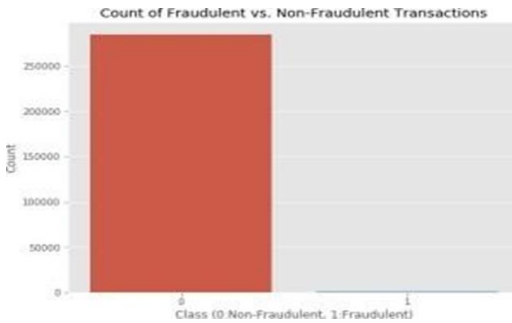


FIGURE 6. Distribution of Monetary values

MAINTENANCE AND TESTING OF THESYSTEM

Testing is critical to the system's success. The assumption in system testing is that if everything is in order, everything will be fine. When all of the components of the system are in place, the goal will be to It was accomplished successfully. We test during the testing procedure. The actual system in a company that collects errors as of now, the new system is fully functional. Stated. The stage of implementation where asystem is tested is called system testing. It is focused towards assuring the system's functionality precisely and effectively We test the actual system during the testing process. In a company and collect faults from new hires system and take steps to rectify the situation. All front- endandback- end. The goal of system testing is to consider all of the possible variations that could occur. We will be recommended, and the system will be pushed to its limits. The focus of the testing method is on logic. The software

at regular times to ensure that all of the statements have been put to the test, as well as the function. Intervals (i.e., performing tests to detect faults) as well as ensuring that defined inputs result in actual results that match the required outcomes. The two most popular methods for testing must be used. Unit testing and integration testing are the first two processes. System testing is carried out as part of the project. Procedure level testing is carried out. First. By providing incorrect inputs, the Errors are reported and corrected. This is the last step in the system's lifecycle.

CONCLUSION

We suggest an application of HMM in credit card fraud detection in this study. The several procedures involved in a creditcard transaction. The underlying processing is represented. An HMM's stochastic process. We have made use of as the observation ranges of transaction amount Symbolshave been used in place of item types. States of the HMM are considered. We've got a method for determining the spending profile of cardholders, as well as its implementation. In determining the worth of observation, knowledge is important. Symbols and a first guess at the model parameters. It's also been explained how the HMM may detect certain things. Whether or not a pending transaction is fraudulent. The performance and outcomes of the experiments are shown below. Illustratethe efficiency of our systemusefulness.

REFERENCES

1. "Global Consumer Attitude Towards On-Line Shopping," http://www2.acnielsen.com/reports/documents/2005_cc_online_shopping.pdf, Mar. 2007.
2. D.J. Hand, G. Blunt, M.G. Kelly, and N.M. Adams, "Data Mining for Fun and Profit," *Statistical Science*, vol. 15, no. 2, pp. 111-131, 2000.
3. "Statistics for General and On-Line CardFraud," <http://www.epaynews.com/statistics/fraud.html>, Mar. 2007.
4. S. Ghosh and D.L. Reilly, "Credit Card Fraud Detection with a Neural-Network," *Proc. 27th Hawaii Int'l Conf. System Sciences: Information Systems: Decision Support and Knowledge-Based Systems*, vol. 3, pp. 621-630,1994.
5. M. Syeda, Y.Q. Zhang, and Y. Pan, "ParallelGranularNetworksforFastCredit Card Fraud Detection," *Proc. IEEE Int'l Conf. Fuzzy Systems*, pp. 572-577, 2002.

6. S.J. Stolfo, D.W. Fan, W. Lee, A.L. Prodromidis, and P.K. Chan, "Credit Card Fraud Detection Using Meta- Learning: Issues and Initial Results," Proc. AAAI Workshop AI Methods in Fraud and Risk Management, pp. 83- 90,1997.
7. S.J. Stolfo, D.W. Fan, W. Lee, A. Prodromidis, and P.K. Chan, "Cost-Based Modeling for Fraud and Intrusion Detection: Results from the JAM Project," Proc. DARPA Information Survivability Conf. and Exposition, vol. 2, pp. 130-144, 2000.
8. E. Aleskerov, B. Freisleben, and B. Rao, "CARDWATCH: A Neural Network Based Database Mining System for Credit Card Fraud Detection," Proc. IEEE/IAFE: Computational Intelligence for Financial Eng., pp. 220- 226,1997.
9. M.J. Kim and T.S. Kim, "A Neural Classifier with Fraud Density Map for Effective Credit Card Fraud Detection," Proc. Int'l Conf. Intelligent Data Eng. and Automated Learning, pp. 378-383,2002.
10. W. Fan, A.L. Prodromidis, and S.J. Stolfo, "Distributed Data Mining in Credit Card Fraud Detection," IEEE Intelligent Systems, vol. 14, no. 6, pp. 67-74,1999.
11. R. Brause,T.Langsdorf,andM.Hepp, "Neural Data Mining for Credit CardFraud Detection," Proc. IEEE Int'l Conf. Tools with Artificial Intelligence, pp. 103-106, 1999.
12. C. Chiu and C. Tsai, "A Web ServicesBased Collaborative Scheme for Credit Card Fraud Detection," Proc.IEEEInt'l Conf. e-Technology, e-Commerce and e-Service, pp. 177-181, 2004.
13. C. Phua, V. Lee, K. Smith, and R. Gayler, "A Comprehensive Survey of Data Mining-Based Fraud Detection Research," <http://www.bsys.monash.edu.au/people/cphua/>, Mar.2007.
14. S. Stolfo and A.L. Prodromidis, "AgentBased Distributed LearningApplied to Fraud Detection," Technical Report CUCS-014-99, Columbia Univ.,1999.
15. C. Phua, D. Alahakoon, and V. Lee, "Minority Report in Fraud Detection: Classification of Skewed Data," ACM SIGKDD Explorations Newsletter, vol. 6, no. 1, pp. 50-59, 2004.

An Encryption and Decryption Technique Using a Complete Graph with Self-Invertible Matrix

Ms. M. Rajeswari*, N. Sharmila** & S. Sarojiny**

* Assistant Professor, PG and Research Department of Mathematics, Theivanai Ammal College for Women (Autonomous), Villupuram Tamilnadu

** M.sc Mathematics., PG and research Department of Mathematics, Theivanai Ammal College for Women (Autonomous), Villupuram Tamilnadu

ABSTRACT

In this paper, we process of message encryption and decryption technique based on the concept of complete graphs and self-invertible matrices. The encryption process involves representing the plaintext as a graph and transforming it using self-invertible matrices derived from the properties of the complete graph. This transformation ensures that the encrypted data retains its structural integrity while achieving a high level of security. We are introduce the enciphering technique with the help of the complete graph, an adjacency matrix, and also generated self-invertible key matrix to encrypt and decrypt the given message to produce complicated cipher text. Using the invertible matrix as a key matrix is always existing, we do not need to compute the inverse of the key matrix. It helps to reduce the complexity involved in the process of finding the inverse of a sum matrix.

Key words: Graph theory, Complete Graph ,Adjacency Matrix, Matrix form, Hill cipher, Encryption Algorithm, Decryption Algorithm and Self -Invertible Matrix.

1. INTRODUCTION

Cryptography derived its name from a Greek word called "Kryptos" which means "Hidden Secrets". Cryptography is the practice and study of hiding information. It is the Art or Science of converting a plain intelligible data into an unintelligible data and again retransforming that message into its original form.

The process of converting plain text into an unintelligible format (cipher text) is called Encryption. The process of converting cipher text into a plain text is called Decryption.

Cryptography is one of the important mathematical techniques that help us protect our data, messages and images from hackers.

Cryptography is the process of converting original messages or plaintexts into an unreadable, unrecognizable form so that only the deliberate recipients can remove the disguised form and read the original plaintext message.

The hackers or intermediates do not identify the data. The message we are sending is known as plain text, and the unrecognizable form of the message is called encrypted text or Ciphertext. Although both plain text and ciphertext are written in the form of alphabets. In certain cases, the messages are written in the form of some special characters like punctuation marks, numerals, and blanks or any other special characters to reduce the possibility of hacking or stealing the information.

Usually, the given plain texts are encoded using the following encoded table.

A	B	C	D	E	F	G	H	I	J
1	2	3	4	5	6	7	8	9	10

K	L	M	N	O	P	Q	R	S	T
11	12	13	14	15	16	17	18	19	20

U	V	W	X	Y	Z
21	22	23	24	25	26

The methods of generating self-invertible matrix for Hill Cipher algorithm have been proposed. The inverse of the matrix used for encrypting the plaintext does not always exist. So, if the matrix is not invertible, the encrypted text cannot be decrypted. In the self-invertible matrix generation method, the matrix used for the encryption is itself self-invertible. So, at the time of decryption, we need not to find inverse of the matrix. Moreover, this method eliminates the computational complexity involved in finding inverse of the matrix while decryption.

2. PRELIMINARIES OF GRAPH THEORY

2.1. Graph:

A graph is simply a collection of vertices and edges (or) a Graph G is an ordered pair (V, E), where V is its vertices and E be the edges.

2.2. Directed / Undirected Graphs:

In an undirected graph every edges as a set of vertices, an edge a, b is going to be the set ab, so it connects {a, b} this is same as the set {b, a} they both are same, there is no direction for the graphs and order does not matter for a graph. For directed graph the directions and order of the graphs are important.

2.3.Path:

A path is a walk with no repeated vertices, If a graph is connected then there is a a-b pathfor all a, b in V.

2.4. Hamiltonian Path:

A connected graph G contains an open walk that visits every vertices of a given graph G exactly once is called Hamiltonian path.

2.5. Adjacency Matrix:

The matrix which is based on the adjacency of vertices of a given graph. The adjacency matrix is a $n \times n$ matrix, where n is the number of vertices of graph.

$$P = \{p_{ij}\} = \begin{cases} 1, & \text{if there is an edge between vertex} \\ 0, & \text{otherwise} \end{cases}$$

2.6. Generation of self-invertible key matrix

A matrix M is said to be self-invertible matrix if $M=M^{-1}$, that is $M \cdot M^{-1} = M \cdot M^{-1} = I$, the self-invertible matrix was generated by using the following procedure, consider any arbitrary $\frac{n}{2} \times \frac{n}{2}$ matrix M_{22} (since n being the order of adjacency matrix) with the help of M_{22} we can compute the remaining $\frac{n}{2} \times \frac{n}{2}$ matrices using the following properties, $M_{11} + M_{22} = 0$, $M_{12} = I^{-2} M_{22}^2$,

$$M_{21} = I + M_{22}.$$

After computing $M_{11,12}, M_{21}, M_{22}$ the self-invertible matrix M was created by

$$M = \begin{bmatrix} M_{11} & M_{12} \\ M_{21} & M_{22} \end{bmatrix} = \begin{bmatrix} M_{11} & \cdots & M_{1n} \\ \vdots & \ddots & \vdots \\ M_{1n} & \cdots & M_{nn} \end{bmatrix}$$

3. Complete graph-based Encryption algorithm:

The given plain text message is converted into their numerical equivalent values with the help of encoded table. These numerical equivalent values are put into the edges of an undirected graph (i.e.) these values are put into the edges of the path, known as weights of the path. Construct a path with n-vertices (n represents the number of plaintext units) begins with the vertex 1, this path is made by connecting the sequential letters in the given plain text message unit, convert this weight assigned path into a Hamiltonian path by connecting dummy edges, and then connects every vertices by drawing edges between each vertices to make the graph into a complete, a false weights was given to the newly created edges and then the adjacency matrix for this corresponding complete graph was computed. For the key matrix, we are generating a selfinvertible key matrix of even order, after generating self-invertible key matrix multiply it with the adjacency matrix, the final matrix is the encrypted data for the original message units, finally this encrypted matrix shared to other user over an unsecure channel, these values are shared either in the form of row wise or column wise also represent the number of vertices, order of a adjacency matrix, $\frac{n}{2} \times \frac{n}{2}$ -matrix which help us to generate a required self-invertible key matrix. i.e.,

$I, n, \langle \text{Adjacency matrix} \rangle \langle \frac{n}{2} \times \frac{n}{2} \text{-matrix} \rangle$, here I is known as the index value of the given graph, n be the size of matrix.

3.1. Complete graph-based Decryption algorithm:

With the help of received data the receiver is able to find the index value, order of the adjacency matrix, the receiver separates the matrices, and with the help of $n2 \times n2$ matrix the receiver is also generating the self-invertible key matrix using the procedures which are explained in Section 3, then the given encrypted matrix can be multiplied with the generated self-invertible key matrix the receiver is able to get the adjacency matrix, tracing back the graph with the help of the resultant

adjacency matrix and write the edge weights of the graph from the given index value, decode these values with their numerical equivalent values using Table 1.0. Then finally the receiver is able to read the original message.

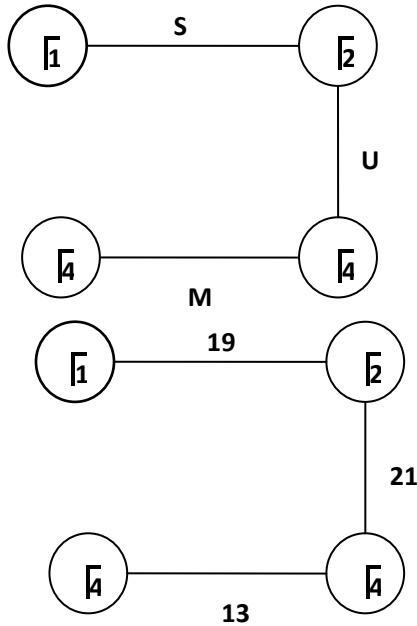
3.2. Implementation example:

Suppose that User A(sender) wants to send the message “SUM” to User B(receiver). Assuming that both the users should know the encryption and decryption techniques of the given procedure.

Encryption- User A (The sender): Encryption is done by the following steps

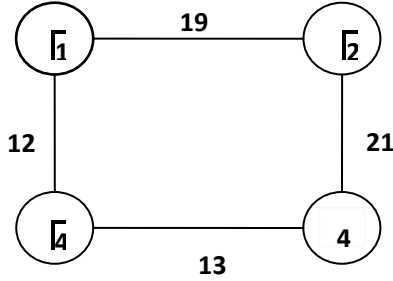
Step 1: The sender converts the message “SUM” into their numerical value using encoding table. S→19, U→21, M→13.

Step 2: Draw a path which starts from 1, the above mentioned value equivalent as the edges of this path. In these vertices are connected by the consecutive letters.



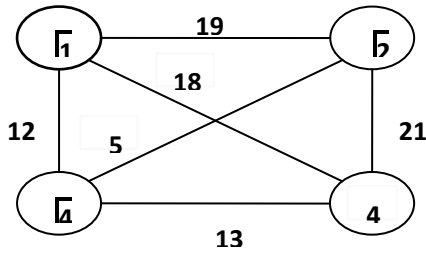
The path for given plain text

Step 3: The Hamiltonian path was constructed with false edge weight



Hamiltonian Path

Step 4: Connecting all the edges to make the given graph into a complete graph



Complete Graph

Step 5: Determine the adjacency matrix by using above complete graph and denoted by P.

$$P = \begin{bmatrix} 0 & 12 & 18 & 19 \\ 12 & 0 & 13 & 5 \\ 18 & 13 & 0 & 21 \\ 19 & 5 & 21 & 0 \end{bmatrix}$$

Step 6: We need to determine the key matrix for that resolve and we construct the self invertible key matrix "M", with the help of $\frac{n}{2}$ -matrix M_{22} .

Let $M_{22} = \begin{bmatrix} 22 & 5 \\ 19 & 0 \end{bmatrix}$ Then

$$M_{11} = \begin{bmatrix} 1 & 21 \\ 7 & 0 \end{bmatrix} M_{12} = \begin{bmatrix} 0 & -21 \\ 7 & -25 \end{bmatrix} = \begin{bmatrix} 0 & 5 \\ 19 & 1 \end{bmatrix} \quad \text{and}$$

$$M_{21} = \begin{bmatrix} 2 & 29 \\ 7 & 1 \end{bmatrix}$$

Therefore, $M = \begin{bmatrix} M_{11} & M_{12} \\ M_{21} & M_{22} \end{bmatrix}$

$$= \begin{bmatrix} 1 & 21 & 0 & 5 \\ 7 & 0 & 19 & 1 \\ 2 & 21 & 25 & 5 \\ 7 & 1 & 19 & 0 \end{bmatrix}$$

Step 7: At last we have compute PM, in this multiplication is called the encrypted data of the original message.

$$C = P.M = \begin{bmatrix} 0 & 12 & 18 & 19 \\ 12 & 0 & 13 & 5 \\ 18 & 13 & 0 & 21 \\ 19 & 5 & 21 & 0 \end{bmatrix} \begin{bmatrix} 1 & 21 & 0 & 5 \\ 7 & 0 & 19 & 1 \\ 2 & 21 & 25 & 5 \\ 7 & 1 & 19 & 0 \end{bmatrix}$$

$$C = \begin{bmatrix} 253 & 397 & 1039 & 102 \\ 73 & 530 & 420 & 125 \\ 256 & 399 & 646 & 103 \\ 96 & 840 & 620 & 205 \end{bmatrix}$$

19 1

25 5

19 0

This *PM* matrix can be converted into either row or column matrix and sent is to the other user over an unsecure channel with index number, size of matrix and the matrix [1,4,253,397,1039,102,73,530,420,125,256,399,646,103,96,840,620,205,25,5,19,0]

DECRYPTION- USER A (THE SENDER):

Decryption is done by the following steps With the received information, the receiver separates the following matrix as follows

$$C = P.M = \begin{bmatrix} 253 & 397 & 1039 & 102 \\ 73 & 530 & 420 & 125 \\ 256 & 399 & 646 & 103 \\ 96 & 840 & 620 & 205 \end{bmatrix}$$

And the self-invertible key matrix be $M = \begin{bmatrix} 1 & 21 & 0 & 5 \\ 7 & 0 & 19 & 1 \\ 2 & 21 & 25 & 5 \\ 7 & 1 & 19 & 0 \end{bmatrix}$

$$CM = PM.M = \begin{bmatrix} 253 & 397 & 1039 & 102 \\ 73 & 530 & 420 & 125 \\ 256 & 399 & 646 & 103 \\ 96 & 840 & 620 & 205 \end{bmatrix} \begin{bmatrix} 1 & 21 & 0 & 5 \\ 7 & 0 & 19 & 1 \\ 2 & 21 & 25 & 5 \\ 7 & 1 & 19 & 0 \end{bmatrix}$$

$$CM = \begin{bmatrix} 5824 & 27234 & 35456 & 6857 \\ 5498 & 10478 & 22945 & 2995 \\ 5062 & 19045 & 25688 & 4909 \\ 8651 & 15241 & 35355 & 4420 \end{bmatrix}$$

Taking modulo 26, we get then we get,

$$5824(\text{mod } 26) = 0$$

$$27234(\text{mod } 26) = 12$$

$$35456(\text{mod } 26) = 18$$

$$6857(\text{mod } 26) = 19$$

$$5498(\text{mod } 26) = 12$$

$$10478(\text{mod } 26) = 0, \dots$$

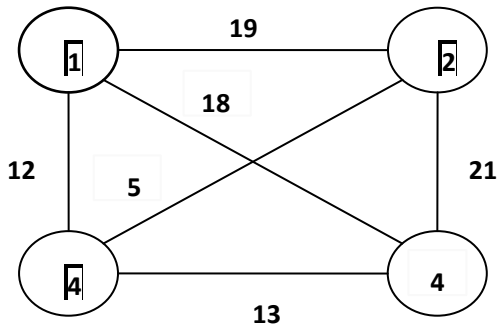
$$SM = \begin{bmatrix} 0 & 12 & 18 & 19 \\ 12 & 13 & 5 \\ 18 & 0 & 21 \\ 19 & 21 & 0 \end{bmatrix}$$

$$0 = P$$

13

5

The Corresponding graph for the above adjacency matrix is



Complete Graph

The edges(weights) of the above path are 12,13,21,19,18,5

Therefore, the original message is S→19, U→21, M→13 (i.e) SUM

CONCLUSION

In this paper, Cryptography algorithm is proposed for providing better security and privacy to the data in any network. Nowadays attacker can easily steal your message and misuse it. The main focus of this paper is to come up with a system where message or a data can be encrypted in a more secure way. One of the important encryption algorithm have been used. That is encryption and decryption algorithm, which encrypts the secret message and convert into a disconnected graph after that introduce the new edge are connected in the disconnected graph, finally we found a complete graph. After that we use the encoding table and construct the matrix form by using the complete graph. According to the system it is capable for giving more security to the message. In this method to easily find the encrypt and decrypt. Moreover system is also very user friendly where any non-technical person can use the system. In this future ,this approach will be modified and to be used for some other graph theory concepts,self -invertible matrix for any order, also to extend your image encryption and decryption, etc.

REFERENCES:

1. Diffie, W., Hellman, M., 1976. New directions in Cryptography, IEEE Trans. Inf. Theory 22(6), 644-654.
2. J. Gallian, a dynamic survey of graph labeling, The electronic journal of combinatorics (2015).
3. Invitation of Graph theory, S .Arumugam, S. Ramachandran, Scitech Publications, 2015.
4. Neal Koblitz, A course in Number Theory and Cryptography, second edition, Springer.
5. W. Stallings, "Cryptography and Network Security", 4th edition, Prentice Hall, 2005.
6. Uma Dixit, Cryptography a Graph Theory approach International journal of Advance Research in Science and engineering, 6(01), 2017.

Ms. R. Suganya*, G. Harini** & D. Priyanka Salomi**

* Assistant Professor, PG and Research Department of Mathematics Theivanai Ammal College For Women (Autonomous), Villupuram, Tamilnadu.
** M.Sc., Mathematics, PG and Research Department of Mathematics Theivanai Ammal College For Women (Autonomous), Villupuram -605 602, Tamilnadu

ABSTRACT

The concept of this paper is to obtain Nano RGB-Closed sets and its new approaches in Nano Topological Spaces. Also investigate its properties. We study the weak form of nano open sets namely nano regular open sets and nano b-open sets in nano topological space. Similarly, we define nano b-closed set and regular closed set and also nano pre closed set, nano semi closed set, nano semi pre closed set. We have introduced a new class of sets on nano topological spaces called nano regular generalized closed sets. The aim of this dissertation is to continue the study on nano generalized closed sets in nano topological spaces.

1. INTRODUCTION

Njastad, Levine and Mashhour et al respectively introduced the notion of α -open, semi open and pre open sets. It was made clear that each α -open set is semi open and pre open, but the converse of each is nano true. Also a new class of generalized open sets called b-open sets in topological spaces was studied by D. Andrijavic, which is contained in the class of semi pre open set and contains all semi open sets and pre open sets.

Levine introduced the class of generalized closed sets, a super class of closed sets in 1970. This concept was introduced as a generalization of closed sets in topological spaces through which new results in general topology were introduced. Ahmad Al-Omari and Mohd Salmi Md. Noorani are introduced "On Generalized b-closed sets" in topological spaces.

Later on N. Palaniappan studies the concept of regular generalized closed set in a topological space. The concept of regular b-closed set in topological spaces are studied by N. Nagaveni and A. Narmadha. The notion of regular generalized b-closed sets introduced by K. Mariappa and S. Sekar.

A rough set can be described by a pair of definable sets called lower and upper approximations. The lower approximation is the greatest definable set contained in the given set of objects, while the upper approximation is the smallest definable set containing the given set. In 2013, the notion of nano topology was introduced by M. Lellis Thivagar which was defined in terms of approximations and boundary region of a universe using an equivalence relation on it. He also established certain weak forms of nano open sets such as nano α -open, nano semi open and nano pre open sets.

In this journal, we have introduced a new class of sets on nano topological spaces called nano regular generalized closed sets. The aim is to continue the study on nano generalized closed sets in nano topological spaces. In particular, we present the notion of nano regular generalized b-closed sets (briefly nano rgb-closed sets) and obtain their characterizations. Also we establish various form of continuities associated to nano regular generalized closed sets.

2. PRELIMINARIES:

2.1. Basic Definitions in Topological spaces.

Definition 2.1.1.

A subset A of a space (U, X) is called,

Pre open set if $A \subseteq \text{int}(\text{cl}(A))$ and Pre closed set if $\text{cl}(\text{int}(A)) \subseteq A$.

Semi open set if $A \subseteq \text{cl}(\text{int}(A))$ and Semi closed set if $\text{int}(\text{cl}(A)) \subseteq A$.

α -open set if $A \subseteq \text{int}(\text{cl}(\text{int}(A)))$ and α -closed set if $\text{int}(\text{cl}(\text{int}(A))) \subseteq A$.

Regular open set if $A = \text{int}(\text{cl}(A))$ and Regular closed set if $A = \text{cl}(\text{int}(A))$.

Definition 2.1.2.

A subset A of a topological space (X, τ) is called a **Generalized Closed Set** (briefly g -closed set) if $cl(A) \subseteq V$ whenever $A \subseteq V$ and V is open in (X, τ) .

2.2. NANO TOPOLOGY SPACE:

Definition 2.2.1.

Let U be the universe, R be an equivalence relation on U and $\tau_R(X) = \{U, \phi, L_R(X), U_R(X), B_R(X)\}$, where $X \subseteq U$. Then by above property, $\tau_R(X)$ satisfies the following axioms:

- i. U and $\phi \in \tau_R(X)$
- ii. The union of the elements of any sub collection of $\tau_R(X)$ is in $\tau_R(X)$.
- iii. The intersection of the elements of any finite sub collection of $\tau_R(X)$ is in $\tau_R(X)$.

That is, $\tau_R(X)$ is a topology on U called the **Nano Topology** on U with respect to X . We call $(U, \tau_R(X))$ as the **Nano Topological Spaces**.

2.3. Nano Continuity.

Definition 2.3.1.

Let $(U, \tau_R(X))$ and $(V, \tau_{R'}(Y))$ be two nano topological spaces. Then a mapping

$f : (U, \tau_R(X)) \rightarrow (V, \tau_{R'}(Y))$ is said to be,

- Nano Continuous if $f^{-1}(B)$ is nano open in U for every nano open set B in V .
- Nano α -Continuous if $f^{-1}(B)$ is nano α -open in U for every nano open set B in V .

3. NANO REGULAR CLOSED SET, NANO B-CLOSED SET AND NANO GENERALIZED CLOSED SET

3.1. Weak Form of Nano Open Sets in Nano Topological Space.

Definition 3.1.1.

If $(U, \tau_R(X))$ is nano topological space with respect to X where $X \subseteq U$ and if $A \subseteq U$, then the **Nano Interior** of A is defined as the union of all nano open subsets of A and it is denoted by $Nint(A)$. $Nint(A)$ is the largest nano open subset of A .

The **Nano Closure** of A is defined as the intersection of all nano closed set containing A and it is denoted by $Ncl(A)$. $Ncl(A)$ is the smallest nano closed set containing A .

Let $(U, \tau_R(X))$ be a nano topological space and $A \subseteq U$. Then A is said to be **Nano Regular Open Set** if $A = \text{Nint}(\text{Ncl}(A))$.

Definition 3.1.2.

Let $(U, \tau_R(X))$ be a nano topological space and $A \subseteq U$. Then A is said to be **Nano Regular Closed Set** (briefly nano r-closed set), if $\text{Ncl}(\text{Nint}(A)) = A$.

3.2. New Class of generalized Nano Open Sets.

Definition 3.2.1.

A subset A of a nano topological space $(U, \tau_R(X))$ is said to be **Nano B-Open** if

$A \subseteq \text{Ncl}(\text{Nint}(A)) \cup \text{Nint}(\text{Ncl}(A))$. The class of all nano b-open sets in X is denoted by $\text{NBO}(U, X)$.

Definition 3.2.2.

A subset A of a space X is called **Nano B-Closed set** if $X - A$ is nano B-open. Thus A is **Nano B-Closed** if and only if $\text{Nint}(\text{Ncl}(A)) \cap \text{Ncl}(\text{Nint}(A)) \subseteq A$ or $\text{Nbcl}(A) = A$.

Definition 3.2.3.

- If A is a subset of a space X is **Nano B-Closure** of A , denoted by $\text{Nbcl}(A)$ is the smallest nano b-closed set containing A .
- The **Nano B-Interior** of A is denoted by $\text{Nbint}(A)$ is the largest nano b-open set contained in A .

3.3. Nano Generalized Closed Set

Definition 3.3.1.

Let $(U, \tau_R(X))$ be nano topological space. A subset A of $(U, \tau_R(X))$ is called **Nano Generalized Closed Set** (briefly NG-Closed set) if $\text{Ncl}(A) \subseteq V$, where $A \subseteq V$ and V is nano open.

4. NANO REGULAR GENERALIZED COSED SET AND NANO GENERALIZED B-CLOSED SET

4.1. Nano Regular Generalized Closed Set in Nano Topological Spaces.

Definition 4.1.1.

If $(U, \tau_R(X))$ is nano topological space with respect to X where $X \subseteq U$ and if $A \subseteq U$ then,

- The **Nano Regular Closure** of A is defined as the intersection of all nano regular closed sets containing A

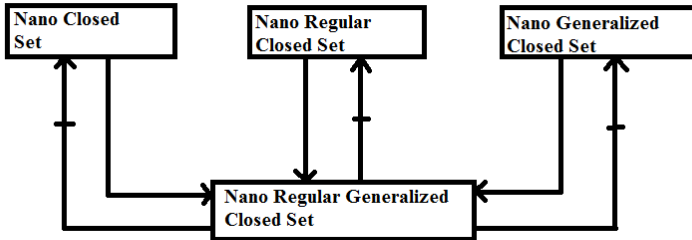
and it is denoted by $Nrcl(A)$, which is the smallest nano regular closed set containing A .

- The **Nano Regular Interior** of A is defined as the union of all nano regular open subsets of A contained in A and it is denoted by $Nrint(A)$, which is the largest nano regular open subsets of A .

Definition 4.1.2.

A subset A of a nano topological space $(U, \tau_R(X))$ is called **Nano Regular Generalized Closed Set** (briefly nano RG-closed set), if $Nrcl(A) \subseteq V$, whenever $A \subseteq V$ and V is nano regular open set.

Note:



4.2. Nano Generalized B-Closed Set in Nano Topological spaces:

Definition 4.2.1.

If $(U, \tau_R(X))$ is nano topological space with respect to X where $X \subseteq U$ and if $A \subseteq U$ then,

- The **Nano B-Closure** of A is defined as the intersection of all nano b-closed sets containing A and it is denoted by $Nbcl(A)$, which is the smallest nano b- closed set containing A .
- The **Nano B-Interior** of A is defined as the union of all nano b-open subsets of A contained in A and it is denoted by $Nbint(A)$, which is the largest nano b- open subsets of A .

Definition 4.2.2.

A subset A of a nano topological space $(U, \tau_R(X))$ is called **Nano Generalized B-Closed Set** (briefly nano GB-closed set), if $Nbcl(A) \subseteq V$, whenever $A \subseteq V$ and V is nano open set.

5. CHARACTERIZATION OF NANO RGB-CLOSED SET IN NANO TOPOLOGICAL SPACES

5.1. Nano RGB-Closed Sets in Nano Topological Spaces.

Definition 5.1.1.

A subset A of a nano topological spaces $(U, \tau_{\text{TR}}(X))$ is said to be **Nano Regular Generalized B-Closed Set** (briefly nrgb-closed set), if $\text{Nbcl}(A) \subseteq V$ whenever $A \subseteq V$ and V is regular open in U .

Theorem 5.1.2.

Let $(U, \tau_{\text{TR}}(X))$ be a nano topological space and $A \subseteq U$, then every nano closed, nano regular closed, nano α -closed, nano semi closed, nano pre closed, nano g -closed, nano gb -closed, nano rg -closed, nano sg -closed, nano gs -closed, nano αg -closed, nano $g\alpha$ -closed sets are nano rgb -closed set.

5.2. Characterization of Nano RGB-Closed Set in Nano Topological Spaces.

Theorem 5.2.1.

Let A be a nano rgb -closed set in (U, X) . Then,

1. $\text{Nbcl}(A) - A$ has no non empty nano regular-closed set.
2. A is nano b -closed set if and only if $\text{Nbcl}(A) - A$ is nano regular-closed set.

Theorem 5.2.2.

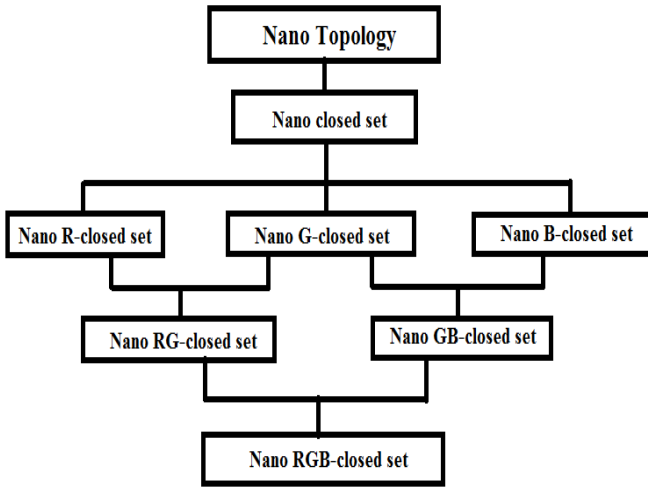
1. If A is nano rgb -closed set and $A \subseteq B \subseteq \text{Nbcl}(A)$ then B is nano rgb -closed set.
2. Suppose that $B \subseteq A \subseteq U$, where A is a nano rgb -closed and nano regular open set. Then B is rgb -closed relative to A if and only if B is a nano rgb -closed relative to U .

5.3. Nano RGB-Open set in Nano Topological Spaces.

Definition 5.3.1.

A subset A of a nano topological space U is called Nano Regular Generalized B-Open (simply Nrgb-open) if A^c is nano rgb -closed. The collection of all nano rgb -open subsets of U is denoted by $\text{NrgbO}(U, X)$.

Flow Chart for New Approaches of Nano RGB-Closed Set:



6. APPLICATIONS

6.1. Nano RGB-Continuous Function between Two Nano Topological Spaces.

Definition 6.1.1.

Let $(U, \tau_R(X))$ and $(V, \tau_R'(Y))$ be nano topological spaces. Then a mapping

$f : (U, \tau_R(X)) \rightarrow (V, \tau_R'(Y))$ is said to be nano regular generalized b-continuous (nano rgb-continuous) if the inverse image of every closed set in V is nano rgb-closed in U .

Theorem 6.1.2.

Let $(U, \tau_R(X))$ and $(V, \tau_R'(Y))$ be nano topological spaces and a mapping $f : (U, \tau_R(X)) \rightarrow (V, \tau_R'(Y))$. Then every nano b-continuous, nano continuous, nano α -continuous, nano semi continuous, nano pre continuous, nano g-continuous, nano sg-continuous functions are nano rgb-continuous.

We characterize nano rgb-continuous functions in terms of inverse image of nano closure.

Theorem 6.1.3.

A function $f : (U, \tau_R(X)) \rightarrow (V, \tau_R'(Y))$ is nano rgb-continuous if and only if $Nrgbcl(f^{-1}(B)) \subseteq f^{-1}(Ncl(B))$.

Theorem 6.1.4.

A function $f: (U, \tau_R(X)) \rightarrow (V, \tau_R'(Y))$ is nano rgb-continuous on U if and only if

$$f^{-1}(\text{Nint}(B)) \subseteq \text{Nrgbint}(f^{-1}(B)) \text{ for every subset } B \text{ of } V.$$

6.2. Nano RGB-Irresolute Function between Two Nano Topological Spaces.

Definition 6.2.1.

Let $(U, \tau_R(X))$ and $(V, \tau_R'(Y))$ be two nano topological spaces. Then a function $f: U \rightarrow V$ is said to be **Nano Regular Generalized B-Irresolute** (nano rgb-irresolute) if the inverse image of every nano rgb-closed set in V is nano rgb-closed in U .

Theorem 6.2.2.

A function $f: U \rightarrow V$ is nano rgb-irresolute if and only if for every nano rgb-open set F in V , $f^{-1}(F)$ is nano rgb-open in U .

Theorem 6.2.3.

A function $f: U \rightarrow V$ is nano rgb-irresolute, then f is nano rgb-continuous.

Theorem 6.2.4.

- ❖ If $f: U \rightarrow V$ is nano rgb-irresolute and $g: V \rightarrow W$ is nano rgb-continuous, then $g \circ f: U \rightarrow W$ is nano rgb-continuous.
- ❖ If $f: U \rightarrow V$ is nano rgb-continuous and $g: V \rightarrow W$ is nano continuous, then $g \circ f: U \rightarrow W$ is nano rgb-continuous.

Theorem 6.2.5.

If $f: U \rightarrow V$ is nano rgb-irresolute and $g: V \rightarrow W$ is nano b-continuous, then

$$g \circ f: U \rightarrow W \text{ is nano rgb-continuous.}$$

Theorem 6.2.6.

If $f: U \rightarrow V$ is nano rgb-irresolute and $g: V \rightarrow W$ is nano α -continuous, then

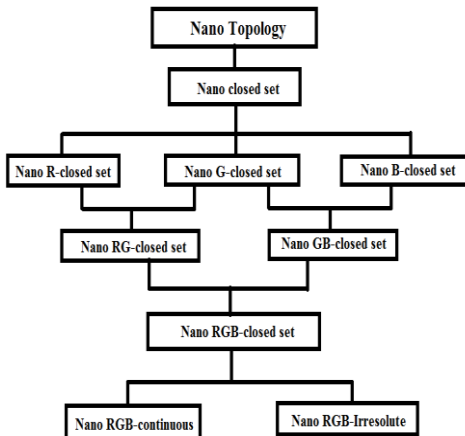
$$g \circ f: U \rightarrow W \text{ is nano rgb-continuous.}$$

Theorem 6.2.7.

If $f : U \rightarrow V$ is nano rgb-irresolute and $g : V \rightarrow W$ is nano semi-continuous, then

$g \circ f : U \rightarrow W$ is nano rgb-continuous.

Overview of This Dissertation can be given in the below Flow Chart:



CONCLUSION

The classes of nano regular generalized b-closed set (Nano RGB-Closed set) is derived using nano regular open set from a nano topology that lies between the class of nano b-closed set and nano rgb-closed set. The nano RGB-closed set can be used to define a new decomposition of continuity such as Nano RGB-Continuity functions and Nano RGB-Irresolute functions in Nano Topological Spaces. This idea can be extended to Fuzzy Topological Spaces.

BIBLIOGRAPHY

1. Levine.N, "Semi Open Sets and Semi Continuity in Topological Spaces", Amer, Math. Monthly 70(1963), 36-41.
2. Mashhour. A. S, AbdEl-Monsef. M. E, and El-Deep. S. N, "On Pre Topological Spaces", Bull. Mat. De la soc.R.S. de Roumanie 28(76) (1984), 39-45.
3. Njastad.O, "On Some Classes of Nearly Open sets", Pacific.J. Math.15(1965), 961- 970.

4. Levine.N (1963), "Generalized Closed Sets in Topology", Rend.Cire. Math. Palermo, 19(2), 89-96.
5. Ahmad Al-Omari and Mohd. Salmi Md. Noorani, "On Generalized b-closed sets", Bull. Malays. Math. Sci. Soc. (2)32(1) (2009), 19-30.
6. Pawlak.Z, "Rough Sets", International Journal of Information and Computer Sciences, 11(1982), 341-356.
7. Nagaveni.N and Narmadha.A, "On Regular B-closed sets in Topological Spaces", Heber International Conference on Applications of Mathematics and Statistics, HICAMS-2012, 5-7 Jan 2012, 81-87.
8. Palaniappan.N and Chandarasekhara Rao.K, "Regular generalized closed sets", Kyungpook math.J, 33(1993), 211-219.
9. Lellis Thivagar.M and Carmel Richard, "Note on Nano topological Spaces", Communicated.
10. Mariappa.K and Sekar.S, "*On Regular Generalized b-Closed Set*", International Journal of Mathematical Analysis, Vol.7, 2013, No.13, 613-624.
11. Dhanis Arul Mary.A, Arockiarani.I, "*On Characterization of Nano RGB- Closed Sets in Nano Topological Spaces*", International Journal of Modern Engineering Research (IJMER), Vol 5, Issue 1, Jan 2015, 68.
12. Dhanis Arul Mary.A, Arockiarani.I, "*On Nano GB-Closed Sets in Nano Topological Spaces*", International Journal of Mathematical Archive-6(2), Feb 2015.
13. Lellis Thivagar.M and Carmel Richard, "*On nano forms of weakly open sets*", International Journal of Mathematics and statistics Invention, Volume 1, Issue 1, August 2013, PP- 31-37.
14. Bhuvanewari. K and Mythili Gnanapriya. K, "*Nano Generalized Closed Sets in Nano Topological Space*", International Journal of Scientific and Research Publications, Vol 4, Issue 5, May 2014.

A. S. Parveen Nisha*, M. Kalaivani**

* Student, Department of Computer Science, Theivanai Ammal College for Women (Autonomous) Villupuram, Tamilnadu

** Assistant Professor, Department of Computer Science, Theivanai Ammal College for Women (Autonomous) Villupuram, Tamilnadu

ABSTRACT

Water conservation is a critical concern in public spaces, particularly at stand posts where water wastage is a prevalent issue. This proposed project introduces a novel solution, the "Touchless Water Tap," designed to prevent unnecessary water loss by incorporating advanced sensor technology. The presence of IR sensor enhances user experience through a touchless interaction, contributing to water conservation efforts in public areas. The system is meticulously designed, leveraging the capabilities of the IR Sensor as a key component. This sensor is strategically integrated into the water tap to detect the proximity of users. The touchless interface ensures that water flow is activated only when a user is within range, effectively addressing the challenge of inadvertent water wastage. The core functionality revolves around the sensor's ability to initiate the water flow upon user detection. This touchless mechanism not only enhances convenience for users but also plays a pivotal role in reducing water consumption. The system is engineered to strike a balance between user accessibility and sustainability, offering an inclusive solution for diverse individuals in public spaces.

Keywords - Touchless Water Tap, IR sensor, Public Stand Posts.

INTRODUCTION

Water, the most valuable and indispensable resource on our planet, is facing unprecedented challenges due to misuse, mismanagement, and depletion of freshwater sources. The ramifications of these issues are dire, with projections indicating a looming global water crisis that could threaten the very survival of humanity. As the population continues to burgeon and urbanization escalates, the demand for water is reaching critical levels, necessitating urgent action to ensure efficient management and conservation of this precious resource.

The Urgency of the Water Crisis

Water scarcity has emerged as a pressing concern in recent years, exacerbated by factors such as population growth, urbanization, and inadequate management practices. The United Nations predicts that by 2025, a staggering 75% of the world's population will lack access to reliable clean water—a sobering statistic that underscores the urgency of addressing the water crisis. Without immediate intervention, the consequences could be catastrophic, with potentially devastating impacts on human health, food security, and socio-economic stability.

Harnessing Technology for Water Management

In response to the growing water crisis, there is an urgent need for innovative solutions that leverage technology to enhance water management and conservation efforts. Revolutionized technologies such as the Internet of Things (IoT), Information and Communication Technology (ICT), and Wireless Sensor Networks (WSN) hold immense potential to address the real-time challenges facing society in the realm of water management. By deploying smart water solutions, we can optimize the distribution of water resources, mitigate wastage, and ensure the sustainable utilization of this vital resource.

The Role of Smart Water Management

Smart water management represents a paradigm shift in how we approach the management of water resources. Also known as the "Internet of Water" or "Smart Water Grid," this approach integrates advanced technologies to monitor, analyze, and optimize water usage across various sectors. By leveraging real-time data and analytics, smart water management systems can identify inefficiencies, detect leaks, and facilitate proactive decision-making to improve overall water efficiency and sustainability.

Addressing Water Wastage and Mismanagement

Water wastage and mismanagement pose significant challenges to water sustainability, particularly in regions with inadequate infrastructure and poor governance. In countries like India, where water resources are abundant yet mismanaged, the consequences of water wastage are acutely felt. Public stand-

posts, intended for community water supply, often suffer from oversupply and neglect, leading to widespread water wastage and scarcity.

LITERATURE REVIEW

Smart Water Management Systems

Chen, Y., Gong, J., Zhang, H., Zhao, X., & Liu, Y. (2020). Design of Smart Water Management System Based on Internet of Things. IOP Conference Series: Materials Science and Engineering, 861(1), 012014.

In the paper titled "Design of Smart Water Management System Based on Internet of Things" by Chen et al. (2020), several scopes can be identified that are relevant for implementing the Touchless Water Tap.

Internet of Things (IoT) Integration

The paper emphasizes the integration of IoT technologies in designing a smart water management system. Similarly, for the Sensor-Based Smart Water Tap project, the focus would be on leveraging IoT principles to develop a tap system that incorporates sensor technologies for efficient water management.

Smart Water Management

The overarching goal of the paper is to design a system for smart water management, which aligns with the objective of the Sensor-Based Smart Water Tap project. By integrating sensors into the tap system, it becomes possible to monitor water usage in real-time and optimize water consumption.

Sensor Deployment

The paper likely discusses the deployment of various sensors within the water management system to collect data on water usage, quality, and other relevant parameters. Similarly, for the Sensor-Based Smart Water Tap project, the deployment of sensors, such as flow sensors or proximity sensors, would be essential for detecting user interactions and monitoring water flow.

Sensor Technologies for Water Conservation

Nabeel, M., Shah, M. A., & Hassan, S. A. (2019). IoT-Based Smart Water Management System Using Artificial Neural Networks. *IEEE Access*, 7, 71358-71369.

In the paper titled "IoT-Based Smart Water Management System Using Artificial Neural Networks" by Nabeel, Shah, and Hassan (2019), several scopes can be identified that are relevant for implementing the Touchless Water Tap.

Sensor Deployment

The paper likely discusses the deployment of various sensors within the water management system to collect data on water usage, quality, and other relevant parameters. Similarly, for the Sensor-Based Smart Water Tap project, the deployment of sensors, such as flow sensors or proximity sensors, would be essential for detecting user interactions and monitoring water flow.

Data Collection and Analysis

Nabeel et al. (2019) may address the collection and analysis of data obtained from sensors deployed within the smart water management system. Likewise, in the Sensor-Based Smart Water Tap project, data collected from sensors embedded in the tap system would be analyzed to gain insights into water usage patterns and identify opportunities for optimization.

Automation and Control

The paper may discuss how IoT technologies enable automation and remote control of water management systems. Similarly, for the Sensor-Based Smart Water Tap project, IoT-enabled features could allow users to remotely control the tap and receive notifications about water usage, leaks, or other issues.

Sensor-Based Water Quality Monitoring Systems:

Soni, N., & Varshney, S. (2019). Real-Time Water Quality Monitoring System Using IoT. 2019 3rd International Conference on Trends in Electronics and Informatics (ICOEI), 1083-1086.

In the paper titled "Real-Time Water Quality Monitoring System Using IoT" by Soni and Varshney (2019), several scopes can be

identified that are relevant for implementing the Sensor-Based Smart Water Tap.

Real-Time Monitoring

Soni and Varshney (2019) likely discuss the importance of real-time monitoring for ensuring water quality and safety. Similarly, for the Sensor-Based Smart Water Tap project, real-time monitoring capabilities could be incorporated into the tap system to detect changes in water flow, temperature, or other parameters instantaneously.

Efficiency and Sustainability

Soni and Varshney (2019) likely highlight the importance of ensuring water quality and sustainability through real-time monitoring and management. Likewise, the Sensor-Based Smart Water Tap project aims to contribute to water conservation efforts by providing a smart, efficient, and sustainable solution for managing water usage and quality at the tap level.

METHODOLOGY

This project aims to build a touchless water tap control system using an ESP8266 microcontroller (NodeMCU), an infrared (IR) sensor, a DC-DC buck converter, a solenoid valve, and a single-channel relay. The system detects hand movement using the IR sensor and activates the water flow through the solenoid valve controlled by the relay, providing a hygienic and convenient way to operate the tap.

The DC-DC buck converter supplies 3.3V power to the NodeMCU. The IR sensor is connected to an appropriate pin of the NodeMCU to receive its signal. The relay is connected to the NodeMCU, with the coil receiving a 5V signal from the microcontroller. The solenoid valve is connected to the relay's output and the 12V power supply. The NodeMCU continuously reads the signal from the IR sensor. When the sensor detects hand movement (high signal), the NodeMCU activates the relay. The activated relay allows current to flow to the solenoid valve coil. The energized solenoid valve opens, allowing water to flow through the tap. Once the hand moves away (low signal), the NodeMCU deactivates the relay. The de-energized solenoid valve closes, stopping the water flow.

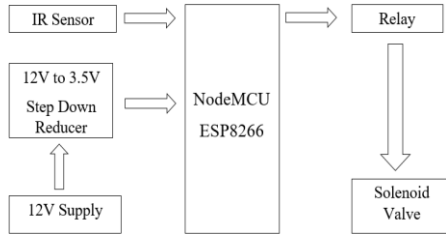


Fig 1. Block Diagram of Touchless Water Tap

HARDWARE REQUIREMENTS

Microcontroller

The heart of NodeMCU is the ESP8266 Wi-Fi Microcontroller Unit (MCU) by Espressif Systems. This tiny chip integrates a CPU, RAM, and networking capabilities, allowing it to connect to the internet and interact with other devices. NodeMCU provides various communication interfaces like UART, SPI, I2C, and I2S, allowing you to connect various sensors, actuators, and displays to expand its functionality.



Fig 2. ESP8266 Microcontroller

IR Sensors

IR sensors are electronic devices that work on the principle of infrared radiation. Just like we can see visible light, these sensors can detect invisible infrared light, which is part of the electromagnetic spectrum. These sensors have both an IR and an

IR detector. The emitter sends out a beam of IR light, and the detector looks for any reflections of that light.



Fig 3. IR Sensor

DC-DC Buck Converters

A DC-DC buck converter is a type of power supply that steps down a higher input DC voltage to a lower output DC voltage. The buck converter uses a combination of switching transistors, an inductor, and a capacitor to step down the voltage.



Fig 4. DC-DC Buck Converter

Solenoid Valves

A solenoid valve is a versatile electromechanical device that controls the flow of liquids or gases in a pipe or system.



Fig 6. Solenoid Valve

Single-Channel 5V Relay

A single-channel 5V relay is an electromechanical switch controlled by a low-voltage signal (5V). It functions like a remotely operated light switch for much higher voltage and current loads than your control circuit can directly handle.



Fig 7. Single-Channel Relay

PCB Board

A Printed Circuit Board (PCB) is the foundation upon which most modern electronic devices are built. It's a thin board made of an insulating material (like fiberglass) laminated with conductive copper layers. These copper layers are etched into intricate patterns called traces, creating electrically conductive pathways that connect the various electronic components mounted on the board.

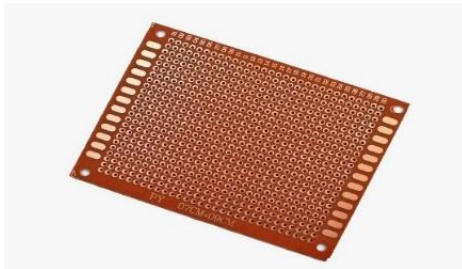


Fig 8. PCB Board

RESULTS AND DISCUSSIONS

Central to the system's functionality is the IR Sensor, strategically integrated into the smart water tap to detect user proximity. Activation of water flow only when a user is within

range effectively addresses inadvertent wastage. This touchless mechanism not only enhances user convenience but also plays a vital role in curbing water consumption, striking a balance between accessibility and sustainability. The environmental benefits of the smart water tap are paramount, as it prevents leaks and optimizes water usage. Field testing confirms the reliability and effectiveness of the touchless sensor technology in real-world scenarios, with user feedback informing ongoing improvements.

CONCLUSION

Water conservation is a pressing issue, especially in public spaces where water wastage is rampant. The "Touchless Water Tap For Preventing Water Loss at Public Stand Posts " project introduces an innovative solution to combat this problem by leveraging advanced sensor technology. By incorporating touchless interaction, this system significantly reduces water loss, contributing to conservation efforts in public areas. Challenges encountered, such as sensor accuracy and durability, are addressed, underscoring the project's commitment to practicality and effectiveness. The project's significance in mitigating water loss in public spaces is emphasized, with future research directions exploring potential enhancements to further advance water conservation technology. In conclusion, the " Touchless Water Tap For Preventing Water Loss at Public Stand Posts" represents a significant step towards sustainable water management in public areas, offering a promising solution for addressing this critical global challenge.

FUTURE ENHANCEMENT

Future enhancements for the " Touchless Water Tap For Preventing Water Loss at Public Stand Posts " project could involve integrating machine learning algorithms to adapt water flow based on user habits, further optimizing water usage. Implementation of remote monitoring and control capabilities through IoT connectivity would enable real-time oversight and management of water consumption in public spaces. Additionally, exploring the use of advanced sensor technologies, such as ultrasonic sensors or pressure sensors, could enhance the precision and reliability of the system, ensuring minimal water wastage. Finally, incorporating self-diagnostic features to detect

and address potential issues proactively would improve the system's longevity and effectiveness in conserving water.

REFERENCE

1. V Saikumar., Kazi Javed Akram, Bobby George, "Capacitive Sensor-based Smart Water Tap: A Feasibility Study", 2023 IEEE 32nd International Symposium on Industrial Electronics (ISIE), pp.1-5, 2023.
2. Patel, D., Singh, K., & Sharma, R., **"Real-Time Hand Gesture Recognition System for Human-Computer Interaction Using Deep Learning"** under Journal of Ambient Intelligence and Humanized Computing, 2021
3. M. Saritha, M. Phil, and U. Abinaya. Research on automatic water tap control system, 01 2021.
4. Chen, Y., Gong, J., Zhang, H., Zhao, X., & Liu, Y. (2020). Design of Smart Water Management System Based on Internet of Things. IOP Conference Series: Materials Science and Engineering, 861(1), 012014.
5. Khalid Abdus Sattar. Automated water tap controlling system using machine vision, 01 2020.
6. Odisha Urban Infrastructure Development Fund (OUIDF), Water Supply, 2020.
7. Chen, L., Zhang, H., & Wang, Y., **"Wireless Gesture Recognition for Smart Home Automation Systems: A Survey"** under Sensors, 2020
8. Smith, J., Johnson, A., & Lee, B., **"Wireless Hand Gesture Recognition Using Inertial Sensors for Human-Computer Interaction"** under IEEE Transactions 2019
9. Nabeel, M., Shah, M. A., & Hassan, S. A. (2019). IoT-Based Smart Water Management System Using Artificial Neural Networks. IEEE Access, 7, 71358-71369.
10. Soni, N., & Varshney, S. (2019). Real-Time Water Quality Monitoring System Using IoT. 2019 3rd International Conference on Trends in Electronics and Informatics (ICOEI), 1083-1086.
11. Dipankar Ghoshal, Helping India Overcome Its Water Woes, <https://www.worldbank.org>, 2019.
12. Gupta, S., Sharma, P., & Singh, A., **"Gesture Recognition Techniques for Human-Computer Interaction: A Review"** under International Journal of Computer Applications, 2018
13. India Education Diary Bureau Admin, Every Indian Wastes Up to 45 litres of Water Per Day, India education diary, 2018.
14. Lopez Farias, R.; Puig, V.; Rodriguez Rangel, H.; Flores, J.J. Multi-Model Prediction for Demand Forecast in Water Distribution Networks. Energies 2018, 11, 660.

15. S. M. Khaled Reza, Shah Ahsanuzzaman Md. Tariq, S.M. Mohsin Reza ,“Microcontroller Based Automated Water Level Sensing and Controlling: Design and Implementation Issue”, 0, San Francisco, USA
16. Wang Y. Xiong B. et al. Xu, D. Mems-based thermoelectric infrared sensors:. A review. *Front. Mech.eng*, 12, 2017.
17. M. Suresh, U. Muthukumar and J. Chandapillai, “A novel smart water meter based on IoT and smartphone app for city distribution management,” 2017 IEEE Region 10 Symposium (TENSymp), Cochin, 2017, pp. 1-5.
18. Ria Sood, Manjit Kaur, Hemant Lenka , “ Design And Development Of Automatic Water Flowmeter”, Mohali, India
19. Asaad Ahmed Mohammedahmed Eltaieb, Zhang Jian Min,“Automatic Water Level Control System”, China - Tianjin
20. Jeffery Perrywade Horwitz Christopher Kirn Saeid Bashash Adam B. Olson Raviteja Datta Akella Omar Awad, System and method for a smart faucet, US20170260722A1, 2016.
21. Managing the water distribution network with a Smart Water Grid. *Smart Water* 1, 4 (2016). <https://doi.org/10.1186/s40713-016-0004-4>.
22. Kartakis, Sokratis, Edo Abraham and Julie A. McCann. *WaterBox: A Testbed for Monitoring and Controlling Smart Water Networks*. (2015).
23. Chen Yongquan, *Water -saving intelligent tap*, CN205155300U, China, 2015.
24. *Programming Embedded Systems in C and C++* by Michael Barr
25. Raymond Jepsen Oliver BradleyDave Morneau, *A piezoelectric touch-controlled faucet*, CA2899109A1, 2014-15.

Analyzing the Shortest Path, Least Cost and Minimum Time by Using Graph Theory and PERT.

Ms. V.S. Selvi*, Ms. R. Ranjani**,
Ms. V. Subashini** & Ms. S. Charumathi**

* Assistant professor, PG and Research department of Mathematics, Theivanai Ammal College for women (autonomous), Villupuram, Tamil Nadu

** M.sc Mathematics, PG and Research department of Mathematics, Theivanai Ammal College for women(autonomous), Villupuram, Tamil Nadu

ABSTRACT

The purpose of this study is to determine the most efficient path, cost, and length of travel for the attraction of visiting tourist spots. This led to the application of graph theory and network analytic methods. The calculation of the distance was done using quantitative analysis and Google Maps.

1.INTRODUCTION

There are many popular tourist destinations in Tamil Nadu. Five primary slots are available. These include Auroville, National Fossil Wood Park, Mailam Murugan Temple, Gingee Fort, and Marakanam Beach. Gingee Fort is one of the busiest tourist destinations. Villupuram has the most potential for natural tourism, according to information from the Gingee with seven tourist destinations: Gingee Fort View Point, Rajagiri Fort, Gingee Fort Bridge, Gingee Fort Lake, Granary, Sculpture Gallery, and Arinagar Anna Library. Similarly, SSS Boating and Vaisakhi Shrimp Hatchery are two locations on Marakanam Beach. The Mailam Murugar Temple is surrounded by tourist attractions such as Mailam Lake, a fish and goat farm, an organic garden, and a PDS agriculture garden. Some of the locations in the National Fossil Wood Park are the Thiruvakarai Redrock Cavern, the GSI Fossil Tree, the Thiruvakarai Sandstone Steam,

and the Thiruvakarai Mariyamman Kovil. Lastly, the primary attractions of Auroville include Matrimandir, the Oxygen tent form land, the Auroville botanical garden, and Sri Ganapathy pottery and Rainbow ECO villa. In this field project a group of ten foreigners visit these places mentioned above and each tourist spot consists more than two visiting spots in Tamil Nadu.

2.PRELIMINARIES:

2.1. Graph theory:

Graph theory is the study of relationship between the vertices and edges. Formally, a graph is denoted as a pair $G (V, E)$. Where V represents the finite set vertices and E represents the finite set edges.

Vertices:

One of the points on which the graph is defined and which may be connected by graph edges **Edges:**

An edge (or link) of a network (or graph) is one of the connections between nodes of the network. Edges can be directed, meaning they point from one node to the next.

Weighted Graph:

A weighted graph is a graph in which each branch is given a numerical weight.

2.2.Floyd warshall:

The Floyd Warshall Algorithm is an algorithm that solves the all-pair shortest path problem in a weighted graph.

2.3.Network analysis:

It defines networks as graphs where the nodes or edges possess attributes.

PERT method:

A PERT chart, also known as a PERT diagram, is a tool used to schedule, organize, and map out tasks within a project.

Critical path:

The critical path is the entire path through the diagram that will take the longest amount of time to complete.

Table 2. Transformation of the Graph to Matrix

	A	B	C	D	E	F	G
A	0	0.8	0.6	1.	∞	∞	∞
B	0.85	0	0.19	∞	1.2	∞	∞
C	1.4	0.19	0	∞	∞	1.4	∞
D	1.4	0	∞	0.7	∞		
E	∞	1.2	∞	∞	0	0.4	∞
F	∞	∞	1.4	0.7	0.4	0	8.1
G	∞	∞	∞	8.1	0		

Next, with $K = 1$ iteration from the sample $K = G$, the values from Table 2 were utilized for the following step. The data from this source can be used to create a matrix from the data in Table 3 in the form of an iterative transformation graph. This matrix can then be used to search for the shortest trip route.

Table 3. Iteration Transform Graph to a Matrix

	A	B	C	D	E	F	G
A	0	0.85	0.65	1.4	2.05	2.05	10.15
B	0.85	0	0.19	2.25	1.2	2.59	9.7
C	1.4	0.19	0	2.05	1.39	1.4	9.5
D	1.4	2.25	2.05	0	1.1	0.7	8.8
E	2.05	1.2	1.39	1.1	0	0.4	8.5
F	2.05	1.59	1.4	0.7	0.4	0	8.1
G	10.15	9.7	9.5	8.8	8.5	8.1	0

The matrix can be used to find the quickest travel route once the distances between each point have been established. The intersection of A and G marked the location of the shortest path,

which was 10.15 kilometers away. The manual distance calculation is provided below to help you verify the accuracy of the data.

DISTANCE

$$\begin{aligned}
 A - B - E - F - G &= 0.85 + 1.2 + 0.4 + 8.1 &= 10.55\text{km} \\
 A - C - F - G &= 0.65 + 1.4 + 8.1 &= 10.15\text{km} \\
 A - D - F - G &= 1.4 + 0.7 + 8.1 &= 10.2\text{km} \\
 A - B - C - F - G &= 0.85 + 0.19 + 1.4 + 8.1 &= 10.84\text{km}
 \end{aligned}$$

These computations demonstrated that the data were accurate, allowing for the determination of the required expenditure and time, which were as follows. (N = number of individuals, where N = 10)

- Time (minutes)

$$A - C - F - G = 14 + 24 + 110 = 148 \text{ minutes}$$

- COST (INR)

$$A - C - F - G = (15 \times N) + (30 \times N) + (160 \times N) = 150 + 300 + 1600 = \text{INR } 2050$$

3.1.1 Network Analysis- PERT Method

In essence, a project is scheduled using the PERT approach. However, PERT was applied in this debate in order to compare graph theory with the analysis of a tourist trip's distance at regular periods. Fig. 2 displays preliminary data.

Caption data = Graph theory (Place distance, Time, Cost)

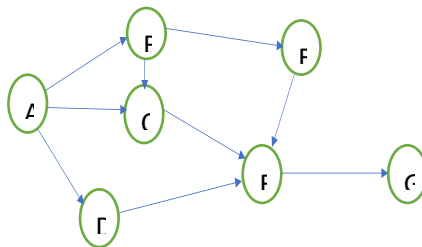


Fig. 2 Preliminary

Resolving

- A network image, which can be seen in Fig. 3 and displays the A through G routes, can be created based on the findings of earlier investigations.

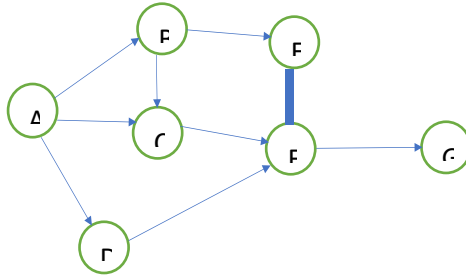


Fig. 3 Network image

Create an activity chart, as shown in Fig. 4.

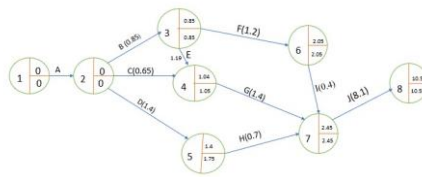


Fig. 4 Activity chart

The critical path is on A, D, E, F, I, J

with normal distance = $0.85 + 1.2 + 0.4 + 8.1 = 10.55$ km
 direct costs = $170 + 210 + 120 + 1700 = \text{INR.}2,200$ and travel time = $19 + 24 + 5 + 110 = 2$ hrs 38 mins

As demonstrated in the previous calculation, the calculation using the graph theory and network analysis yielded the same results.

GINGEE TO MARAKANAM

Distance = 66 km
 Cost = INR 1500
 Time = 1 hour 44 minutes

3.2 Floyd Warshall Graph Theory:

2) MARAKANAM BEACH

Route description:

- A. = SSS Boating
- B. = Vaisakhi shrimp Hatchery

Table 1. Cost and Travel Time Determination

ROU	DISTAN	TIM	COST
A-B	04k	5mi	₹

Fig. 1 displays a map of the mileage within one kilometer of each predetermined route.



The data from this source can be used to create a matrix from the data in Table 2 by use of an iterative transformation graph. This matrix can then be used to search for the shortest trip route.

	A	B
A	0	0.4
B	0.4	0

The shortest path can be discovered using the matrix once the distances between each location have been calculated. At the intersection of A and B, the shortest route which was 0.55 km long was found. The manual distance calculation is provided below so that you can verify the accuracy of the data.

$$A - B = 0.4\text{km}$$

These calculations demonstrated the accuracy of the data, allowing for the determination of the required expenditure and time, which are as follows.

- Cost (INR)

$$A - B = \text{INR } 90$$

- Time (minutes)

$$A - B = 5 \text{ minutes}$$

3.2.1. Network Analysis- PERT Method

Essentially, a project is scheduled using the PERT approach. In contrast, PERT was applied in this discussion to compare graph

theory with the analysis of a tourist trip's distance at regular periods. Figure 2 displays preliminary data.

Caption data = Graph theory (Place, Cost, Time)



Fig. 2 Preliminary data

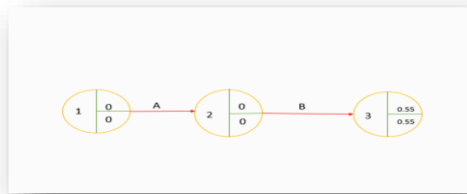
a. Resolving

• A network image that displays the A through B routes can be created using the findings of earlier investigations, as shown in Fig. 3.



Create an activity chart, as shown in Fig. 4.

Fig. 4 Activity chart.



The critical path is on A, B

with normal distance = $0 + 0.55 = 0.55$ km direct costs = INR 120 and travel time = 8 minutes

The computation employing network analysis and graph theory produced the same findings as the preceding calculation, as shown.

Marakanam to National Fossil Wood Park

Distance = 59km
 Cost = INR 860

Time = 1 hour 30 minutes

3.3. Floyd Warshall Graph Theory:

3) National Fossil wood park

Route Description

A = Thiruvakarai redrock cavern

C= Great Fossil Tree

B = GSI Fossil Wood Enclosure
Sandstone stream

D = Thiruvakarai

E = Thiruvakarai mariyamman kovil

$$A - B - C - E = 0.8 + 1.6 + 1.4 = 3.8 \text{ km}$$

$$A - B - D - C - E = 0.8 + 1.4 + 0.18 + 1.4 = 3.78 \text{ km}$$

Based on these calculations, the data were proven to be correct, so that it could determine the cost and time needed, namely as follows.

- Time(minutes)

$$A - B - D - C - E = 11 + 20 + 2 + 20 = 53 \text{ minutes}$$

- Cost (INR)

$$A - B - D - C - E = 150 + 230 + 230 + 60 = 670$$

3.3.1. Network Analysis- PERT Method

The critical path is on A, B, C, F

with normal distance = $0.8 + 1.6 + 1.4 = 3.8 \text{ km}$ direct costs = $200 + 320 + 300 = \text{INR.820}$ and travel time = $11 + 22 + 20 = 53 \text{ minutes}$

As demonstrated in the previous calculation, the calculation using the graph theory and network analysis yielded the same results.

NATIONAL FOSSIL WOOD PARK TO MAILAM MURUGAN TEMPLE

Distance = 14km

Cost = INR 400

Time = 27 minutes

3.4. Floyd Warshall Graph Theory:

4) MAILAM MURUGAN TEMPLE

Route Description:

A = Mailam Lake

C= Organic Garden

B = Goat and fish farm
Garden

D = PDS Agriculture

E = Mailam engineering college
Ground

E= KFG Cricket

$$A - B - C - E - F = 0.7 + 0.9 + 3.3 + 1.6 = 6.5 \text{ km}$$

$$A - D - E - F = 2.1 + 4 + 1.6 = 7.7 \text{ km}$$

$$A - D - C - E - F = 2.1 + 0.7 + 3.3 + 1.6 = 7.7 \text{ km}$$

Based on these calculations, the data were proven to be correct, so that it could determine the cost and time needed, namely as follows.

• *Time(minutes)*

$$A - B - C - E - F = 9 + 12 + 40 + 23 = 84 \text{ minutes}$$

• *Cost (INR)*

$$A - B - C - E - F = 170 + 200 + 530 + 400 = \text{INR } 1300$$

3.4.1. Network Analysis- PERT Method The critical path is on A, D, C, E, F with normal distance = $2.1 + 0.7 + 3.3 + 1.6 = 7.7 \text{ km}$
direct costs = $480 + 170 + 630 + 380 = \text{INR } 1600$ and travel time = $27 + 9 + 40 + 23 = 99 \text{ minutes}$

As demonstrated in the previous calculation, the calculation using the graph theory and network analysis yielded the same results. **Mailam Muruga Temple to Auroville**

Distance = 33km

Cost = INR 550

Time = 42minutes

3.5. Floyd Warshall Graph Theory:

5). *Auroville*

Route Description:

A = Matrimandir

C= Sri Ganapathy pottery

B = Auroville Botanical garden

D = Rainbow ECO villa

E = Oxygen tent Farm land

$$A - B - C - D - E = 4.1 + 3.4 + 2.6 + 0.2 = 10.3 \text{ km}$$

$$A - D - E - F = 3 + 2.6 + 0.2 = 5.8 \text{ km}$$

Based on these calculations, the data were proven to be correct, so that it could determine the cost and time needed, namely as follows.

- *Time(minutes)*

$$A - C - D - E = 40 + 35 + 3 = 78 \text{ minutes}$$

- *Cost (INR)*

$$A - C - D - E = 600 + 550 + 50 = 1200$$

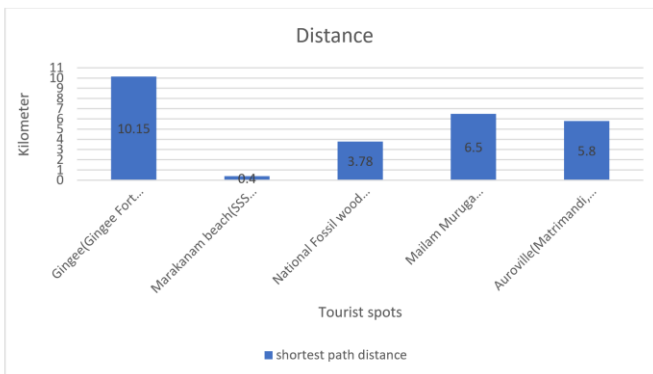
3.5.1. Network Analysis- PERT Method The critical path is on **A, B, C, D, E** with normal distance = $4.1 + 3.4 + 2.6 + 0.2 = 10.3 \text{ km}$ direct costs = $820 + 650 + 470 + 120 = \text{INR } 2060$ and travel time = $55 + 40 + 35 + 3 = 133 \text{ minutes}$

As demonstrated in the previous calculation, the calculation using the graph theory and network analysis yielded the same results.

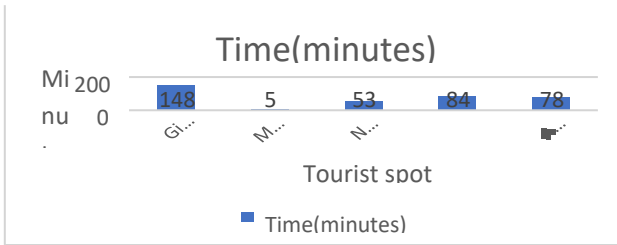
4. Statement of Results

This section discusses the findings of the graph-based recapitulation of time, cost, and distance based on network analysis and the Floyd Warshall method computation of graph theory.

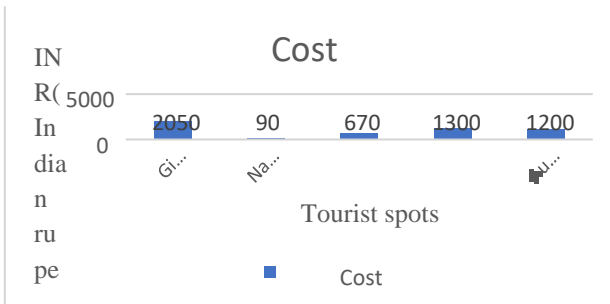
Distance Recapitulation



Time Recapitulation

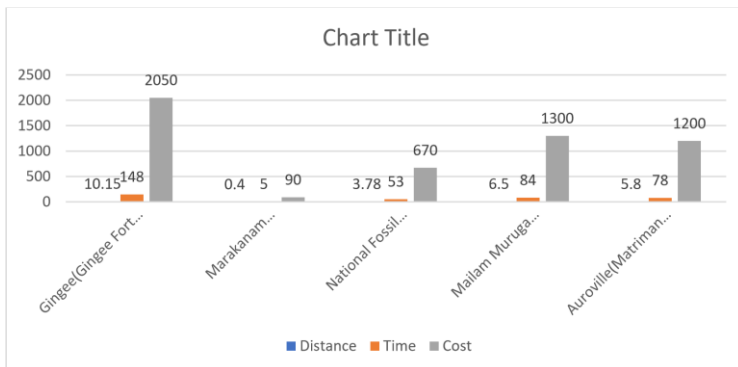


Cost Recapitulation



5.Explanatory Text

The following is the determination of the optimal distance, cost, and travel time based on graph theory using the Floyd Warshall method and network analysis using the PERT method.



In which exhibits results from using the graph theory of Floyd Warshall method ,natural tourism in Gingeel , Marakanam beach,

National Fossil wood , Mailam murugan temple , Auroville with the optimal distance, cost, and time travel :

Gingee: Mailam murugan temple: Distance 10.15 km Distance : 6.5 km Cost INR 2050 Cost INR 1300 Time 148 minutes Time 84 minutes

Marakanam beach: Auroville:

Distance : 0.4 km Distance : 5.8 km

Cost INR 90 Cost INR 1200

Time 5 minutes Time 78 minutes

National Fossil wood:

Distance : 3.78 km

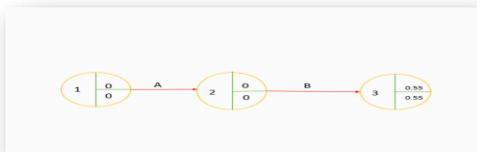
Cost : INR 670

Time : 53 minutes

5.1.Network Analysis Using the PERT Method:



The analysis of the PERT method. Based on the calculation results using the PERT method. The distance, cost, and normal travel time of the Gingee tourism were obtained with a normal distance of 10.55 km, a normal cost of INR.2,200, and a normal travel time of 2 hrs 38 mins.



The analysis of the PERT method. Based on the calculation results using the PERT method. The distance, cost, and normal travel time of the Marakanam Beach tourism were obtained with

a normal distance of 0.55 km, a normal cost of INR 120, and a normal travel time of 8 minutes.

CONCLUSION

As previously discussed, the Floyd Warshall approach is more efficient in identifying the tourist destination with the shortest route when compared to network analysis using the PERT method. Normal routes were the only outcomes of the PERT technique network study. This research has improved the use of graph theory, in contrast to the previous study's conclusions. It is supported by the use of Google Maps to calculate journey time and distance as well as the Grab app to calculate costs.

The graph theory and network analysis for determining the shortest distance can be deduced from the conducted research. In this field project a group of ten foreigners visit to take on 5 major area tourist spot and each tourist spot consists more than two visiting spots in Tamil Nadu. As in They recommended a shortest path, low cost, less amount of time during that travel compared to the google map. In which they used Floyd method for this operating calculation for to finding shortest route, least cost and minimum amount of travelling time for the foreigners.

REFERENCES

1. R. Paryanti and A. Thobirin, "Penerapan Teori Graf untuk Mencari Lintasan Tercepat Bus Trans-Jogja," Undergraduate thesis, Universitas Ahmad Dahlan, Umbulharjo, Yogyakarta, 2019.
2. U.M. Rifanti and B. Arifwido, "Implementasi Algoritma Floyd dalam Penentuan Rute Terpendek," *Jurnal Ilmiah Teknologi Sistem Informasi*, vol. 5, no. 2, pp. 140-151, Jul. 2019, doi: 10.26594/register.v5i2.1683.
3. F.D. Putra, "Implementasi Teori Graf Sistem Angkutan Kendaraan Umum di Kota Medan," Undergraduate thesis, UIN Sumatera Utara, Seli Serdang, Sumatera Utara, 2021.
5. E.T. Susdarwono, "Pemrograman Dinamis: Analisis Jaringan Menggunakan PERT dan Prosedur AHP dalam Menyelesaikan Masalah Ekonomi Pertahanan," *Jurnal El-Hamra*, 5, no. 1, pp. 1-9, Feb. 2020.
6. Kuntarto and T.H. Purwanto, "Penggunaan Analisa Jaringan Sistem Informasi Geografis Untuk Perencanaan Rute Wisata di Kabupaten Sleman," *Jurnal Bumi Indonesia*, vol. 1, no. 2, pp. 140-148, 2012.



G – MAP of 5 Tourist Spot

Analysis of Waiting Time in Hospital by Application of Queueing Theory

Dr. N. Velmurugan*, S. Pratheepa**,
K. Ragavi** & T. Pragatheeswari**

** Research Head & Assistant Professor, PG and Research
Department of Mathematics, Theivanai Ammal College for
women (Autonomous), Villupuram, Tamil Nadu*

*** M.Sc Mathematics, PG and Research Department of Mathematics, Theivanai
Ammal College for women (Autonomous), Villupuram, Tamil Nadu*

ABSTRACT

The following paper presents an examination of queueing systems within hospital management, employing mathematical methodologies to analyze waiting lines across various settings characterized by arrival rates. The paper aims to elucidate the challenges posed by the urgency of medical cases, particularly concerning patient allocation and the utilization of waiting lines. It adopts the principle of "FIRST COME FIRST SERVED" queue discipline as the basis for its analysis.

INTRODUCTION:

Agner Krarup Erlang considered the father of queueing theory, Erlang, a Danish Mathematician, made foundational contributions to the field in the early 20th century. He developed mathematical models to describe the relationship between the capacity of a telephone exchange and the probability of call blocking.

Queueing theory is a branch of applied probability theory that deals with the study of queues (lines or waiting lines) in systems where entities, such as customers or tasks, arrive at a service point for processing. It provides mathematical models to analyze and predict various performance measures of queueing systems, such as average waiting time, queue lengths, and system utilization. Queueing theory finds applications in diverse fields such as telecommunications, computer networks, transportation systems, manufacturing, and healthcare, helping to optimize system performance, resource allocation, and design.

Queueing systems is of two types,

Single-Server Queue: There is only one server serving the queue of customers.

Multi-Server Queue: There are multiple servers serving the queue of customers.

CONCEPT OF QUEUEING THEORY:

Queue management poses a significant challenge for healthcare institutions worldwide. While extensive research has been conducted globally to enhance queue systems in hospitals, developing countries have not received adequate attention in this regard. This study aims to fill this gap by examining queue dynamics in government-run hospitals and offering practical insights to improve decision-making processes within these facilities. Utilizing queuing theory, a robust mathematical framework, we analyze performance metrics of waiting lines in healthcare delivery systems. This approach has emerged as a valuable management tool for informed decision-making in more advanced healthcare settings.

Hospital Out Patient Departments (OPDs) are vital components of multi-specialty hospitals, playing a pivotal role in delivering high-quality healthcare services. Often serving as a profit center within hospital operations, the OPD not only facilitates investments in cutting-edge technology but also helps mitigate losses incurred by inpatient services. Despite its significance, hospitals frequently overlook complaints regarding prolonged waiting times, primarily attributed to visible queues, leading to patient dissatisfaction. Consequently, there is a pressing need for hospital service operations to ensure seamless workflows that meet patient expectations. This can be achieved through system redesign and adoption of best practices and tools to optimize processes, particularly in developing economies like India, where there is ample room for improvement.

The OutPatient Department (OPD) serves as a vital link between the hospital and the community, underscoring the importance of strategic planning aimed at maximizing utilization and ensuring swift turnover. Effective cooperation between medical services and support line services is crucial to meet the diverse needs of the OPD efficiently. This collaborative approach ensures

seamless operations and enhances the overall quality of care provided to patients accessing outpatient services.

The success of managing the OutPatient Department (OPD) hinges on various factors, including the interpersonal skills of medical staff, the availability of medication, hospital infrastructure, and access to medical information. These elements collectively contribute to patient satisfaction. Therefore, it is crucial to prioritize the optimization of waiting times within hospital operations. Doing so benefits patients by enhancing their overall experience and well-being.

The OutPatient Department (OPD) of a hospital serves as a vital connection between the institution and the community it serves. Therefore, it is crucial to strategize the planning of the OPD with the goal of maximizing its utilization and ensuring quick turnover of patients. Effective planning is essential for the successful establishment of a hospital. A well-thought-out plan sets the foundation for smooth operations and desired outcomes. Conversely, inadequate planning can lead to delays and hinder progress. Initiating the planning process involves establishing clear goals for the hospital platform, providing a definitive direction and focus. This is followed by a comprehensive assessment of the external environment surrounding the hospital, as well as an evaluation of both internal and external resources available to achieve the established goals. Through this process, suitable strategies can be identified to achieve goals efficiently while staying within budget constraints.

QUEUEING THEORY IN HOSPITAL:

Queueing theory finds various applications in hospitals and healthcare systems to optimize resource utilization, improve patient flow, reduce waiting times, and enhance overall system efficiency. Some key applications include:

Emergency Department (ED) Management: Utilizing queueing theory enables hospitals to optimize staffing levels, bed allocation, and triage processes in the emergency department. By modeling patient arrivals and service times, hospitals can predict and manage patient flow more effectively, reducing overcrowding and improving wait times for urgent care.

Outpatient Clinic Scheduling: Queueing models play a vital role in optimizing appointment scheduling and resource allocation in

outpatient clinics. By considering patient arrivals, service times, and clinic capacities, hospitals can minimize patient waiting times, decrease no-show rates, and enhance overall clinic efficiency.

Operating Room (OR) Scheduling: Queueing theory aids in optimizing the scheduling of surgeries and allocation of operating room resources. By modeling surgical case arrivals, procedure durations, and OR utilization rates, hospitals can improve OR utilization, decrease delays, and increase the efficiency of surgical services.

Inpatient Ward Management: Queueing models assist hospitals in managing patient admissions, bed allocations, and discharge processes in inpatient wards. By analyzing patient flow patterns and bed availability, hospitals can optimize bed utilization, reduce patient wait times for admissions, and ensure timely discharges, thus enhancing overall ward efficiency.

Pharmacy and Laboratory Services: Queueing theory can be applied to optimize workflows and resource allocation in hospital pharmacies and laboratories. By modeling prescription fill times, test processing times, and staffing levels, hospitals can decrease wait times for medications and test results, enhance patient satisfaction, and improve overall service quality.

Telemedicine and Virtual Care: With the rise of telemedicine and virtual care platforms, queueing theory can help optimize appointment scheduling, resource allocation, and service delivery in virtual healthcare settings. By analyzing virtual visit demand patterns and provider capacities, hospitals can enhance access to care, decrease wait times for virtual appointments, and improve patient experience.

In summary, queueing theory equips hospitals and healthcare systems with valuable tools and methodologies to effectively manage patient flow, allocate resources efficiently, and enhance the quality-of-care delivery across various clinical and administrative processes.

QUEUEING SYSTEM:

In a basic queueing system within a hospital setting, patients are analogous to the "arrivals," while the servers represent the resources or personnel providing the required service. In the

context of analyzing time delays for patients awaiting admission to the hospital from the Emergency Department (ED), the relevant servers would be the inpatient beds.

This means that when patients arrive at the ED and require admission to the hospital, the inpatient beds become the critical resources or servers responsible for providing the service of accommodating and caring for these patients. The time delays experienced by patients in the ED awaiting admission would be influenced by factors such as the availability of these inpatient beds, the efficiency of bed turnover, and any bottlenecks in the admission process. Therefore, optimizing the utilization of inpatient beds and streamlining the admission process are essential for reducing wait times and improving the overall efficiency of the hospital's operations.

COLLECTION OF DATA:

Arrival and Departure of Queuing in Hospital (OPD) of a Primary Health Care Centre,

Time Interval Per 30 Min	No. of Arrivals Per 30 Min	No of Departure Per 30 Min
10:30-11:00	25	26
11:00-11:30	45	45
11:30-12:00	48	49
12:00-12:30	40	42
12:30-01:00	32	33
TOTAL	190	195

EVALUATION OF CHARACTERIZATION:

From the above table

- 1) Average number of arrivals to the system per 30 min(λ)=38 per 30 min
- 2) Average number of departures from the system per 30 min (μ)=39 per 30 min
- 3) Since $c=3$, $\mu=13$ per 30 min

To find the crowd intensity $\rho = \lambda / c\mu$

Here $\lambda=38$

$\mu=39$ and

$c=3, \rho=0.974$

4) To find P_0

$$P_0 = \left[\sum_{n=0}^{c-1} \frac{\lambda^n}{n!} + \frac{\lambda^c}{c!} \left(\frac{\lambda}{\mu} \right)^c \right]^{-1}$$

$$= [1 + 2.923 + 4.272 + 162.343]^{-1}$$

$$= [170.538]^{-1}$$

$$P_0 = 0.00586$$

THE RESULTS OF CHARACTERISTICS OF OUR SYSTEM:

$P(n>c)$ =probability that an arrival has to wait

Arrival rate (λ) = 38 customers per unit time

Service rate (μ) = 39 customers per unit time

Number of servers (c) = 3

Utilization factor (ρ) = 0.974

Probability of zero customers in the system (P_0) = 0.00586

$P(n>c)$ =probability that an arrival has to wait

$$P(n>c) = \frac{\lambda^c \rho}{\mu^c (1-\rho)}$$

$P(n>c) \approx 0.1101$

Probability that an arrival enters the service without wait

$$= 1 - \rho$$

$$= 1 - 0.1101$$

$$= 0.8899$$

Average queue length [L_q]

$$L_q = \frac{\lambda^c \rho}{\mu^c (1-\rho)^2}$$

$$L_q \approx 31.86$$

Average number of customers in the system [L_s]

$$L_s = L_q + \lambda / \mu$$

$$= 31.86 + 2.92$$

$$L_s = 34.78$$

Average waiting time of an arrival [W_q]

$$Wq = Lq / \lambda$$

$$Wq = 0.8384$$

Average waiting time an arrival spends in the system [Ws]

$$Ws = Wq + 1 / \lambda$$

$$Ws = 0.8647$$

VERIFICATION OF THE LITTLE'S FORMULAE:

The relationships between the characteristics are given by means of the following formulae known as little formulae there are

$$Ls = \lambda Ws$$

$$Ls = \lambda Ws$$

Our findings also satisfy the little's formula.

To verify $Ls = \lambda Ws$ from equation

In this section, we have obtained that $Ls = 34.78$

$$\begin{aligned} \text{From equation we have found that } \lambda Ws &= 38 * 0.8647 \\ &= 32.8586 \end{aligned}$$

$$Ls \text{ (appr.)} = 32.8586$$

To prove: $= \lambda Wq$

From the equation we see that $Lq = 31.86$

Also from equation, $\lambda Wq = 38 * 0.8384$

$$= 31.8592$$

$$Lq \text{ (Appr.)} = 31.8592$$

OBSERVATIONS:

In our study we have made the following observations the following results.

- a) Traffic intensity, $\rho = 0.974$
- b) Probability that there are no customers in the system, $P_0 = 0.00586$
- c) Probability that an arrival has to wait, $P(n > c) = 0.1101$
- d) Probability that an arrival enters the service without wait $1 - P(n > c) = 0.8899$
- e) Average queue length at any time $Lq = 31.8592$ patients

- f) Average number of customers in the system at any time $L_s = 34.78$ patients
- g) Average waiting time of an arrival in the queue, $Wq = 0.8384$
- h) Average waiting time of arrival spend in the system $W_s = 0.8647$
- i) Average number of arriving rate, $\lambda = 38$ per 30 min
- j) Average number of service rate, $\mu = 13$ per 30 min

SUMMARY:

- a) An average of 38 patient is arriving to the hospital in 30 min
- b) Average of 39 patient is being served in the hospital in 30 min
- c) The crowd intensity $\rho = \lambda / c\mu = 0.974$ and therefore the queuing system followed in the hospital
- d) At any time, an average of 31 patients are found waiting in the queue.
- e) At any time, an average of 34 patients are found waiting in the system.

CONCLUSION:

In our study, the analyzed system not only caters to the needs of individuals seeking services within hospitals but also optimizes their time for engaging in other activities. The utilization of open-source solutions presents a significant advantage, extending benefits to society as a whole. This system design and setup are not limited to benefiting a single hospital; rather, multiple hospitals can simultaneously leverage its advantages. Each hospital can manage its own queues with designated power users serving as queue administrators. Such a design facilitates cost-sharing arrangements among hospitals without necessitating additional development expenditures. Multi-server queuing methodologies prove invaluable in estimating various performance metrics, including average waiting time, queue length, number of servers, and service rates, thereby enhancing operational efficiency across healthcare facilities.

REFERENCES:

1. Rao, Rajiv.; Applications of queuing theory, International Journal of Applied Statistics, Vol-56, 150-160
2. Rajesh Amudhan, Theory of Queue, III-Edition (2019), PHI publications, Delhi

3. Rio, D, G, (1972) : Management breakthrough inHospital Management opsearch 9(384), 143-167
4. Bisham Sharma, Hospital Science, Applied SciencePeriodical, Vol-III,Number-1 February-2001
5. FoadsMahdavisPasjough, ManjunaithKamath, Applications of Queueing Models in Hospitals, Queueing Applications in Hospitals.

OVERVIEW:

Nowadays peoples are suffer from CKD (Chronic Kidney Disease) due to kidney failure which can be detected by some of the symptoms or else by the lab tests. In world probably 20 million peoples are suffered and die due to this disease without the improper detection of advanced stages. There are lot of techniques to detect and prevent the CKD. This paper aims to use Machine Learning and data mining technique for decrease the amount of patient and death rate by predicting their stages. The doctors can detect and prevent the disease by machine learning classifier algorithm on time to cure it. Chronic kidney disease prediction model using three machine learning classifiers Logistic Regression, Decision Tree and Support Vector. The dataset of the patient has been collected and then classified by the classifier algorithm of c5.0 decision tree. In existing it uses CNN method for predicting it gives 93.28% accuracy. This paper promote ANN method for predicting with an accuracy 98.93%.

Keywords – Artificial Neural Network, C5.0 Decision tree, Machine Learning

INTRODUCTION

In early stages kidney diagnose treatment are used but which is not work in all the time. So that the avoiding the risky situation, find the good way of cure the kidney disease. The proposing the technologies of predict renal stages from the dataset. In existing there any missing of values which leads to drop of prediction. But in the advances machine learning algorithm proposed the correct prediction of there is missing of values in a patient's data

In today's world probably all disease is detected and predicted in an efficient manner with more accuracy by using many technologies in internet. These can be analysis by using the

patient's dataset. Every dataset contains the collection of data which gives more amount of information about the disease. These collected datasets can be trained and classified by some algorithms.

CKD which is abbreviated as Chronic Kidney Disease is one of the major disease in the world. The Global Burden of Disease Study (GBDS) announces in 2010 that CKD is one of the top 20th disease in the world. Probably 500 million people are suffered from the mostly from Africa and south Asia. In an research they find 33% people who affected by CKD are 30 years old in urban countries

CKD can be from improper consumption of water, irregular sleepiness, smoking, alcohol and improper diet. It can affect females, males and children. Probably males are suffered from this disease due to the consumption of alcohol. This can affect the parts of the body, urine and at last kidney failure

The previous method of diagnosing the CKD based on the report of patients which contain urine examination, history of checkups and also screened the relatives who had this disease. This tool works on the principle of multivariate analysis, which can help predict, explain, describe, and classify the outcome.

The patient who suffer from CKD can follow some of the tips like regular exercise, following diet, avoid smoking and alcohol, be active and so all physical works and so on

By this summary we proposed to calculate GFR and ACR of first level using artificial neural networks .This paper aims to get efficient prediction of disease using machine learning techniques. Machine Learning algorithm techniques have played a very important role in CKD prediction

LITERATURE SURVEY

M.P.M.N WIKRAMSINGHNE gives the diet plan to control CKD. It uses Multilevel Descion Forest, Multilevel Neural network algorithm to predict the disease using blood potassium and classifier algorithm gives the diet plan to the users

H.A.WIBAWA can evaluated and proposed kernel extreme learning machine to predict CKD by using four kernel levels such as RBF-ELM, Linear-ELM, Polynomial-ELM and Wavelet - ELM are compared the methodologies to predict the disease

The author M.Chen, Y.Hao, K.Hwang, I.Wang states that they used prediction algorithm for chronic verbal infraction disease from the data. They used Convolution neural networks to predict and KNN classifier to disease

M. J. Lysaght states the patient in CKD to develop End Stage Rental disease which is expensive way of dialysis and kidney transplantation

P. Yildirim has try to predict with incomplete data with an accuracy of 0.975 and 0.960 using neural networks. By this research they find Hypertension can also cause CKD. By eliminating some characteristics which lead to decrease the accuracy

C. A. Johnson, A.S.Levey ,J.Coresh,A.Lwvin and J.G.I Eknoyan uses MCAR method to do prediction in the missing data, thirreserch shows the cereum value is normal but others are to be changed

PROPOSED SYSTEM

The framework utilizes the CKD prediction dataset. After preprocessing and feature selection, ANN and c5.0 decision tree algorithms have been used.

The early stages of prediction uses CNN based model with K-nearest neighbor’s algorithm. In proposed the prediction can be done by ANN based model with c5.0 decision tree classifier

Using structured and unstructured data of patients can be classified by Machine Learning algorithm

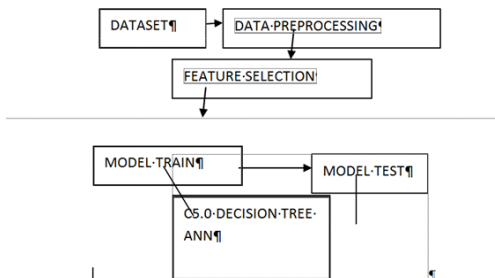


Figure 2.1 Block Diagram

The figure 2.1 represent the block diagram of predicting Chronic Kidney Disease. First the dataset of the patients to be collected, the process the structure and unstructured data in the dataset in data Preprocessing. After preprocessing the feature of data that is Blood Pressures, WBC count level are to be checked finally using classifier algorithm the data of the patients to be trained and tested

DATASET

The data of patients can be collected from hospital. Here we can take 500 dataset of the patients '0' represent thepatient not suffer from CKD and '1' represent the patient suffer from CKD

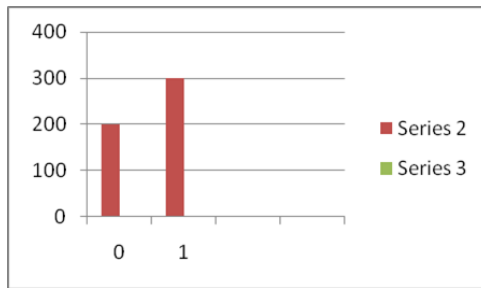


Figure 3.1 describes the overall CKD patients and Non-CKD patients. From the collected dataset there are 300 CKDpatients and 200 Non CKD patients which represents as 1 and 0 respectively

DATA PROCESSING

This stage the data in the dataset can be preprocessed which means it could remove unwanted data i.e., noisy data during processing the dataset for help to predict the stages

Data Preprocessing has the strategy of change raw information into clean dataset. Every machine learning classifier algorithm used this as first step

It can also process both structured and unstructured data in a dataset and also predict the accuracy of there is also from the incomplete data

Sr. No	Attribute Name	Description
1	Age	Patient age (It is in years)
2	Bp	Patient blood pressure (It is in mmHG)
3	Sg	Patient urine specific gravity
4	Al	Patient albumin ranges from 0-5
5	Sa	Patient sugar ranges from 0-5
6	Rbc	Patient red blood cells two value normal and abnormal
7	Pe	Patient pus cell two value normal and abnormal
8	Pcc	Patient pus cell clumps two values present and not present
9	Ba	Patient bacteria two values present and not present
10	Bgr	Patient blood glucose random in mg/dl
11	Bu	Patient blood urea in mg/dl
12	Sc	Patient serum creatinine
13	Sod	Patient sodium
14	Pot	Patient potassium
15	Hemo	Patient hemoglobin (protein molecule in red blood cells)
16	Pcv	Patient packed cell volume % of red blood cells in circulating blood
17	Wc	Patient white blood cell counts in per microliter
18	Re	Patient red blood cell count in million cells per microliter
19	Htn	Patient hypertension two value Yes and No
20	Dm	Patient diabetes mellitus two value Yes and No
21	Cad	Patient coronary artery disease two value Yes and No

Figure 4.1 Data Abbreviation

Data to be collected are (Figure 4.1) age, blood pressure, urine specific, and aluminide so on

FEATURE SELECTION

The dataset contains blood pressure, albumin, sugar, blood urea, serum creatinine, potassium, white blood cell count, and hypertension of the patient.

In the urine protein test albumin is accessed if the level is high in urine test there possible of failures in filtration. The WBC count should be 4.5 to 11 mgl if it is exceed or in low due to kidney failure, heart disease.

The serum creatinine count contains both creatinine and creatinine are in same level in the body for metabolic cycle of muscle contraction.

Hypertension can result of heart attack, tension and headaches

ALGORITHMS

- C5.0 decision tree
- ANN

C5.0 DECISION TREE

The C5.0 is one of the decision tree algorithms used to build a decision tree or rule set. It can split the maximum field and convert it into sub-fields. Then again split the sub-sample into another sub it will repeat until the sub cannot be able to split. It need not require large estimate dataset. This algorithm can predict also from the missing values

C5.0 DT can predict continuous and discrete values in the dataset. This Machine Learning uses supervised learning approach by that it can give priority to the important data. This algorithm can find which input column is used to predict the disease

C5.0 is a type of decision tree because it creates the decision tree from the input. The tree has the number of branches. It utilizes the tree structure to model the relationship between features and potential outcomes. At each node of the tree, the attribute of the dataset is chosen. It can handle nominal and numeric features both. C5.0 is the extended version of the C4.5 classification algorithm and uses information entropy concept. Entropy is used for finding the impurity of features. Information entropy is produced based on the calculation of parent and child entropy values. This process is iterative and works until there is no further split.

CHAID Chi-square automatic interaction detection (CHAID) is a type of decision tree technique. It is used to determine the relationship between variables. Nominal, ordinal and continuous data can be used in CHAID for finding the outcome. For each categorical predictor, all possible cross-tabulation is created in the CHAID model and its process works until the best outcome is attained. The target or dependent variable becomes a root node in the tree, the target variable

Two or more parts as per the categories in target variable and child of the root node are created using the statistical method and variable relationship. Such a process will be till leaf nodes of the tree. F-test is used for the continuous dependent variable and the Chi-square test is used for the categorical dependent variable

ANN

ANN is Artificial Neural Network, It used to preprocess the dataset of patient which helps in complex data to predict the problem, classifies the stages of CKD and make the decision. It

can connect large amount of data to process it. Previously CNN can be used.

The ANN approach enables automatic diagnosis of Chronic Kidney Disease. This approach can help the classifier algorithm to the evaluation of treatment for Kidney. Artificial Neural Network can train the data by selecting the feature values

And is a type of artificial intelligence and also supervised machine learning type. It work same as the human brain like every neuron connected here also connected to every network like neuron which are the node. Ann can solve the complex problem which the human does not solve. It consist of input, hidden and output layers. The input layer can take the input of the function and the operation of function are performed in hidden layer and then output produce by output layer which gives the predicted result. Ann work based on backpropagation

Ann used the logistic regression supervised learning techniques for predict the disease which is a statistical model. It divided the result as "True" or "False", 0 or 1, success or not success

It return 1 if it is success else return 0 if it is not success

$$P = 1/(1 + e^{-(b_0 + b_1x + b_2x^2)})$$

Where P is the predicted value, b0, b1, b2 are biases and x is an attribute. It is used in various field of machine learning application in social sciences and medical arena, for example, for spam detection, diabetes detection, cancer detection, etc. Logistic regression is the advanced version of linear regression

EXPERIMENTAL RESULT

The prediction of health sickness and advances stages can be done by utilizing c5.0 and ANN. The result is high accurate when compared with existing result

PERFORMANCE FACTOR

- Memory allocation depend upon the size of dataset
- Number of scan depends upon the disease
- Execution time based on the number of patients

- Figure 7.1 gives the number of positive and negative result of CKD patient and Non-CKD patient from the dataset using the classifier algorithm from neural networks
- Figure 7.2 represent the result of different algorithm which varies depend upon the accuracy level of test results. By this result the finding the highest accuracy test result classifiers among the others.

	Positive (1)	Negative (0)
Positive (1)	TP	FN
Negative (0)	FP	TN

Figure 7.1 Result Sample

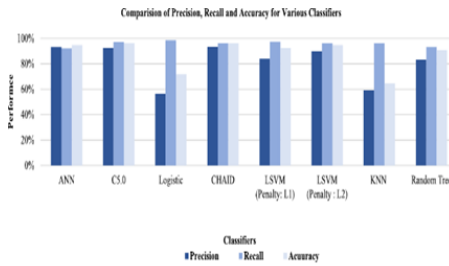


Figure 7.2 Comparision of Others Result

CONCLUSION

The aim of the project is to detect and predict CKD in early stages predictions can also be done for which types by their symptoms. By the medical database it can classify the types and disease in an automation way. C5.0 decision tree can classify the types of stages and predict its level and an economical faster manner

By conclude that decision tree classifier c5.0 can predict accurately CKD. The existing methods are 95 percent and it can give 98 percent accuracy. There is large amount of dataset can be used to predict. The use of this technology to make the patient to become aware and take prior treatment to prevent the disease or

death, which reduces the death rate of people and also suffer of people

REFERENCES

1. Veenithakunwar, KhushbooChandel, A.SaiSabitha, Abhay Bansal, Chronic Kidney Disease Analysis Using Data Mining Classification Techniques, [1], 2016.
2. Mircea GH, Robert J. Howlett, Lakhmi G. Jain, (2004) "Knowledge-Based Intelligent Information and Engineering Systems", 8th International Conference, KES 2004, Wellington, New Zealand, Sep 20-25. Proceedings, e-book Springer publication 12. Ramya. S, Senthil Kumar. R, (2014)
3. World Health Organization, *Preventing Chronic Disease: A Vital Investment*, WHO, Geneva, Switzerland, 2005.
4. B. Bikbov, N. Perico, and G. Remuzzi, "Disparities in chronic kidney disease prevalence amongmales and females in 195 countries: analysis of the global burden of disease 2016 study," *Nephron*, vol. 139, no. 4, pp. 313-318, 2018.View at: Publisher Site | Google Scholar
5. Z. Chen, X. Zhang, and Z. Zhang, "Clinical risk assessment of patients with chronic kidney disease by using clinical data and multivariate models," *International Urology and Nephrology*, vol. 48, no. 12, pp. 2069-2075, 2016.View at: Publisher Site | Google Scholar
6. *Glomerular Filtration Rate (GFR)*, National Kidney Foundation, New York, NY, USA, 2020, <https://www.kidney.org/atoz/content/gfr>.
7. T. H. Aldhyani, A. S. Alshebami, and M. Y. Alzahrani, "Soft computing model to predict chronic diseases," *Information Science and Engineering*, , vol. 36, no. 2, pp. 365-376, 2020.View at: Google Scholar
8. T. S. Furey, N. Cristianini, N. Duffy, D. W. Bednarski, M. Schummer, and D. Haussler, "Support vector machine classification and validation of cancer tissue samples using microarray expression data," *Bioinformatics*, vol. 16, no. 10, pp. 906-914, 2000.View at: Publisher Site | Google Scholar
9. R. M. Pujari and V. D. Hajare, "Analysis of ultrasound images for identification of Chronic Kidney Disease stages," in *Proceedings of the 2014 First International Conference on Networks & Soft Computing (ICNSC2014)*, pp. 380-383, IEEE, Guntur, India, August 2014.View at: Google Scholar
10. S. Ahmed, M. T. Kabir, N. T. Mahmood, and R. M. Rahman, "Diagnosis of kidney disease using fuzzy expert system," in *Proceedings of the 8th International Conference on Software, Knowledge, Information Management and Applications (SKIMA 2014)*, pp. 1-8, IEEE, Dhaka, Bangladesh, December 2014.View at: Google Scholar

- A. Khamparia, G. Saini, B. Pandey, S. Tiwari, D. Gupta, and A. Khanna, "KDSAE: chronic kidney disease classification with multimedia data learning using deep stacked autoencoder network," *Multimedia Tools and Applications*, vol. 79, no. 47-48, pp. 35425–35440, 2019. View at: [Publisher Site](#)

Dr. Kaustubh Kumar Shukla*, Dr. Saket Kumar &
Dr. C Venkataraman*****

** Associate Professor, ECE, Dronacharya Group of Institutions,
Greater Noida, Uttar Pradesh*

*** Assistant Professor, Deptt. of Mechanical Engineering,
Dronacharya Group of Institutions, Greater Noida, Uttar Pradesh*

**** Professor, Deptt. of ECE, Sri Eshwar College of Engineering,
Coimbatore, Tamil Nadu*

ABSTRACT

The integration of drones and artificial intelligence (AI) has revolutionized aviation by enabling autonomous navigation, data collection, logistics, security, and surveillance. AI-powered drones can analyze real-time data to avoid obstacles, adapt flight paths, and operate without human intervention. They can also optimize data collection and analysis in agriculture, construction, and environmental conservation. The combination of drones and AI is reshaping supply chains, reducing delivery times and energy consumption. They are also strengthening security and surveillance in border security, disaster response, and urban safety. However, challenges include regulatory hurdles, ethical concerns, and technical barriers. Despite these challenges, the drone revolution represents a defining moment in aviation history, driving innovation and improving efficiency, safety, and sustainability. Drones, or unmanned aerial vehicles, have revolutionized various industries, including agriculture, filmmaking, and search and rescue. They reduce human casualties, improve efficiency, and improve crop yields. However, privacy and safety concerns have led to regulations. Advancements in drone technology include AI, autonomous drones, swarm drones, 5G connectivity, and smaller drone sizes. Challenges include regulatory issues, battery life limitations, and cyber security. Governments are developing safe drone operation frameworks and exploring alternative power sources.

Keywords: *Artificial Intelligence, Aviation, Drones, Robotics, Sensors and Electronics.*

INTRODUCTION

A technological transformation known as the "drone revolution" is changing our lives, logistics, and entire industries. With artificial intelligence (AI) enhancing their capabilities, drones are becoming a necessary component of our contemporary environment. Precision farming, disaster relief, infrastructure inspection, distribution and logistics, media and video, environmental monitoring, and autonomous drone swarms are some of the main uses. More ground-breaking uses, such as autonomous drone swarms, drone traffic control systems, and sophisticated drone sensors, are anticipated as AI and drone technology develop further. A universe of creativity and opportunity can be unlocked by embracing this technological revolution.

Unmanned aerial vehicles, or drones, are a cutting-edge technology that has broad applications in many different industries [1]. Their growth and widespread use have been fuelled by commercial popularity, downsizing, and advancements in electronics. Drones are flying robots with embedded flight plans that are controlled by programming [2]. Search and rescue, surveillance, traffic checks, environmental detection, fire fighting, private robots, robot photography, videography, and agriculture are just a few of the non-military uses for them [3]. Military drones with sensors and camera units were later developed after the 1930s saw the creation of the first aircraft with a reusable radio control system [4]. Drones that can carry groups from the air without a considerable distance are being developed by companies such as Google and Amazon [5-6].

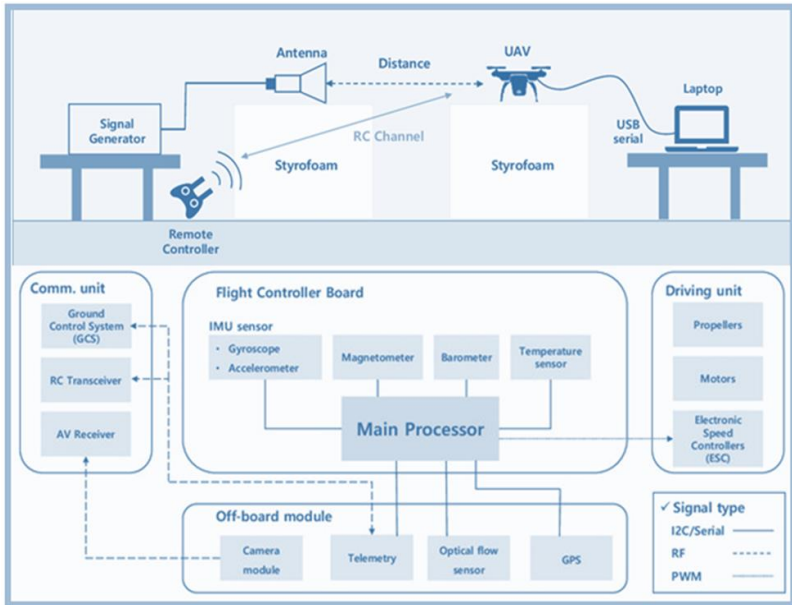


Fig.-1 Block diagram of the proposed system

LITERATURE SURVEY AND BACKGROUND

Drones, or Unmanned Aerial Vehicles (UAVs), have a rich history dating back to 1849. The first military use of a drone occurred during the Austrian-Italian War in 1898. Throughout World Wars, drone technology advanced significantly, with countries like the U.S. and Germany developing various types of drones for reconnaissance and target practice. Post-War, drones continued to evolve, with increased focus on military and civilian applications. In the 21st century, drones have become increasingly popular for civilian applications, including aerial photography, agriculture, delivery services, search and rescue, infrastructure inspection, and scientific research. Recent trends include advancements in AI and machine learning, integration with 5G technology, drone delivery services, and drone swarms.

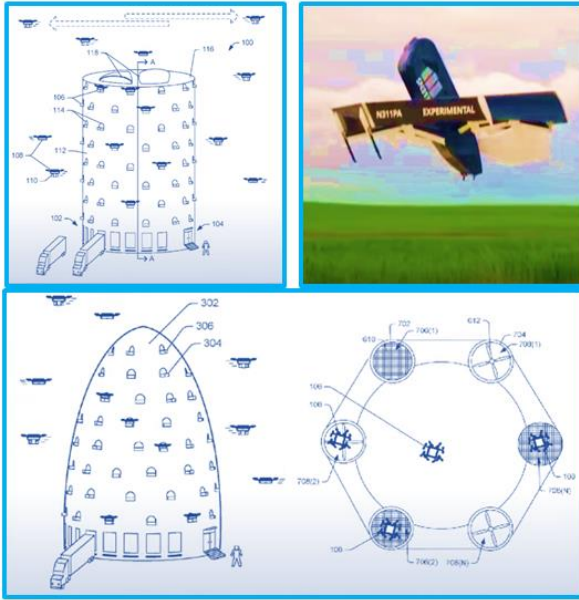


Fig-2(a) Real Time device (Drone)

Drones, also known as automated flying vehicles (UAVs), were first used in 1918 and have existed since the middle of the 20th century. With the development of the first radio-controlled airplane in the 1930s, they have experienced tremendous technological improvements. In the 1960s, plane-powered drones for observation were introduced as part of the ongoing drone technology exploration by the US, Japan, and Germany [7]. When drones with satellite control were developed in the 1970s, they were used in military operations like as the Vietnam War. With the advent of remote-controlled quad copters in the 1990s, there was a notable change in the use of drones for both business and recreational purposes.

Drone use underwent a dramatic change in the twenty-first century as a result of technological breakthroughs that let them to carry larger payloads and carry out a greater variety of jobs. Drones have been used in the War on Terror since 2002, when the US military started employing them for targeted strikes in Afghanistan. These days, drones are utilized in movies and television shows, as well as in environmental observation, search and rescue operations, and disaster relief initiatives [8].

However, the growing usage of drones raises health and safety issues. Guidelines to guarantee the safe and dependable use of drones are being developed by state-run administrations across the globe [9].

Thanks to advancements in technology, a variety of drone types are now available and on the horizon, each with a specific purpose. Over time, drones have changed dramatically, and now there are many different kinds of drones for different uses. For corporate applications including aerial photography, planning, and evaluation, fixed-wing drones – which are made to look like airplanes – are frequently utilized [11][12]. For accurate data collecting, they can be outfitted with cameras and high-performance sensors. The most popular kind of drones are rotational drones, sometimes referred to as multi-rotor drones, which have rotors attached to a focus point enabling vertical take-off and landing.

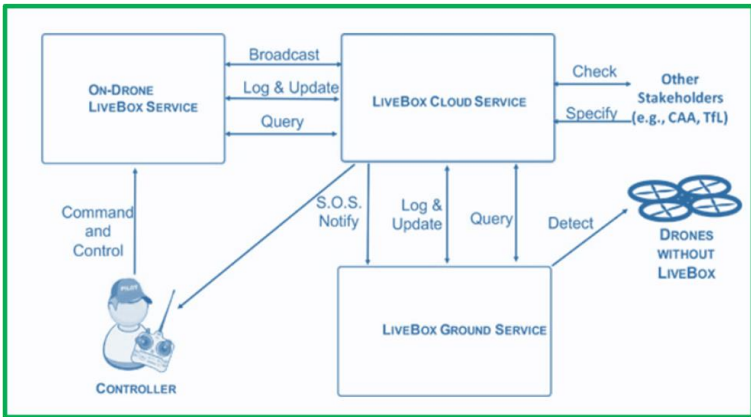


Fig.-2(b) Control Process of Drone[10]

Crossbreed drones are appropriate for both short- and long-range missions since they incorporate aspects of both varieties. Larger and more sophisticated single-rotor helicopters are ideal for intricate tasks including freight transportation, observation, and search and rescue. Drones with flapping wings that imitate the flight patterns of birds and insects are employed for study and monitoring. With the added capacity to take off and land higher, fixed-wing VTOL drones are appropriate for military operations in confined locations. Drones powered by sunlight are perfect for long-distance observation and natural checking

because they rely on the sun's energy as their main power source. Drones using hydrogen power modules can fly for longer periods of time and carry greater loads because they rely on hydrogen gas as their main power source.

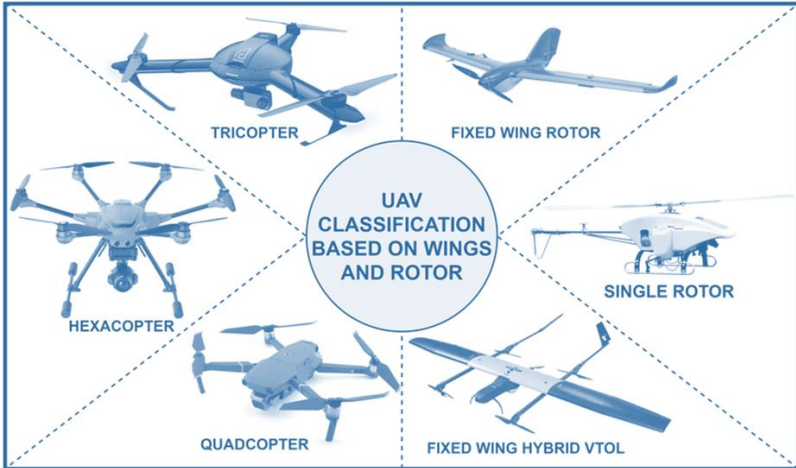


Fig-3 Types of Drones

Real drones and various drone kinds that cover nearly every engineering field have been demonstrated with the aid of Figures 2 and 3.

DESIGN AND WORKING

The process of designing a drone includes establishing its objectives, specifications, features, performance requirements, financial constraints, type, electrical system, software, assembly, testing, and certifications. It is seen in Figure 4. Establishing the drone's target market, desirable features, performance requirements, and financial constraints is the first step in the process. The type of drone – multi-rotor, fixed-wing, or hybrid – is selected. Weight and durability, motors and ESCs, propellers, battery capacity, flight controller, sensors, and optional payload are all factors in the selection of components. The design of the electrical system includes battery management and power distribution systems. Ground control stations, payload integration, and flight control algorithms are all included in software development. For best results, the drone is put together, tested, calibrated, and adjusted. Licenses or qualifications are acquired as needed [13].

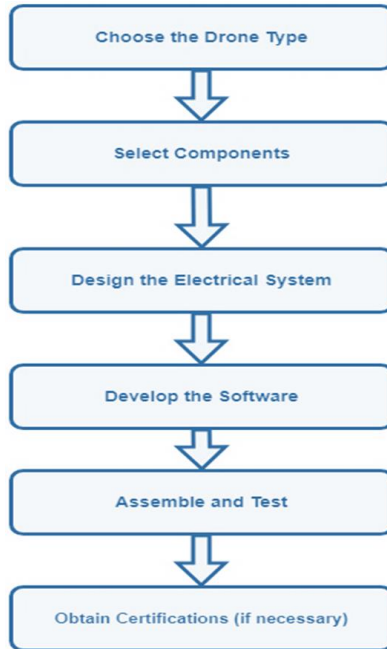


Fig.-4 Design steps of drones

Despite the fact that drone designs may differ based on their intended purpose [14], the main body of a drone is composed of the following parts:

Frame: The UAE's fundamental design preserves the integrity of its numerous components. Robots can be made of a number of materials, including carbon fiber, aluminum, and plastic, depending on their size and nature.

Motors and propellers: Drones' propellers are powered by electric engines, which provide push and lift. The number and size of the drone's engines and propellers are determined by its weight and dimensions. In order to handle their increased weight, larger drones typically feature larger propellers and more powerful engines.

Battery: The drone's battery serves as its main power source. It supplies the vital energy required for the operation of engines and other electronic devices. The type and quantity of batteries used depends depend on the drone's size, weight, and required flight time.

Flight regulator: The flight regulator is the drone's brain. It converts commands from the controller or a nearby PC into particular drone advances. It also modifies engine speeds to keep the drone level and under control.

Sensors: UAs are outfitted with a range of sensors, such as gyrotors, accelerometers, and magnetometers, to collect information on their area, speed, and direction. This data is used by the flight regulator to keep the drone stable and under control.

Camera and gimbal: Many are outfitted with cameras and gimbals to record and take high-quality pictures. The camera is held in place by a gimbal, a settling component that keeps the camera consistent while the robot is moving.

The same trip regulations that apply to ordinary airplanes also apply to drones. Drones use the lift produced by the propellers to counteract gravity and maintain altitude. Additionally, they use the criterion of streamlined qualities to govern their development and bearing [15]. Based on input from the pilot or an installed PC, the flight regulator adjusts the engines' speed and propellers' direction to provide the required development. Drones are operated remotely using a controller or a PC that has been installed. The pilot instructs the robot using the controller, and the robot complies. Furthermore, certain drones can fly and do duties without human aid because they are autonomous.

MULTIDISCIPLINARY NATURE AND APPLICATIONS OF DRONES

There are numerous applications for drones. The most well-known applications of UAs are probably as follows:

Airborne photography and videography: Drones with high-end cameras and gimbals are commonly used by the film and media sectors to take breathtaking high-altitude images. They are also employed in land photography, event inclusion, and sports broadcasting.

Farming: Drones are utilized in horticulture to gather information about crops, including soil moisture content, plant health, and expected yield. Ranchers can use this information to make educated decisions about harvesting, board preparation, and the water system.

Military: In the military, drones have been employed for observation, knowledge collection, and targeted attacks.

Conveyance services: Businesses like UPS and Amazon are looking into a number of options for product delivery via drone. Drones can move bundles faster and more effectively in places with a lot of traffic or difficult terrain.

Disaster board: Executives utilize drones fitted with thermal imaging cameras and other sensors to look for survivors and evaluate the damage in remote locations.

FUTURE IMPLICATIONS



Fig.-5 Future prediction of Drone

Figure 5 displays the study report and drone predictions for the future. The inventiveness behind rambles is expanding, as are the possible applications and suggestions for them. Drones are also being investigated for practical and medicinal applications in addition to the companies already listed. Organs and medical supplies can be transported by robots in the clinical setting, especially in isolated or rural locations (Ling, 2018). In humanitarian disaster response, drones can be used to transport aid and medical supplies to impacted areas (Schroth, 2016). Drones may possibly be used in freight and passenger transportation in the future. Companies like Uber and Airbus are currently developing drones for freight and taxis (Ride, 2019).

Although this development raises questions over safety and regulations, it also has the potential to transform transportation.

Additionally, there may be health risks associated with the extensive use of drones. As more UAEs take to the skies, the likelihood of mishaps and collisions increases, particularly in places with a high population density. Drone administrators urgently need appropriate planning and processes to lower these hazards. All things considered, drones will have a significant influence on the future and hold great potential for a number of businesses. They can improve productivity, well-being, and supportability in sectors like development, agriculture, transportation, and conveyance. In any case, stringent laws and moral considerations must be taken into account to guarantee that drone use does not negatively impact security, safety, or well-being. It is crucial to thoroughly examine and address the possible ramifications of drones as innovation develops in order to optimize their benefits and reduce their drawbacks.

CONCLUSION

Finally, because of their adaptability, affordability, and creative potential, drones are transforming a number of industries; nevertheless, obstacles related to electricity, security, and regulations must be addressed before they can be widely used. Since the 1980s, drone use has grown, helping sectors like delivery, agriculture, and cinematography. But they need to be regulated and present possible risks. Drones will have a huge impact on society in the future as technology develops. For safe and responsible use, advantages and dangers must be balanced. Drones may become more versatile as technology develops, but ethical use requires addressing safety and security issues. In conclusion, the versatility, efficiency, and technological advancements of drones are radically altering a variety of industries. Thanks to AI-powered autonomous systems and integration with 5G networks, drones are moving beyond their initial military use into sectors including logistics, agriculture, environmental monitoring, and even urban air mobility. Their potential applications in areas including construction, medical emergencies, and space exploration show how significantly they could influence future innovation. Despite the abundance of options, there are still problems with things like regulation, power supply, and cyber security. As research and technology develop, drones have the potential to completely transform both industry and everyday life, creating exciting new opportunities for the future.

REFERENCES

1. M. Hassanalian and A. Abdelkefi, "Classifications, applications, and design challenges of drones: A review," *Prog. Aerosp. Sci.*, vol. 91, pp. 99–131, May 2017, doi: 10.1016/j.paerosci.2017.04.003.
2. M. Ayamga, S. Akaba, and A. A. Nyaaba, "Multifaceted applicability of drones: A review," *Technol. Forecast. Soc. Change*, vol. 167, p. 120677, Jun. 2021, doi: 10.1016/j.techfore.2021.120677.
3. D. Floreano and R. J. Wood, "Science, technology and the future of small autonomous drones," *Nature*, vol. 521, no. 7553, pp. 460–466, May 2015, doi: 10.1038/nature14542.
4. M. Gharibi, R. Boutaba, and S. L. Waslander, "Internet of Drones," *IEEE Access*, vol. 4, pp. 1148–1162, 2016, doi: 10.1109/ACCESS.2016.2537208.
5. A. Intelligence *et al.*, "4670848 Artificial intelligence system," *Robot. Comput. Integr. Manuf.*, vol. 3, no. 4, p. iii, 1987, doi: 10.1016/0736-5845(87)90065-2.
6. Kaustubh Kumar Shukla, T.Muthumanickam, and T.Sheela, *Effects of Thermally Induced Deformations and Surface Radiosity for 3D Heat Transfer and Its Applications*, Technology. Singapore: Springer Nature Singapore Pte Ltd. 2022, 2022. doi: 10.1007/978-981-16-7909-4.
7. K. Kumar Shukla and T. Muthumanickam, "A smart sensor using MEMS technology for artificial environmental monitoring," *Mater. Today Proc.*, Jul. 2022, doi: 10.1016/J.MATPR.2022.07.160.
8. S. Mishra, M. Jaiswal, K. K. Shukla, H. Mittal, S. Dubey, and B. K. Sharma, "Design and Analysis of a Novel Microbattery using Multiphysics based on Artificial Intelligence Applications," in *2024 Third International Conference on Smart Technologies and Systems for Next Generation Computing (ICSTSN)*, IEEE, Jul. 2024, pp. 1–6. doi: 10.1109/ICSTSN61422.2024.10671311.
9. C. Manning, "Artificial Intelligence Definitions," *HAI Stanford Univ.*, no. September, p. 1, 2020.
10. Y. Yu, D. Barthaud, B. A. Price, A. K. Bandara, A. Zisman, and B. Nuseibeh, "LiveBox: A Self-Adaptive Forensic-Ready Service for Drones," *IEEE Access*, vol. 7, pp. 148401–148412, 2019, doi: 10.1109/ACCESS.2019.2942033.
11. K. K. Shukla, T. Muthumanickam, and T. Sheela, "Comparative Study of Sensitivity Improvement through Mechanical Properties

- of Micro-Cantilever," *J. Inf. Comput. Sci.*, vol. 9, no. 11, pp. 1103–1110, 2019.
12. V. Kangunde, R. S. Jamisola, and E. K. Theophilus, "A review on drones controlled in real-time," *Int. J. Dyn. Control*, vol. 9, no. 4, pp. 1832–1846, Dec. 2021, doi: 10.1007/s40435-020-00737-5.
 13. J. A. Besada, A. M. Bernardos, L. Bergesio, D. Vaquero, I. Campana, and J. R. Casar, "Drones-as-a-service: A management architecture to provide mission planning, resource brokerage and operation support for fleets of drones," in *2019 IEEE International Conference on Pervasive Computing and Communications Workshops (PerCom Workshops)*, IEEE, Mar. 2019, pp. 931–936. doi: 10.1109/PERCOMW.2019.8730838.
 14. H. Na and Y. S. Chang, "Study on the Policies, Regulations of Drone-Based Logistics," in *2024 2nd International Conference on Cyber Resilience (ICCR)*, IEEE, Feb. 2024, pp. 1–4. doi: 10.1109/ICCR61006.2024.10533097.
 15. A. Alsawy, A. Hicks, D. Moss, and S. Mckeever, "An Image Processing Based Classifier to Support Safe Dropping for Delivery-by-Drone," in *2022 IEEE 5th International Conference on Image Processing Applications and Systems (IPAS)*, IEEE, Dec. 2022, pp. 1–5. doi: 10.1109/IPAS55744.2022.10052868.

About the Editors



Dr. Vijayalakshmi Chintamaneni

Associate Professor Department of Electronics and Communication Engineering, Vignan Institute of Technology & Science, Hyderabad, Telangana



Dr. Amit Kumar Dutta

Professor & Head, Amity Institute of Biotechnology, Amity University Jharkhand, Ranchi



Dr. Kaustubh Kumar Shukla

Associate Professor, Department of ECE, Dronacharya Group of Institutions, Greater Noida, Uttar Pradesh



Dr. G Madhukar

Associate Professor, CSE Department CMR Technical Campus, Hyderabad, Telangana



Mrs. M Rekhasree

Assistant Professor, CSE Department, KUCE & T, Kakatiya University, Warangal



SIDVI Foundation, Visakhapatnam



Bharti Publications, New Delhi

E-mail: bhartipublications@gmail.com, info@bhartipublications.com.
www.bhartipublications.com

978-81-19757-24-4



9 788119 757244

Price - 1180/-